Playing Tetris with Porphyrins – The Synthesis of Porphyrinic Materials for Self-Assembly Studies

Thesis submitted to The University of Nottingham for the degree of Doctor of Philosophy

Tim Hames, MSci

October 2016

Abstract

This thesis focuses on the synthesis of porphyrinic materials for self-assembly studies. It begins with the synthesis of a large number of 'building block' molecules, terminated with bromo-, alkyne- and TMS- groups. These molecular building blocks are combined to form porphyrin compounds also terminated with bromo- alkyne- and TMS- groups at carefully selected positions. A series of porphyrin arrays inspired by the computer game Tetris was designed to be synthesised from these porphyrin units. The Tetris compounds are comprised of four square-like tetraphenylporphyrin (TPP) units, linked together with alkyne bridges to create arrays shaped like the T, I, L/J, S/Z and O Tetriminos. The NMR spectroscopy of the Tetris compounds is thoroughly explored to highlight the slight structural differences between the molecules.

The synthesis of two bromoaryl-terminated porphyrin dimers for ultimate incorporation into covalent organic frameworks (COFs) is also described. The X-ray diffraction data collected showed that crystals grown were of trifluoroacetic acid (TFA) salts of the target compounds. The presence of the TFA anions resulted in significant distortion of the porphyrin ring which is described in full.

Finally, the synthesis of a series of poly(acetylene) anthracene dimer compounds that have potential use in the field of organic electronics has also been explored. The electrochemical and fluorescence properties of the molecules across the series are investigated and the crystal structures are described.

Acknowledgments

Firstly, I would like to thank my supervisor Neil Champness, primarily for his guidance and encouragement throughout my PhD but also for providing many amusing stories about the more bizarre aspects of life which always entertained.

Thank-you to Stephen Davies for supervising all of the electrochemical and fluorescence experiments described in this thesis (as well as many more attempted experiments for less well-behaved compounds) and for teaching the theory whilst the measurements were being collected.

Thanks to William Lewis, Stephen Argent, Jeremiah Tidey and especially Connie Pfeiffer for all (at one point or another) offering extensive help with crystallography, the structures within this thesis would be much worse off without them.

I have been lucky enough to receive help and advice from many postdocs over the years and so I wish to thank Lixu Yang, Connie Pfeiffer (again), Stephen Argent (again), Andrea Laybourn and Anna Slater.

I would like to thank Graham Coxhill, Ben Pointer-Gleadhill and Mick Cooper for keeping the spectrometers running and for all their time spent collecting high-resolution data of my compounds. I would also like to thank Shaz Aslam, Kev Butler and Adrienne Davies for maintaining the NMR facilities and helping explain some of the more unusual data collected during this research. Thanks also to Stephen Boyer of London Metropolitan University for conducting elemental analysis experiments.

The people in the lab have varied during my stay but they have all made a fantastic impact on my life and I wouldn't have enjoyed working in B52 nearly as much if it wasn't for them. A final thank-you to Nic, Ben, Sam Quinn, Harry, Sarah, Charlie, Harry, Phil, Razan, Dan, Barry, Tom, Vics, Simon and Irina.

List of Abbreviations

1D	One-Dimensional
2D	Two-Dimensional
3D	Three-Dimensional
AFM	Atomic force microscopy
A.U.	Arbitrary units
BDBA	1,4-Benzenediboronic acid
BPEA	9,10-Bis(phenylethynyl)anthracene
Bipy	4,4'-Bipyridine
DCC	Dynamic covalent chemistry
DCM	Dichloromethane
COF	Covalent organic framework
COSY	Correlation Spectroscopy
CTF	Covalent triazine framework
CV	Cyclic voltammetry
DABCO	1,4-Diazabicyclo(2.2.2)octane
DCTB	Trans-2-(3-(4-tert-butylphenyl)-2-methyl-2-propenylidene)malononitrile
DDQ	2,3-Dichloro-5,6-dicyano-1,4-benzoquinone
DMF	N,N-Dimethylformamide
DNA	Deoxyribonucleic acid
EI	Electron ionisation
ESI	Electrospray ionisation
FD	Field desorption
HHTP	2,3,6,7,10,11-Hexa-hydroxytriphenylene
HMBC	Heteronuclear multiple bond correlation

HMWM	Higher molecular weight material
HOMO	Highest occupied molecular orbital
HOPG	Highly ordered pyrolytic graphite
IUPAC	International union of pure and applied chemistry
LUMO	Lowest unoccupied molecular orbital
MALDI	Matrix assisted laser desorption/ionisation
MOF	Metal organic framework
MS	Mass spectrometry
NIR	Near-infrared
NMP	1-Methyl-2-pyrrolidine
NMR	Nuclear magnetic resonance
OTFT	Organic thin film transistors
PEG	Polyethylene glycol
PTFE	Polytetrafluoroethylene
PXRD	Powder X-ray diffraction
RT	Room temperature
SCOF	Surface covalent organic framework
SEC	Size exclusion chromatography
SEM	Scanning electron microscope
SLG	Single layer graphene
STM	Scanning tunnelling microscope
TBAF	Tetrabutylammonium fluoride
TEM	Transmission electron microscopy
TFA	Trifluoroacetic acid
THF	Tetrahydrofuran
TLC	Thin layer chromatography

TMEDA	Tetramethylethylenediamine
TMS	Trimethylsilyl
TOF	Time of flight
TPP	Tetraphenylporphyrin
TPTC	p-Terphenyl-3,5,3',5'-tetracarboxylic acid
UHV	Ultra-high vacuum
UV	Ultraviolet
Vis	Visible

Contents

Chapter 1: Introduction 1

Self-Assembly 2

Dipoles 2

Hydrogen Bonds 3

π-Interactions 4

Metal-Ligand Coordination 5

Mechanical Bond 5

Reactions Forming Carbon-Carbon Bonds 8

Surface Studies 11

Surface Preparation 13

Tiling 15

Overview of Thesis/Project Aims 20

General Synthetic Methods 21

Reagents and Purification 21

General Analytical Methods 21

Cyclic Voltammetry 22

Fluorescence Measurements 22

X-Ray Diffraction 23

References 24

Chapter 2: Molecular Building Blocks 29

Introduction 30

Results and Discussion 31

Aldehydes 31

Pyridyl Thioesters 33

Dipyrromethanes 35

Acylated Dipyrromethanes 38

Conclusions 44

Experimental 46

4-TMS-ethynylbenzaldehyde (1) 46

4-Ethynylbenzaldehyde (2) 46

4,4'-Dicarbaldehydebiphenyl (3) 47

S-2-pyridyl-benzothioate (4) 48

S-2-Pyridyl-4-bromobenzothioate (5) 48

S-2-Pyridyl-4-iodobenzothioate (6) 49

S-2-Pyridyl-4-(2-TMS-ethynyl)benzothioate (7) 50

5-Phenyldipyrromethane (8) 50

5-(4-Bromophenyl)dipyrromethane (9) 51

5-(4-(2-TMS-ethynyl)phenyl)dipyrromethane (10) 51

5-(4-Ethynylphenyl)dipyrromethane (11) 52

1,4-Bis(dipyrromethane)benzene (12) 52

4,4'-Bis(dipyrromethane)biphenyl (13) 53

1,9-Bis(benzoyl)-5-phenyldipyrromethane (14) 54

1,9-Bis(4-bromobenzoyl)-5-(4-bromophenyl)dipyrromethane (15) 54

1,9-Bis(benzoyl)-5-(4-(2-(TMS)-ethynyl)phenyl)dipyrromethane (16) 55

1-(Benzoyl)-5-(4-(2-TMS)ethynylphenyl)dipyrromethane (17) 56

1-(Benzoyl)-5-(4-(2-TMS)ethynylphenyl)-9-(4-bromobenzoyl)dipyrromethane (18) 57

1-(4-(2-(TMS)-ethynyl)benzoyl)- 5-(4-ethynylphenyl)dipyrromethane (19) 58

1-(4-(2-(TMS)-ethynyl)benzoyl)-5-(4-ethynylphenyl)-9-benzoyldiprromethane (20) 58

1-(4-Bromobenzoyl)-5-(4-bromophenyl)dipyrromethane (21) 59

1-(4-Bromobenzoyl)-5-(4-bromophenyl)-9-benzoyldipyrromethane (22)..... 60

References 62

Chapter 3: Porphyrins 64

Introduction 65

Structure and Nomenclature 65

Porphyrin Synthesis 66

Spectroscopic Properties of Porphyrins 70

Results and Discussion 74

Metallation 80

Statistical Method for Porphyrins 23, 25 and 30 80

Comparison of Zn-Porphyrin and Freebase Porphyrin. 82

UV/Vis Spectroscopy 88

Conclusions 90

Experimental 91

General Procedure A for Porphyrin Formation Reaction 91

5-(4-Bromophenyl)-10,15,20-tri(phenyl)porphyrin (23) 91

Zn-5-(4-bromophenyl)-10,15,20-tri(phenyl)porphyrin (Zn-23) 92

5-(4-Ethynylphenyl)-10,15,20-triphenylporphyrin (24) 92

Zn-5-(4-ethynylphenyl)10,15,20-tri(phenyl)porphyrin (Zn-24) 93

5,10,15-tri(4-Bromophenyl)-20-phenylporphyrin (25) 93

5-(4-(2-(TMS)-ethynyl)phenyl)-10-phenyl-15-(4-bromophenyl)-20-phenylporphyrin (26) 94

5-(4-(2-(TMS)-ethynyl)phenyl)-10-phenyl-15-(4-ethynylphenyl)-20-phenylporphyrin (27) 94

5-(4-(2-(TMS)-ethynyl)phenyl)-10-(4-bromophenyl),15,20-diphenylporphyrin (28) 95

5-(4-(2-(TMS)-ethynyl)phenyl)-10-(4-ethynylphenyl),15,20-diphenyl porphyrin (29) 95

5-(4-Bromophenyl)-10-(4-bromophenyl),15,20-diphenyl porphyrin (30) 96

References 97

Chapter 4: The Synthesis of Porphyrin Dimers for Covalent Organic Frameworks 100

Introduction 101

Covalent Organic Frameworks 101

Design 101

Synthesis 103

Porphyrin-Based COFs 106

Results and discussion 111

Synthesis of Porphyrin Dimers 31 and 32 111

Crystallographic Analysis of 31 114

Crystallographic Analysis of 32 119

UV/Vis Spectroscopy for 31 and 32 133

Conclusions 136

Experimental 138

1-(5,10,15-tri(4-bromophenyl)-20-porphyrinyl)-4-(5,10,15-tri(4-bromophenyl-20-porphyrinyl)phenyl (31) 138

4-(5,10,15-tri(4-bromophenyl)-20-phenylporphyrin)-4'-(5,10,15-tri(4-bromophenyl)-20-phenylporphyrin)biphenyl (32) 139

References 140

Chapter 5: Porphyrin Tetris 143

Introduction 144

Synthesis of Porphyrin Arrays 144

Results and Discussion 148

Porphyrin Tetris 148

Synthesis of Porphyrin Dimers 33 and 34 152

Synthesis of Tetrimino T 156

Synthesis of Tetrimino J/L 160

Synthesis of Tetrimino S/Z 163

Synthesis of Tetrimino I 165

Synthesis of Tetrimino O 168

NMR Spectra of Tetris Products 171
Conclusions 180
Experimental 181
1,2-bis(4-(10,15,20-triphenylporphyrin-5-yl)phenyl)ethyne (33) 181
Zn_2-1,2-bis(4-(10,15,20-triphenylporphyrin-5-yl)phenyl)ethyne (34) 181
Tetrimino T (35) 182
Tetrimino J/L protected precursor (36) 182
Tetrimino J/L deprotected precursor (37) 183
Tetrimino J/L (38) 184
Tetrimino S/Z protected precursor (39) 184
Tetrimino S/Z deprotected precursor (40) 185
Tetrimino S/Z (41) 186
Tetrimino I protected precursor (42) 186
Tetrimino I deprotected precursor (43) 187
Tetrimino I (44) 188
Tetrimino O protected precursor (45) 188
Tetrimino O deprotected precursor (46) 189
Tetrimino O (47) 189
References 191
Chapter 6: Anthracenes 193
Introduction 194
Results and Discussion 198

Crystallographic Analysis of 50 206

Crystallographic Analysis of 51 209

Crystallographic Analysis of 54 212

Cyclic Voltammetry 214

Fluorescence Measurements 217

Conclusions 221

Experimental 223

4-(Anthracen-9-yl)-2-methylbut-3-yn-2-ol (48) 223

9-Ethynylanthracene (49) 223

1,2-Di(9-anthrancenyl)ethyne (50) 224

1,4-Di(9-anthracenyl)1,3-butadiyne (51) 224

9-((Z)-4-Chlorobut-3-en-1-ynyl)anthracene (52) 225

9-(Buta-1,3-diynyl)anthracene(53) 225

1,8-Di(9-anthracenyl)1,3,5,7octatetrayne (54) 226

1,2,4-Tri(9,9',9"-anthracenyl)benzene (55) 226

References 228

Chapter 7: Conclusions 230

Chapter 1:

Introduction

Self-Assembly

The term self-assembly can be used to describe a diverse range of processes involving the spontaneous generation of order arising from disordered components binding with each other *via* non-covalent interactions. It is one of the most fundamental concepts in supramolecular chemistry, a field which is defined as 'chemistry beyond the molecule'.[1,2] Dipole interactions,[3] π- interactions[4] and metal-ligand coordination[5] all fall under the non-covalent bond category and so can be used to create self-assembled architectures. These interactions may also be exploited so that a mechanical bond is formed, a crucial feature of many increasingly researched supramolecular systems.[6] Self-assembled systems usually result in new properties arising that were not present in the discrete components.[7] Ultimately, the aim of self-assembly is to create molecular machines that are capable of arranging their components in a specific way when exposed to a stimulus so that useful information or motion may be gleaned from the system.[8] This 'bottom-up' approach has received a lot of attention and so a great amount of research has been conducted to find systems which exhibit self-assembly and the properties that arise from that process.[9]

Dipoles

A dipole occurs within a molecule when the electronic charge is not spread out equally between all of its atoms. Atoms which have a higher electronegativity pull electronic charge closer to themselves resulting in a partially negative charge at these sites and a partially positive charge where the electronic charge was pulled from. Molecules which due to their geometry have dipoles which cancel each other out (*e.g.* CO_2) are non-polar, whereas molecules with an overall dipole (*e.g.* HCl) are polar. When two polar molecules approach each other, they can interact so that the partially positive end of one molecule will attract the partially negative end of another molecule.

In non-polar molecules, intermolecular interactions are still possible through induced dipoles. These types of interactions are very weak and are known as London dispersion forces.[10] Fluctuations of electronic charge density can occur within the molecule causing a temporary dipole which is able to interact with another molecule nearby. On the condition that the molecules stay near to each other, their individual polarities will fluctuate synchronistically so that the attraction between the molecules remains.

Hydrogen Bonds

Hydrogen bonds are a specific class of dipole-dipole interactions and certainly one of the most important for self-assembly. They occur between a hydrogen, bonded to a highly electronegative atom, and another electronegative atom either as part of another molecule, or as an ion. They are among the strongest non-covalent interactions, a representative selection of which is listed below in table 1.1.

Table 1.1 Bond enthalpies of hydrogen bonds.[11]

Hydrogen bond	Bond enthalpy (kJ mol^{-1})
$H_2N\text{-}H\cdots NH_3$	17
$HO\text{-}H\cdots OH_2$	22
$F\text{-}H\cdots FH$	29
$HO\text{-}H\cdots Cl^-$	55

The most obvious instance of hydrogen bonding can be found in water, as oxygen has high electronegativity, it creates a strong dipole in the molecule. The slightly positive hydrogen can interact with a slightly negative oxygen on a neighbouring molecule to form a hydrogen bond. This results in water having some very interesting properties, including having a much higher boiling point than other small molecules (100 °C compared

to -161 °C for methane) and being one of the few substances which is less dense in its solid phase than its liquid phase. Hydrogen bonding is also a vital phenomenon within DNA, holding the two strands of the double helix together. The four base pairs that make up our DNA, adenine, thymine, cytosine and guanine and the hydrogen bonding that occurs between them are pictured in figure 1.1.

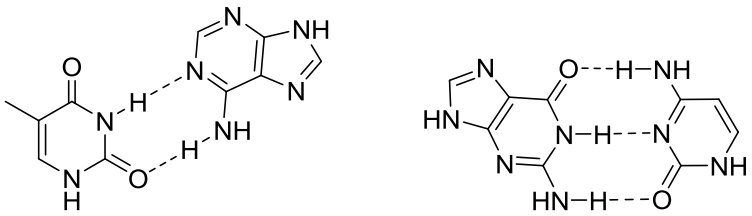


Figure 1.1 Hydrogen bonding between adenine and thymine (left) and cytosine and guanine (right).

π-Interactions

π-π interactions are another form of non-covalent interaction which have great importance in self-assembly.[12] They most commonly occur between two molecules containing aromatic rings when they approach each other in various orientations, three of which are displayed in figure 1.2. The sandwich π-π interaction is less favourable than both the parallel displaced and the T-shaped interactions. The interactions have to overcome the electrostatic repulsion of electrons in π-orbitals to be attracted to the positively charged σ-framework and vary in bond strength up to 50 kJ mol^{-1} for extended aromatic systems.[13]

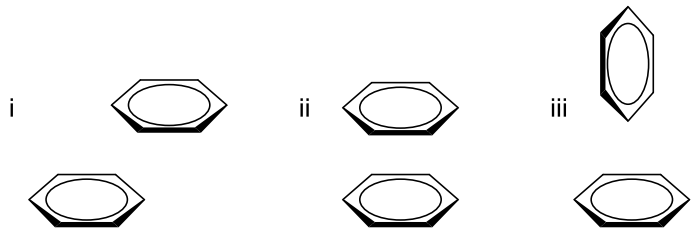


Figure 1.2 (i) Parallel displaced, (ii) Sandwich (iii) T-shaped π-π interactions.

Cation-π interactions[14] can be stronger than π-π interactions, up to 80 kJ mol^{-1} and occur between either a metallic or organic cation and an aromatic π-region. More recently, evidence for anion-π interactions has been uncovered and used for self-assembly processes[15] having a typical energy of 50 kJ mol^{-1}.[16]

Metal-Ligand Coordination

In designing supramolecular structures, using metal-ligand coordination gives access to a range of geometries based upon the transition metal of choice, and the denticity of the associated ligand. This type of interaction can be very strong and is commonly in the region of 150 kJ mol^{-1}.[17] The high degree of directional control makes this type of interaction of particular use in creating three-dimensional networks, which was exploited by Yaghi in the construction of MOFs,[18] an area that has since seen huge interest from the scientific community with potential to be used in many areas including gas storage,[19] separation[20] and catalysis.[21]

Mechanical Bond

The mechanical bond is the term used to describe the interaction between two molecules that are not covalently bonded to each other but are locked together so that they are inseparable.[22] Catenanes,[23] rotaxanes,[24] Borromean rings,[25] Solomon links[26] and trefoil knots[27] are all examples of mechanically bonded molecules shown in figure 1.3 that have been synthesised by various research groups.



Figure 1.3 Cartoon depictions of catenanes, rotaxanes, Borromean rings, Solomon links and trefoil knots (from left to right).[28]

Catenanes derive their name from the latin *catena* meaning 'chain' and have a naming convention in which the number of macrocycles connected together shown between square brackets.[29,30] They are composed of two or more interlocked rings, either in a linear conformation as presented in the [5]-catenane, olympiadane[31] or in a branched conformation.[32]

Rotaxanes derive their name from the latin word *rota* meaning 'wheel' and an axle and are comprised of one or more macrocycles encircling an axle component with stopper groups on the ends of the axle to prevent dethreading of the macrocycle components.[33] A rotaxane-like molecule without these stopper groups is known as a pseudo-rotaxane.[34]

Molecules that are linked together in this way have attracted significant attention, not only for their unusual structures but also for their potential to be used in or as molecular machines.[35-37] Figure 1.4 demonstrates schematically how a [2]-rotaxane or a [2]-catenane could have two positions (representing a 0 or 1) meaning that they can act as a molecular switch.[38] This movement between two recognition sites can be induced and controlled in a variety of ways, including photochemically,[39] electrochemically,[40] *via* changes in pH[41] or by ion coordination.[42]

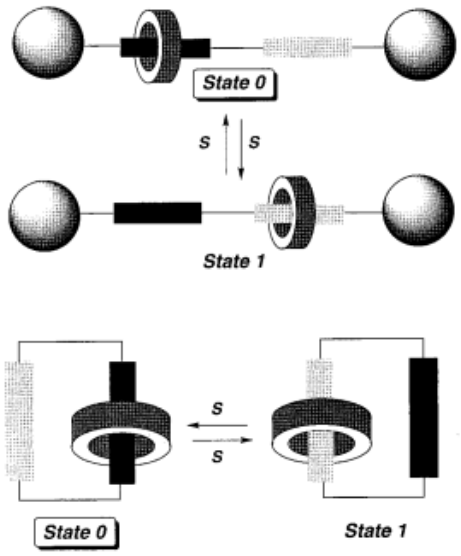


Figure 1.4 Mechanical movements of a [2]-rotaxane (top) and a [2]-catenane (bottom) to two states.[38]

Reactions Forming Carbon-Carbon Bonds

Reactions which form carbon–carbon bonds are of incredible importance in organic chemistry but can involve dangerous or impractical components. Over time, a vast range of coupling reactions have been developed that can be used as powerful tools to combine two smaller molecules together to form one larger one. There are far too many to name individually so instead a selection of the most significant coupling reactions for the research described in this thesis are briefly discussed below.

Glaser coupling,[43] discovered by Carl Glaser in 1869 uses a copper salt such as copper (I) chloride to combine two terminal alkynes to form a diacetylene. The reaction is carried out using water or an alcohol as the solvent and ammonia as the base. Only catalytic amounts of copper are needed but the system must be exposed to oxygen. This reaction has since been modified to make the reaction more versatile. One such modification is the Eglinton reaction.[44] This typically uses pyridine as the solvent and importantly uses stoichiometric amounts of a copper (II) salt, typically copper (II) acetate as the oxidant. Another modification, the Hay reaction,[45] uses a catalytic amount of a copper-tetramethylethylenediamine (TMEDA) complex which is soluble in a wide range of solvents.

A similar reaction known as the Ullmann reaction,[46] named after its innovator Fritz Ullmann, takes place between two aryl halides and is also catalysed by copper. The development of the Cadiot-Chodkiewicz coupling reaction,[47] between a terminal alkyne and a haloalkyne meant that asymmetrically substituted diacetlyenes could be synthesised more efficiently.

The Sonogashira coupling reaction is one of many palladium catalysed reactions. Building one the work done by Heck[48] and Cassar[49] which classically use high temperatures, the protocol introduced by Sonogashira, Tohda and Higahara allows the coupling of a carbon (sp^2) halide and a terminal alkyne to take place at room temperature with the addition of a copper co-catalyst.[50] Figure 1.5 below shows the suggested mechanism for a co-catalysed Sonogashira reaction.[51] The use of copper as a co-catalyst often results in an undesired Glaser reaction occurring, hence an array of copper-free Sonogashira coupling conditions have been reported.[52-55]

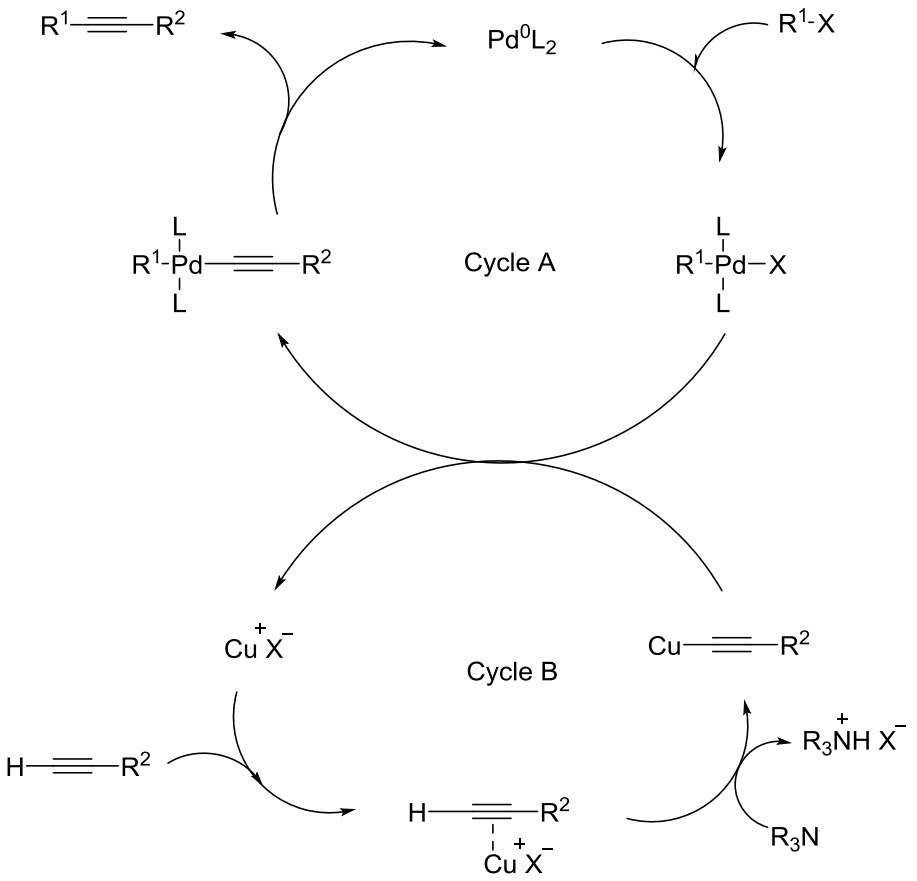


Figure 1.5 Suggested mechanism for copper co-catalysed Sonogashira coupling reaction. R^1,R^2 = aryl, heteroaryl, vinyl; X = I, Br, Cl, OTf).

In cycle A, the palladium cycle, the Pd^0L_2 species is generated from the reduction of a palladium (II) species by amines and phosphines. Following this, fast oxidative addition

of R^1-X to the palladium catalyst occurs. The next step intersects cycle B and involves a transmetallation from the copper acetylide species to form a palladium complex containing both the R^1 and alkyne groups as ligands. Finally a reductive elimination gives the coupled product. The mechanism for cycle B is less well understood. It is thought that the amine base abstracts the acetylenic proton to form a copper acetylide species which can then interact with the palladium species in cycle A.[51]

Grignard reagents, having the general formula R-MgX (R = alkyl, aryl; X = halogen), are very versatile compounds that can be used to couple together many different compounds and so are widely used in organic synthesis. However, they are very susceptible to hydrolysis and oxidation so any reaction that employs Grignard reagents must be done in dry, inert conditions.[56] To aid this, typically anhydrous diethyl ether or tetrahydrofuran (THF) is used as the volatility of the solvent creates vapours which provide a blanketing effect to the bulk reaction volume. The scope of the Grignard reaction is vast; various carbonyl derivatives including aldehydes, ketones, amides, esters have all been shown to react with Grignard reagents, as have epoxides. An example mechanism of a Grignard reaction with a ketone is illustrated below in figure 1.6, showing a nucleophilic Grignard reagent that forms a six-membered ring with the carbonyl as a transition state. The magnesium then coordinates with the oxygen before addition of acid affords the alcohol.

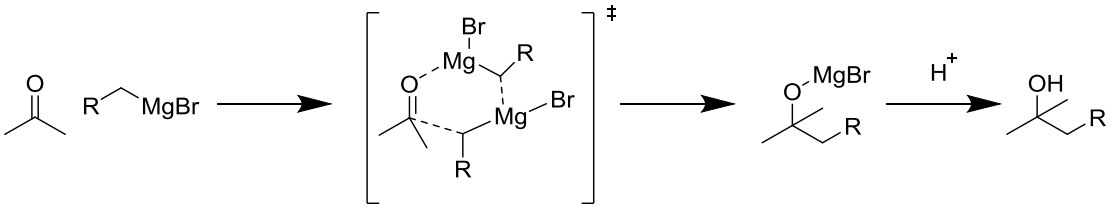


Figure 1.6 Mechanism of Grignard reaction.

Surface Studies

The scanning tunnelling microscope (STM) was invented by Binnig and Rohrer in 1981, and was quickly deemed one of the most important and influential innovations in surface science, earning them both the 1986 Nobel prize in physics in conjunction with Ernst Ruska for his design of the first electron microscope.[57]

A conventional microscope works by light reflecting off an object which then passes through a lens and into your eye. However, it is ultimately limited in its resolution by the wavelength of visible light (approximately 400 nm) so in order to view fine detail of surfaces another technique is required. A scanning electron microscope (SEM) uses a focused beam of high energy electrons instead of light as the source of illumination. Theoretically, the resolution is limited by the wavelength of the electrons. In practice however, the resolution is limited by the lens' ability to focus, which is hindered by spherical aberration. Recently aberration-corrected electron microscopy techniques have been reported, with the resolution of these systems now being limited by the size of the electron probe so that astonishingly, resolution as fine as 50 pm can be achieved.[58-60] The magnification of the electron microscope can be varied extensively to provide detailed pictures of macroscopic and microscopic objects as shown in figure 1.7, as well as showing atomic detail of surfaces.

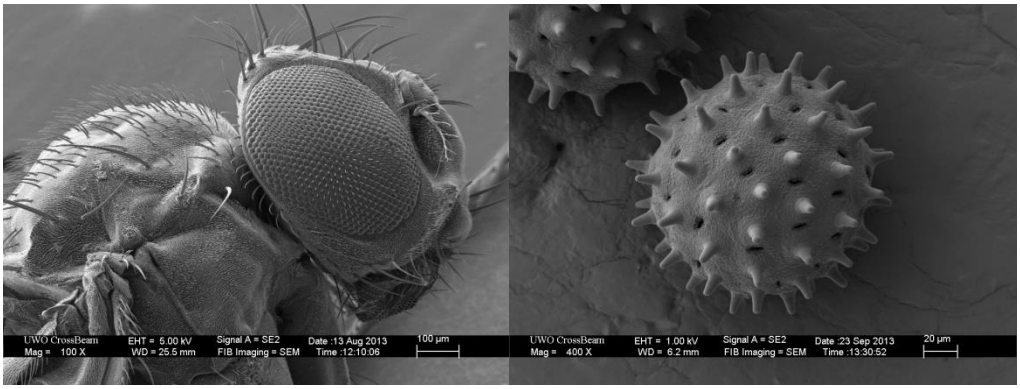


Figure 1.7 SEM images of a fruit fly (left) and pollen and stamen (right).[61]

The technique of STM is notably different to standard electron microscopy. Instead of firing a beam of electrons at a surface, a conducting tip scans over a surface, a schematic of this is shown in figure 1.8. A known, precise potential energy difference is setup between the tip and the surface, allowing electrons to travel between the two, creating a tunnelling current. The current depends on the distance of the tip from the sample, the density of states and the applied voltage, which is predetermined value. To obtain useful data one of two techniques is employed. In constant current mode, the position of the piezoelectric tube is controlled so that the current detected remains constant. The data collected represents a topological map travelled by the STM tip which can then be related to charge density. A faster technique appropriate only for atomically flat surfaces is constant height mode. This keeps the height of the piezoelectric tube and voltage constant and again the changes in current observed are related to changes in charge density.

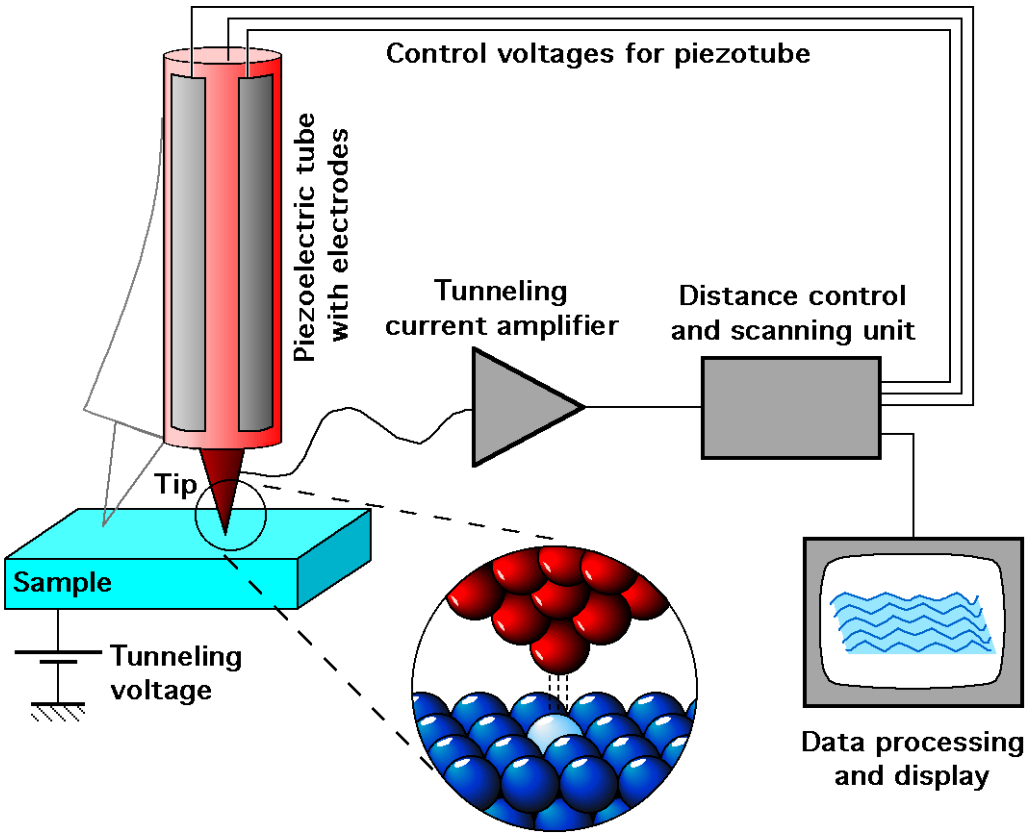


Figure 1.8 Schematic diagram of a STM.[62]

The STM has resolution good enough to observe individual atoms within a molecule and so is a suitable technique for observing how molecules pack on a surface. In addition, the STM tip allows the operator to manually select and move single atoms to create any arrangement they desire. This aspect was taken advantage of by IBM in their short film 'A boy and his atom', in which they celebrated STM technology by creating a stop-motion film.[63]

Surface Preparation

Briefly, there has been a lot of research conducted on pure metal surfaces using STM, in particular to discover which relaxation or reconstruction processes occur upon heating of the surface. Surface relaxation refers to a situation when the position of entire layers of atoms shift relative to the bulk. Surface reconstruction refers to when there is a change in

the two-dimensional structure of the surface layer in comparison to the bulk. Certain reconstructions are beneficial for certain depositions and so careful selection of a suitable metal along with the appropriate reconstruction may be required to achieve the desired surface chemistry. Au(110) has a 'missing row' structure, giving it a striped appearance which highly favours one-dimensional structure growth evidenced by the work conducted by Tchalala *et al.* in which silicon nanoribbons were reported to self-assemble on an Au(110) surface.[64] Similarly, deposition of silicon on an Ag(111) surface was found to produce a continuous two-dimensional sheet of honeycomb-structured silicene.[65]

Sample deposition may be achieved in a number of ways with the technique chosen depending on the properties such as solubility, thermal stability and molecular weight of the molecules being deposited. One common method of deposition is sublimation from a Knudsen cell. The sample is placed in a Knudsen cell which is carefully degassed so that the process is performed at ultra-high vacuum (UHV). The Knudsen cell is then heated to a temperature that causes the sample to sublime and effuse through a pinhole opening onto the surface. However, for larger, more complex molecules deposition using this technique becomes difficult as the thermal energy the molecule is exposed to reaches the intramolecular binding energies and as a result, molecular fragments are deposited rather than whole molecules.[66] Samples may also be deposited through solution deposition, which has the advantage of being performed at ambient pressure and temperature. Several different solvents have been shown to be effective including water,[67] acetone[68] and alkanoic acids.[69] Similarly, electrospray techniques have been developed that can safely deposit samples onto surfaces that would not survive the thermally intensive conditions of sublimation.[70]

Tiling

The phenomenon of tiling is one that we are all able to recognise, on a surface, two-dimensional shapes arrange themselves into a tessellation so that there are no gaps visible between the shapes. This tiling can be periodic, whereby you can identify a region covering an area that when moved using translational operations tiles that area completely. M. C. Escher is an artist well known for his works which often feature this type of tiling, a couple of which are displayed in figure 1.9 below.



Figure 1.9 Artworks by M. C. Escher 'Lizard' (left) and 'Butterfly' (right) demonstrating periodic tiling.[71]

Probably the most famous example of aperiodic tiling is Penrose tiling, named after Roger Penrose.[72] The first type of Penrose tiling (type P1) to be discovered is shown in figure 1.10. This tiling uses pentagons, five-pointed stars, diamonds and boats (3/5 of a star) which are placed together using matching rules to ensure aperiodicity. The tiling exhibits both reflectional and five-fold rotational symmetry and self-repeating sections can be found throughout the design. Penrose developed two other tilings that share these characteristics; the kite and dart tiling (type P2) consists of kite and dart shapes that fit together following matching rules to exclude the formation of rhombuses. The rhombus

tiling (type P3) consists of two different rhombuses of equal length but different angles. Penrose tilings can also be considered as a representation of quasicrystals, and there has been some success in designing molecular equivalents of these systems by a couple of research groups.[73,74]

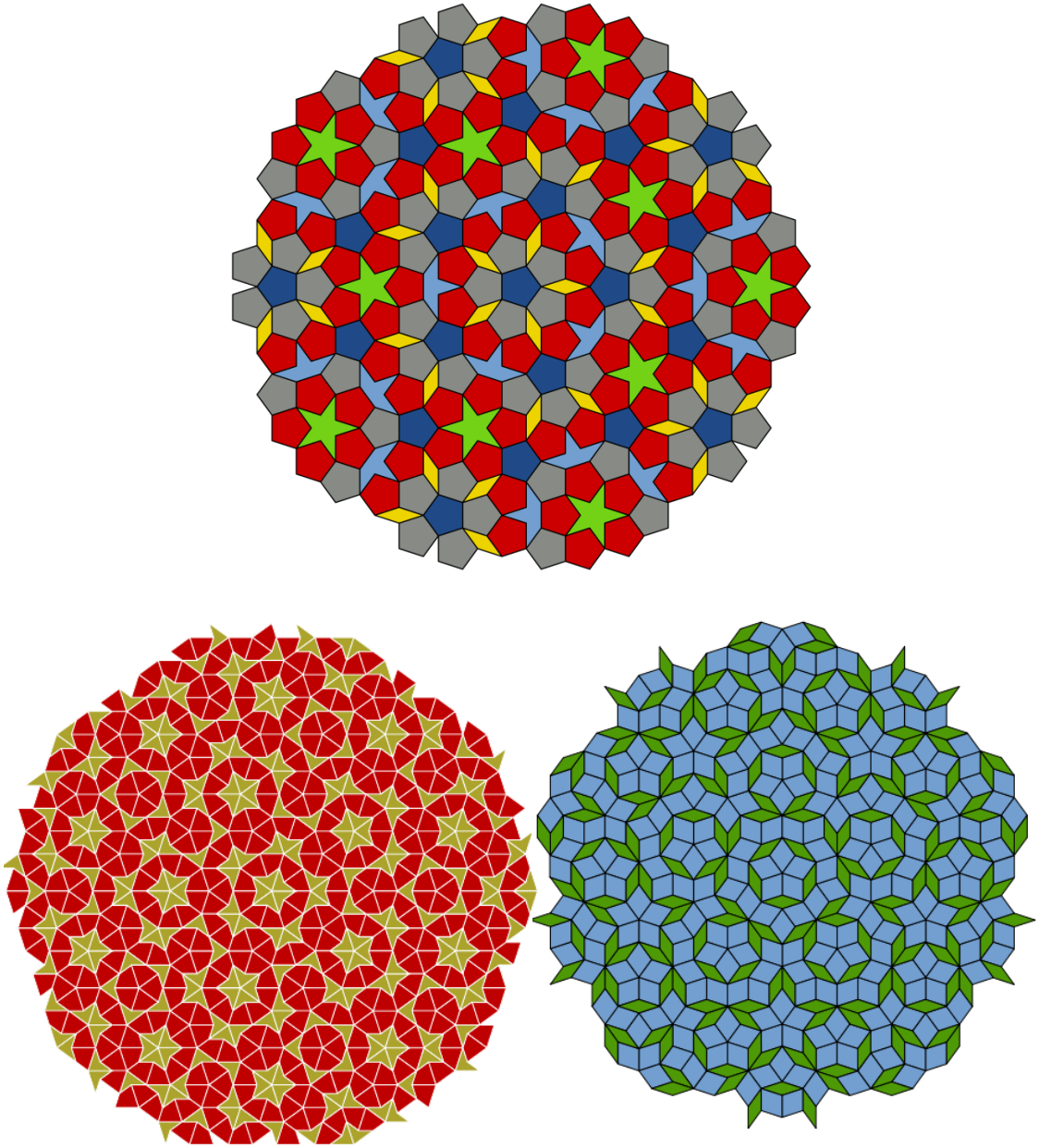


Figure 1.10 Penrose tilings P1 (top) P2 (bottom left) and P3 (bottom right).[75]

Other aperiodic tilings include Wang dominoes, first created by Hao Wang in 1961.[76] Wang tiles are best modelled using any number of coloured squares termed as the set. The squares within the set are not allowed to be rotated or reflected, *i.e.* a square with the same pattern as another square rotated 90° clockwise would count as a separate tile within the set. These squares are then arranged so that the colours along the edges of adjacent squares match up. Winfree *et al.* were able to move this from a concept to a real-world example when they created a set of DNA-based Wang tiles in which the preferential binding of the base pairs led to self-assembly in a periodic fashion.[77] When he first proposed the system, Wang posited that for any set of tiles that are able to tile a plane, a periodic tiling of that set must exist. However, in 1964, Robert Berger was able to show that this was untrue and was able to construct a set of Wang dominoes that only tiled aperiodically. The number of tiles within such a set was first found by Berger to be 20,426 which he later improved to 104 but now rests at 13 due to work done by Karel Culik.[78,79] This tiling system can be modified so that instead of matching colours, it consists of matching jigsaw-like protrusions and indents and allows rotations and reflections of the tiles.

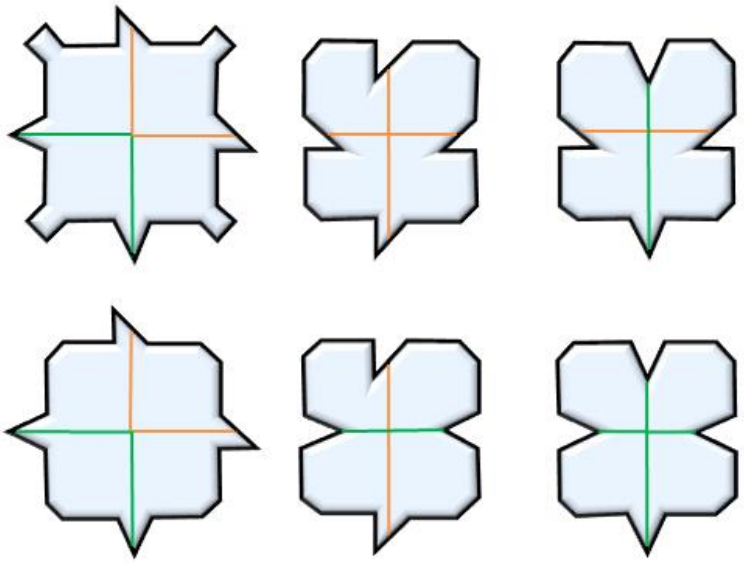


Figure 1.11 The six Wang tiles designed by Raphael Robinson that ensure aperiodic tiling.[80]

In this system, Raphael Robinson proved that it is possible to ensure an aperiodic tiling using just six tiles shown in figure 1.11.[80] Any valid arrangement of these tiles results in a hierarchical structure. From figure 1.12 we can see that each small orange square that is formed is itself on a corner of a larger orange square, which again is on a corner of a larger orange square, ad infinitum.

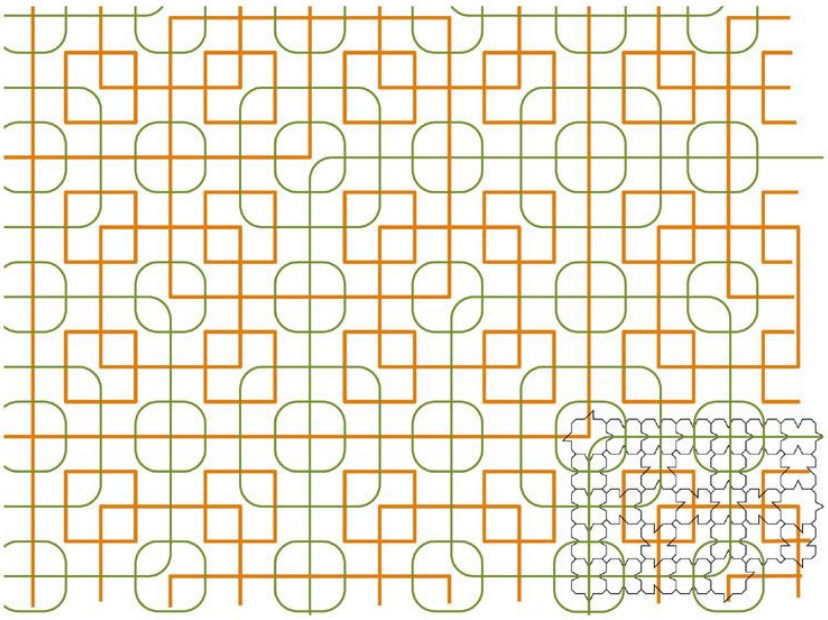


Figure 1.12 Aperiodic tiling formed from Robinson's tiles.[81]

This concept of hierarchical structure is very common in aperiodic tiling being important not only for Penrose and Wang tilings but also for rep-tiles, that is, tiles that can be dissected into smaller copies of themselves. Some rep-tiles such as the square would result in a periodic tiling, but most result in an aperiodic tiling. The sphinx pentagon illustrates this in figure 1.13 up to its fourth generation. As this shape takes four smaller copies of itself to generate a larger copy, it is termed as a rep-4 tile. These types of tiles have many mathematical curiosities associated with them, any rep-4 tile can also be a rep-9 tile, polygons for rep-k exist for any value of k and repeated subdivision and subtraction of a rep-tile results in a fractal pattern being generated.

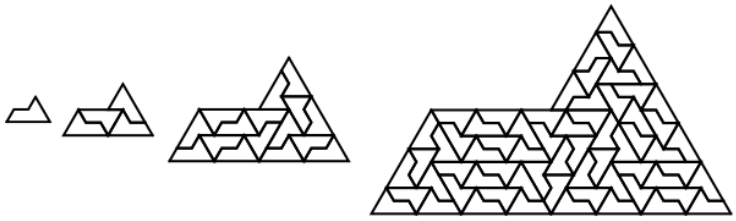


Figure 1.13 Tiling of the 'sphinx' rep-4 pentagon.

Aperiodic tiling has also been achieved by depositing p-terphenyl-3,5,3',5'-tetracarboxylic acid (TPTC) shown in (A) in figure 1.14 on a highly ordered pyrolytic graphite (HOPG) surface.[82] The carboxylic acid groups of TPTC promote the formation of directional, intermolecular hydrogen bonds. As there are multiple orientations TPTC can take, illustrated in part (B) an aperiodic rhombus tiling is formed. Using STM, long-range order was observed, along with localised tiling defects which propagated slowly through the system leading to further work discussing the similarities between structural glass formers and this system.[83]

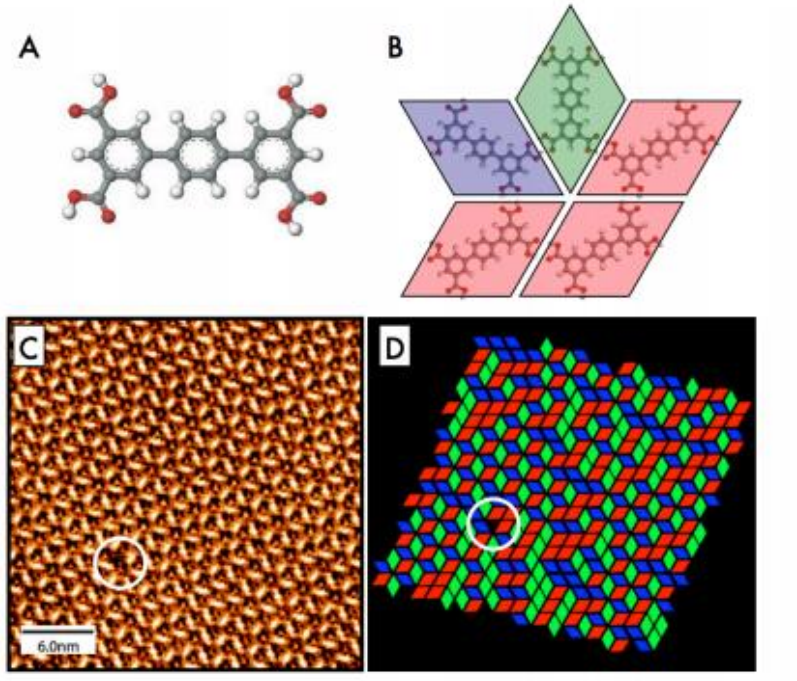


Figure 1.14 (A) Molecular ball and stick diagram of TPTC. (B) Example of an arrangement of TPTC molecules linked *via* hydrogen bonds. (C) An STM image of a typical area of TPTC network adsorbed on HOPG. (D) Corresponding rhombus tiling to (C). The white circle shows the position of a tiling defect.[83]

Overview of Thesis/Project Aims

This project focused on the synthesis of porphyrinic materials for surface deposition studies. In order to achieve this, a number of smaller molecules acting as 'building blocks' must first be synthesised. Chapter 2 discusses the synthesis of these small molecules. This is continued in chapter 3 which discusses the formation of monomeric porphyrin units terminated with bromo-, alkyne- and TMS-protection groups which make them suitable to undergo further coupling reactions to form larger porphyrin arrays. The first major aim of the project was to synthesise a series of bromoaryl-terminated porphyrin dimers as these have been highlighted as candidates for synthesising Covalent Organic Frameworks (COFs). The synthesis of two bromoaryl- terminated porphyrin dimers is described in chapter 4. The second major aim of this research is explored in chapter 5; a series of porphyrinic 'Tetris' molecules was designed to investigate how the molecules arrange themselves on a surface and to discover if any emergent properties arise from this process. This research also aimed to synthesise a series of anthracene dimer compounds containing varying numbers of consecutive linking alkyne moieties to investigate the fluorescence properties across the series, the results of which are discussed in chapter 6. Finally, the conclusions drawn from this research are summarised in chapter 7.

General Synthetic Methods

Reagents and Purification

All starting materials were obtained from commercial sources and used without further purification, with the exception of pyrrole which was distilled for use at the beginning of each experiment. Anhydrous toluene was prepared over a potassium mirror under a nitrogen atmosphere. Anhydrous triethylamine, DMF, THF and 1,4-dioxane were stored over 4 Å sieves under a nitrogen atmosphere. Column chromatography was performed using silica (pore size 60 Å 40-63 μm) or alumina (neutral, Brockmann I, 60 Å, 50-200 μm) as the stationary phase. Size exclusion chromatography (SEC). SEC was performed using Bio-Beads SX-1 or SX-3. The beads were swelled with toluene or chloroform and packed into a 1.2 x 60 cm glass column under gravity flow. Unlike silica and alumina column chromatography, SEC media can be used repeatedly. After a few separations have been performed a slight pink-brown discolouration can be observed of the media however this does not have a noticeable impact on the quality of separation.

General Analytical Methods

Nuclear magnetic resonance (NMR) experiments were carried out using either a Bruker DPX400 (400 MHz), Bruker AV400 (400 MHz), Bruker AV3400hd (400 MHz), Bruker 3400 (400 MHz) or a Bruker AV3500 (500 MHz) spectrometer. J values were calculated using ACD Labs NMR processing software. When 2D COSY experiments were run, full analysis was possible enabling an average J value to be calculated between coupling protons. In the instances where 2D COSY experiments were not run and the protons involving in coupling could not be identified, the J values listed are unchanged from those generated by the software. Electrospray (ESI) mass spectrometry (MS) was carried out on a Bruker Daltonics micrOTOF spectrometer. Matrix-assisted laser

desorption/ionisation time of flight (MALDI-TOF) MS was conducted using a Bruker Ultraflex III spectrometer using trans-2-[3-(4-tert-butylphenyl)-2-methyl-2-propenylidene]malononitrile (DCTB) as the matrix. A polyethylene glycol standard was used to calibrate the spectrometer when collecting high resolution spectra. Electron ionisation (EI) MS data was collected using a Bruker Apex IV 4.7 T mass spectrometer. Field desorption (FD) MS data was collected using JEOL GCv4G spectrometer. Elemental analysis was carried out at London Metropolitan University by Stephen Boyer. UV-Vis data was collected using a PerkinElmer Lambda 25 UV-Vis spectrometer in 10 mm quartz cells.

Cyclic Voltammetry

Cyclic voltammetry (CV) was carried out using an Autolab PGSTAT20 potentiostat. Measurements were recorded using a three-electrode arrangement in a single compartment cell which contained a glassy carbon working electrode, a Pt wire secondary electrode and a saturated calomel reference electrode, chemically isolated from the test solution *via* a bridge tube containing electrolyte solution and fitted with a porous vycor frit. Concentration of solutions were 10^{-3} M for the test compound and 0.4 M for the supporting electrolyte, $[^{n}Bu_4N][BF_4]$. Redox potentials are quoted versus the ferrocenium-ferrocene (Fc^{+}/Fc) couple used as an internal reference. Compensation for internal resistance was not applied.

Fluorescence Measurements

Fluorescence measurements were recorded using a Horiba FluoroMax-3 using a 10 mm quartz fluorescence cuvette. Quantum yields were calculated using coumarin-153 as the reference compound.

X-Ray Diffraction

Single crystal X-ray data was collected either at the UK Diamond Light Source, or on a 'Supernova' or an 'Agilent GV1000' Atlas CCD area detector diffractometer at 120 K using monochromated Cu Kα radiation (λ = 1.54184 Å). CrysAlisPRO software was used for initial data processing followed by OLEX2 for structure solution and refinement.

References

1. F. Schreiber, *Prog. Surf. Sci.*, 2000, **65**, 151-256.

2. J. M. Lehn, *Angew. Chem. Int. Ed.*, 1988, **27**, 89-112.

3. J. T. Davis and G. P. Spada, *Chem. Soc. Rev.*, 2007, **36**, 296-313.

4. L. Zang, Y. Che and J. S. Moore, *Acc. Chem. Res.*, 2008, **41**, 1596-1608.

5. J. B. Beck, J. M. Ineman and S. J. Rowan, *Macromolecules*, 2005, **38**, 5060-5068.

6. P. L. Anelli, P. R. Ashton, R. Ballardini, V. Balzani, M. Delgado, M. T. Gandolfi, T. T. Goodnow, A. E. Kaifer, D. Philp, M. Pietraszkiewicz, L. Prodi, M. V. Reddington, A. M. Z. Slawin, N. Spencer, J. F. Stoddart, C. Vicent and D. J. Williams, *J. Am. Chem. Soc.*, 1992, **114**, 193-218.

7. M. P. Pileni, *J. Phys. Chem. B*, 2001, **105**, 3358-3371.

8. V. Balzani, A. Credi and M. Venturi, *Chem. Eur. J.*, 2002, **8**, 5524-5532.

9. V. Balzani, *Pure Appl. Chem.*, 2008, **80**, 1631-1650.

10. H. Margenau, *J. Chem. Phys.*, 1938, **6**, 896-899.

11. P. Atkins, T. Overton, J. Rourke, M. Weller and F. Armstrong, Oxford University Press, 2006, ch. 9, p. 248.

12. C. G. Claessens and J. F. Stoddart, *J. Phys. Org. Chem.*, 1997, **10**, 254-272.

13. C. A. Hunter and J. K. M. Sanders, *J. Am. Chem. Soc.*, 1990, **112**, 5525-5534.

14. J. Wouters, *Protein Sci.*, 1998, **7**, 2472-2475.

15. B. L. Schottel, H. T. Chifotides, M. Shatruk, A. Chouai, L. M. Perez, J. Bacsa and K. R. Dunbar, *J. Am. Chem. Soc.*, 2006, **128**, 5895-5912.

16. B. L. Schottel, H. T. Chifotides and K. R. Dunbar, *Chem. Soc. Rev.*, 2008, **37**, 68-83.

17. M. T. Rodgers and P. B. Armentrout, *Mass Spectrom. Rev.*, 2000, **19**, 215-247.

18. O. M. Yaghi, M. O'Keeffe, N. W. Ockwig, H. K. Chae, M. Eddaoudi and J. Kim, *Nature*, 2003, **423**, 705-714.

19. M. Eddaoudi, J. Kim, N. Rosi, D. Vodak, J. Wachter, M. O'Keeffe and O. M. Yaghi, *Science*, 2002, **295**, 469-472.

20. J. S. Seo, D. Whang, H. Lee, S. I. Jun, J. Oh, Y. J. Jeon and K. Kim, *Nature*, 2000, **404**, 982-986.

21. J. Lee, O. K. Farha, J. Roberts, K. A. Scheidt, S. T. Nguyen and J. T. Hupp, *Chem. Soc. Rev.*, 2009, **38**, 1450-1459.

22. R. Jager and F. Vogtle, *Angew. Chem. Int. Ed.*, 1997, **36**, 930-944.

23. M. Asakawa, P. R. Ashton, V. Balzani, A. Credi, C. Hamers, G. Mattersteig, M. Montalti, A. N. Shipway, N. Spencer, J. F. Stoddart, M. S. Tolley, M. Venturi, A. J. P. White and D. J. Williams, *Angew. Chem. Int. Ed.*, 1998, **37**, 333-337.

24. M. J. Blanco, M. C. Jimenez, J. C. Chambron, V. Heitz, M. Linke and J. P. Sauvage, *Chem. Soc. Rev.*, 1999, **28**, 293-305.

25. K. S. Chichak, S. J. Cantrill, A. R. Pease, S. H. Chiu, G. W. V. Cave, J. L. Atwood and J. F. Stoddart, *Science*, 2004, **304**, 1308-1312.

26. Y. H. Song, N. Singh, J. Jung, H. Kim, E.-H. Kim, H.-K. Cheong, Y. Kim and K.-W. Chi, *Angew. Chem. Int. Ed.*, 2016, **55**, 2007-2011.

27. C. O. Dietrichbuchecker and J. P. Sauvage, *Angew. Chem. Int. Ed.*, 1989, **28**, 189-192.

28. K. E. Griffiths and J. F. Stoddart, *Pure Appl. Chem.*, 2008, **80**, 485-506.

29. E. Wasserman, *J. Am. Chem. Soc.*, 1960, **82**, 4433-4434.

30. P. R. Ashton, C. L. Brown, E. J. T. Chrystal, T. T. Goodnow, A. E. Kaifer, K. P. Parry, D. Philp, A. M. Z. Slawin, N. Spencer, J. F. Stoddart and D. J. Williams, *J. Chem. Soc. Chem. Comm.*, 1991, 634-639.

31. D. B. Amabilino, P. R. Ashton, A. S. Reder, N. Spencer and J. F. Stoddart, *Angew. Chem. Int. Ed.*, 1994, **33**, 1286-1290.

32. D. B. Amabilino, P. R. Ashton, V. Balzani, S. E. Boyd, A. Credi, J. Y. Lee, S. Menzer, J. F. Stoddart, M. Venturi and D. J. Williams, *J. Am. Chem. Soc.*, 1998, **120**, 4295-4307.

33. P. L. Anelli, N. Spencer and J. F. Stoddart, *J. Am. Chem. Soc.*, 1991, **113**, 5131-5133.

34. J.-P. Collin, F. Durola, P. Mobian and J.-P. Sauvage, *Eur. J. Inorg. Chem.*, 2007, 2420-2425.

35. J. P. Sauvage, *Acc. Chem. Res.*, 1998, **31**, 611-619.

36. A. R. Pease, J. O. Jeppesen, J. F. Stoddart, Y. Luo, C. P. Collier and J. R. Heath, *Acc. Chem. Res.*, 2001, **34**, 433-444.

37. J. P. Collin, C. Dietrich-Buchecker, P. Gavina, M. C. Jimenez-Molero and J. P. Sauvage, *Acc. Chem. Res.*, 2001, **34**, 477-487.

38. V. Balzani, M. Gomez-Lopez and J. F. Stoddart, *Acc. Chem. Res.*, 1998, **31**, 405-414.

39. A. Livoreil, J. P. Sauvage, N. Armaroli, V. Balzani, L. Flamigni and B. Ventura, *J. Am. Chem. Soc.*, 1997, **119**, 12114-12124.

40. P. R. Ashton, R. Ballardini, V. Balzani, A. Credi, M. T. Gandolfi, S. Menzer, L. Perezgarcia, L. Prodi, J. F. Stoddart, M. Venturi, A. J. P. White and D. J. Williams, *J. Am. Chem. Soc.*, 1995, **117**, 11171-11197.

41. P. R. Ashton, R. Ballardini, V. Balzani, I. Baxter, A. Credi, M. C. T. Fyfe, M. T. Gandolfi, M. Gomez-Lopez, M. V. Martinez-Diaz, A. Piersanti, N. Spencer, J. F. Stoddart, M. Venturi, A. J. P. White and D. J. Williams, *J. Am. Chem. Soc.*, 1998, **120**, 11932-11942.

42. D. B. Amabilino, C. O. DietrichBuchecker, A. Livoreil, L. PerezGarcia, J. P. Sauvage and J. F. Stoddart, *J. Am. Chem. Soc.*, 1996, **118**, 3905-3913.

43. C. Glaser, *Ber. Dtsch. Chem.*, 1869, **2**, 422-424.

44. G. Eglinton and A. R. Galbraith, *Chem. Ind. (London)*, 1956, 737-738.

45. A. S. Hay, *J. Org. Chem.*, 1962, **27**, 3320-3321.

46. F. Ullmann and J. Bielecki, *Ber. Dtsch. Chem. Ges.*, 1901, **34**, 2174-2185.

47. T. Chodkiewicz, *Ann. Chim. (Paris)*, 1957, **2**, 819-869.

48. H. A. Dieck and F. R. Heck, *J. Organomet. Chem.*, 1975, **93**, 259-263.

49. L. Cassar, *J. Organomet. Chem.*, 1975, **93**, 253-257.

50. K. Sonogashira, Y. Tohda and N. Hagihara, *Tetrahedron Lett.*, 1975, 4467-4470.

51. R. Chinchilla and C. Najera, *Chem. Rev.*, 2007, **107**, 874-922.

52. V. P. W. Bohm and W. A. Herrmann, *Eur. J. Org. Chem.*, 2000, 3679-3681.

53. B. Liang, M. J. Dai, J. H. Chen and Z. Yang, *J. Org. Chem.*, 2005, **70**, 391-393.

54. A. Soheili, J. Albaneze-Walker, J. A. Murry, P. G. Dormer and D. L. Hughes, *Org. Lett.*, 2003, **5**, 4191-4194.

55. D. Mery, K. Heuze and D. Astruc, *Chem. Comm.*, 2003, 1934-1935.

56. M. T. Goebel and C. S. Marvel, *J. Am. Chem. Soc.*, 1933, **55**, 1693-1696.

57. G. Binnig and H. Rohrer, *Rev. Mod. Phys.*, 1987, **59**, 615-625.

58. P. E. Batson, N. Dellby and O. L. Krivanek, *Nature*, 2002, **418**, 617-620.

59. R. Erni, M. D. Rossell, C. Kisielowski and U. Dahmen, *Phys. Rev. Lett.*, 2009, **102**, 096101.

60. P. D. Nellist, M. F. Chisholm, N. Dellby, O. L. Krivanek, M. F. Murfitt, Z. S. Szilagyi, A. R. Lupini, A. Borisevich, W. H. Sides and S. J. Pennycook, *Science*, 2004, **305**, 741-1741.

61. Zeiss Microscopy, https://www.flickr.com/photos/zeissmicro/sets/72157641357585124, (accessed 06/2016).

62. IAP, http://www.iap.tuwien.ac.at/www/surface/stm_gallery/stm_schematic, (accessed 06/2016).

63. IBM, http://www.research.ibm.com/articles/madewithatoms.shtml#fbid=oPQXovO3TID, (accessed 02/2016).

64. M. R. Tchalala, H. Enriquez, A. J. Mayne, A. Kara, S. Roth, M. G. Silly, A. Bendounan, F. Sirotti, T. Greber, B. Aufray, G. Dujardin, M. A. Ali and H. Oughaddou, *Appl. Phys. Lett.*, 2013, **102**, 5.

65. B. Lalmi, H. Oughaddou, H. Enriquez, A. Kara, S. Vizzini, B. Ealet and B. Aufray, *Appl. Phys. Lett.*, 2010, **97**.

66. L. Grill, *J. Phys. Condens. Matter.*, 2010, **22**, 084023.

67. E. S. Skibinski, A. Song, W. J. I. DeBenedetti, A. G. Ortoll-Bloch and M. A. Hines, *J. Phys. Chem. C*, 2016, **120**, 11581-11589.

68. C. C. Chusuei, X. Lai, K. A. Davis, E. K. Bowers, J. P. Fackler and D. W. Goodman, *Langmuir*, 2001, **17**, 4113-4117.

69. M. Lackinger, S. Griessl, W. A. Heckl, M. Hietschold and G. W. Flynn, *Langmuir*, 2005, **21**, 4984-4988.

70. G. Rinke, S. Rauschenbach, S. Schrettl, T. N. Hoheisel, J. Blohm, R. Gutzler, F. Rosei, H. Frauenrath and K. Kern, *Int. J. Mass. Spectrom.*, 2015, **377**, 228-234.

71. http://www.mcescher.com/gallery/symmetry/, (accessed 06/2016).

72. R. Penrose, *Inst. Math. Appl.*, 1974, **10**, 266-271.

73. Z. Zhou and K. D. M. Harris, *Chemphyschem*, 2006, **7**, 1649-1653.

74. D. N. Laikov, *RSC Adv.*, 2014, **4**, 17925-17930.

75. http://tex.stackexchange.com/questions/61437/penrose-tiling-in-tikz, (accessed 06-2016).

76. H. Wang, *AT&T Tech. J.*, 1961, **40**, 1-41.

77. E. Winfree, F. R. Liu, L. A. Wenzler and N. C. Seeman, *Nature*, 1998, **394**, 539-544.

78. K. Williams and M. J. Ostwald, *Architecture and Mathematics from Antiquity to the Future Volume II: The 1500s to the Future*, Birkhäuser, 2015.

79. K. Culik, *Disc. Math*, 1996, **160**, 245-251.

80. R. M. Robinson, *Invent. Math.*, 1971, **12**, 177-209.

81. C. G. Strauss, https://en.wikipedia.org/wiki/Aperiodic_tiling, (accessed 06/2016).

82. M. O. Blunt, J. C. Russell, M. d. C. Gimenez-Lopez, J. P. Garrahan, X. Lin, M. Schroder, N. R. Champness and P. H. Beton, *Science*, 2008, **322**, 1077-1081.

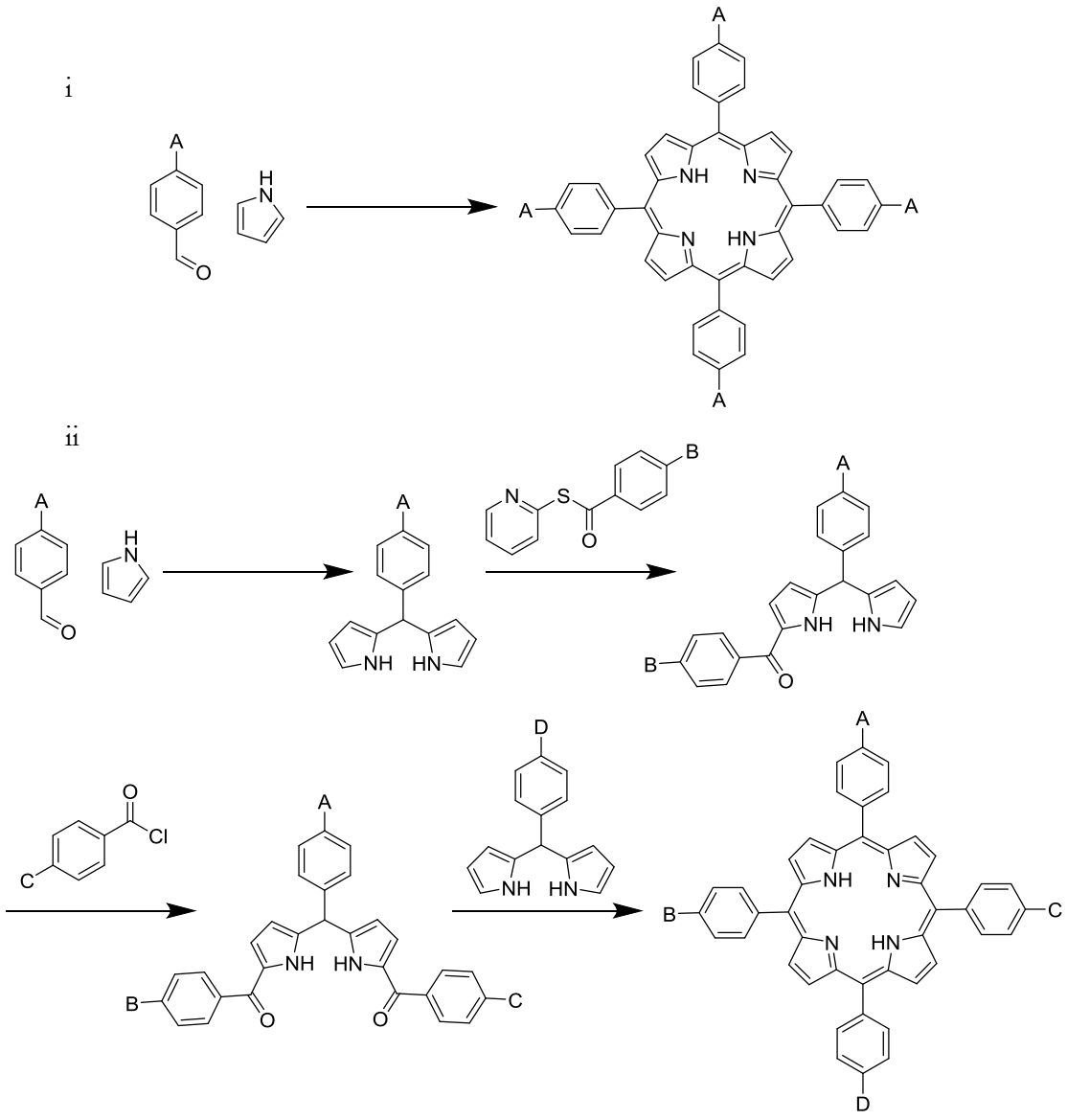
83. J. P. Garrahan, A. Stannard, M. O. Blunt and P. H. Beton, *Proc. Natl. Acad. Sci. USA*, 2009, **106**, 15209-15213.

Chapter 2:

Molecular Building Blocks

Introduction

The synthesis of porphyrins requires a variety of smaller molecules, or building blocks. If a simple Adler-Longo method[1] as shown in scheme 2.1 is employed, then a combination of aldehydes and pyrroles are sufficient but if a more directed approach is desired, a wider range of components are required. A generalised example of a more directed strategy which was made popular by Lindsey is also shown in scheme 2.1.[2] The ultimate aim of this research is to synthesise porphyrin species for surface deposition studies. This chapter describes the synthesis of the building blocks required for porphyrin synthesis.

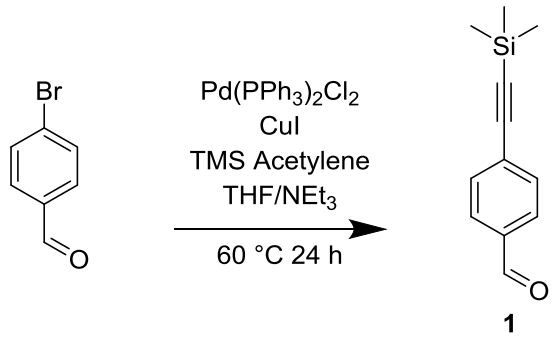


Scheme 2.1 (i) Adler-Longo synthesis (ii) Lindsey synthesis.

Results and Discussion

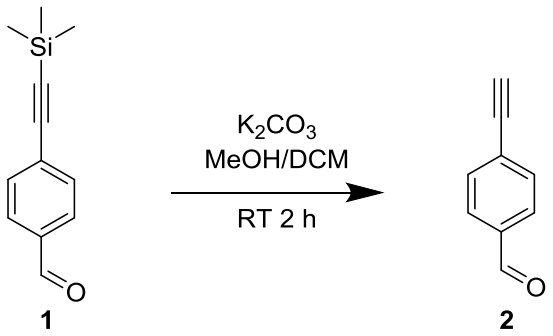
Aldehydes

All of the aldehydes required for this study were commercially available, however as large quantities of the 'building block' compounds are needed due to the low yields typical of porphyrin reactions, the more expensive aldehydes were synthesised when needed. Scheme 2.2 below describes the formation of 4-((trimethylsilyl)ethynyl)benzaldehyde,[3] which is a useful building block for the preparation of alkynyl- functionalised porphyrins. The alkyne is introduced in its silyl- protected form and can be subsequently deprotected under mild conditions, *e.g.* K_2CO_3 whilst leaving the porphyrin unmodified.



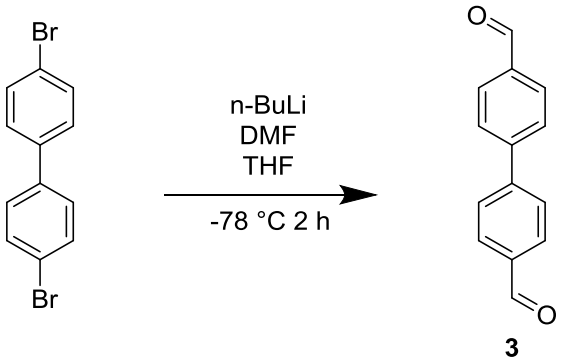
Scheme 2.2 Synthesis of 4-TMS-ethynylbenzaldehyde.

This reaction was performed in anhydrous solvents under an inert atmosphere of N_2. A syringe pump was used to ensure continuous slow addition over the first two hours of the reaction. The reaction proceeded very efficiently, resulting in 98% conversion of starting material to desired product. There were no other identifiable products isolated from the reaction; however a small amount of starting material was detected by NMR. The unreacted bromobenzaldehyde could be removed by vacuum distillation to give the pure aldehyde **1**.



Scheme 2.3 Synthesis of 4-ethynylbenzaldeyhde.

Adapting a known procedure, aldehyde **1** was dissolved in methanol (MeOH) and dichloromethane (DCM) followed by an addition of K_2CO_3 (scheme 2.3).[4] The mixture was stirred for 2 h, after which additional DCM was added and the mixture washed with 2 M HCl, water and brine. After the removal of solvents, column chromatography gave **2** in 79% yield. This reaction was able to be performed open to air and without using dry solvents. Initial attempts at forming **2** were performed in 100% MeOH but it was found that addition of DCM marginally improved the yield and increased the solubility of both the starting material and product.



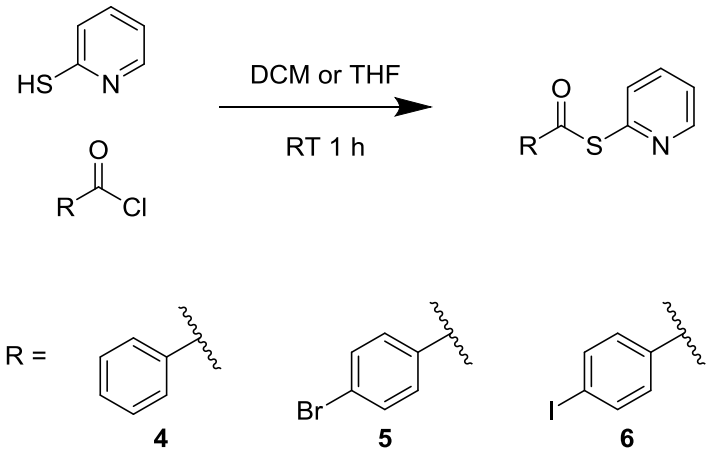
Scheme 2.4 Synthesis of 4,4'-dicarbaldehydebiphenyl.

In a modified procedure from the literature,[5] dibromobiphenyl was dissolved in degassed tetrahydrofuran (THF) and then cooled to -78 °C. n-Butyllithium was added slowly to this to minimise any rise in temperature. After completion of addition, dimethylformamide (DMF) was added and the mixture was allowed to slowly warm to

room temperature after 15 min (scheme 2.4). After the work-up process, it was determined that two products had formed which were readily separated *via* column chromatography. The major product was found to be the monoaldehyde yielding 52% whereas the desired dicarbaldehyde only yielded 16%, both being white and crystalline in appearance.

Pyridyl Thioesters

Pyridyl thioesters have been shown to be useful in the production of β-lactams, a core structure in many antibiotics, as part of an enantioselective one-pot synthesis.[6] They have also found use in the production of ketones[7] in general but most recently the same methods have been applied to specifically make monoacylated dipyrromethanes,[8] see later in the chapter. A range of pyridyl thioesters was synthesised that would allow for the subsequent synthesis of the desired substituted dipyrromethanes. The general synthetic procedure for synthesising pyridyl thioesters is described in scheme 2.5 below.

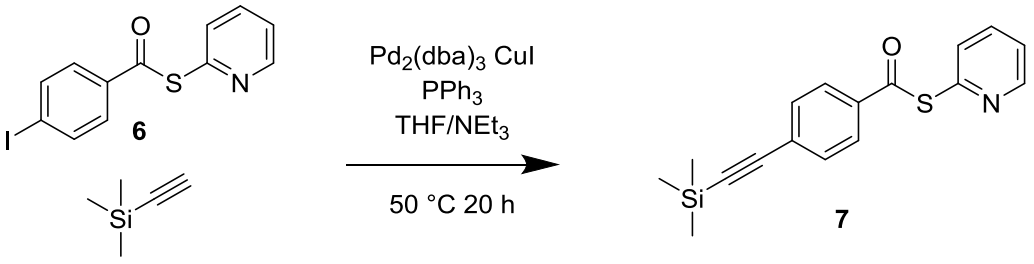


Scheme 2.5 General synthesis of pyridyl thioesters.

For each reaction, a solution of 2-mercaptopyridine was prepared and then slowly added *via* pipette to a separate solution of the appropriate acid chloride. Both THF and DCM are suitable solvents for this reaction with each solvent giving similar yields. A white

precipitate quickly formed in each instance within a couple of minutes of initial addition. After an hour of stirring at RT, diethylether and 2 M NaOH were added, and the organic layer was separated, dried and solvents removed.

In the case of compound **4,** this produced a yellow oil which was left to crystallise overnight. The crystals produced were very large, flat plates which had to be washed with cold toluene to remove oil coated to the surface of the crystals. A second crop of crystals was obtained by removing toluene from the oil under reduced pressure and repeating the procedure of leaving the oil to crystallise overnight. Compounds **5** and **6** both formed small white needles upon evaporation of solvent which were collected and washed with cold diethylether. NMR data collected from these crystals indicated that no further purification was necessary.[9]

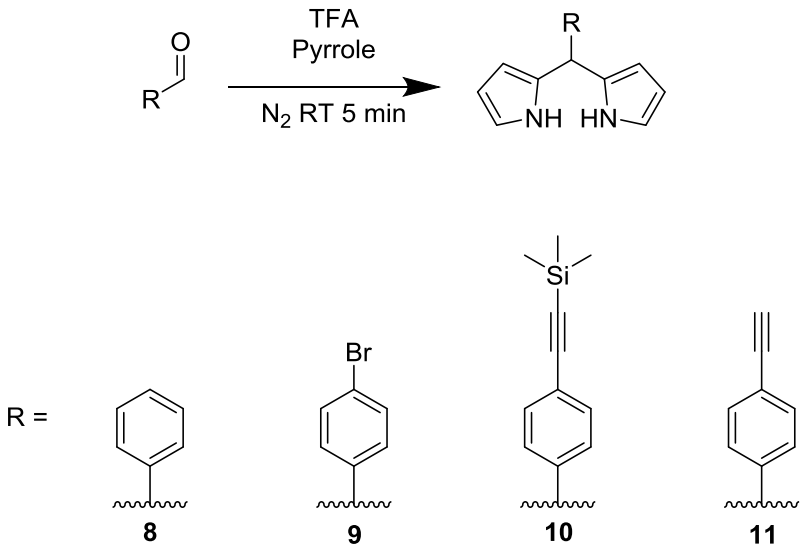


Scheme 2.6 Synthesis of S-2-pyridyl-4-(2-TMS-ethynyl)benzothioate.

The acid chloride required to make **7** directly was not commercially available so instead had to be synthesised *via* an intermediate. The route chosen was to do a Sonogashira coupling between **6** and TMS-acetylene as shown in scheme 2.6.[2] The reaction produced an orange product in 70% yield with spectroscopic data that is consistent with previous literature reports.[8]

Dipyrromethanes

The general one-pot procedure used for synthesising dipyrromethanes is shown below in scheme 2.7, though other step-wise syntheses have also been developed.[10] The reaction involves an aldehyde, pyrrole and a catalyst, in these instances, trifluoroacetic acid (TFA). Typically reactions are performed without any other solvents, instead using a large (40 - 100 fold) excess of pyrrole,[11] though alternative conditions have been developed where the reaction is performed in organic solvents[12] or water without using excess pyrrole.[13]



Scheme 2.7 General synthesis of dipyrromethanes.

Compounds **8**-**11** were chosen with the intention of creating a series of *meso*-substituted porphyrin molecules that would be suitable for Sonogashira coupling reactions. By having different combinations of protected alkyne, terminal alkyne, phenyl and halogen groups on different porphyrins it allows the directed construction of larger porphyrin oligomers *via* successive Sonogashira coupling and deprotection reactions.

Regardless of the synthetic route, pyrrole is an essential component in the reaction forming dipyrromethanes. In storage, pyrrole polymerises *via* a light catalysed reaction to

form polypyrrole which is easily identifiable by its brown appearance rather than being colourless. When pyrrole is used in reactions without removing the polypyrrole, undesirable by-products form so to remove the polypyrrole impurities, pyrrole was freshly distilled under reduced pressure before its use in a reaction.

Alternative catalysts can be used in the synthesis of dipyrromethanes instead of TFA such as acetic acid,[14] $InCl_3$[15] and $BF_3.Et_2O$.[16] To compare the effects of choice of catalyst on the reaction, TFA and $InCl_3$ were used as catalysts in the synthesis of **9.** The reaction that employed $InCl_3$ as the catalyst resulted in an almost identical yield to the corresponding synthesis involving TFA but it took a lot longer, 2 h verses 5 min. It was decided from this that subsequent reactions would be done using TFA as the catalyst. When $BF_3.Et_2O$ is used as the catalyst a significant amount of N-confused dipyrromethane (structure shown in figure 2.1) is produced alongside the desired product.[16] Although this can be removed by successive recrystallisations, the use of $BF_3.Et_2O$ as a catalyst has fallen out of fashion in favour of TFA which only produces trace amounts of N-confused dipyrromethane. Other impurities known to arise from TFA catalysed reactions are tripyrromethane and higher oligomer pyrromethane products.[17]

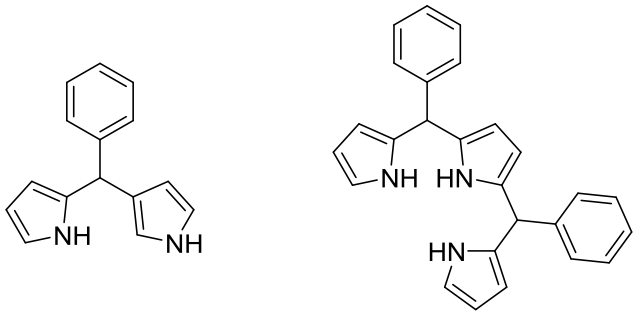
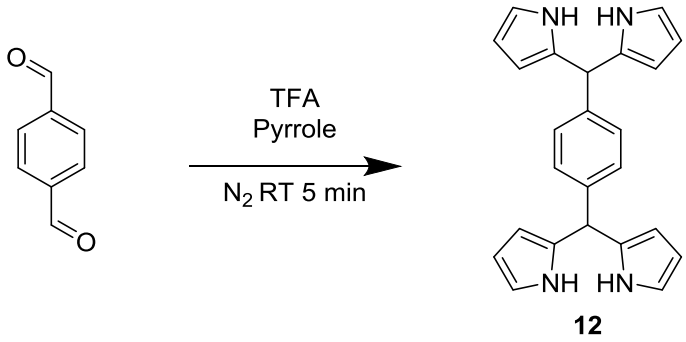


Figure 2.1 N-confused dipyrromethane (left) and tripyrrane (right).

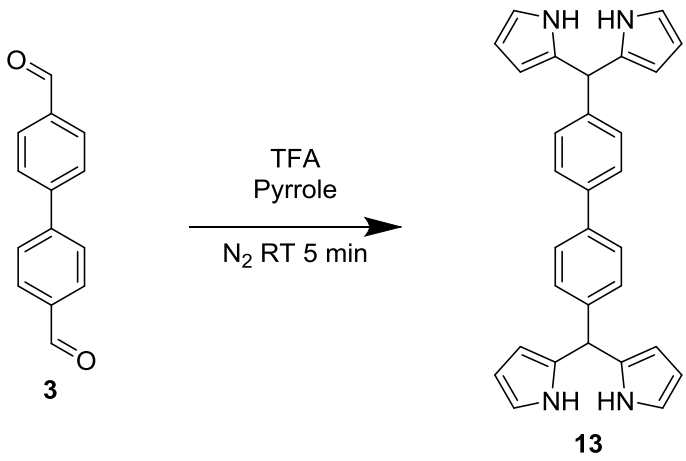
In each instance of dipyrromethanes **8-11**, we were able to isolate the desired dipyrromethane from these impurities by column chromatography. The dipyrromethane

was subsequently washed with hexanes as this was found to remove some soluble, unknown, coloured impurities.

The following dipyrromethanes were synthesised using the same conditions but result in molecules with two dipyrromethane units. These were synthesised with the intention of performing subsequent reactions that would form porphyrin dimers. Compound **12** has dipyrromethane groups at the 1- and 4- positions of a phenyl ring so that when the porphyrin dimer is formed, the porphyrin units themselves will be separated by a single phenyl unit (scheme 2.8).



Scheme 2.8 Synthesis of 1,4-bis(dipyrromethane)benzene.



Scheme 2.9 Synthesis of 4,4'-bis(dipyrromethane)biphenyl.

Compound **13** was designed as simple extension of **12** by another phenyl ring unit, keeping the dipyrromethane groups at the 1- and 4- positions and is synthesised from aldehyde **3** (scheme 2.9). The porphyrin dimer formed from **13** will have two phenyl groups to link the porphyrin units together. Compounds **12** and **13** both proceeded in slightly lower yields than compounds **8-11**. It is thought that this is due to two dipyrromethane units being required to form at once on the same molecule which increases the likelihood of forming oligomeric impurities.

Acylated Dipyrromethanes

A common method for synthesising porphyrins is to perform a condensation reaction between a dipyrromethane and a dicarbinol. Dicarbionols can be formed in a number of ways, one direct method is by performing a Friedel-Craft alkylation on the dipyrromethane.[18] Another common route is *via* a reduction of a diacylated dipyrromethane, the synthesis of a number of these (compounds **14**-**22**, figure 2.2) is described in the following pages.

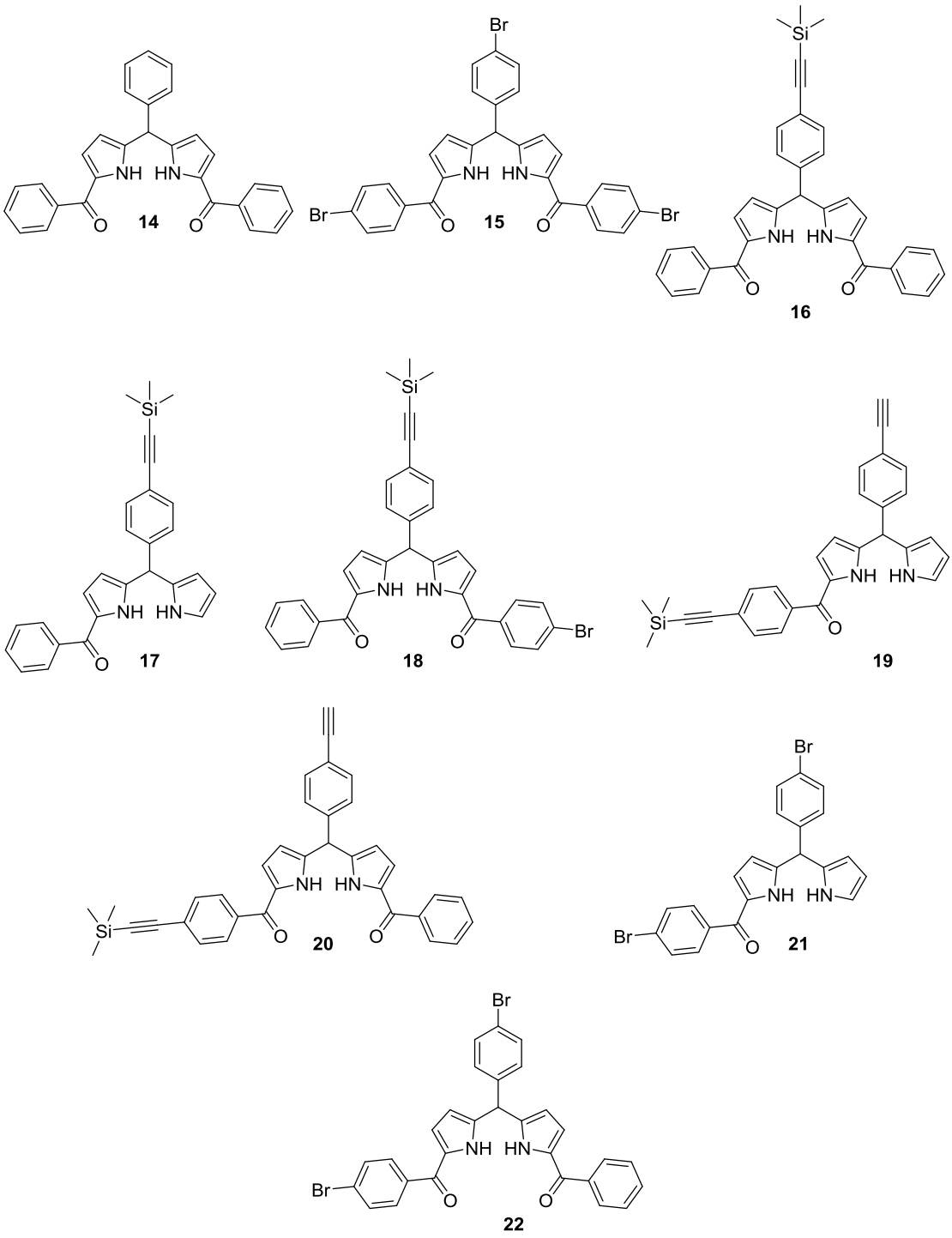
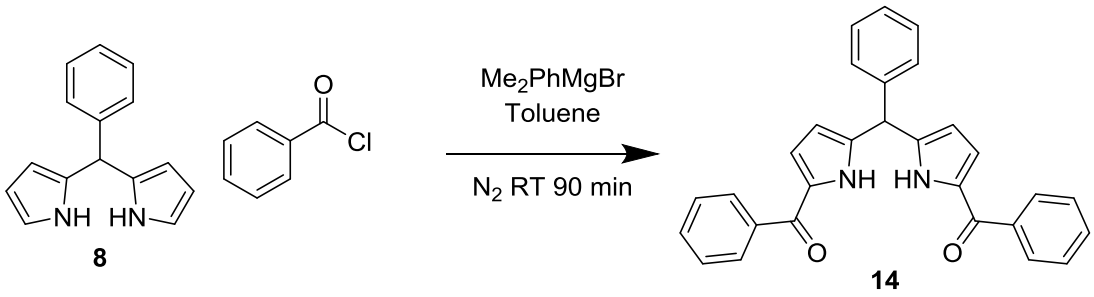


Figure 2.2 Chemical structures of the acylated dipyrromethanes 14-22 synthesised.

One problem often encountered in the synthesis of acylated dipyrromethanes is in the purification stage as often the compounds streak on column chromatography media. To help relieve this problem, a tin complexation strategy has been devised that helps to easily isolate 1,9-diacyldipyrromethanes, complexing exclusively with the diacylated

dipyrromethane and decomplexing readily when exposed to TFA.[19] Similarly, a boron complexation strategy that selectively complexes with the monoacylated dipyrromethane and decomplexes with TFA in good yields has also been created.[20]



Scheme 2.10 Synthesis of 1,9-bis(benzoyl)-5-phenyldipyrromethane.

Compounds **14**-**16** are all symmetrically substituted dipyrromethanes. The synthesis of **14** is shown in scheme 2.10, with compounds **15** and **16** being synthesised in a similar manner from diprromethanes **9** and **10** respectively. Compounds **14**-**16** were synthesised by reacting the suitable 5-substituted dipyrromethane with an acid chloride in the presence of a Grignard reagent. Addition of a Grignard reagent to the dipyrromethane forms a dipyrromethane-Grignard reagent. Electrophilic substitution occurs preferentially at the α- position of the pyrrole moiety upon addition of the acid chloride as three resonance structures are available to stabilize the intermediate, rather than two for the β-position. Compounds **14**-**16** were both produced in good-moderate yields, (75%, 67% and 60% respectively). Purification for these compounds was achieved by column chromatography using alumina as the stationary media. Alumina is available as both a basic or neutral medium whereas silica is acidic. Compounds that are unstable to acidic conditions are better purified using alumina.

During initial attempts to synthesise **15**, it was discovered that employing the sterically hindered Grignard reagent 2,6-dimethylphenylmagnesium bromide ($Me_2PhMgBr$) in the

acylation reactions resulted in higher yields (67%) than when using the less sterically hindered reagent EtMgBr (46%).[21] Also produced in this reaction are the products shown in figure 2.3. The hindered Grignard is less likely to form its undesired by-product from the reaction and this is the most likely reason for why the hindered Grignard gave better yields than the non-hindered Grignard. $Me_2PhMgBr$ was then chosen to be used in all subsequent Grignard reactions without prior screening of other Grignard reagents.

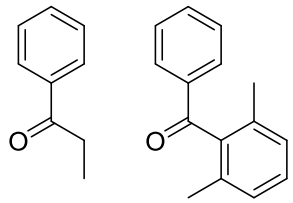
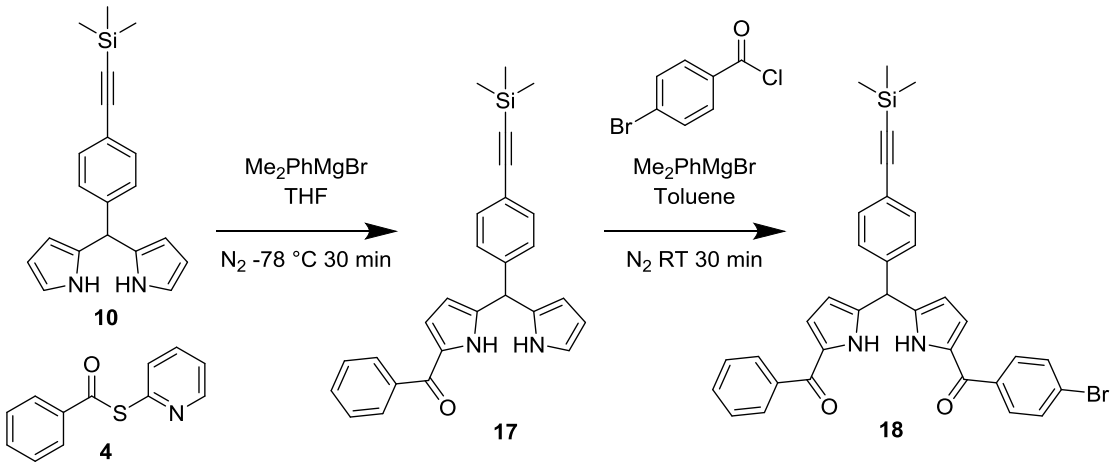


Figure 2.3 Primary undesired product in reactions employing EtMgBr (left) and $Me_2PhMgBr$ (right).

Another route to acylated dipyrromethanes is *via* a Vilsmeier-Haack reaction.[22] In an attempt to synthesise **15**, 4-(4-bromobenzoyl)morpholine was stirred in phosphoryl chloride under an atmosphere of N_2 and heated to 65 °C. After 3 h stirring, the mixture was allowed to cool and a solution of 5-(4-bromophenyl)dipyrromethane in anhydrous toluene was added. The mixture was heated to reflux and stirred for a further 2 h. A 50:50 mixture of EtOAc and NH_4Cl solution was added to quench the reaction, the organics were collected and washed with water, brine and then dried with anhydrous magnesium sulfate. The resulting mixture was filtered and the solvent removed under reduced pressure. Analysis showed that this reaction did not produce the desired product.

Barbero *et al.* first showed that 1,3-Benzoxathiolium salts can be used to synthesise diacyl pyrroles.[23] Their procedure has since been adapted for the synthesis of 1,9-diacyldipyrromethanes.[24]



Scheme 2.11 Synthesis of 1-(benzoyl)-5-(4-(2-TMS)ethynylphenyl)-9-(4-bromobenzoyl)dipyrromethane.

Compounds **17**, **19** and **21** are all monoacylated dipyrromethanes. When used with Grignard reagents and dipyrromethanes at reduced temperatures, pyridyl thioesters ensure that only one acylation reaction occurs, so that the monoacylated dipyrromethane is the major product. This is very useful in synthesising porphyrins with A_2B_2, A_2BC, and ABCD configurations and particularly useful for trans-A_2B_2 porphyrins as the monoacylated dipyrromethane can be reduced to form a dipyrromethane carbinol and then undergo a self-condensation reaction to form the desired product.

In the synthesis of **17** (scheme 2.11), dipyrromethane **11** was dissolved in thoroughly degassed THF and then cooled to -78 °C. Following this, a solution of pyridyl thioester **4** in THF was added in a single portion with vigorous stirring and the reaction vessel was allowed to gradually warm up to room temperature. The reaction was quenched with NH_4Cl solution and extracted with diethylether before solvents were removed. The residue was purified by column chromatography, using silica as the stationary medium to produce **17** as an amorphous grey solid in 83% yield.

18 was synthesised from **17** in another Grignard reaction. In this instance, a solution of **17** in toluene and a 4 mol equivalents solution of 4-bromobenzoyl chloride in toluene were

prepared separately. A 2 mol equivalent portion of Grignard reagent was added to **17** and after 5 min stirring approximately half of the 4-bromobenzoyl chloride solution was transferred. Additional amounts of Grignard reagent and 4-brombeznoyl chloride solution were added after 10 min stirring.

Compounds **19** and **21** were synthesised in a similar fashion to **17**, by reacting dipyrromethanes **11** and **9** with pyridyl thioesters **4** and **5** respectively. Compounds **20** and **22** were subsequently made from Grignard reactions involving the appropriate acid chloride and monoacylated dipyrromethane.

Conclusions

A variety of compounds designed to be used in the construction of larger porphyrin motifs have successfully been synthesised.

Aldehydes **1**-**3** have been converted into their respective dipyrromethanes **10**, **11**, and **13.** The reaction to form aldehyde **1** could reliably make multi-gram quantities at exceptionally high yields (>95%). Similarly, the reaction forming aldehyde **2** was sufficiently high yielding that synthesising it was much more economical than buying an otherwise commercial product. The reaction forming aldehyde **3** needs further optimisation to favour the production of the dicarbaldehyde product rather than the single aldehyde product.

The reactions forming the pyridyl thioesters in general gave good yields (59% - 81%) and with the exception of **7**, produced a crystalline product after work-up that did not need further purification.

Dipyrromethanes **8**-**13** have been synthesised in multi-gram quantities from relatively cheap starting materials in excellent (93% for **11)** to moderate (47% for **13**) yields. Whilst performing column chromatography, the dipyrromethane compounds would decompose slightly in solution. Washing the columned product with hexanes to remove traces of impurity was essential to ensure long-term stability of the product. Once purified, these dipyrromethane compounds were found to be stable for several months when stored at -20 °C. Dipyrromethanes **8**-**11** have been substituted as deemed appropriate *via* Grignard reactions so that the entire range of porphyrins required in later chapters can be made from a combination of these and their unsubstituted counterparts.

Dipyrromethanes **12** and **13** have been designed with two dipyrromethane units each; ready to be used as the linking moieties in the synthesis of porphyrin dimers explored in greater detail in chapter 4.

Experimental

4-TMS-ethynylbenzaldehyde (1)

4-Bromobenzaldehyde (4.00 g, 21.6 mmol), CuI (82 mg, 0.861 mmol) and $Pd(PPh_3)_2Cl_2$ (210 mg, 0.598 mmol) were placed in a flask purged with N_2. A solution of THF (30 mL) and NEt_3 (6.60 mL) was degassed by bubbling with N_2 for 10 min. A solution of TMS-acetylene (9.60 mL, 67.9 mmol) was prepared in THF (10 mL) and was slowly added to the mixture *via* syringe pump over 2 h. upon initial addition of the TMS-acetylene solution, the mixture was heated to 60 °C. The mixture was stirred at 60 °C for 24 h before being left to cool. The room temperature mixture was passed through kieselguhr with washings of hexane. The solvent was removed *in vacuo*, the residue dissolved in a minimum amount of hexane and passed through a silica plug using hexane as an eluent until the washings became colourless. Hexane was removed *in vacuo* to give the nearly pure title compound. Any remaining impurity was removed *via* sublimation to give the title compound as a light brown solid. (4.29 g, 21.2 mmol, 98%).

^{1}H NMR (400 MHz, $CDCl_3$): δ = 10.01 (s, 1 H), 7.82 (d, J = 8.35 Hz, 2 H), 7.61 (d, J = 8.35 Hz, 2 H), 0.28 (s, 9 H) ppm. ^{13}C NMR (101 MHz, $CDCl_3$): δ = 191.40, 135.57, 132.46, 129.42, 129.33, 103.81, 99.01, -0.23 ppm. MS: (EI) m/z calculated for $[C_{12}H_{14}OSi]^+$: 202.08084 Found: 202.08185. Elemental analysis calculated for $C_{12}H_{14}OSi.0.5H_2O$: C, 68.20; H, 7.15; N, 0.00. Found: C, 68.53; H, 7.61; N, 0.00.

4-Ethynylbenzaldehyde (2)

4-TMS-ethynylbenzaldehyde (2.00 g, 9.88 mmol) was dissolved into a solution of methanol (40 mL) and DCM (4 mL). Potassium carbonate (125 mg, 0.904 mmol) was added and the mixture was stirred at RT for 2 h. DCM (50 mL) was added and the mixture was washed with aqueous HCl (2 M, 100 mL), water (100 mL), brine (100 mL)

and the organic phase dried over anhydrous magnesium sulfate. This was then filtered and the solvent was removed *in vacuo*. The residue was subjected to column chromatography (silica, 1:1 hexane/DCM) to give the title compound as a pale yellow crystalline solid (1.02 g, 7.84 mmol, 79%).

^{1}H NMR (400 MHz, $CDCl_3$): δ = 10.03 (s, 1 H), 7.85 (d, J = 8.41 Hz, 2 H), 7.65 (d, J = 8.41 Hz, 2 H), 3.30 (s, 1 H) ppm. ^{13}C NMR (101 MHz, $CDCl_3$): δ = 191.37, 135.93, 132.69, 129.47, 128.29, 82.60, 81.03 ppm. MS (EI) *m/z* calculated for $[C_9H_6O]^+$: 130.04132. Found: 130.04118. Elemental analysis calculated for C_9H_6O: C, 83.06; H, 4.65; N, 0.00. Found: C, 80.82; H, 4.54; N, 0.00.

4,4'-Dicarbaldehydebiphenyl (3)

4,4'-Dibromobiphenyl (10.0 g, 32.1 mmol) was stirred in anhydrous THF (100 mL) at -78 °C to form a solution. n-Butyllithium (2.5 M in hexanes, 16.4 mL, 41 mmol) was added dropwise to the solution, upon completion of addition, DMF (20 mL) was added and the mixture was stirred for 15 min at -78 °C after which, the mixture was stirred for a further 2 h being allowed to warm up gradually to 0 °C. Water (100 mL) was added to the mixture. The organics were collected and washed with water (100 mL), brine (100 mL) and then dried with anhydrous magnesium sulfate. The resulting mixture was filtered and the solvent removed *in vacuo*. After column chromatography (silica, 1:1, hexane/DCM) the target compound was collected as pale yellow crystalline solid (1.10 g, 5.23 mmol, 16%).

^{1}H NMR (400 MHz, $CDCl_3$): δ = 10.12 (s, 2 H), 8.03 (d, J = 8.35 Hz, 4 H), 7.83 (d, J = 8.35 Hz, 4 H) ppm. ^{13}C NMR (101 MHz, $CDCl_3$): δ = 191.71, 145.52, 135.94, 130.34, 128.01 ppm. MS: (ESI) *m/z* calculated for $[C_{14}H_{10}O_2 + H]^+$: 211.0754 Found: 211.0764.

S-2-pyridyl-benzothioate (4)

A solution of benzoyl chloride (5.80 mL, 50.0 mmol) in DCM (100 mL) was prepared and transferred over slowly to a stirred solution of 2-mercaptopyridine (5.56 g, 50.0 mmol) in DCM (250 mL) at RT. Upon completion of addition, the solution was allowed to stir for a further 1 h, after which point sodium hydroxide solution (1 M, 200 mL) was added. The layers were separated, the aqueous phase extracted with DCM and the organic layers combined. This was then dried over anhydrous magnesium sulfate, filtered and the solvents removed *in vacuo* to give a yellow oil. The oil was left to crystallise overnight at RT to produce large, colourless crystals which were collected and washed with a small amount of cold toluene (6.30 g, 29.3 mmol, 59%).

^{1}H NMR (400 MHz, $CDCl_3$): δ = 8.69 (ddd, J = 4.86, 1.89, 0.88 Hz, 1 H), 8.00 - 8.06 (m, 2 H), 7.80 (ddd, J = 7.80, 7.40, 1.89 Hz, 1 H), 7.74 (ddd, J = 7.80, 1.32, 0.88 Hz, 1 H), 7.60 - 7.66 (m, 1 H), 7.47 - 7.55 (m, 2 H), 7.35 (ddd, J = 7.40, 4.86, 1.32 Hz, 1 H) ppm. ^{13}C NMR (101 MHz, $CDCl_3$): δ = 189.36, 151.31, 150.53, 137.17, 136.53, 133.90, 130.86, 128.81, 127.56, 123.64 ppm. MS: (ESI) *m/z* calculated for $[C_{12}H_9NOS + Na]^+$: 238.0297. Found: 238.0310. Elemental analysis calculated for $C_{12}H_9NOS$: C, 66.95; H, 4.21; N, 6.51. Found: C, 66.87; H, 4.36; N, 6.48.

S-2-Pyridyl-4-bromobenzothioate (5)

A solution of 4-bromobenzoyl chloride (6.60 g, 30.1 mmol) in THF (50 mL) was prepared and transferred *via* pipette to a stirred solution of 2-mercaptopyridine (3.35 g, 30.1 mmol) in THF (50 mL). Upon completion of addition, the solution was allowed to stir for a further 1 h. The white precipitate was collected and washed with hexanes (200 mL). The precipitate was added to a stirred, biphasic solution of diethyl ether (100 mL) and saturated sodium hydrogen carbonate (100 mL). The layers were separated and the aqueous layer was extracted with diethyl ether. The organic phases were

combined, dried over anhydrous magnesium sulfate, filtered and the solvent removed *in vacuo* to give the title compound as small white needles (7.17 g, 24.4 mmol, 81%).

^{1}H NMR (400 MHz, $CDCl_3$): δ = 8.69 (ddd, J = 4.86, 1.94, 0.88 Hz, 1 H), 7.87 - 7.91 (m, 2 H), 7.81 (ddd, J = 7.83, 7.47, 1.94 Hz, 1 H), 7.73 (ddd, J = 7.83, 1.18, 0.88 Hz, 1 H), 7.63 - 7.67 (m, 2 H), 7.36 (ddd, J = 7.47, 4.86, 1.18 Hz, 1 H) ppm. ^{13}C NMR (101 MHz, $CDCl_3$): δ = 188.46, 150.83, 150.61, 137.26, 135.31, 132.15, 130.83, 129.05, 128.97, 123.81 ppm. MS: (ESI) *m/z* calculated for $[C_{12}H_8NOSBr + H]^+$: 293.9583. Found: 293.9586. Elemental analysis calculated for $C_{12}H_8BrNOS$: C, 49.00; H, 2.74; N, 4.76. Found: C, 48.92; H, 2.73; N, 4.89.

S-2-Pyridyl-4-iodobenzothioate (6)

A solution of 4-iodobenzoyl chloride (6.65 g, 25.0 mmol) in THF (50 mL) was prepared and transferred *via* pipette to a stirred solution of 2-mercaptopyridine (2.78 g, 25.0 mmol) in THF (50 mL). Upon completion of addition, the solution was allowed to stir for a further 1 h. The white precipitate was collected and washed with hexanes (200 mL). The precipitate was added to a stirred, biphasic solution of diethyl ether (100 mL) and saturated sodium hydrogen carbonate (100 mL). The layers were separated and the aqueous layer was extracted with diethyl ether. The organic phases were combined, dried over anhydrous magnesium sulfate, filtered and the solvent removed *in vacuo* to give the title compound as small white needles (6.82 g, 20.0 mmol, 80%).

^{1}H NMR (400 MHz, $CDCl_3$): δ = 8.69 (ddd, J = 4.86, 1.88, 0.88 Hz, 1 H), 7.84 - 7.89 (m, 2 H), 7.80 (ddd, J = 7.80, 7.47, 1.88 Hz, 1 H), 7.68 - 7.76 (m, 3 H), 7.36 (ddd, J = 7.47, 4.86, 1.13 Hz, 1 H) ppm. ^{13}C NMR (101 MHz, $CDCl_3$): δ = 188.81, 150.86, 150.65, 138.17, 137.29, 135.92, 130.87, 128.85, 123.84, 101.86 ppm. MS: (ESI) *m/z* calculated for $[C_{12}H_8NOSI + H]^+$: 341.9444. Found: 341.9452. Elemental analysis calculated for $C_{12}H_8INOS.0.5H_2O$: C, 41.16; H, 2.59; N, 4.00; Found: C, 40.77; H, 2.19; N, 4.45.

S-2-Pyridyl-4-(2-TMS-ethynyl)benzothioate (7)

Pyridyl thioester **6** (3.41 g, 10.0 mmol), $Pd_2(dba)_3$ (153 mg, 0.167 mmol), CuI (190 mg, 1.00 mmol) and PPh_3 (350 mg, 1.33 mmol) were placed in a schlenk flask. A degassed mixture of THF (15 mL) and trimethylamine (7 mL) was added and the mixture was allowed to stir. To this mixture, TMS-acetylene (1.42 mL, 10.0 mmol) in degassed THF (5 mL) was added over 10 min. The reaction mixture was heated to 50 °C and stirred for 20 h. This was then allowed to cool, filtered and the solvents removed *in vacuo*. The residue was subjected to column chromatography (silica, 4:1, hexane/ethyl acetate) to produce the title compound as an orange solid (2.185 g, 7.02 mmol, 70%).

^{1}H NMR (400 MHz, $CDCl_3$): δ = 8.69 (ddd, J = 4.86, 1.88, 0.88 Hz, 1 H), 7.93 - 7.98 (m, 2 H), 7.80 (ddd, J = 7.80, 7.47, 1.88 Hz, 1 H), 7.73 (ddd, J = 7.80, 1.25, 0.88 Hz, 1 H), 7.54 - 7.59 (m, 2 H), 7.35 (ddd, J = 7.47, 4.86, 1.25 Hz, 1 H), 0.28 (s, 9 H) ppm. ^{13}C NMR (101 MHz, $CDCl_3$): 188.58, 151.06, 150.58, 137.22, 135.77, 132.25, 130.85, 128.84, 127.37, 123.73, 103.73, 98.80, -0.22 ppm. MS: (ESI) *m/z* calculated for $[C_{17}H_{17}NOSSi + H]^+$: 312.0873. Found: 312.0885.

5-Phenyldipyrromethane (8)

Benzaldehyde (3.37 mL, 33.0 mmol) was stirred in pyrrole (200 mL) at RT under nitrogen. After 10 min TFA (200 μL, 2.61 mmol) was added. After 5 min, sodium hydroxide (2.00 g, 50.0 mmol) was added. After a further 5 min the reaction mixture was filtered and the solvent removed *in vacuo*. The resulting brown solid was purified by column chromatography (silica, 1:1, chloroform/hexane) to give the title compound as a beige solid which was washed with hexanes to give the title compound as an off-white solid (4.20 g, 18.9 mmol, 57%).

^{1}H NMR (400 MHz, $CDCl_3$): δ = 7.90 (br, s, 2 H), 7.28 - 7.34 (m, 2 H), 7.19 - 7.26 (m, 3 H), 6.64 - 6.72 (m, 2 H), 6.16 (m, 2 H), 5.91 (m, 2 H), 5.46 (s, 1 H) ppm. ^{13}C NMR

(101 MHz, $CDCl_3$): δ = 142.06, 132.46, 128.62, 128.37, 126.95, 117.19, 108.41, 107.20, 43.96 ppm. MS: (ESI) *m/z* calculated for $[C_{15}H_{14}N_2]^+$: 222.1157. Found: 222.1069. Elemental analysis calculated for $C_{15}H_{14}N_2$: C, 81.05; H, 6.35; N, 12.60. Found: C, 80.92; H, 6.45; N, 12.48.

5-(4-Bromophenyl)dipyrromethane (9)

4-bromobenzaldehyde (2.50 g, 13.5 mmol) was stirred in pyrrole (100 mL) at RT under nitrogen. After 10 min, TFA (100 μL, 1.31 mmol) was added. After 5 min, sodium hydroxide (2.00 g, 50.0 mmol) was added. After a further 5 min the reaction mixture was filtered and the solvent removed *in vacuo*. The resulting brown solid was purified by column chromatography (silica, 3:1, DCM/hexane) to give a pale yellow solid which was washed with hexanes to give the title compound as an off-white solid (3.17 g, 10.5 mmol, 78 %).

^{1}H NMR (400 MHz, $CDCl_3$): δ = 7.92 (br, s, 2 H), 7.39 - 7.50 (m, 2 H), 7.04 - 7.15 (m, 2 H), 6.71 (ddd, J = 2.60, 1.60 Hz, 2 H), 6.18 (m, 2 H), 5.86 - 5.95 (m, 2 H), 5.44 (s, 1 H) ppm. ^{13}C NMR (101 MHz, $CDCl_3$): δ = 141.15, 131.82, 131.66, 130.09, 120.81, 117.47, 108.53, 107.39, 43.40 ppm. MS: (ESI) *m/z* calculated for $[C_{15}H_{13}BrN_2 + Na]^+$: 323.0160. Found: 323.0146. Elemental analysis calculated for $C_{15}H_{13}BrN_2$: C, 59.82; H, 4.35; N, 9.30. Found: C, 59.87; H, 4.36; N, 9.29.

5-(4-(2-TMS-ethynyl)phenyl)dipyrromethane (10)

Aldehyde **1** (4.00 g, 19.8 mmol) was stirred in pyrrole (200 mL) at RT under nitrogen. After 10 min TFA (0.20 mL, 2.61 mmol) was added. After 5 min sodium hydroxide (2.00 g, 50.0 mmol) was added. After a further 5 min the reaction mixture was filtered and the solvent removed *in vacuo*. The resulting brown solid was purified by column chromatography (silica, 2:1, DCM/hexane). The solvent was removed to give a pale

yellow crystalline solid which was washed with hexane to give an off-white crystalline solid (5.39 g, 16.9 mmol, 85%).

^{1}H NMR (400 MHz, $CDCl_3$): δ = 7.91 (br, s, 2 H), 7.39 - 7.45 (m, 2 H), 7.16 (d, J = 8.16 Hz, 2 H), 6.71 (m, 2 H), 6.17 (m, 2 H), 5.87 - 5.92 (m, 2 H), 5.47 (s, 1 H), 0.26 (s, 9 H) ppm. ^{13}C NMR (101 MHz, $CDCl_3$): δ = 142.48, 132.20, 131.88, 128.28, 121.77, 117.38, 108.49, 107.36, 104.78, 94.25, 43.80, -0.09 ppm. MS: (ESI) *m/z* calculated for $[C_{20}H_{22}N_2Si + H]^+$: 319.1625. Found: 319.1616. Elemental analysis calculated for $C_{20}H_{22}N_2Si.0.5H_2O$: C, 73.35; H, 7.08; N, 8.55. Found: C, 73.83; H, 7.14; N, 8.81.

5-(4-Ethynylphenyl)dipyrromethane (11)

Aldehyde **2** (500 mg, 3.84 mmol) was stirred in pyrrole (25 mL) at RT under nitrogen. After 10 min TFA (31 μL, 0.405 mmol) was added. After 5 min sodium hydroxide (400 mg, 10.0 mmol) was added. After a further 5 min the reaction mixture was filtered and the solvent removed *in vacuo*. The resulting brown solid was purified by column chromatography (silica, 1:1, DCM/hexane). The solvent was removed to give a pale yellow crystalline solid which was washed with hexane to give the title compound as an off-white crystalline solid (877 mg, 3.56 mmol, 93%).

^{1}H NMR (400 MHz, $CDCl_3$): δ = 7.95 (br, s, 2 H), 7.47 (d, J = 8.16 Hz, 2 H), 7.18 (d, J = 8.16 Hz, 2 H), 6.71 (d, J = 1.51 Hz, 2 H), 6.17 - 6.22 (m, 2 H), 5.91 (br, s, 2 H), 5.47 (s, 1 H), 3.08 (s, 1 H) ppm. ^{13}C NMR (101 MHz, $CDCl_3$): δ = 142.97, 132.43, 131.88, 128.43, 120.76, 117.49, 108.57, 107.46, 83.45, 77.25, 43.86 ppm. MS: (ESI) *m/z* calculated for $[C_{17}H_{14}N_2 + H]^+$: 247.1230. Found: 247.1232. Elemental analysis calculated for $C_{17}H_{14}N_2$: C, 82.90; H, 5.73; N, 11.37. Found: C, 82.91; H, 5.81; N, 11.24.

1,4-Bis(dipyrromethane)benzene (12)

Terephthalaldehyde (1.50 g, 11.2 mmol) was stirred in pyrrole (100 mL) at RT under nitrogen. TFA (100 μL, 1.31 mmol) was added and the reaction was allowed to stir for a further 5 min. Sodium hydroxide (2.00 g, 50.0 mmol) was added, the reaction mixture was filtered and the solvent removed *in vacuo*. The resulting yellow solid was purified by column chromatography (silica, DCM) to give an off white solid (2.05 g, 6.09 mmol, 52%). ^{1}H NMR (400 MHz, CD_3CN): δ = 8.91 (br, s, 4 H), 7.15 (s, 4 H), 6.63 (m, 4 H), 6.00 (m, 4 H), 5.77 (dddd, J = 3.28, 2.49, 1.69, 0.69 Hz, 4 H), 5.39 (s, 2 H) ppm. ^{13}C NMR (101 MHz, CD_3CN): δ = 142.93, 134.45, 129.46, 118.33, 108.79, 107.66, 44.73 ppm. MS: (ESI) *m/z* calculated for $[C_{24}H_{22}N_4 + H]^+$: 367.1918. Found: 367.1917. Elemental analysis calculated for $C_{24}H_{22}N_4.0.5H_2O$: C, 76.77; H, 6.17; N, 14.92. Found: C, 76.92; H, 6.48; N, 15.11.

4,4'-Bis(dipyrromethane)biphenyl (13)

Aldehyde **3** (500 mg, 2.38 mmol) was stirred in 100 mL freshly distilled pyrrole under an inert atmosphere. After 10 min, TFA (250 μL, 3.26 mmol) was added. After 5 min, sodium hydroxide (2.00 g, 50.0 mmol) was added. After a further 5 min the reaction mixture was filtered and the solvent removed *in vacuo*. The resulting brown solid was purified by column chromatography (silica, DCM) followed by a recrystallisation in DCM/hexane to give the title compound as a light brown solid (492 mg, 1.11 mmol, 47%).

^{1}H NMR (400 MHz, CD_3CN): δ = 8.98 (br, s, 4 H), 7.56 (d, J = 8.29 Hz, 4 H), 7.27 (d, J = 8.29 Hz, 4 H), 6.65 (m, 4 H), 6.02 (m, 4 H), 5.80 (m, 4 H), 5.46 (s, 2 H) ppm. ^{13}C NMR (101 MHz, CD_3CN): δ = 143.87, 139.91, 134.20, 129.88, 127.91, 118.31, 108.66, 107.57, 44.57 ppm. MS: (ESI) *m/z* calculated for $[C_{30}H_{26}N_4 + H]^+$: 443.2230. Found: 443.2234.

Elemental analysis calculated for $C_{30}H_{26}N_4$: C, 81.42; H, 5.92; N, 12.66. Found: C, 81.32; H, 5.95; N, 12.57.

1,9-Bis(benzoyl)-5-phenyldipyrromethane (14)

Dipyrromethane **8** (4.20 g, 18.9 mmol) was dissolved in anhydrous toluene (200 mL) and placed under an inert atmosphere. $Me_2PhMgBr$ (1 M in THF, 94.5 mL, 94.5 mmol) was added and the reaction was stirred at RT for 90 min. A solution of benzoyl chloride (11.0 mL, 94.7 mmol) in toluene (100 mL) was added dropwise and the reaction mixture was stirred for a further 90 min after which, a 1:1 mixture of saturated aqueous NH_4Cl solution and ethyl acetate was added to the reaction solution. The organics were collected and washed with water (100 mL), brine (100 mL) and then dried over anhydrous magnesium sulfate. The resulting mixture was filtered and the solvent removed *in vacuo*. The resulting red solid was purified using column chromatography (alumina, DCM) to produce a light pink solid (6.08 g, 14.1 mmol, 75%).

^{1}H NMR (400 MHz, $CDCl_3$): δ = 11.22 (br, s, 2 H), 7.75 - 7.85 (m, 4 H), 7.47 - 7.56 (m, 4 H), 7.37 - 7.47 (m, 6 H), 7.34 (s, 1 H), 6.62 (dd, J = 3.76, 2.51 Hz, 2 H), 5.97 - 6.04 (m, 2 H), 5.70 (s, 1 H) ppm. ^{13}C NMR (101 MHz, $CDCl_3$): δ = 184.52, 140.65, 140.05, 138.23, 131.65, 131.02, 129.43, 128.94, 128.75, 128.05, 127.56, 120.72, 111.17, 44.90 ppm. MS: (ESI) *m/z* calculated for $[C_{29}H_{22}N_2O_2 + H]^+$: 431.1767. Found: 431.1754. Elemental analysis calculated for $C_{29}H_{22}N_2O_2.0.5H_2O$ C, 79.25; H, 5.27; N, 6.37. Found: C, 79.13, H, 5.26, N, 6.19.

1,9-Bis(4-bromobenzoyl)-5-(4-bromophenyl)dipyrromethane (15)

Dipyrromethane **9** (4.00 g, 16.9 mmol) was dissolved in anhydrous toluene (200 mL) and placed under an inert atmosphere. $Me_2PhMgBr$ (1 M in THF, 83.1 mL, 83.1 mmol) was added and the reaction was stirred at RT for 45 min. A solution of 4-bromobenzoyl

chloride (14.6 g, 66.5 mmol) in toluene (50 mL) and THF (50 mL) was added dropwise and the reaction mixture was stirred for a further 30 min after which, a 1:1 mixture of saturated aqueous NH_4Cl solution and ethyl acetate was added to the reaction solution. The organics were collected and washed with water (100 mL), brine (100 mL) and then dried over anhydrous magnesium sulfate. The resulting mixture was filtered and the solvent removed *in vacuo*. The resulting solid was purified using column chromatography (alumina, 7:2:1, hexane/DCM/ethyl acetate) to produce a light pink solid (7.47g, 11.2 mmol, 67%)

^{1}H NMR (400 MHz, $(CD_3)_2CO$): δ = 11.34 (br, s, 2 H), 7.76 - 7.82 (m, 4 H), 7.66 - 7.72 (m, 4 H), 7.51 - 7.56 (m, 2 H), 7.28 - 7.33 (m, 2 H), 6.81 (dd, J = 3.89, 2.38 Hz, 2 H), 6.07 (dd, J = 3.64, 2.38 Hz, 2 H), 5.92 (s, 1 H) ppm. ^{13}C NMR (101 MHz, $(CD_3)_2CO$): δ = 183.78, 142.13, 141.83, 139.11, 132.98, 132.91, 132.17, 132.08, 132.05, 127.10, 121.99, 121.01, 111.91, 44.68 ppm. MS: (ESI) *m/z* calculated for $[C_{29}H_{19}Br_3N_2O_2 - H]^-$: 662.8924. Found: 662.8925.

1,9-Bis(benzoyl)-5-(4-(2-(TMS)-ethynyl)phenyl)dipyrromethane (16)

Dipyrromethane **10** (800 mg, 2.52 mmol) was dissolved in toluene (20 mL). In a separate flask, a solution of benzoyl chloride (1.46 mL, 12.57 mmol) in toluene (20 mL) was prepared. $Me_2PhMgBr$ (1 M in THF, 6.3 mL, 6.3 mmol) followed by approximately half volume of the benzoyl chloride solution was added to the flask containing the dipyrromethane, which was then allowed to stir for 10 min. After this time, the reaction mixture was treated with a further addition of $Me_2PhMgBr$ (1 M in THF, 6.3 mL, 6.3 mmol) and the remaining benzoyl chloride solution. After an additional 20 min stirring, the mixture was quenched with saturated aqueous NH_4Cl solution (100 mL). The mixture was extracted with diethyl ether, the organic layers were combined, washed with water, brine, dried over anhydrous magnesium sulfate and filtered. Solvents were

removed *in vacuo* and the residue was subjected to column chromatography (alumina, 25:1, DCM:ethyl acetate) to produce the title compound as a dark green solid (800 mg, 1.52 mmol, 60%).

^{1}H NMR (400 MHz, $CDCl_3$): δ = 11.53 (br, s, 2 H), 7.73 - 7.79 (m, 4 H), 7.46 - 7.54 (m, 6 H), 7.38 - 7.44 (m, 4 H), 6.56 (dd, J = 3.89, 2.38 Hz, 2 H), 5.94 - 5.98 (m, 2 H), 5.69 (s, 1 H), 0.27 (s, 9 H) ppm. ^{13}C NMR (101 MHz, $CDCl_3$): δ = 184.56, 140.72, 140.40, 138.09, 132.46, 131.68, 131.08, 129.56, 128.74, 128.01, 122.28, 120.85, 111.28, 104.77, 94.57, 44.85, -0.04 ppm. MS: (ESI) *m/z* calculated for $[C_{34}H_{30}N_2O_2Si + H]^+$: 527.2149. Found: 527.2149. Elemental analysis calculated for $C_{34}H_{30}N_2O_2Si$: C, 77.53; H, 5.74; N, 5.32. Found: C, 77.64; H, 5.81; N, 5.31.

1-(Benzoyl)-5-(4-(2-TMS)ethynylphenyl)dipyrromethane (17)

Dipyrromethane **10** (2.00 g, 6.28 mmol) was dissolved in THF (10 mL) and $Me_2PhMgBr$ (1 M in THF, 16 mL, 16 mmol) was added to this. After stirring for 10 min, the solution was cooled to -78 °C and a solution of pyridyl thioester **4** (1.36 g, 6.32 mmol) in THF (10 mL) was added. The reaction mixture was allowed to gradually warm up to room temperature, and after a further 30 min of stirring, the mixture was quenched with saturated aqueous NH_4Cl solution. The mixture was extracted with diethyl ether, the organic layers were combined, washed with water, brine, dried over anhydrous magnesium sulfate and filtered. Solvents were removed *in vacuo* and the residue was subjected to column chromatography (silica, DCM) to afford an amorphous grey solid (2.21 g, 5.23 mmol, 83%).

^{1}H NMR (400 MHz, $CDCl_3$): δ = 9.73 (br, s, 1 H), 8.19 (br, s, 1 H), 7.79 - 7.85 (m, 2 H), 7.53 - 7.58 (m, 1 H), 7.38 - 7.50 (m, 4 H), 7.15 (d, J = 8.03 Hz, 2 H), 6.82 (dd, J = 3.76, 2.51 Hz, 1 H), 6.71 (m, 1 H), 6.17 (m, 1 H), 6.04 - 6.08 (m, 1 H), 5.97 (m, 1 H), 5.55 (s, 1 H), 0.26 (s, 9 H) ppm. ^{13}C NMR (101 MHz, $CDCl_3$): δ = 184.65, 141.13, 141.01, 138.26,

132.32, 131.77, 130.76, 130.32, 128.89, 128.28, 128.22, 122.17, 120.78, 118.01, 110.70, 108.56, 107.98, 104.64, 94.57, 43.98, -0.06 ppm. MS: (ESI) *m/z* calculated for $[C_{27}H_{26}N_2OSi + H]^+$: 423.1887. Found: 423.1890. Elemental analysis calculated for $C_{27}H_{26}N_2OSi$: C, 76.74; H, 6.20; N, 6.63; Found: C, 76.73; H, 6.24; N, 6.76.

1-(Benzoyl)-5-(4-(2-TMS)ethynylphenyl)-9-(4-bromobenzoyl)dipyrromethane (18)

Dipyrromethane **17** (1.00 g, 2.37 mmol) was dissolved in degassed toluene (15 mL). $Me_2PhMgBr$ (1 M in THF 5.00 mL, 5.00 mmol) was added at RT and the solution was stirred for 5 min. A solution of 4-bromobenzoyl chloride (2.08 g, 9.48 mmol) in THF (15 mL) was prepared and half was transferred to the reaction flask. After stirring for 10 min, a further addition of Grignard reagent (5.00 mL, 5.00 mmol) and the remaining 4-bromobenzoyl solution was performed. The reaction was quenched after 20 min with saturated aqueous NH_4Cl solution (100 mL). The mixture was extracted with ethyl acetate, the organic layers were combined, washed with water, brine, dried over anhydrous magnesium sulfate and filtered. Solvents were removed *in vacuo* and the residue was subjected to column chromatography (silica, 20:1, DCM/ethyl acetate) to afford the title compound as a light brown solid (1.27 g, 2.10 mmol, 89%).

^{1}H NMR (400 MHz, $(CD_3)_2CO$): δ = 11.30 (br, s, 1 H), 11.24 (br, s, 1 H), 7.85 (m, 2 H), 7.80 (m, 2 H), 7.71 (m, 2 H), 7.59 (m, 1 H), 7.48 (m, 4 H), 7.35 (d, J = 8.18 Hz, 2 H), 6.82 (dd, J = 3.87, 2.41 Hz, 1 H), 6.79 (dd, J = 3.80, 2.34 Hz, 1 H), 6.06 (ddd, J = 6.21, 3.65, 2.41 Hz, 2 H), 5.94 (s, 1 H), 0.23 (s, 9 H) ppm. ^{13}C NMR (101 MHz, $(CD_3)_2CO$): δ = 184.52, 183.27, 142.80, 141.78, 141.18, 139.77, 138.74, 132.88, 132.49, 132.46, 132.02, 131.67, 131.58, 129.69, 129.66, 129.24, 126.58, 122.83, 120.47, 120.21, 111.41, 111.21, 105.85, 94.71, 44.57, 0.07 ppm. MS: (ESI) *m/z* calculated for $[C_{34}H_{29}N_2O_2BrSi - H]^-$: 603.1149. Found: 603.1130. Elemental analysis calculated for $C_{34}H_{29}N_2O_2BrSi$: C, 67.43; H, 4.83; N, 4.63; Found: C, 67.35; H, 4.91; N, 4.75.

1-(4-(2-(TMS)-ethynyl)benzoyl)- 5-(4-ethynylphenyl)dipyrromethane (19)

Dipyrromethane **11** (1.00 g, 4.06 mmol) was dissolved in THF (10 mL) and $Me_2PhMgBr$ (1 M in THF, 10.0 mL, 10.0 mmol) was added to this. After stirring for 10 min, the solution was cooled to -78 °C and a solution of pyridyl thioester **7** (1.26 g, 4.05 mmol) in THF (10 mL) was added. The reaction mixture was allowed to gradually warm up to room temperature, and after a further 30 min of stirring, the mixture was quenched with saturated aqueous NH_4Cl solution (50 mL). The mixture was extracted with diethyl ether, the organic layers were combined, washed with water (100 mL), brine (100 mL), dried over anhydrous magnesium sulfate and filtered. Solvents were removed *in vacuo* and the residue was subjected to column chromatography (silica, DCM) to produce the title compound as a honeycomb yellow solid (710 mg, 1.59 mmol, 39%).

^{1}H NMR (400 MHz, $CDCl_3$): δ = 10.05 (br, s, 1 H), 8.31 (br, s, 1 H), 7.69 - 7.79 (m, 2 H), 7.50 - 7.58 (m, 2 H), 7.40 (d, J = 8.28 Hz, 2 H), 7.14 (d, J = 8.16 Hz, 2 H), 6.79 (dd, J = 3.89, 2.51 Hz, 1 H), 6.69 (m, 1 H), 6.16 (m, 1 H), 6.06 - 6.12 (m, 1 H), 5.93 - 6.01 (m, 1 H), 5.56 (s, 1 H), 3.08 (s, 1 H), 0.28 (s, 9 H) ppm. ^{13}C NMR (101 MHz, $CDCl_3$): δ = 183.72, 141.49, 141.30, 137.71, 132.47, 131.79, 130.67, 130.16, 128.78, 128.27, 126.70, 121.13, 120.85, 118.08, 110.89, 108.59, 108.05, 104.16, 97.36, 83.20, 77.49, 43.95, -0.16 ppm. MS: (ESI) *m/z* calculated for $[C_{29}H_{26}N_2OSi + H]^+$ 447.1887. Found: 447.1892.

1-(4-(2-(TMS)-ethynyl)benzoyl)-5-(4-ethynylphenyl)-9-benzoyldiprromethane (20)

A solution of dipyrromethane **19** (700 mg, 1.57 mmol) in degassed toluene (10 mL) was prepared. $Me_2PhMgBr$ (1 M in THF, 3.15 mL, 3.15 mmol) was added and the solution was stirred for 5 min. A solution of benzoyl chloride (0.73 mL, 6.28 mmol) in degassed toluene (10 mL) was prepared and half of this was transferred to the reaction flask. After 10 min stirring an additional amount of $Me_2PhMgBr$ (1 M in THF, 3.15 mL) was added

followed immediately by the remaining benzoyl chloride solution. After 20 min additional stirring, the reaction was quenched with saturated aqueous NH_4Cl solution. The mixture was extracted with ethyl acetate the organic layers were combined, washed with water (100 mL), brine (100 mL), dried over anhydrous magnesium sulfate and filtered. Solvents were removed *in vacuo* and the residue was subjected to column chromatography (silica, 20:1 DCM/ethyl acetate) to produce the title compound as a dark green solid (400 mg, 0.726 mmol, 46%).

^{1}H NMR (400 MHz, $CDCl_3$): δ = 11.93 (br, s, 1 H), 11.88 (br, s, 1 H), 7.71 - 7.77 (m, 2 H), 7.68 (d, J = 8.41 Hz, 2 H), 7.52 - 7.56 (m, 4 H), 7.47 - 7.52 (m, 3 H), 7.37 - 7.43 (m, 2 H), 6.45 - 6.54 (m, 2 H), 5.94 (m, 2 H), 5.70 (s, 1 H), 3.12 (s, 1 H), 0.27 (s, 9 H) ppm. ^{13}C NMR (101 MHz, $CDCl_3$): δ = 184.56, 183.45, 141.06, 140.82, 140.41, 137.96, 137.47, 132.61, 131.74, 131.52, 131.08, 130.95, 129.63, 129.47, 128.85, 128.59, 128.00, 126.55, 121.27, 120.91, 111.53, 111.35, 104.19, 97.32, 83.36, 77.50, 44.88, -0.17 ppm. MS: (ESI) *m/z* calculated for $[C_{36}H_{30}N_2O_2Si + H]^+$: 551.2149. Found: 551.2152. Elemental analysis calculated for $C_{36}H_{30}N_2O_2Si.0.5H_2O$: C, 77.25; H, 5.58; N, 5.00. Found: C, 77.13; H, 6.09; N, 5.21.

1-(4-Bromobenzoyl)-5-(4-bromophenyl)dipyrromethane (21)

Dipyrromethane **9** (1.50 g, 4.98 mmol) was dissolved in THF (10 mL) and $Me_2PhMgBr$ (1 M in THF, 12.5 mL, 12.5 mmol) was added to this. After stirring for 10 min, the solution was cooled to -78 °C and a solution of pyridyl thioester **5** (1.47 g, 5.00 mmol) in THF (10 mL) was added. The reaction mixture was allowed to gradually warm up to room temperature, and after a further 30 min of stirring, the mixture was quenched with saturated aqueous NH_4Cl solution (50 mL). The mixture was extracted with diethylether, the organic layers were combined, washed with water (100 mL), brine (100 mL), dried over anhydrous magnesium sulfate and filtered. Solvents were removed *in vacuo* and the

residue was subjected to column chromatography (silica, DCM) to produce the title compound as a honeycomb yellow solid (1.95 g, 4.03 mmol, 81%).

^{1}H NMR (400 MHz, $CDCl_3$): δ = 9.74 (br, s, 1 H), 8.15 (br, s, 1 H), 7.69 (m, 2 H), 7.61 (m, 2 H), 7.43 (m, 2 H), 7.07 (m, 2 H), 6.79 (dd, J = 3.76, 2.51 Hz, 1 H), 6.73 (ddd, J = 2.70, 1.60 Hz, 1 H), 6.18 (m, 1 H), 6.08 (m, 1 H), 5.98 (dddd, J = 3.36, 2.54, 1.63, 0.75 Hz, 1 H), 5.51 (s, 1 H) ppm. ^{13}C NMR (101 MHz, $CDCl_3$): δ = 183.29, 141.11, 139.67, 136.92, 131.92, 131.61, 130.48, 130.40, 130.04, 130.02, 126.70, 121.38, 120.60, 118.15, 110.85, 108.76, 108.12, 43.63 ppm. MS: (ESI) *m/z* calculated for $[C_{22}H_{16}Br_2N_2O + Na]^+$: 504.9522. Found: 504.9525. Elemental analysis calculated for $C_{22}H_{16}Br_2N_2O$: C, 54.57; H, 3.33; N, 5.79. Found: C, 54.64; H, 3.42; N, 5.76.

1-(4-Bromobenzoyl)-5-(4-bromophenyl)-9-benzoyldipyrromethane (22)

A solution of dipyrromethane **21** (1.00 g, 2.07 mmol) in degassed toluene (10 mL) was prepared. $Me_2PhMgBr$ (1 M in THF, 4.00 mL, 4.00 mmol) was added and the solution was stirred for 5 min. A solution of benzoyl chloride (0.94 mL, 8.09 mmol) in degassed toluene (10 mL) was prepared and half of this was transferred to the reaction flask. After 10 min stirring an additional amount of $Me_2PhMgBr$ (1 M in THF, 4.00 mL, 4.00 mmol) was added followed immediately by the remaining benzoyl chloride solution. After 40 min additional stirring, the reaction was quenched with saturated aqueous NH_4Cl solution. The mixture was extracted with ethyl acetate the organic layers were combined, washed with water (100 mL), brine (100 mL), dried over anhydrous magnesium sulfate and filtered. Solvents were removed *in vacuo* and the residue was subjected to column chromatography (silica, 20:1 DCM/ethyl acetate) to produce the title compound as a light grey solid (800 mg, 1.36 mmol, 66%).

^{1}H NMR (400 MHz, $CDCl_3$): δ = 11.74 (s, 1 H), 11.78 (s, 1 H), 7.81 (dd, J = 8.34, 1.32 Hz, 1 H), 7.72 - 7.77 (m, 2 H), 7.59 - 7.64 (m, 2 H), 7.49 - 7.57 (m, 5 H), 7.39 - 7.47

(m, 4 H), 6.55 (dd, J = 3.76, 2.38 Hz, 1 H), 6.52 (dd, J = 3.83, 2.45 Hz, 1 H), 5.97 (ddd, J = 8.50, 3.10 Hz, 2 H), 5.66 (s, 1 H) ppm. ^{13}C NMR (101 MHz, $CDCl_3$): δ = 132.58, 131.08, 128.64, 127.70, 126.60, 126.52, 125.61, 116.58, 105.19, 78.86, 66.24, 31.85 ppm. MS: (ESI) m/z calculated for $[C_{29}H_{21}Br_2N_2O_2 + H]^+$: 586.9964. Found: 586.9943.

References

1. A. D. Adler, F. R. Longo, J. D. Finarell, J. Goldmach, J. Assour and L. Korsakof, *J. Org. Chem.*, 1967, **32**, 476.

2. P. D. Rao, S. Dhanalekshmi, B. J. Littler and J. S. Lindsey, *J. Org. Chem.*, 2000, **65**, 7323-7344.

3. S. Thorand and N. Krause, *J. Org. Chem.*, 1998, **63**, 8551-8553.

4. W. B. Austin, N. Bilow, W. J. Kelleghan and K. S. Y. Lau, *J. Org. Chem.*, 1981, **46**, 2280-2286.

5. J.-C. Poupon, D. Marcoux, J.-M. Cloarec and A. B. Charette, *Org. Lett.*, 2007, **9**, 3591-3594.

6. R. Annunziata, M. Benaglia, M. Cinquini and F. Cozzi, *Tetrahedron Lett.*, 1995, **36**, 613-616.

7. M. Araki, S. Sakata, H. Takei and Mukaiyam.T, *B. Chem. Soc. Jpn.*, 1974, **47**, 1777-1780.

8. P. D. Rao, B. J. Littler, G. R. Geier and J. S. Lindsey, *J. Org. Chem.*, 2000, **65**, 1084-1092.

9. S. H. H. Zaidi, K. Muthukumaran, S. Tamaru and J. S. Lindsey, *J. Org. Chem.*, 2004, **69**, 8356-8365.

10. D. M. Wallace, S. H. Leung, M. O. Senge and K. M. Smith, *J. Org. Chem.*, 1993, **58**, 7245-7257.

11. C. H. Lee and J. S. Lindsey, *Tetrahedron*, 1994, **50**, 11427-11440.

12. T. P. Wijesekera, *Can. J. Chem.*, 1996, **74**, 1868-1871.

13. A. Sobral, N. Rebanda, M. da Silva, S. H. Lampreia, M. R. Silva, A. M. Beja, J. A. Paixao and A. Gonsalves, *Tetrahedron Lett.*, 2003, **44**, 3971-3973.

14. T. P. Wijesekera, J. B. Paine and D. Dolphin, *J. Org. Chem.*, 1985, **50**, 3832-3838.

15. J. K. Laha, S. Dhanalekshmi, M. Taniguchi, A. Ambroise and J. S. Lindsey, *Org. Process. Res. Dev.*, 2003, **7**, 799-812.

16. B. J. Littler, M. A. Miller, C. H. Hung, R. W. Wagner, D. F. O'Shea, P. D. Boyle and J. S. Lindsey, *J. Org. Chem.*, 1999, **64**, 1391-1396.

17. J. W. Ka and C. H. Lee, *Tetrahedron Lett.*, 2000, **41**, 4609-4613.

18. Y. Terazono, E. J. North, A. L. Moore, T. A. Moore and D. Gust, *Org. Lett.*, 2012, **14**, 1776-1779.

19. S. Tamaru, L. H. Yu, W. J. Youngblood, K. Muthukumaran, M. Taniguchi and J. S. Lindsey, *J. Org. Chem.*, 2004, **69**, 765-777.

20. K. Muthukumaran, M. Ptaszek, B. Noll, W. R. Scheidt and J. S. Lindsey, *J. Org. Chem.*, 2004, **69**, 5354-5364.

21. D. Gryko and J. S. Lindsey, *J. Org. Chem.*, 2000, **65**, 2249-2252.

22. R. G. Khoury, L. Jaquinod, K. Aoyagi, M. M. Olmstead, A. J. Fisher and K. M. Smith, *Angew. Chem. Int. Ed.*, 1997, **36**, 2497-2500.

23. M. Barbero, S. Cadamuro, I. Degani, R. Fochi, A. Gatti and V. Regondi, *J. Org. Chem.*, 1988, **53**, 2245-2250.

24. C. H. Lee, F. R. Li, K. Iwamoto, J. Dadok, A. A. Bothnerby and J. S. Lindsey, *Tetrahedron*, 1995, **51**, 11645-11672.

Chapter 3:

Porphyrins

Introduction

Porphyrins are found abundantly in nature, being a vital component in heme, the pigment found in red blood cells, vitamin B_{12} and for the process of photosynthesis.[1] Studies into porphyrins and porphyrin-containing systems are of considerable interest as they have a broad range of applications including optoelectronic devices,[2] chiral sensors,[3] sensitisers in photodynamic therapy,[4] molecular memory storage[5] and liquid crystals.[6] Developing reliable synthetic routes for new porphyrin containing systems will provide an opportunity to advance these and related areas.

Structure and Nomenclature

The structure of porphyrin was a matter of some contention between a few of the pioneers of porphyrin chemistry. Fischer originally proposed a bicyclic system of two eight-membered rings joined together[7] whereas tetrapyrrylethylene structures were proposed by Willstatter.[8] Kuster was the first to suggest the familiar cyclic, tetrapyrrolic system that we know to be correct today.[9]

Macrocyclic compounds can be difficult to name so it is vital that their naming systems are regulated to avoid confusion. With porphyrins, there are two nomenclature systems to be aware of, the Fischer system and the IUPAC system. Using the Fischer system, the four rings are labelled clockwise A-D and the eight β-pyrrolic carbons are labelled clockwise 1-8 so that β-pyrrolic carbons 1 and 2 are on ring A. The four *meso*-positions are labelled α, β, γ and δ. This system does not label every carbon atom and so its use is decreasing in favour of the IUPAC method. The IUPAC method starts at an α-pyrrolic carbon and in a clockwise fashion labels each carbon with a number. If there is a group branching off from one of the carbons of the porphyrin, the carbons within that substituent are given their own labels consisting of the carbon number they branched

from plus a superscript number to denote which carbon it is on the substituent chain. The notation used for Fischer and IUPAC nomenclature is shown in figure 3.1 below.

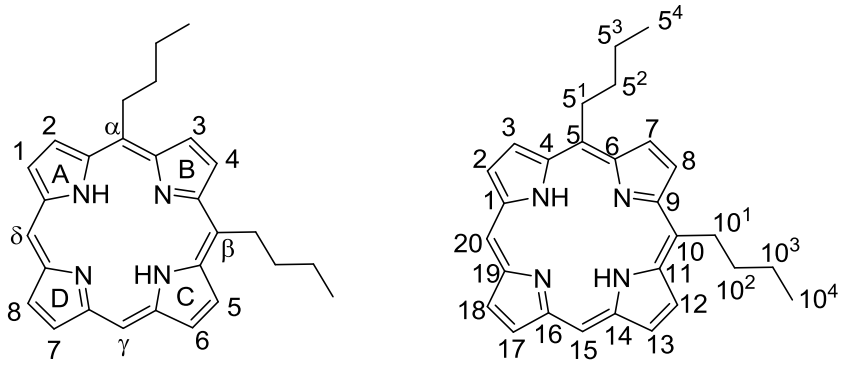
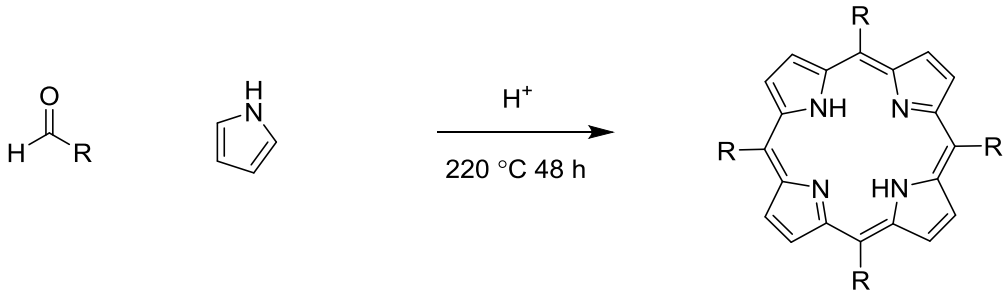


Figure 3.1 showing the Fischer (left) and IUPAC (right) nomenclature of porphyrins.

Porphyrin Synthesis

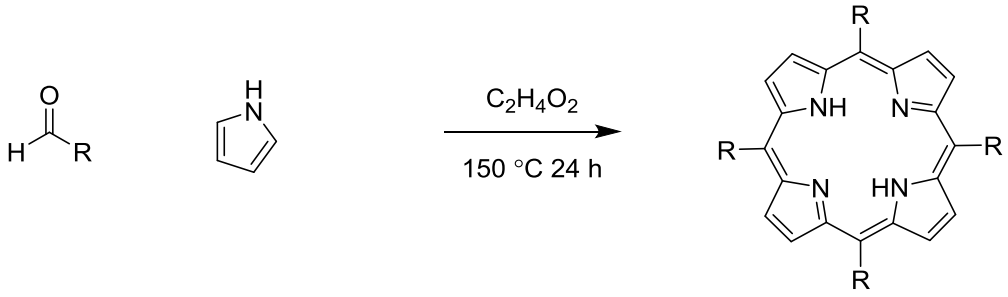
Porphyrins were first successfully prepared by Thudichum in 1867 by a treatment of haemoglobin with sulfuric acid.[10] Since this was reported, there have been many advances in porphyrin synthesis. Fischer was the first to report the synthesis of several other porphyrins such as protophorphyrin IX, the freebase porphyrin of hemin.[11]

Another chemist responsible for a lot of the groundwork of modern porphyrin synthesis is Paul Rothemund (scheme 3.1). The structurally simplest porphyrin, porphine was synthesised by Rothemund *via* a condensation and oxidation reaction using pyrrole, formaldehyde and an acid catalyst in a sealed tube.[12] Rothemund went on to create other porphyrins showing that by using a different aldehyde, substituents can be placed at the *meso*- positions.[13] The general method used was to heat the aldehyde and pyrrole together in a sealed tube at high temperatures (140 - 220 °C) for 24 - 48 h.



Scheme 3.1 Rothemund synthesis R = aryl, alkyl.

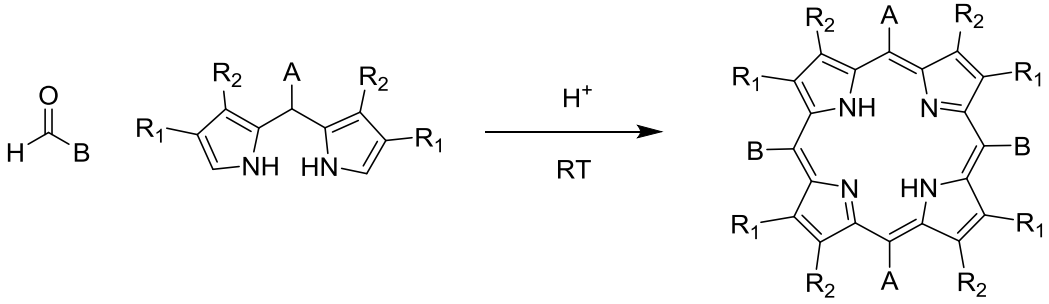
Since the synthesis of porphine by Rothemund, alternative synthetic methods have been devised by various research groups. The Adler-Longo method (scheme 3.2) uses relatively mild conditions when compared to the Rothemund method, but still very harsh compared to other methods used today. The aldehyde and pyrrole are refluxed together in the presence of acetic acid for 24 - 48 h, giving a yield of up to 20% for the synthesis of tetraphenylporphyrin (TPP).[14] This method, although an improvement on the Rothemund method which gave an 11% yield of TPP[13] causes a large amount of a tar-like substance to be produced in the reaction, making purification difficult.



Scheme 3.2 Adler-Longo synthesis R = aryl, alkyl.

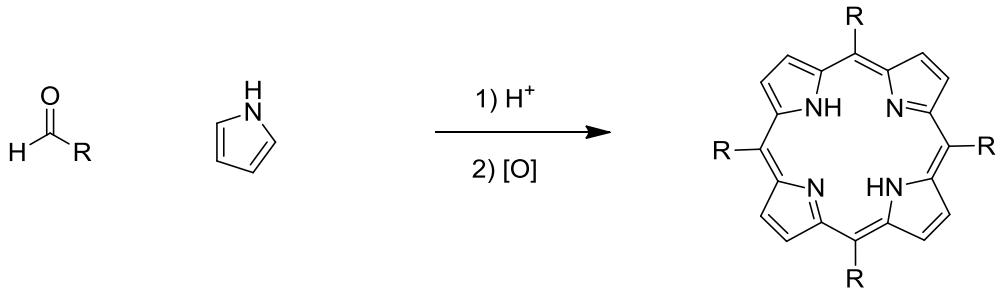
MacDonald employed a strategy of coupling dipyrromethanes and aldehydes together in acidic conditions at room temperature, known as the MacDonald [2+2] method.[15] This method allowed for the synthesis of both asymmetric and symmetric porphyrins depending on the dipyrromethanes being coupled. Scheme 3.3 shows the production of a single *trans*-porphyrin using a MacDonald [2+2] method. The nucleophilicity of the

pyrrole is affected by substituent groups present on the ring. Electron withdrawing groups such as carboxylic acids, nitro- and cyano- decrease the nucleophilicity and thereby, the reactivity of the pyrrole. However, electron donating groups such as alkyls, amines and alcohols increase the nucleophilicity and reactivity. The realisation and utilisation of this effect allows for a more controlled synthesis of porphyrins.



Scheme 3.3 Macdonald [2+2] coupling A, B, R = Aryl, alkyl.

The method developed by Lindsey showed that porphyrins could be formed in mild, equilibrium conditions. The Lindsey method (scheme 3.4) uses a condensation reaction between an aldehyde and pyrrole in the presence of a Lewis acid catalyst such as trifluoroacetic acid (TFA) to form a porphyrinogen which is then followed by oxidation using an agent such as p-chloranil or 2,3-dichloro-5,6-dicyano-1,4-benzoquinone (DDQ) to form a porphyrin.[16]



Scheme 3.4 Lindsey method R = aryl, alkyl.

Possible side products arising from porphyrin synthesis include chlorins,[17] N-confused porphyrins,[18] and other porphyrin species arising from a process known as scrambling.[19]

Scrambling, depicted in figure 3.2, forms a porphyrin product that would not be possible to produce directly by a reaction between the starting materials as a consequence of the acid catalyst generating a highly reactive intermediate.[20] Ordinarily, the Macdonald coupling between 'dipyrromethane A' and 'aldehyde B' results in a *trans*-A_2B_2 porphyrin product, however due to scrambling it is possible for a *cis*-A_2B_2 product to form.

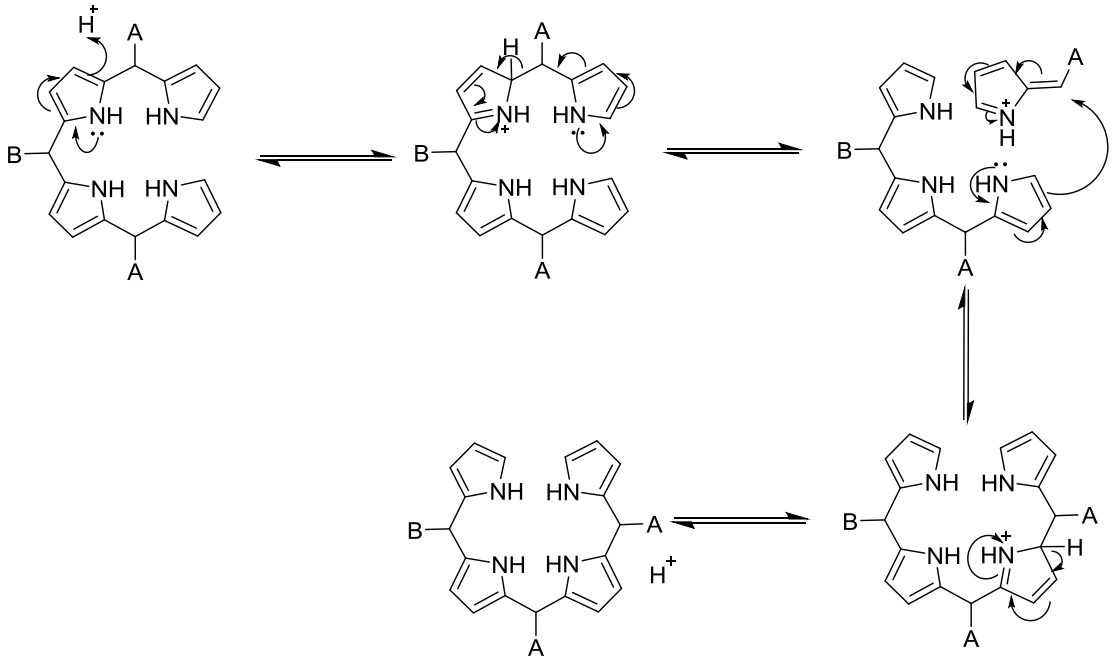


Figure 3.2 Mechanism of 'scrambling' process.

Spectroscopic Properties of Porphyrins

Porphyrins obey Huckel's 4n + 2 rule of aromaticity and also conform to the other criteria of being planar and cyclic. The aromatic 18 π-electron pathway of porphine is highlighted in bold in figure 3.3, however there is delocalisation of electrons across the whole molecule.[21]

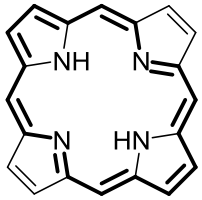


Figure 3.3 Aromatic pathway of porphine.

The UV-vis spectra of porphyrins (an example of which can be seen in figure 3.4) can be understood by considering using Gouterman's four-orbital model which states that π-π* transitions occur between two HOMOs, calculated to be an a_{1u} and an a_{2u} orbital and two LUMOs, calculated to be a degenerate set of e_g orbitals.[22] Orbital mixing splits the pair of degenerate e_g orbitals into a higher energy and a lower energy orbital. Transitions to the higher energy orbital can be represented as S_0 ➔ S_2 and are responsible for the feature known as the Soret or B band.[23] Transitions to the lower energy orbital can be represented as S_0 ➔ S_1 and are responsible for the Q-bands.[24] If the aromaticity of the porphyrin is removed, the Soret and Q-bands will no longer be observed.[25] However, a coordinating metal or substituents on the porphyrin will shift the wavelengths being absorbed.[26]

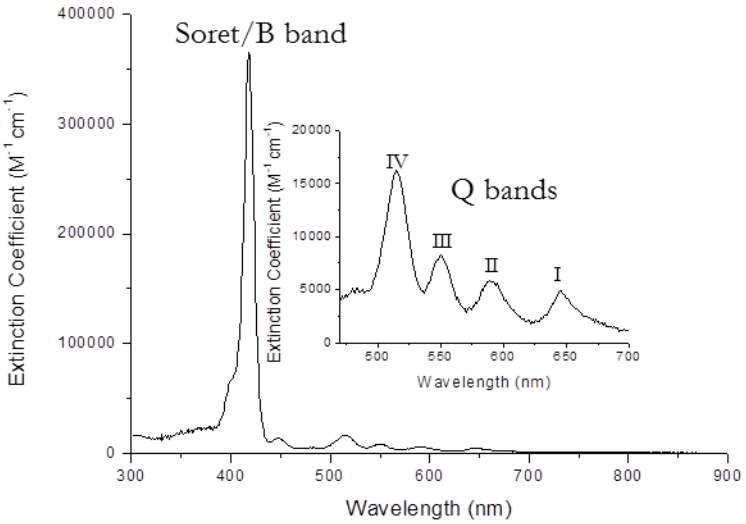


Figure 3.4 UV/Vis spectrum of a tetra-aryl porphyrin.

The Soret band is a very strong UV-Vis absorption in the order of $\varepsilon_0 = 100000\ M^{-1}\ cm^{-1}$ and is present at approximately 420 nm. It consists of two perpendicularly polarized transitions, labelled as B_x and B_y in figure 3.5. Although the transitions B_x and B_y are not fully degenerate in freebase porphyrins (one transition occurs through the NH-NH axis, the other through the N-N axis) there is no sizeable splitting observed of the two components, and so a single transition is observed in UV-Vis spectra.[27]

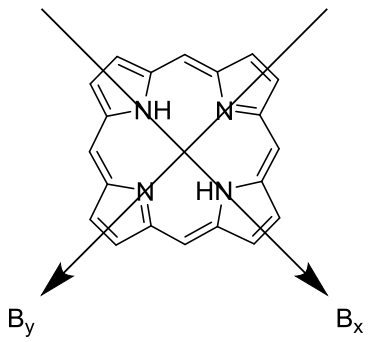


Figure 3.5 Electric transitions B_x and B_y displayed on porphine.

The Q-bands are approximately 20 times less intense than the Soret band and are found between 450-700 nm. The Q-bands also occur along the same axes as the Soret band but

have significant splitting. Furthermore, they are also split due to vibrational excitations which gives rise to four distinct peaks for the transitions $Q_x(0,0)$, $Q_y(0,0)$, $Q_x(1,0)$ and $Q_y(1,0)$.[28] When metallated, the Q_x and Q_y transitions are fully degenerate due to the symmetry of the molecule increasing from point group D_{2h} to D_{4h}. However, vibrational excitations still cause the Q- transitions to split, resulting in two Q-peaks being observed.[29] For the freebase species the Q-peaks are labelled I-IV, increasing in energy whereas for metallated species, these peaks are often labelled as α and β.[30]

Using ^{1}H NMR spectroscopy, it is possible to observe the N-H protons at the centre of the porphyrin ring as a signal that can range from -4 to -2 ppm. This type of signal is archetypal of protons within an anisotropic shielding cone. The β-pyrrolic and meso-protons on the other hand are deshielded and are observed downfield, also as a result of the aromatic ring current.[31]

Porphyrins are able to undergo multiple redox processes, with the number of which depending on metal coordination, substitution of the porphyrin macrocycle and the potential range of the solvent being used.[32, 33] Table 3.1 displays a number of oxidation and reduction potentials to show the effect various metals have when coordinated to tetraphenylporphryin (TPP).[34]

Table 3.1 Showing redox potentials of porphyrins (vs. Ag/AgCl) in CH_2Cl_2 containing $TBAPF_6$ as supporting electrolyte at 298 K.

Compound	Oxidation (I)	Oxidation (II)	Reduction (I)	Reduction (II)
H_2TPP	1.00	1.34	-1.23	-1.54
ZnTPP	0.84	1.15	-1.36	-1.77
CuTPP	0.97	1.35	-1.30	-1.70
CoTPP	1.06	1.32	-1.38	-
NiTPP	1.02	1.32	-1.28	-1.72

Altering the *meso*-substituents also has an effect on redox potentials, it has been observed that the introduction of an ethynylene group significantly decreased the HOMO – LUMO gap of the porphyrin by shifting its first reduction to the positive.[35] The tunable metrics of such compounds such as these has led to their incorporation in devices such as dye sensitised solar cells[36, 37] and information storage systems.[38, 39]

Results and Discussion

The synthesis of porphyrins can either be done using a multi-step, rational, directed methodology or by using a single-step statistical method of reacting aldehydes with pyrrole. If two aldehydes in a 1:1 ratio were to be reacted together with pyrrole to form a porphyrin, assuming equal reactivity from both aldehydes we get a product distribution that can be summarised in table 3.2.[40] However, it should be noted that experimentally, the statistical distribution attained will differ from these figures depending on the reactivity of the aldehydes and can be manipulated by altering the ratios of the aldehydes accordingly.

Table 3.2 Statistical distribution of porphyrin products resulting from aldehydes A and B.

Porphyrin Type	Statistical amount (%)
A_4	6.25
A_3B	25
cis-A_2B_2	25
trans-A_2B_2	12.5
AB_3	25
B_4	6.25

Once synthesised, column chromatography is required to separate out each product. Separations are very often difficult and occasionally not possible, in particular for the *trans*- and *cis*- isomers of A_2B_2 porphyrins.[41] Additionally, for the purposes of the research presented, four of the target compounds would require three aldehydes to be reacted together. This would potentially give twenty-one different products were a statistical

method used. This is clearly inefficient and so because of this, the multi-step directed method was chosen.

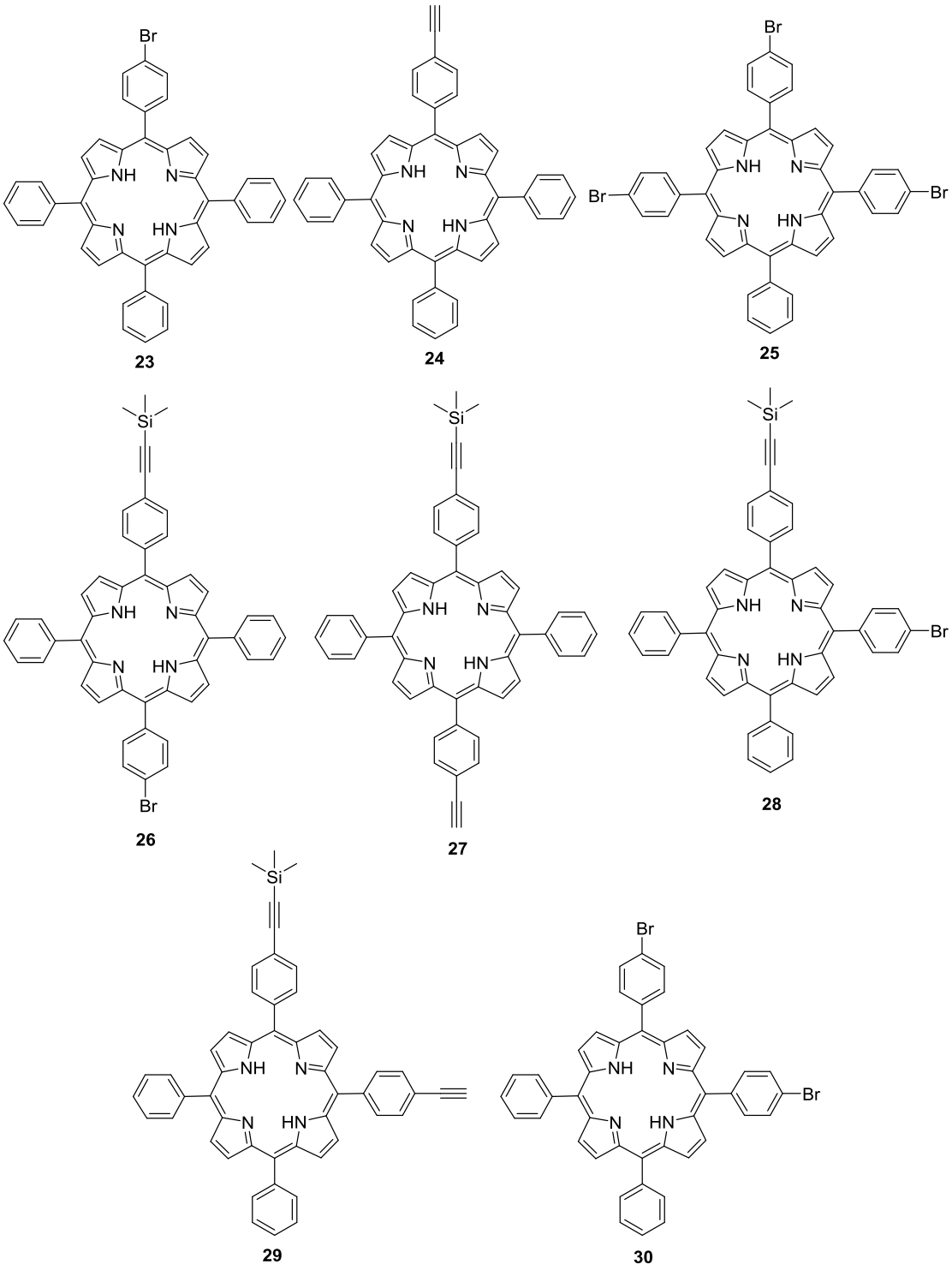
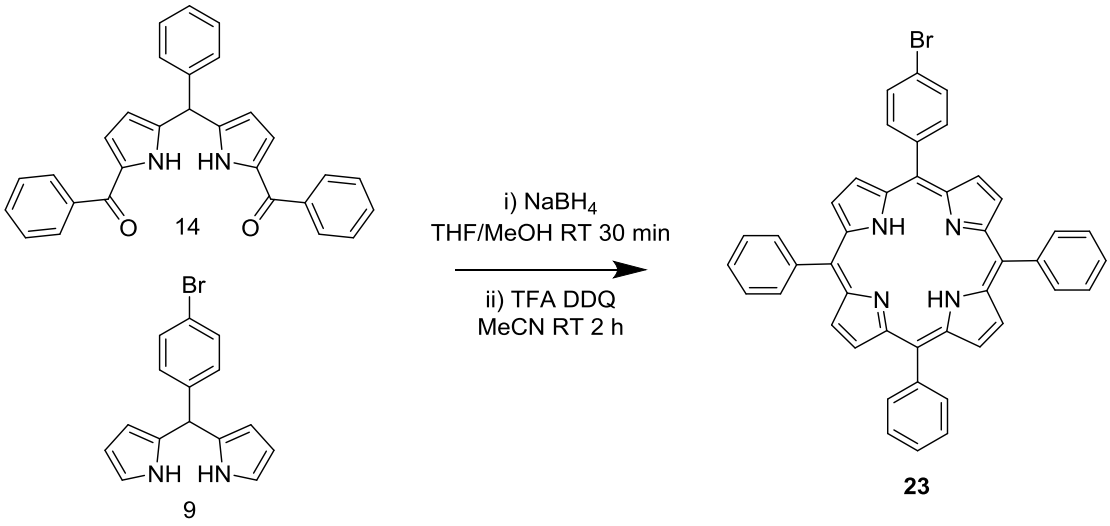


Figure 3.6 Chemical structures of porphyrins 23-30 synthesised using the Lindsey method.

The method used to synthesise porphyrins **23**-**30** (figure 3.6) is the same as the one developed by Lindsey and co-workers.[16] This method is advantageous because it only generates one main porphyrin product, with very little, often undetectable scrambling.



Scheme 3.5 Synthesis of 5-(4-bromophenyl)-10,15,20-triphenylporphyrin.

The procedure illustrated in scheme 3.5 is for the synthesis of **23**. However, similar conditions were used to synthesise a wide range of porphyrins, all of which are shown in figure 3.6 from the relevant building block molecules presented in chapter 2.

The first stage of the reaction is a reduction of the diacylated dipyrromethane by a large excess of sodium borohydride in a THF/MeOH solvent mix to form a dicarbinol species. The reaction was quenched with aqueous NH_4Cl and was worked up in a standard fashion. It was found that the solvent used to extract the dicarbinol during the work-up phase had to be fairly volatile due to the instability of the dicarbinol species; if the dicarbinol solution was exposed to temperatures exceeding 40 °C, the solution would rapidly darken from pale yellow, to orange, then red and finally brown.

The dicarbinol species was not usually isolated but it was in the case of reducing dipyrromethane **15** during the synthesis of porphyrin **25.** Following the work-up, an

alumina column was prepared. It was essential to conduct column chromatography in alumina as exposure to an acidic silica column would cause the dicarbinol species to decompose within minutes. The desired fractions were collected and solvents were removed. Analysis by NMR showed several differences between the diacylated species and the dicarbinol species, illustrated in figure 3.7. Two new broad peaks are present at 4.75 ppm and 5.74 ppm, both representing two protons. The peak at 4.75 ppm is assigned as the alcohol group and the peak at 5.74 ppm is assigned as the protons attached to the same carbon as these alcohol groups. The peak representing the NH protons in the diacylated species shifts upfield when reduced to the dicarbinol species from 11.34 ppm to 9.36 ppm. The protons on the phenyl groups at the 1- and 9-positions also shift upfield, but to a much lesser extent, approximately 0.4 ppm each. The protons on the phenyl group at the 5-position have shifted between 0.15 ppm and 0.2 ppm upfield. One set of β-pyrrolic protons appears to be much more affected by the reduction than the other as one set shifts upfield by 1.12 ppm and the other just by 0.5 ppm. Finally, the central proton at the 5-position shifts upfield by 0.55 ppm. Overall, it can be said that the reduction of the acyl group to an alcohol results in a shielding effect that can be felt across the entire molecule.

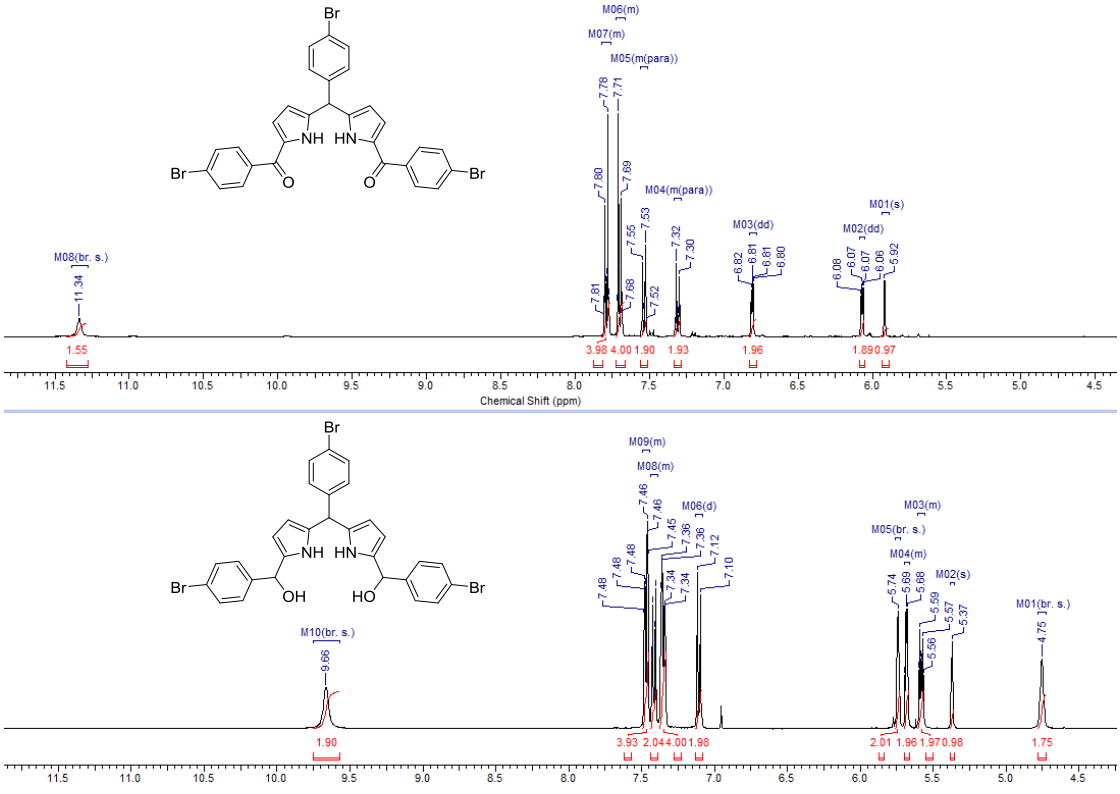


Figure 3.7 ^{1}H NMR spectra of 1,9-bis(4-bromobenzoyl)-5-(4-bromophenyl)dipyrromethane 15 (top) and of 1,9-bis(4-bromobenzylalcohol)-5-(4-bromophenyl)dipyrromethane (bottom).

For the synthesis of porphyrins **23**-**30**, the relevant dicarbinol species would usually be reacted after work-up without further purification. The dicarbinol would be dissolved in acetonitrile, followed by addition of TFA. Figure 3.8 shows the intermediate product of the dicarbinol and the dipyrromethane after addition of TFA. This intermediate had two options for further reactions, the desired *intramolecular* route or the undesired *intermolecular* route. The intramolecular route results in cyclisation of the molecule to form a porphyrinogen. The intermolecular route involves a reaction between two molecules to form a larger bilane chain, this chain itself could then go on to cyclise (although this is very unlikely) or it could continue reacting with other molecules to form a polymeric substance.[42]

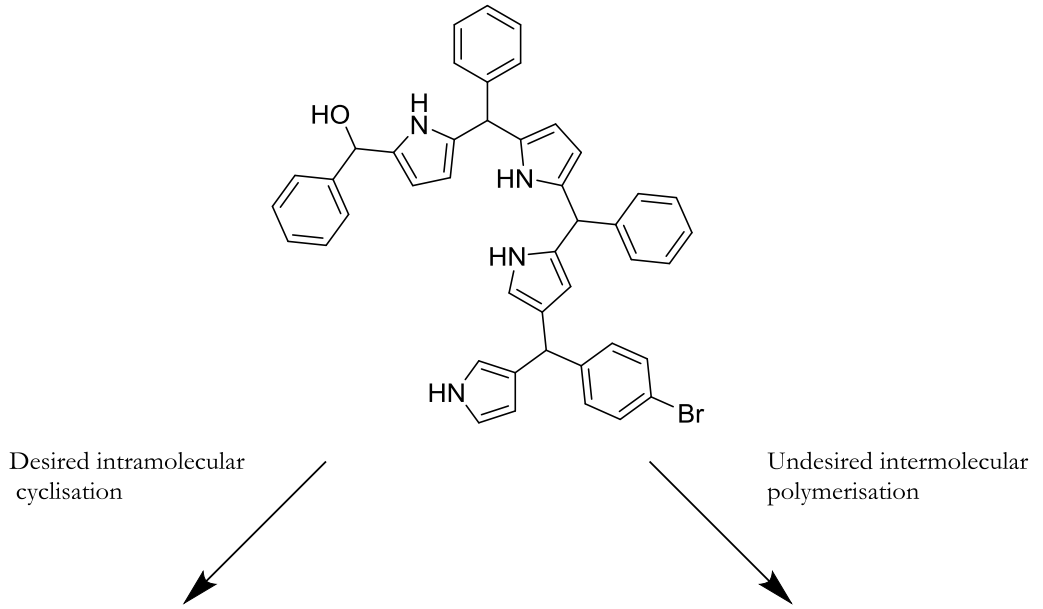
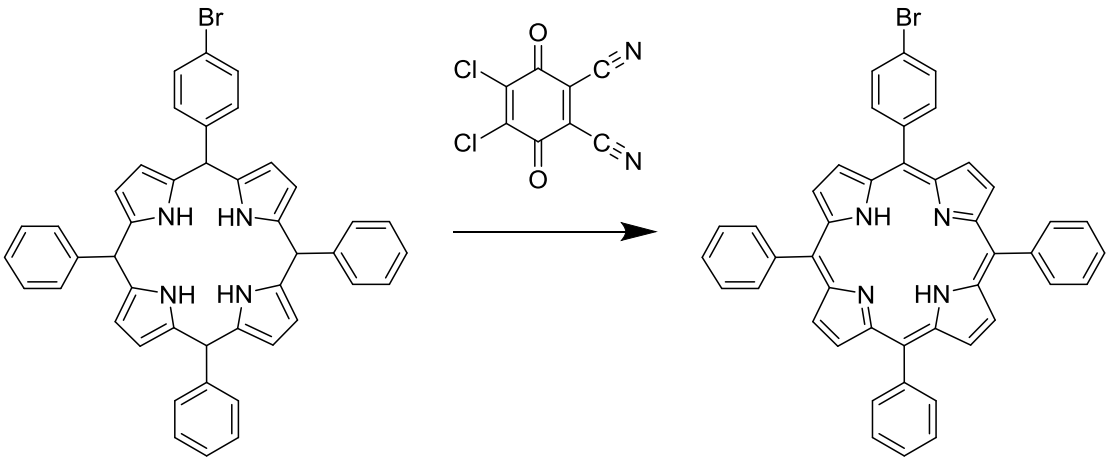


Figure 3.8 Intermediate bilane-OH product.

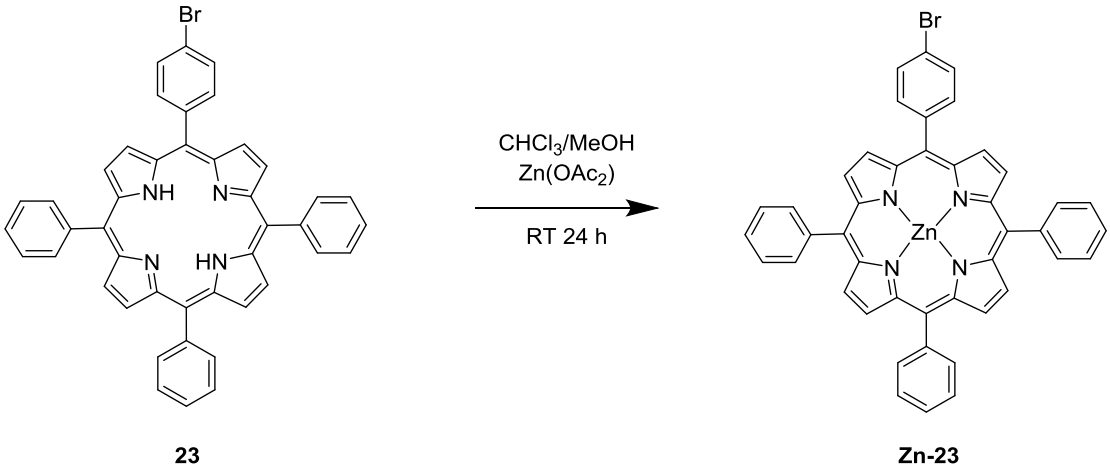
The final stage of the reaction is an oxidation of the porphyrinogen to a porphyrin by dichlorodicyanobenzoquinone (DDQ), shown in scheme 3.6. Oxidation occurs very rapidly, with the solution becoming very dark in colour so that it appeared completely opaque within seconds of addition. The structure of DDQ can be seen in scheme 3.6. Each molecule of DDQ is able to abstract two protons from the porphyrinogen. As a porphyrinogen has six protons that need to be removed before oxidation to a porphyrin is complete, three molar equivalents of DDQ are needed.



Scheme 3.6 Oxidation of porphyrinogen to porphyrin using DDQ as oxidant.

Metallation

As previously discussed, metallation of porphyrins alters their spectroscopy in interesting ways. Another effect of metallation has been suggested as being that the interaction between metallated porphyrins when deposited on a surface would be different between other metallated porphyrins and non metallated porphyrins. To investigate this, porphyrins **23** and **24** were metallated with zinc.



23 **Zn-23**

Scheme 3.7 Metallation of porphyrin 23 to form Zn-23.

Metallation was achieved by preparing a solution of zinc acetate in methanol and adding this to a solution of the porphyrin in DCM. This was stirred at room temperature for 24 h, after which the solvents were removed and the residue subjected to column chromatography (scheme 3.7). This reaction proceeded very efficiently, with almost complete metallation of **24** and 92% conversion of **23** with the remaining material being unreacted porphyrin.

Statistical Method for Porphyrins 23, 25 and 30

As mentioned previously, another method of synthesising porphyrins developed by Adler and Longo involves reacting aldehydes with pyrrole at high temperatures. As porphyrins **23**, **25** and **30** could in theory be produced from the same mixed-aldehyde reaction, an Adler-Longo style reaction was conducted.

Equal amounts of benzaldehyde and 4-bromobenzaldehyde were refluxed together in propionic acid. Pyrrole was added to this and the reaction was kept at reflux for a further 2 h and subsequently left to cool. The mixture was filtered to collect the porphyrinic species, which was then washed successively with methanol and hexane. Column chromatography was carried out on silica using DCM/hexane as the eluent. The ratios of porphyrins did not match up with the statistical distribution listed in table 3.2 but instead showed a distinct shift weighted in favour of the 4-bromobenzaldeyhde containing porphyrins, suggesting that the 4-bromobeznaldeyhde is a more reactive species than the benzaldehyde. Tetra(4-bromophenyl)porphyrin was isolated in approximately 2%. Porphyrin **25** was isolated in approximately 5% yield. Porphyrin **23** was isolated in approximately 2% yield and TPP was isolated in 0.5% yield. Porphyrin **30**, a *cis*-isomer could not be separated from its *trans*- isomer and the combioned isomers had a yield of 3.5%. As it is essential for the porphyrins to be isomerically pure, this statistical method was not pursued for porphyrin **30**. To assess the suitability of the method for porphyrins **23** and **25** we must compare the yields obtained to the overall yield *via* the directed method.

For porphyrin **23**, the stepwise approach involved the synthesis of dipyrromethane **8** (57%) before a Grignard reaction to give **14** (75%, 43% overall). This was followed by a reduction to a dicarbinol species (approaching stoichiometric conversion), condensation with dipyrromethane **9** (78%) and finally oxidation by DDQ (28%, 9% overall). From this we can see that despite requiring multiple reaction steps, the Lindsey-style directed approach results in significantly higher yields than an Adler-Longo approach.

For porphyrin **25**, synthesis of dipyrromethane **9** (78% yield) was followed by a Grignard reaction to give **15** (67% for final step; 52% overall). This was followed by a reduction to

a dicarbinol species, condensation with dipyrromethane **8** (57%) and finally oxidation by DDQ (31%, 9% overall). This also shows an increased yield when using the directed approach.

Although it would be possible to manipulate the product ratios to favour the desired products by increasing the amount of 4-bromobenzaldehyde for the synthesis of **25** and the amount of benzaldehyde for the synthesis of **23**, it is not possible to do both at once, which nullifies the benefit of the Adler-Longo method of producing multiple desired porphyrin products in the same reaction. The versatility of the directed method is such that, although multiple steps are required to synthesise the porphyrins, the precursor molecules can be 'swapped' in and out of reactions to create a variety of porphyrins requiring very little purification.

Comparison of Zn-Porphyrin and Freebase Porphyrin.

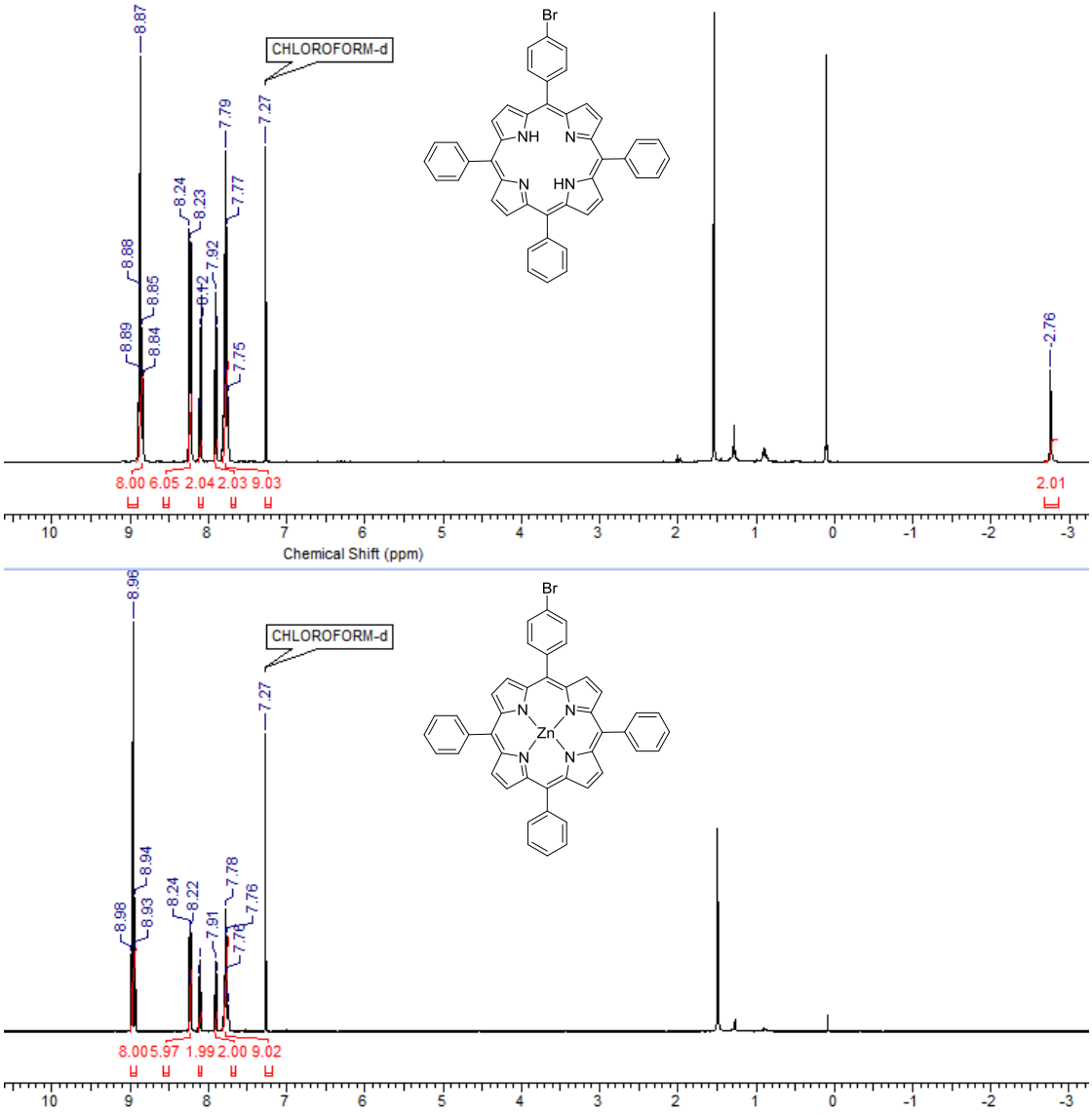


Figure 3.9 ^{1}H NMR spectra of 23 (top) and Zn-23 (bottom).

The ^{1}H NMR spectra of **23** and **Zn-23** are shown in figure 3.9 and are, in general, fairly similar. The only significant difference is the signal at -2.76 ppm present in the freebase porphyrin relating to the protons in the centre of the porphyrin ring that is removed when zinc is coordinated. The other minor difference is the slight downfield shift (0.09 ppm) of the pyrrolic β-protons of the zinc coordinated porphyrin compared to the freebase porphyrin. The other signals relating to protons on the *meso*- phenyl groups are unaffected.

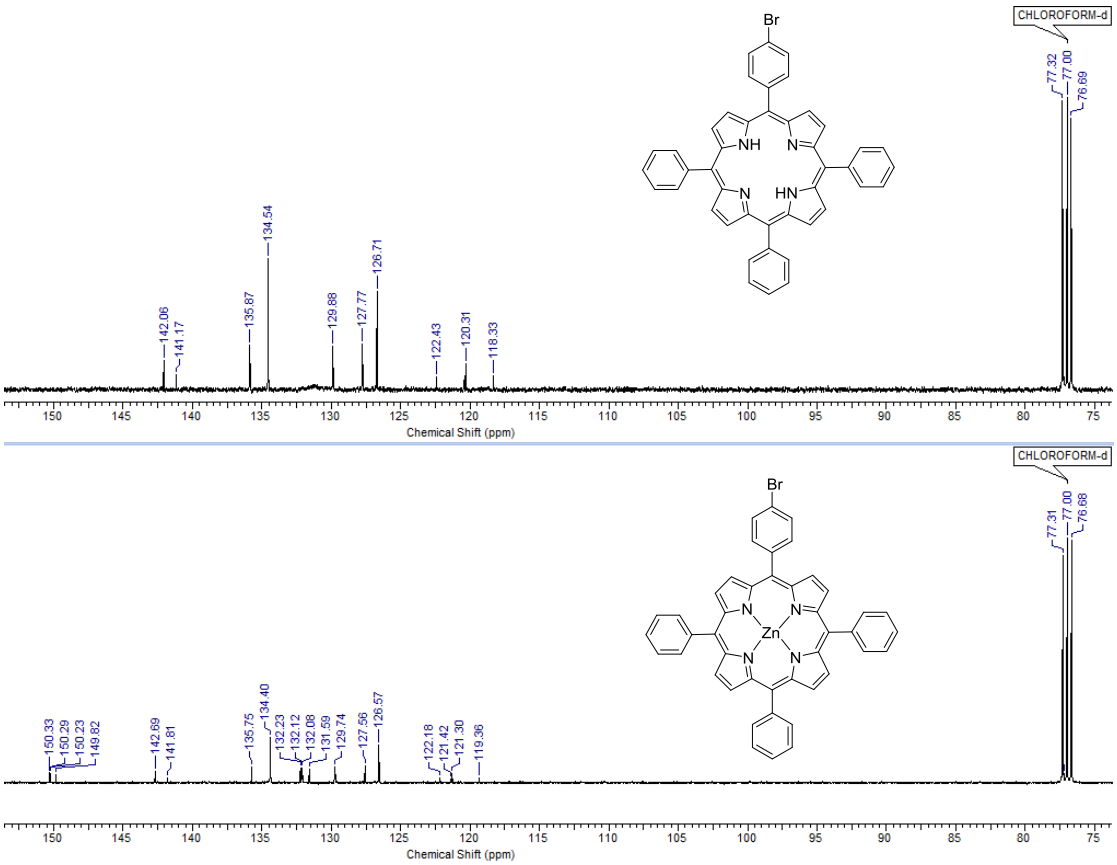


Figure 3.10 ^{13}C NMR Spectra of 23 (top) and Zn-23 (bottom).

The ^{13}C NMR spectra of porphyrins differ dramatically depending on whether there is a metal coordinated at the centre or if the porphyrin is freebase. Although it is possible to view every carbon environment by Carbon-13 enriched synthesis,[43, 44] not all the carbon environments are visible in conventional synthesis, due to restricted motion of the porphyrin, which takes the form of flexing. The NMR experiments run during the course of this research resulted in eleven environments being detected for the freebase porphyrin **23**. The coordinated metal provides a more rigid structure to the porphyrin (it was thought that little to no flexing would be able to occur) allowing more environments to be observed, nineteen environments were detected for the A_3B porphyrin **Zn-23** shown in figure 3.10. However, if every environment were detected, twenty-three environments should be seen.

During NMR experiments, restricted rotation or movement within a molecule causes the same carbon atom to appear in different environments. When there is free rotation/movement within a molecule (*e.g.* an unhindered alkyl chain), rotation occurs very rapidly causing an average signal to be taken for each carbon atom resulting in a single peak for a single atom. Similarly, if movement within the molecule is completely hindered (e.g. benzene) a single environment is observed. Porphyrins possess restricted movement due to a flexing motion of the ring. These motions do not occur fast enough for an average signal to be determined, the relaxation time for the nuclei involved is long and so appear as very broad signals.[45] To combat these effects, we can either decrease the temperature to reduce the speed of motion, possibly resulting in multiple signals for a single carbon atom relating to different rotational conformations or we can increase the temperature to speed up the motion so that a better average can be taken. High temperature NMR experiments were performed on **23** and **Zn-23** to observe the effects on their NMR spectra.

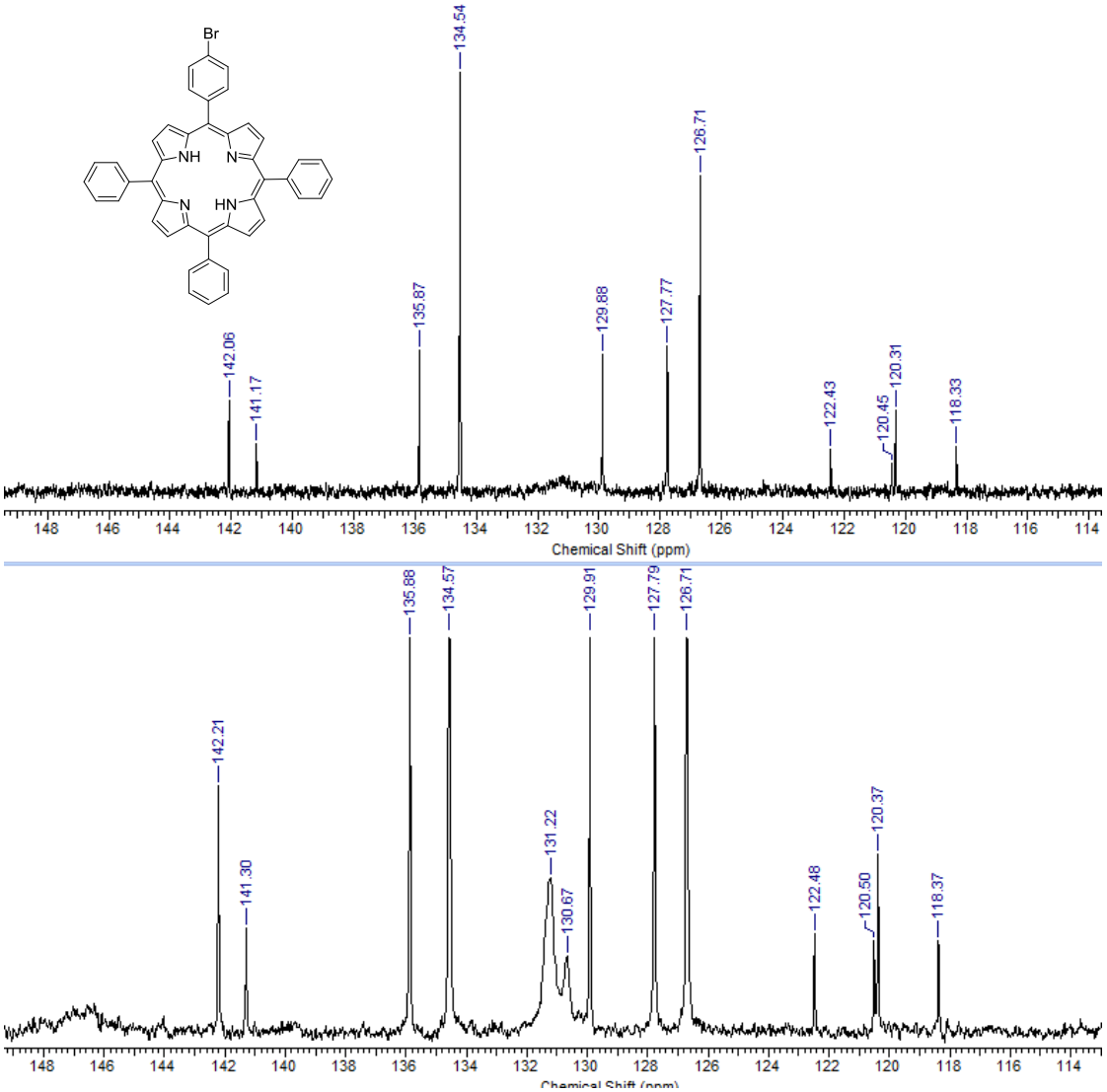


Figure 3.11 ^{13}C NMR of 23 collected at 25 °C (top) and at 50 °C (bottom).

The inability to observe all carbon environments can be compensated for slightly by performing the NMR experiments at an elevated temperature. Figure 3.11 shows a comparison between a ^{13}C NMR spectrum of **23** collected at RT and a ^{13}C NMR spectrum collected at 50 °C. The broad signal observed in the RT spectrum sharpens into two distinct peaks around 131 ppm and a new broad signal that was not detected at the lower temperature is observed at 147 ppm. Additionally, 2D HMBC NMR experiments were run for **23** at 25 °C and 50 °C. No coupling was observed between the pyrrolic β-protons (approximately 8.9 ppm) and nearby carbons at 25 °C. At 50 °C coupling was

observed between the pyrrolic β-protons and carbons with signals around 131 ppm and 147 ppm, indicating that these 'new' signals relate to pyrrolic carbons.

Another experiment was performed on a sample of **Zn-23** in an attempt to elucidate the missing carbon peaks. Two ^{13}C NMR experiments in DMSO were performed, one at RT, the other at 90 °C, as if flexing was occurring it was thought this temperature should be high enough to obtain an averaged signal for the 'missing' carbons. Interestingly, no new peaks were discovered at the higher temperature indicating that all the environments had already been observed. It is thought that the coordinating zinc inhibits the flexing motion completely, in turn cause more efficient relaxations to occur of the nuclei in the molecule. It is likely that the missing carbon peaks lie within such similar environments to other carbon peaks that should formally be in a separate environment, that the peaks overlap and appear as one.

UV/Vis Spectroscopy

The spectra collected for porphyrins **23**-**30** are remarkably similar to one another and are displayed in figure 3.12. As expected for the freebase porphyrins, we can observe the Soret band at approximately 420 nm followed by four less intense Q-bands at longer wavelengths.

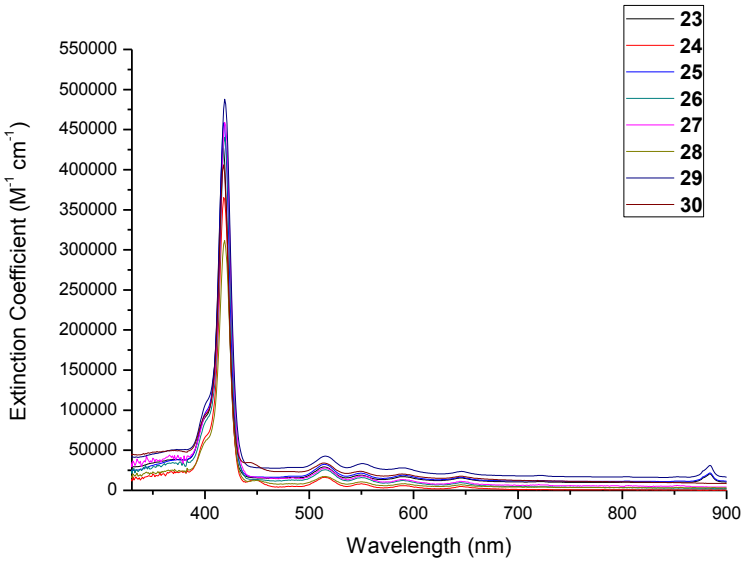


Figure 3.12 UV/Vis spectra for porphyrins 23-30.

The metallated porphyrin **Zn-23** showed essentially no change in the position of the Soret band but a slight decrease in intensity (figure 3.13). The data also showed only one Q-peak, which correlated well with one of the Q-peaks recorded for the freebase species with the other expected Q-peak from theory being indistinguishable from the baseline. The metallated porphyrin **Zn-24** again showed essentially no shift in the Soret peak but in this instance displayed an increase in intensity (figure 3.14). Only one Q-peak was detected, with the other transition that was expected to occur being indistinguishable from the baseline.

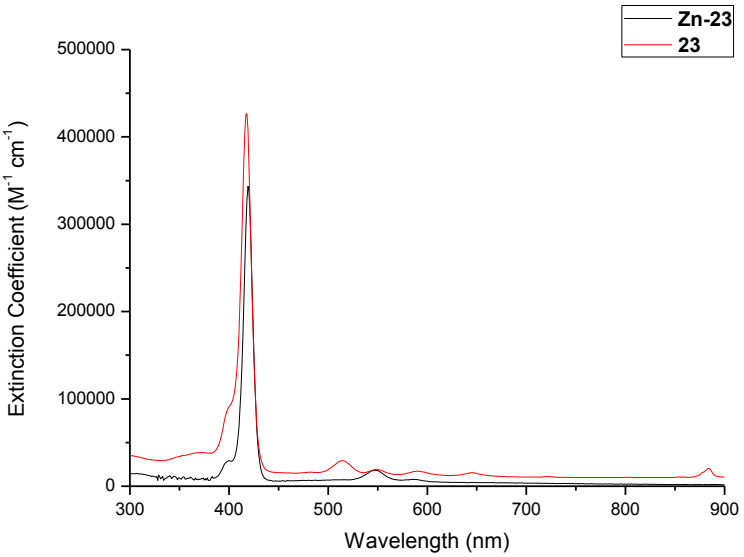


Figure 3.13 UV/Vis spectra for 23 and Zn-23.

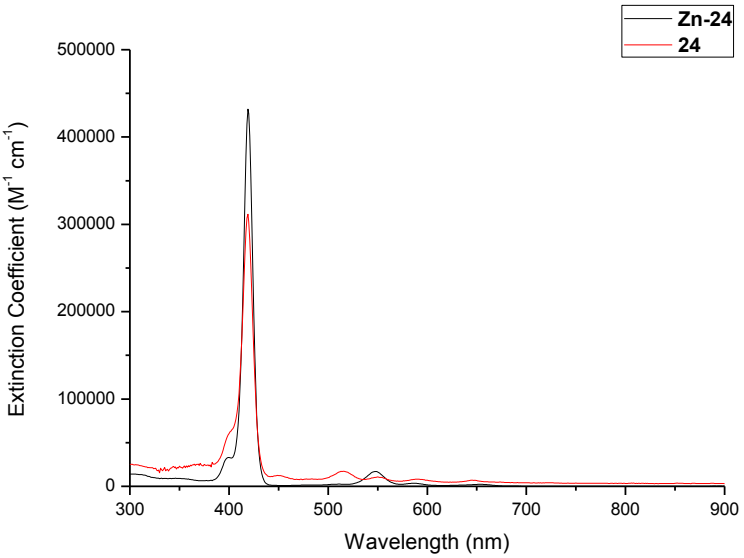


Figure 3.14 UV/Vis spectra for 24 and Zn-24.

Conclusions

Compounds **23** - **30** were synthesised by the Lindsey method obtaining good yields ranging from 21-31%. These porphyrins have terminal bromo-, ethynyl-, and TMS-groups that make them suitable for successive Sonogashira coupling and deprotection reactions to create larger porphyrin arrays such as the Tetris compounds discussed in chapter 5.

Metallation of porphyrins **23** and **24** proceeded very efficiently at over 90% in both cases and with unreacted starting material being easily recovered.

Elevating the temperature at which NMR data was collected marginally improved the data for freebase porphyrins, whilst still leaving many environments undetected. Elevating the temperature at which NMR data was collected for metallated porphyrins did not have any effect on the appearance of their spectra.

The statistical method of synthesising porphyrins **23**, **25** and **30** was compared to the directed approach. The statistical method was found to be unsuitable for the synthesis of **30** as the *trans*- isomer could not be separated from the *cis*- isomer. The statistical method was also found to be inferior to the directed approach for the synthesis of porphyrins **23** and **25**, despite being less reaction intensive.

Experimental

General Procedure A for Porphyrin Formation Reaction

Diacylated dipyrromethane (1 eq) was dissolved in THF (75 mL) and methanol (12.5 mL). Sodium borohydride (40 eq) was added and the reaction mixture stirred at room temperature for 1 h after which a saturated aqueous ammonium chloride/diethyl ether mixture (1:1, 100 mL) was added. The organics were collected and washed with water (100 mL), brine (100 mL) and then dried over anhydrous magnesium sulfate. The resulting mixture was filtered and the solvent removed *in vacuo*. The residue, along with dipyrromethane (1 - 1.2 eq) was dissolved in acetonitrile (2.5 mmol solution). TFA (12 eq) was added and the solution stirred for 1 h. DDQ (3 eq) was added and the solution stirred for a further 1 h at room temperature after which, the solvent was removed *in vacuo*. The residue was dissolved in DCM and filtered through a silica column to collect the porphyrinic species.

5-(4-Bromophenyl)-10,15,20-tri(phenyl)porphyrin (23)

General procudure A was used for diacylated dipyrromethane **14** (1.00 g, 2.32 mmol) and dipyrromethane **9** (840 mg, 2.78 mmol). Purification was achieved by column chromatography (silica, chloroform) affording the title compound as a purple solid (450 mg, 0.649 mmol, 28%).

^{1}H NMR (400 MHz, $CDCl_3$): δ = 8.82 - 8.93 (m, 8 H), 8.20 - 8.27 (m, 6 H), 8.07 - 8.14 (m, 2 H), 7.87 - 7.94 (m, 2 H), 7.70 - 7.84 (m, 9 H), -2.76 (s, 2 H) ppm. ^{13}C NMR (101 MHz, $CDCl_3$): 142.1, 141.2, 135.9, 134.58, 129.9, 127.8, 126.7, 122.5, 120.5, 120.3, 118.4. MS: (MALDI-TOF, DCTB/MeCN) m/z calculated for $[C_{44}H_{29}N_4Br]^+$: 692.1570. Found: 692.1592. Elemental analysis calculated for $C_{44}H_{29}BrN_4$: C, 76.19; H, 4.21; N, 8.08.

Found: C, 73.96; H, 4.41; N, 7.62. UV/Vis λ_{abs} ($CHCl_2$)/nm (ε/$dm^3mol^{-1}cm^{-1}$): 418 (427,000), 514 (29,000), 549 (19,100), 589 (17,100), 645 (15,400).

Zn-5-(4-bromophenyl)-10,15,20-tri(phenyl)porphyrin (Zn-23)

Porphyrin **23** (100 mg, 0.144 mmol) was dissolved in chloroform (50 mL). A solution of zinc acetate dehydrate (158 mg, 0.720 mmol) in methanol (6 mL) was prepared and added to the porphyrin solution. The reaction mixture was allowed to stir at RT for 24 h, after which the solvents were removed *in vacuo*. The purple residue was separated by column chromatography (silica, 5:4, hexane/DCM) to afford the title compound as a purple solid (100 mg, 0.132 mmol, 92%).

^{1}H NMR (400 MHz, $CDCl_3$): δ = 8.96 (m, 8 H) 8.23 (dd, *J* = 7.72, 1.57 Hz, 6 H) 8.11 (d, *J* = 8.36 Hz, 2H) 7.90 (d, *J* = 8.36 Hz, 2H) 7.77 (m, 9 H) ppm. ^{13}C NMR (101 MHz, $CDCl_3$): δ = 150.3, 150.3, 150.2, 149.8, 142.7, 141.8, 135.7, 134.4, 132.2, 132.1, 132.1, 131.6, 129.7, 127.6, 126.6, 122.2, 121.4, 121.3, 119.4 ppm. MS: (MALDI-TOF, DCTB/MeCN) *m/z* calculated for $[C_{44}H_{27}N_4BrZn]^+$: 754.0705. Found: 754.0697. UV/Vis λ_{abs} (CH_2Cl_2)/nm (ε/$dm^3mol^{-1}cm^{-1}$): 419 (343,000), 547 (18,400).

5-(4-Ethynylphenyl)-10,15,20-triphenylporphyrin (24)

General procudure A was used for diacylated dipyrromethane **14** (1.00 g, 2.32 mmol) and dipyrromethane **11** (630 mg, 2.56 mmol). Purification was achieved by column chromatography (silica, chloroform) affording the title compound as a purple solid (460 mg, 0.721 mmol), 31%).

^{1}H NMR (400 MHz, $CDCl_3$): δ = 8.83 - 8.99 (m, 8 H), 8.18 - 8.32 (m, 8 H), 7.93 (d, *J* = 8.07 Hz, 2 H), 7.72 - 7.86 (m, 9 H), 3.35 (s, 1 H), -2.71 (br. s., 2 H) ppm. ^{13}C NMR (126 MHz, $CDCl_3$): δ = 142.86, 142.10, 142.08, 134.54, 134.46, 130.50, 127.75, 126.70, 121.60, 120.42, 120.30, 118.93, 83.66, 78.26 ppm. MS: (MALDI-TOF, DCTB/MeCN)

m/z calculated for $[C_{46}H_{30}N_4]^+$: 638.2465. Found: 638.2453. UV/Vis λ_{abs} ($CHCl_2$)/nm (ε/$dm^3mol^{-1}cm^{-1}$): 418 (365,000), 515 (16,300), 550 (8,300), 589 (5,900), 646 (4,900).

Zn-5-(4-ethynylphenyl)10,15,20-tri(phenyl)porphyrin (Zn-24)

Porphyrin **24** (100 mg, 0.157 mmol) was dissolved in chloroform (50 mL). A solution of zinc acetate dihydrate (172 mg, 0.784 mmol) in methanol (6 mL) was prepared and added to the porphyrin solution. The reaction mixture was allowed to stir at RT for 24 h, after which the solvents were removed *in vacuo*. The purple residue was subjected to column chromatography (silica, 5:4, hexane/DCM) to afford a magenta solid (110 mg, 0.156 mmol, 99%).

^{1}H NMR (400 MHz, $CDCl_3$): δ = 8.92 - 8.99 (m, 8 H), 8.18 - 8.27 (m, 8 H), 7.90 (d, *J* = 8.28 Hz, 2 H), 7.73 - 7.82 (m, 9 H), 3.32 (s, 1 H) ppm. ^{13}C NMR (101 MHz, $CDCl_3$): δ = 150.3, 150.3, 150.3, 149.8, 143.6, 142.7, 134.4, 134.4, 132.2, 132.1, 132.1, 131.7, 130.4, 127.6, 126.6, 121.4, 121.4, 121.3, 120.0, 83.8, 78.1 ppm. MS: (MALDI-TOF, DCTB/MeCN) *m/z* calculated for $[C_{46}H_{28}N_4Zn]^+$: 700.1600. Found: 700.1587. UV/Vis λ_{abs} (CH_2Cl_2)/nm (ε/$dm^3mol^{-1}cm^{-1}$): 419 (432,000), 448 (17,000).

5,10,15-tri(4-Bromophenyl)-20-phenylporphyrin (25)

General procudure A was used for diacylated dipyrromethane **15** (600 mg, 0.899 mmol) and dipyrromethane **8** (240 mg, 1.08 mmol). Purification was achieved by column chromatography (silica, 1:1, $CHCl_3$/hexane) affording the title compound as a purple solid (220 mg, 0.258 mmol), 29%).

^{1}H NMR (400 MHz, $CDCl_3$): δ = 8.80 - 8.91 (m, 8 H), 8.21 (dd, *J* = 7.78, 1.51 Hz, 2 H), 8.04 - 8.12 (m, 6 H), 7.87 - 7.94 (m, 6 H), 7.73 - 7.83 (m, 3 H), -2.84 (s, 2 H) ppm. ^{13}C NMR (101 MHz, $CDCl_3$): δ = 141.83, 140.93, 139.95, 135.83, 134.51, 129.94, 127.88, 126.76, 122.56, 120.77, 118.80, 118.67 ppm. MS: (MALDI-TOF, DCTB/MeCN) *m/z*

calculated for $[C_{44}H_{27}N_4Br_3]^+$: 847.9780. Found: 847.9753. UV/Vis λ_{abs} (CH_2Cl_2)/nm (ε/$dm^3mol^{-1}cm^{-1}$): 418 (458,000), 515 (32,300), 550 (21,400), 589 (18,800), 644(16,300).

5-(4-(2-(TMS)-ethynyl)phenyl)-10-phenyl-15-(4-bromophenyl)-20-phenylporphyrin (26)

General procudure A was used for diacylated dipyrromethane **16** (350 mg, 0.665 mmol) and dipyrromethane **9** (240 mg, 1.01 mmol). Purification was achieved by column chromatography (silica, 3:2 hexane/chloroform) affording the title compound as a purple solid (130 mg, 0.165 mmol), 25%).

^{1}H NMR (400 MHz, $CDCl_3$): δ = 8.81 - 8.90 (m, 8 H), 8.22 (dd, *J* = 7.72, 1.44 Hz, 4 H), 8.18 (d, *J* = 8.22 Hz, 2 H), 8.09 (d, *J* = 8.22 Hz, 2 H), 7.86 - 7.93 (m, 4 H), 7.74 - 7.83 (m, 6 H), 0.35 - 0.42 (m, 9 H), -2.79 (s, 2 H) ppm. ^{13}C NMR (101 MHz, $CDCl_3$): δ = 142.38, 141.96, 141.08, 135.84, 134.51, 134.39, 130.34, 129.88, 127.80, 126.72, 122.61, 122.45, 120.43, 119.40, 118.55, 104.97, 95.59, 0.05 ppm. MS: (MALDI-TOF, DCTB/MeCN) *m/z* calculated for $[C_{49}H_{37}N_4BrSi]^+$: 788.1965. Found: 788.1948. Elemental analysis for $C_{49}H_{37}BrN_4Si$: C, 74.51; H, 4.72; Br, 10.12; N, 7.09; Si, 3.56. UV/Vis λ_{abs} (CH_2Cl_2)/nm (ε/$dm^3mol^{-1}cm^{-1}$): 419 (440,000), 515 (25,700), 550 (16,000), 590 (12,400), 646 (9,700).

5-(4-(2-(TMS)-ethynyl)phenyl)-10-phenyl-15-(4-ethynylphenyl)-20-phenylporphyrin (27)

General procudure A was used for diacylated dipyrromethane **16** (550 mg, 1.04 mmol) and dipyrromethane **11** (310 mg, 1.26 mmol). Purification was achieved by column chromatography (silica, 3:2, hexane/chloroform) affording the title compound as a purple solid (160 mg, 0.218 mmol, 21%).

^{1}H NMR (400 MHz, $CDCl_3$): δ = 8.81 - 8.90 (m, 8 H), 8.15 - 8.25 (m, 8 H), 7.87 - 7.93 (m, 4 H), 7.73 - 7.81 (m, 6 H), 3.33 (s, 1 H), 0.40 (s, 9 H), -2.78 (s, 2 H) ppm. ^{13}C NMR

(101 MHz, $CDCl_3$): δ = 142.76, 142.40, 141.98, 134.50, 134.44, 134.39, 130.49, 130.33, 127.79, 126.71, 122.59, 121.61, 120.41, 119.37, 119.14, 104.98, 95.57, 83.63, 78.29, 0.04 ppm. MS: (MALDI-TOF, DCTB/MeCN) m/z calculated for $[C_{51}H_{38}N_4Si]^+$: 734.2860. Found: 734.2889. UV/Vis λ_{abs} (CH_2Cl_2)/nm (ε/$dm^3mol^{-1}cm^{-1}$): 419 (459,000), 515 (28,200), 550 (18,000), 590 (13,400), 646 (11,400).

5-(4-(2-(TMS)-ethynyl)phenyl)-10-(4-bromophenyl),15,20-diphenylporphyrin (28)

General procudure A was used for diacylated dipyrromethane **18** (600 mg, 0.991 mmol) and dipyrromethane **8** (263 mg, 1.18 mmol). Purification was achieved by column chromatography (silica, 1:1 hexane/chloroform) affording the title compound as a purple solid (240 mg, 0.304 mmol, 31%).

^{1}H NMR (400 MHz, $CDCl_3$): δ = 8.86 (m, 8 H), 8.23 (dd, *J* = 7.65, 1.63 Hz, 4 H), 8.18 (d, *J* = 8.28 Hz, 2 H), 8.09 (d, *J* = 8.28 Hz, 2 H), 7.87 - 7.94 (m, 4 H), 7.78 (m, 6 H), 0.38 - 0.43 (m, 9 H), -2.78 (s, 2 H) ppm. ^{13}C NMR (101 MHz, $CDCl_3$): δ = 142.37, 141.98, 141.07, 135.83, 134.52, 134.39, 130.35, 129.90, 127.79, 126.71, 122.63, 122.47, 120.56, 120.53, 119.28, 118.46, 104.96, 95.61, 0.06 ppm. MS: (MALDI-TOF, DCTB/MeCN) m/z calculated for $[C_{49}H_{37}N_4BrSi]^+$: 788.1965. Found: 788.1990. UV/Vis λ_{abs} (CH_2Cl_2)/nm (ε/$dm^3mol^{-1}cm^{-1}$): 419 (312,000), 515 (17,300), 550 (10,700), 591 (8,200), 646 (7,000).

5-(4-(2-(TMS)-ethynyl)phenyl)-10-(4-ethynylphenyl),15,20-diphenyl porphyrin (29)

General procudure A was used for diacylated dipyrromethane **20** (350 mg, 0.636 mmol) and dipyrromethane **8** (170 mg, 0.765 mmol) Purification was achieved by column chromatography (silica, 2:1 hexane/chloroform) affording the title compound as a purple solid (100 mg, 0.136 mmol, 21%).

^{1}H NMR (400 MHz, $CDCl_3$): δ = 8.82 - 8.93 (m, 8 H), 8.18 - 8.29 (m, 8 H), 7.92 (m, 4 H), 7.77 - 7.84 (m, 6 H), 3.36 (s, 1 H), 0.42 (s, 9 H), -2.76 (s, 2 H) ppm. ^{13}C NMR (101 MHz,

$CDCl_3$): δ = ppm 142.76, 142.39, 142.01, 134.80, 134.52, 134.44, 134.40, 130.51, 130.35, 127.79, 126.71, 124.60, 123.39, 122.63, 121.65, 120.54, 119.27, 119.05, 104.98, 95.59, 83.64, 78.30, 0.06 ppm. MS: (MALDI-TOF, DCTB/MeCN) m/z calculated for $[C_{51}H_{38}N_4Si]^+$: 734.2860. Found: 734.2843. UV/Vis λ_{abs} (CH_2Cl_2)/nm (ε/$dm^3mol^{-1}cm^{-1}$): 419 (488,000), 516 (42,600), 551 (33,400), 590 (28,000), 646 (23,600).

5-(4-Bromophenyl)-10-(4-bromophenyl),15,20-diphenyl porphyrin (30)

General procudure A was used for diacylated dipyrromethane **22** (750 mg, 1.27 mmol) and dipyrromethane **8** (320 mg, 1.44 mmol). Purification was achieved by column chromatography (silica, 3:2, hexane/chloroform) affording the title compound as a purple solid (282 mg, 0.366 mmol, 29%).

^{1}H NMR (400 MHz, $CDCl_3$): δ = 8.81 - 8.89 (m, 8 H), 8.20 - 8.24 (m, 4 H), 8.07 - 8.11 (m, 4 H), 7.88 - 7.93 (m, 4 H), 7.75 - 7.81 (m, 6 H), -2.84 - -2.77 (m, 2 H) ppm. ^{13}C NMR (101 MHz, $CDCl_3$): δ = 141.96, 141.04, 135.85, 134.53, 129.92, 127.82, 127.76, 126.73, 122.50, 120.61, 118.50 ppm. MS: (MALDI-TOF, DCTB/MeCN) m/z calculated for $[C_{44}H_{28}N_4Br_2]^+$: 770.0675. Found: 770.0642. UV/Vis λ_{abs} (CH_2Cl_2)/nm (ε/$dm^3mol^{-1}cm^{-1}$): 418 (406,000), 514 (34,100), 548 (23,700), 589 (20,500), 644 (17,600).

References

1. J. Barber, *Nat. Struct. Biol.*, 2001, **8**, 577-579.

2. R. W. Wagner and J. S. Lindsey, *J. Am. Chem. Soc.*, 1994, **116**, 9759-9760.

3. Y. Furusho, T. Kimura, Y. Mizuno and T. Aida, *J. Am. Chem. Soc.*, 1997, **119**, 5267-5268.

4. R. Wormald, J. Evans, L. Smeeth and K. Henshaw, *Cochrane Db. Syst. Rev.*, 2007, **3**, CD002030.

5. K. M. Roth, N. Dontha, R. B. Dabke, D. T. Gryko, C. Clausen, J. S. Lindsey, D. F. Bocian and W. G. Kuhr, *J. Vac. Sci. Technol. B*, 2000, **18**, 2359-2364.

6. Q. M. Wang and D. W. Bruce, *Tetrahedron Lett.*, 1996, **37**, 7641-7644.

7. H. Fischer and H. Orth, *Die Chemie des Pyrroles*, Johnson Reprint Corporation, New York and London, 1968.

8. R. Willstatter, *Untersuchungen Uber Chlorophyll*, Springer, Berlin, 1913.

9. W. Kuster, *Z. Physiol. Chem.*, 1912, **82**, 463-483.

10. J. L. W. Thudichum, Report Med. Off. Privy Council, 1867.

11. H. Fischer and K. Zeile, *Liebigs. Ann. Chem.*, 1929, **468**, 98-116.

12. P. Rothemund, *J. Am. Chem. Soc.*, 1936, **58**, 625-627.

13. P. Rothemund and A. R. Mentoni, *J. Am. Chem. Soc.*, 1941, **63**, 267-270.

14. A. D. Adler, Shergali.W and F. R. Longo, *J. Am. Chem. Soc.*, 1964, **86**, 3145.

15. G. P. Arsenault, E. Bullock and S. F. Macdonald, *J. Am. Chem. Soc.*, 1960, **82**, 4384-4389.

16. J. S. Lindsey, I. C. Schreiman, H. C. Hsu, P. C. Kearney and A. M. Marguerettaz, *J. Org. Chem.*, 1987, **52**, 827-836.

17. R. H. Ball, G. D. Dorough and M. Calvin, *J. Am. Chem. Soc.*, 1946, **68**, 2278-2281.

18. H. Furuta, T. Asano and T. Ogawa, *J. Am. Chem. Soc.*, 1994, **116**, 767-768.

19. G. R. Geier, B. J. Littler and J. S. Lindsey, *J. Chem. Soc. Perkin Trans. 2*, 2001, 701-711.

20. B. J. Littler, Y. Ciringh and J. S. Lindsey, *J. Org. Chem.*, 1999, **64**, 2864-2872.

21. P. Rothemund, *J. Am. Chem. Soc.*, 1935, **57**, 2010-2011.

22. M. Gouterman, *J. Chem. Phys.*, 1959, **30**, 1139-1161.

23. C. Rimington, *Biochem. J.*, 1960, **75**, 620-623.

24. R. Wiglusz, J. Legendziewicz, A. Graczyk, S. Radzki, P. Gawryszewska and J. Sokolnicki, *J. Alloy. Compd.*, 2004, **380**, 396-404.

25. C. Weiss, *J. Mol. Spectrosc.*, 1972, **44**, 37-80.

26. R. F. Pasternack, E. J. Gibbs and J. J. Villafranca, *Biochemistry (US)*, 1983, **22**, 2406-2414.

27. X. F. Huang, K. Nakanishi and N. Berova, *Chirality*, 2000, **12**, 237-255.

28. M. Uttamlal and A. S. Holmes-Smith, *Chem. Phys. Lett.*, 2008, **454**, 223-228.

29. A. Stradomska and J. Knoester, *J. Chem. Phys.*, 2010, **133**, 094701.

30. M. R. Dayer, A. A. Moosavi-Movahedi and M. S. Dayer, *Protein Peptide Lett.*, 2010, **17**, 473-479.

31. E. D. Becker, R. B. Bradley and C. J. Watson, *J. Am. Chem. Soc.*, 1961, **83**, 3743.

32. M. Kadish and E. Van Caemelbecke, *J. Solid State Electr.*, 2003, **7**, 254-258.

33. A. Wolberg and J. Manassen, *J. Am. Chem. Soc.*, 1970, **92**, 2982-&.

34. K. Prakash, R. Kumar and M. Sankar, *RSC Adv.*, 2015, **5**, 66824-66832.

35. C.-W. Lee, H.-P. Lu, C.-M. Lan, Y.-L. Huang, Y.-R. Liang, W.-N. Yen, Y.-C. Liu, Y.-S. Lin, E. W.-G. Diau and C.-Y. Yeh, *Chem. Eur. J.*, 2009, **15**, 1403-1412.

36. A. Yella, H.-W. Lee, H. N. Tsao, C. Yi, A. K. Chandiran, M. K. Nazeeruddin, E. W.-G. Diau, C.-Y. Yeh, S. M. Zakeeruddin and M. Graetzel, *Science*, 2011, **334**, 629-634.

37. L.-L. Li and E. W.-G. Diau, *Chem. Soc. Rev.*, 2013, **42**, 291-304.

38. Z. M. Liu, A. A. Yasseri, J. S. Lindsey and D. F. Bocian, *Science*, 2003, **302**, 1543-1545.

39. D. T. Gryko, C. Clausen, K. M. Roth, N. Dontha, D. F. Bocian, W. G. Kuhr and J. S. Lindsey, *J. Org. Chem.*, 2000, **65**, 7345-7355.

40. K. Kadish, *The Porphyrin Handbook: Synthesis and Organic Chemistry*, Elsevier, 2000.

41. L. R. Milgrom, *J. Chem. Soc. Perk. T. 1.*, 1984, 1483-1487.

42. S. H. H. Zaidi, F. M. Fico and J. S. Lindsey, *Org. Process. Res. Dev.*, 2006, **10**, 118-134.

43. S. G. Boxer, G. L. Closs and J. J. Katz, *J. Am. Chem. Soc.*, 1974, **96**, 7058-7066.

44. J. J. Katz and T. R. Janson, *Ann. NY. Acad. Sci.*, 1973, **206**, 579-603.

45. University of Wisconsin, http://www.chem.wisc.edu/areas/reich/nmr/08-tech-01-relax.htm, (accessed 10/2016).

Chapter 4:

The Synthesis of Porphyrin Dimers for Covalent Organic Frameworks

Introduction

Covalent Organic Frameworks

Covalent organic frameworks (COFs) are a family of porous, crystalline materials which are constructed from molecular building blocks composed entirely of light elements (C, H, Si, B, O and N) which are linked together *via* strong covalent bonds. These, along with other porous, crystalline materials are of considerable interest due to their potential applications in gas storage[1], catalysis[2] and optoelectronics.[3] Crystalline materials usually show superior performance over amorphous materials in these areas due to the fact they have well defined, stable pore structures of uniform size distribution, have tuneable metrics and they can have organic functionality incorporated into their structure.[4, 5]

Design

COFs are produced using the principles of dynamic covalent chemistry (DCC) and reticular synthesis in which predesigned molecular building blocks are brought together in order to create a well-ordered extended network.[6] Throughout the formation of the network, the structural integrity of the building blocks is retained. This principle was first used to create metal organic frameworks (MOFs); networks of metal ions or clusters of metal ions held together by multi-dentate organic linkers.[7] There are a vast number of routes to creating MOFs due to the numerous different coordination preferences of the metal ions combined and the diversity of size, shape and functionality of the organic linker, so it is understandable that there has been a considerable amount of research undertaken in this area.[8-10] DCC allows for the formation, breakage and reformation of covalent bonds, offering control of a reaction with thermodynamics rather than kinetics which form irreversible covalent bonds.[11] The reversibility of covalent bond formation allows for greater control of network formation as any errors in structure can be broken and reformed to a more favourable configuration. The fact that structural defects are

essentially detected and repaired by systems using DCC means that highly ordered crystalline products form, possessing high thermal stability.[12]

Depending on the building units used, COFs will form either 2D or 3D structures.[13] 2D structures present themselves as sheets that can stack on top of each other to create periodically aligned columns (figure 4.1), generating ordered π-systems that can be difficult to achieve by others means.[14] The ordered π-systems can be used for charge transfer applications, making them useful in fields such as optoelectronics and photovoltaics.[15, 16] 3D structured COFs are porous networks with very high surface areas, numerous open sites and low densities; all properties which make them more suitable for gas storage applications.[1]

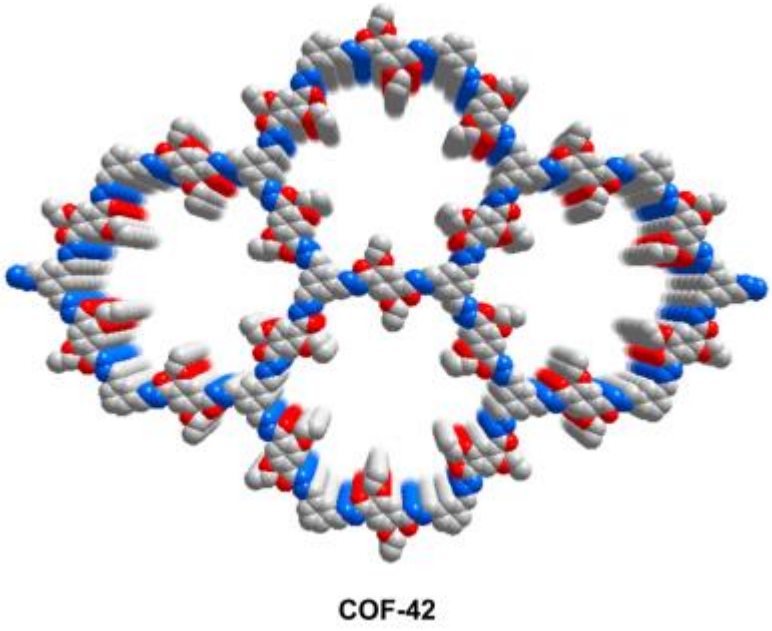


Figure 4.1 COF-42 showing 2D sheets stacking so that the pores are aligned.[17]

A careful selection of the building units allows control of the pore size and shape. Tilford *et al.* showed how this could be achieved by affixing varying lengths of alkyl chains onto the building blocks of the COFs.[18] It has been shown that boronate-ester based COFs,

although thermodynamically stable, have a high susceptibility to attack and are easily hydrolysed, especially 'bare pore' COFs. The method of alkylating the pores has been utilised to reduce the degree of COF hydrolysis.[19] Other connecting groups such as imine and hydrazone COFs have been used, demonstrating that COFs can be made from a variety of starting materials.[20, 21]

Synthesis

In 2005, Yaghi showed that the principle of reticular synthesis could be used to form covalent bonds to produce COFs and introduced this new family of materials to the scientific community.[22] Various reaction media and conditions have been tried for the synthesis of COFs, one of the most common methods is solvothermal synthesis. In solvothermal synthesis, monomers and mixed solvents are placed in sealed tubes that have been degassed. The solution is then heated to a certain temperature for the designated reaction time. A sealed reaction vessel is used to allow for the presence of water molecules needed for the reverse reaction, a key requirement if the reaction is to be under thermodynamic control.[23] The COF forms as a precipitate which is collected by washing with suitable solvents and drying.

The reaction Yaghi's team designed was a condensation reaction using solvothermal conditions, as shown below in figure 4.2. 1,4-benzenediboronic acid (BDBA) and 2,3,6,7,10,11-hexa-hydroxytriphenylene (HHTP) are reacted together for 72 h at 100 °C in a solution of mesitylene/1,4-dioxane. In the condensation reaction between BDBA and HHTP, boronate esters are formed. The boronate esters link the two molecules together *via* covalent bonds to produce COF-5.

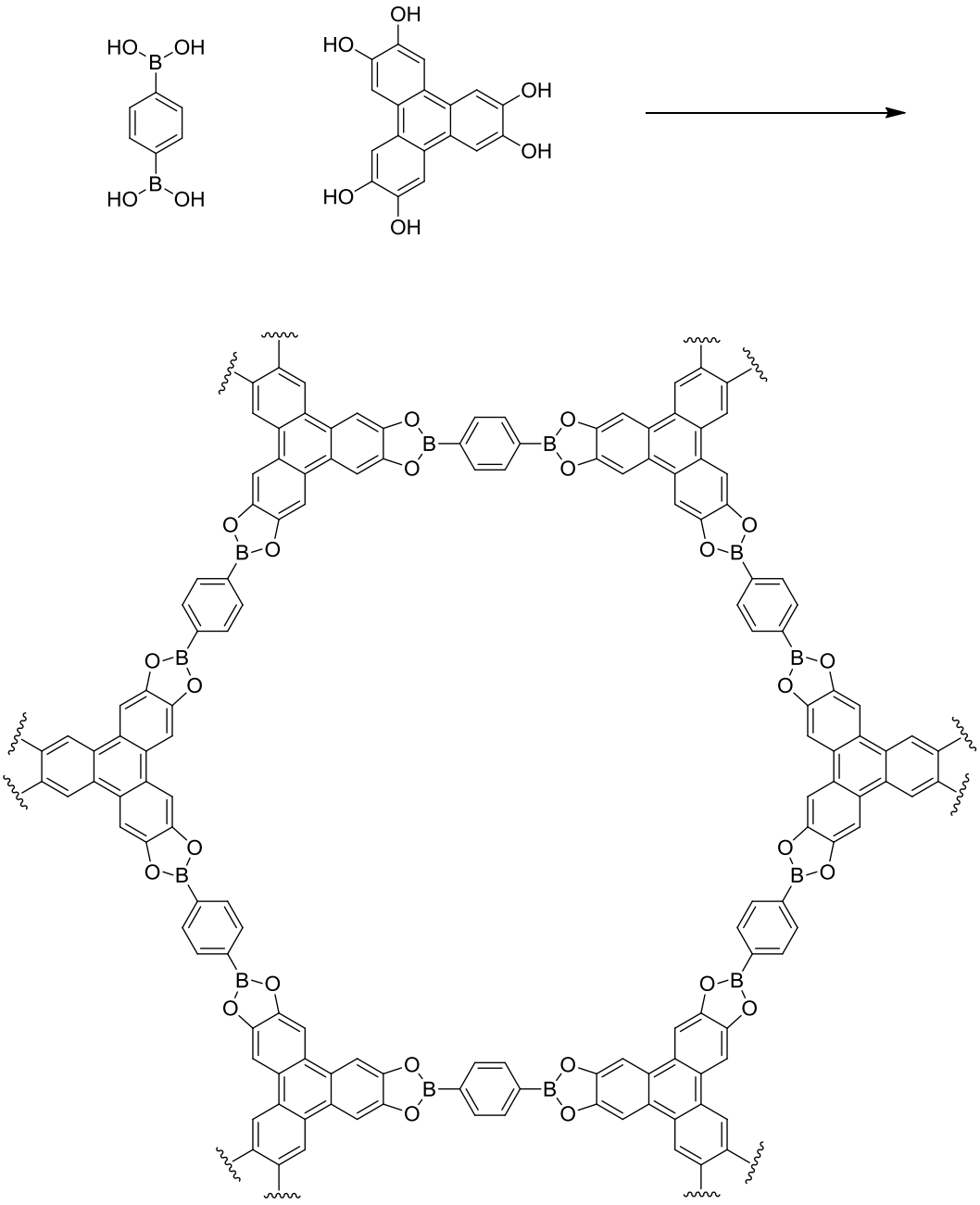


Figure 4.2 Synthesis of COF-5.

A related method, ionothermal synthesis, has been used to create covalent triazine frameworks (CTFs), a specific type of COF which have triazine units incorporated into their structure.[24] Aromatic nitrile monomers are heated in one equivalent of molten $ZnCl_2$ and trimerised. The trimer units then combine to form the CTF. The metal salt is removed from the product by crushing the samples into powders and washing with dilute HCl solution.[25] CTFs are often more chemically stable than other COFs but

accompanying this is a lower degree of crystallinity due to the poor reversibility of the cyclical trimerisation reaction.[26]

Microwave synthesis has been used as an alternative method of creating COFs.[27, 28] COF-5 was produced by heating HHTP and BDBA together using microwave irradiation to 100 °C for 20 min in a 1:1 mixture mesitylene and 1,4-dioxane, in a sealed tube under a dinitrogen atmosphere with stirring.[29] The resulting mixture was filtered, washed with dry acetone and heated again in acetone to give the COF in 68% yield. In comparison, the work done by Yaghi's team achieved 73% yield of the same COF after heating at 100 °C for 72 h.[22] This shows that COF formation can be a quick process and that previous synthetic strategies could be altered for microwave synthesis while still achieving the same final product.

The synthesis of COFs on surfaces has led to the term surface covalent organics frameworks (SCOFs). The incorporation of COFs onto substrates is of great significance as it should allow them to be more effectively connected to real devices *via* electrodes. This would help in fully utilising their potential in molecular electronic devices.[30] SCOF-2 (analogous to COF-5) has been prepared from sublimation of HHTP and BDBA from separate molybdenum crucibles onto an Ag (111) surface in UHV conditions. This method resulted in a near monolayer being formed, dominated by the hexagonal conformations but also presenting some faults in 5, 7 and 8 membered ring structures.[30] Other surfaces such as highly ordered pyrolytic graphite (HOPG) have also been used to prepare SCOFs. Biphenyldiboronic acid was deposited onto a HOPG surface and heated to 150 °C for 1 h in the presence of $CuSO_4.5H_2O$. $CuSO_4.5H_2O$ is needed as a water 'reservoir' to help regulate the chemical equilibrium, water molecules being released as the

sample is heated to participate in the reverse reaction. The monolayer coverage was increased from 7% without any $CuSO_4.5H_2O$ to 98% when it was included.[31]

The preparation of COF thin films on single layer graphene on SiO_2 (SLG/SiO_2) substrate has been demonstrated by Dichtel. For the synthesis, SLG/SiO_2 was placed in a reaction tube with the desired building units under solvothermal conditions. The SCOFs were then formed on the SLG/SiO_2 in a directional manner. [32]

To characterise the COFs, properties such as the crystallinity, porosity and morphology need to be assessed. As of yet, there have only been a couple of instances of single crystals being produced of COF materials[33, 34] so structure analysis is usually done using powder X-ray diffraction (PXRD) with the Pawley method used to refine the structure.[35] NMR spectroscopy is a powerful tool in assessing composition and connectivity within the COF since COFs are composed of many elements that have NMR active isotopes (^{1}H, ^{11}B, ^{13}C, ^{15}N, ^{17}O and ^{29}Si). Surface area and porosity can be assessed using gas absorption/desorption measurements. Morphology can be observed using scanning electron microscopy (SEM) and pore sizes can be estimated using transmission electron microscopy (TEM). Photoconductivity can be explored using an on-off experiment, where the current passing through the COF is measured while it is exposed to a light source being turned on and off and I-V curves can be constructed by sandwiching the COF between platinum electrodes and doing a linear sweep of voltages and measuring the current.

Porphyrin-Based COFs

For molecules to possess efficient charge transport and stability, strong covalent bonds are needed.[36] Charge transport occurs more readily if the charge transporting material has

ordered conducting channels. As porphyrins possess a planar π-conjugated structure, they are able to stack neatly into well-defined crystalline arrangements.[37] The planar nature of porphyrins also means that the π-π interactions of the molecule are more favourable compared to non-planar molecules, stabilising the channelled structure. This makes porphyrins ideal candidates to be made into COFs.

There have already been examples of porphyrin containing COFs reported within the literature; in one study, a team found that the charge that was transported by the COF could be altered depending on what was coordinating at the centre of the porphyrin ring.[38] The research conducted by Feng *et al.* showed that when freebase porphyrin was present in the COF depicted in figure 4.3, holes were the charge carriers being transported. When Cu (II) was coordinated to the porphyrin, electrons were transported and Zn (II) coordinated porphyrins were found to be ambipolar.

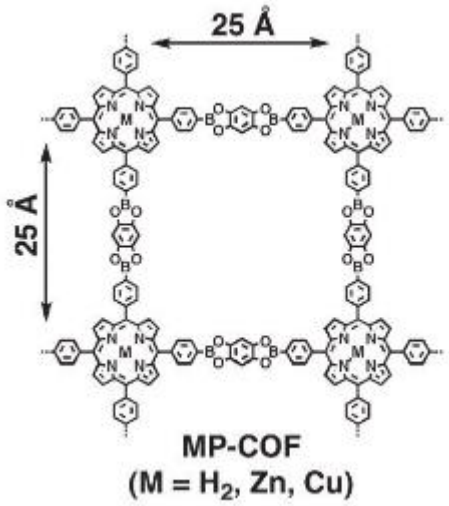


Figure 4.3 Porphyrin containing COF that exhibits charge transfer abilities.[38]

Porphyrin networks have also been used for catalysis, the system developed by Chen *et al.* is illustrated in figure 4.4. The framework is able to transform a large range of sulfides

into sulfoxides with very little or no over-oxidisation observed.[39] The catalytic system was able to be recycled at least three times without noticeable loss of activity and selectivity. Similar porphyrin-based frameworks acting as catalytic systems for oxidation reactions, such as the epoxidation of styrene, have also been reported.[40] Though current literature has few other examples, more research into this area is needed before we can fully appreciate the scope of these framework materials.

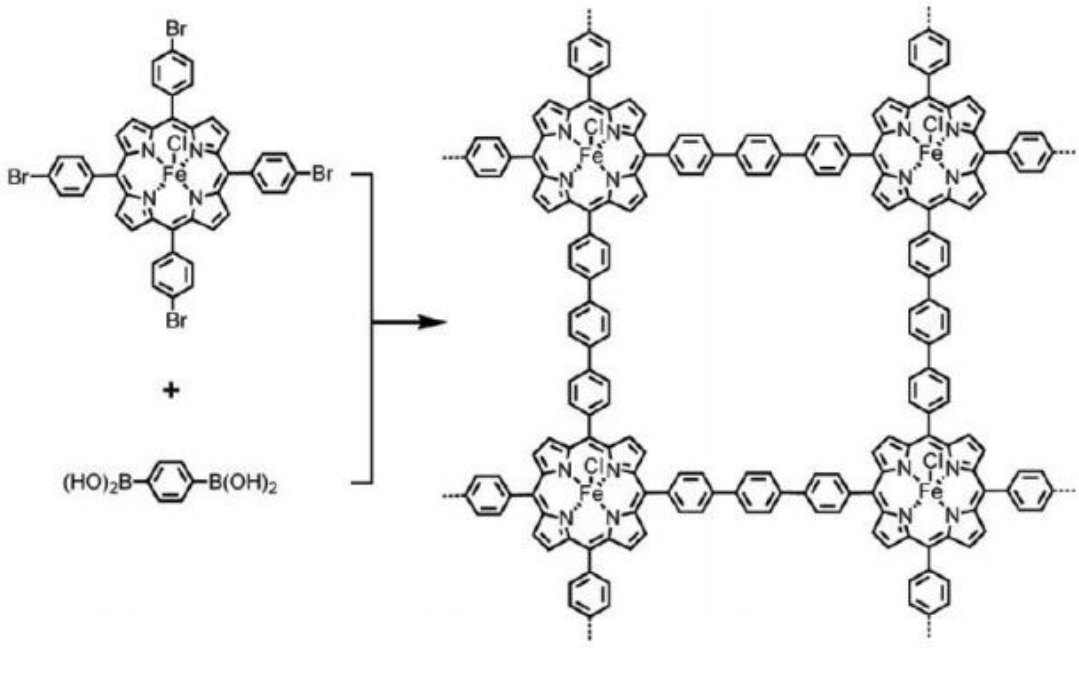


Figure 4.4 Porphyrin based COF that catalyses the oxidation of sulfides to sulfoxides.[39]

Recently a method of forming porphyrin COFs has been developed by Grill which takes molecular building blocks with reactive side groups termed 'legs'.[41] The legs act as the connection points to form the permanent covalent bonds upon activation. In this method, it is important that the legs are able to be activated selectively, without breaking other covalent bonds so that a well-defined, regular structure results. For this purpose, Grill selected carbon-halogen bonds as these have much lower bonding energies that the rest of the core structure. It is also important to note that, as this process is not

reversible, it is not an example of self-assembly whereas the other common methods of COF formation are.

There are two different variations to the method that Grill devised to create COFs. In the first variation, the sample is placed in a Knudsen cell and heated to remove halogen atoms generating carbon radicals. The sample effuses from the cell and is deposited onto a surface where the radicals recombine forming carbon-carbon bonds. In the second variation, the sample is deposited onto a surface which is then heated to cleave halogen-carbon bonds, generating carbon radicals. The radicals then combine with each other to form carbon-carbon bonds. It is thought that the recombining of radicals takes place on the surface for both methods. Although formation of dimers may be possible in the Knudsen cell, the sublimation of dimers and large systems from the Knudsen cell would require high evaporator temperatures that would actually cause the decomposition of the structures.[42] Some production of dimer could result from recombination in the air, however due to the low molecular density the quantities would be very low, if any.

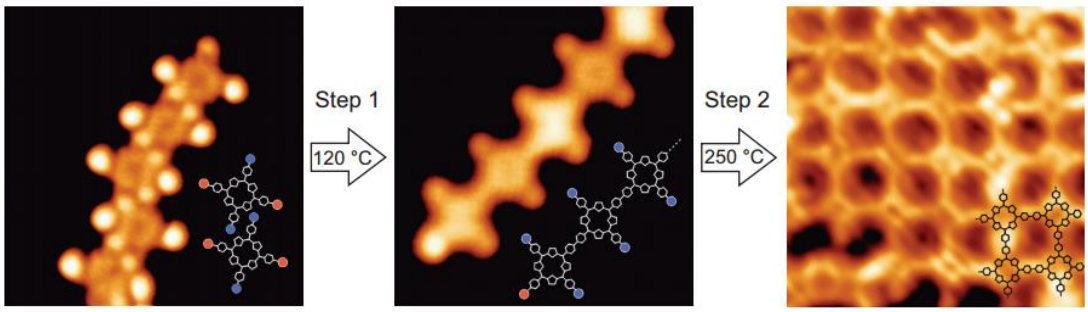


Figure 4.5 Hierarchical growth of trans-Br_2I_2TPP on an Au (111) surface. [43]

In a study by Grill, 5,15-bis(4'-bromophenyl)-10,20-bis(4'-iodophenyl)porphyrin (*trans*-Br_2I_2TPP) was used to explore the idea of hierarchical growth on surfaces (figure 4.5).[43] *Trans*-Br_2I_2TPP has two carbon-bromine bonds and two carbon-iodine bonds. The concept of hierarchical growth arises from the fact that these two types of bonds have different dissociation energies. In this system, there would be initial activation of the

iodine sites, followed by activation at the bromine sites at higher temperatures. In the work done by Grill, molecules of *trans*-Br_2I_2TPP are deposited onto an Au (111) surface at RT from an evaporator. The STM images shown in figure 4.5 depict the COF formation process using *trans*-Br_2I_2TPP monomers (left). The monomers are heated at 120 °C, selectively breaking the carbon-iodine bonds to from radicals which recombine to from 1D arrays (centre). The bromine sites are then activated by heating the sample to 250 °C in a second step to form the 2D array (right).

The main aim for the work presented in this chapter was to create porphyrin dimer molecules terminated with bromo- substituents (figure 4.6). In a similar manner to the work previously published by Grill, it was hoped that by depositing the target molecules onto as surface with subsequent heating, the bromine atoms would dissociate and the resultant radical species would recombine on the surface to create COFs.

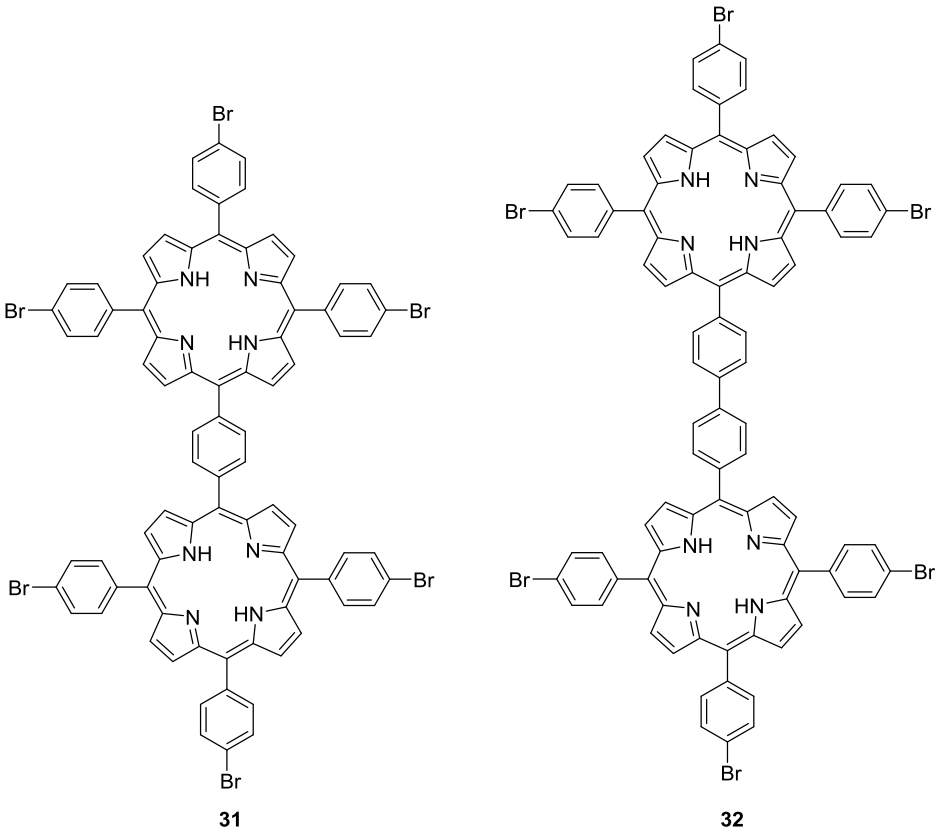
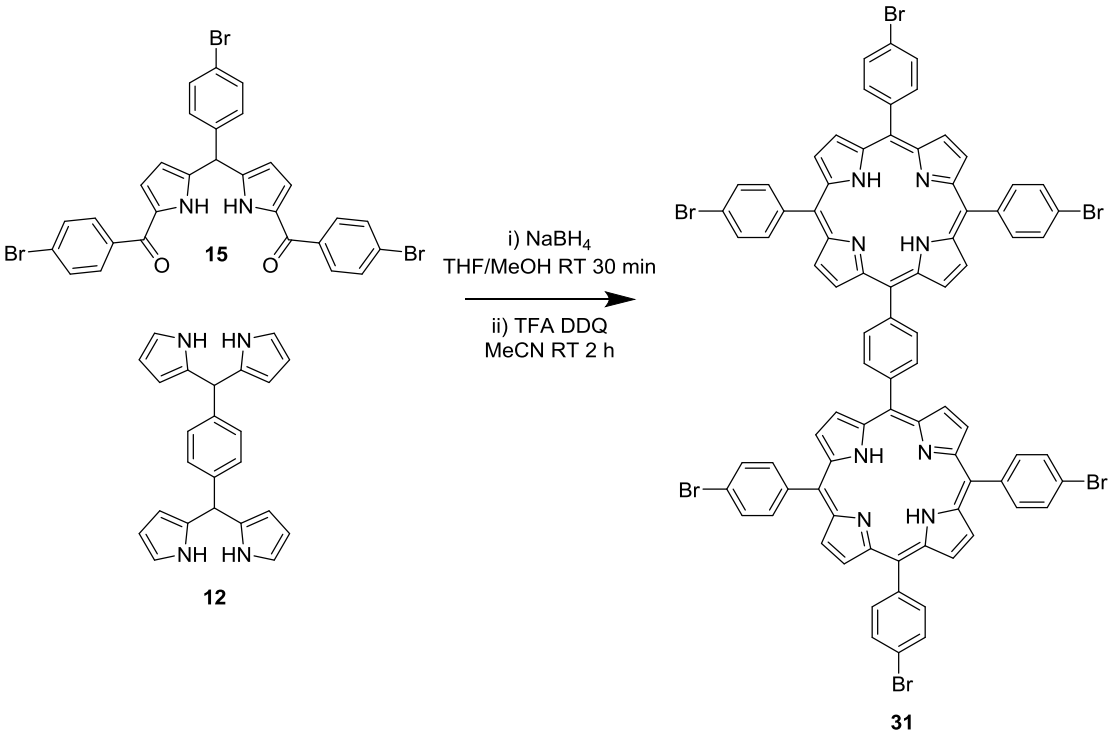


Figure 4.6 Structures of porphyrin dimers 31 and 32

Results and discussion

Synthesis of Porphyrin Dimers 31 and 32



Scheme 4.1 Synthesis of porphyrin dimer 31.

Porphyrin dimers **31** and **32** were designed with the intention of using them to form COFs with the methodology of Grill in mind.[43] Porphyrin dimer **31** was synthesised from **12** and **15** in a yield of 4% (scheme 4.1). Porphyrin dimer **32** was synthesised from **13** and **15** in the same manner as porphyrin dimer **31**, in a yield of 6% (scheme 4.2). As discussed in the previous chapter, the initial step is a reduction of **15** from a diacylated-dipyrromethane to a dipyrromethane-dicarbinol species. Following this, the condensation reaction to form the porphyrinogen dimer requires two equivalents of the dicarbinol reacting with one equivalent of the dipyrromethane species. As this reaction involves forming two porphyrinogen rings, the potential for intermolecular reactions to occur, forming polymeric materials is much higher than in the previous chapter (see figure 4.7) and so lower yields are expected.

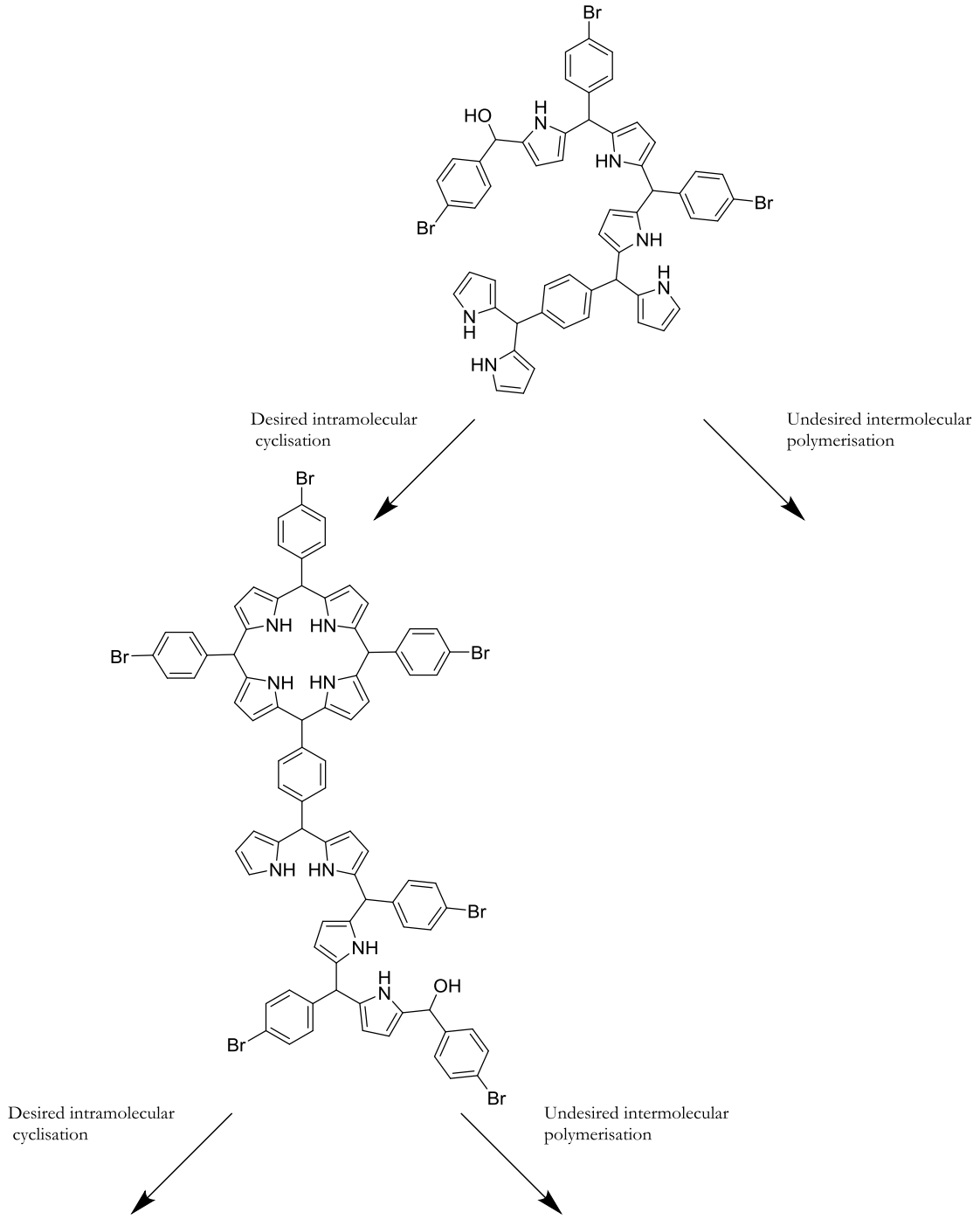
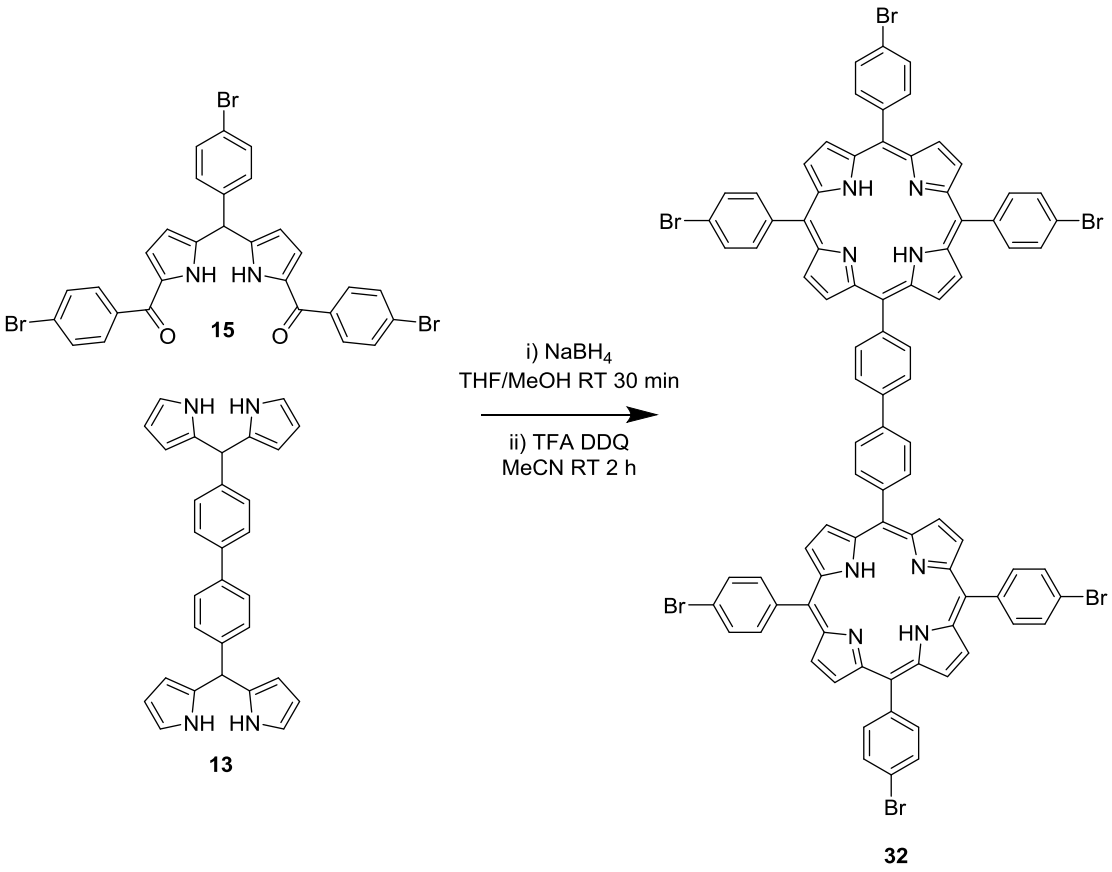


Figure 4.7 Possible reaction pathways when forming porphyrin dimer 31.

To minimise the potential for the unwanted intermolecular polymerisation reactions to occur, the reaction was conducted in high dilution, 1 mM with respect to the dicarbinol species. Despite this precaution the majority of the reactants do not follow the ideal reaction pathway as is evidenced by the low yields of **31** and **32**. The low yields from synthesising porphyrin dimers using this method can perhaps be explained by looking at

the reaction to from the first porphyrinogen as a 20% yield reaction (which is typical for monomeric porphyrin synthesis), this is then followed by another 20% yield reaction to form the second porphyrinogen giving an approximate yield of 5%.



Scheme 4.2 Synthesis of porphyrin dimer 32.

Porphyrin dimers **31** and **32** were able to be purified by column chromatography. Initially the attempts had a chloroform/hexane mix as the mobile phase, but this resulted in a significant amount of purple material remaining at the start of the column. Although some of the desired target compound did elute, complete separation was not achieved so that impurities were also eluted at the same time. As the target compounds had low solubility, the eluent system was modified so that it contained TFA. The introduction of TFA protonates the porphyrin molecules, increasing the solubility by helping to reduce stacking and aggregation. This had the desired effect and spectroscopically pure samples of dimers **31** and **32** were able to be obtained using this eluent system.

Crystallographic Analysis of 31

Single crystals suitable for X-ray diffraction were grown of $[\mathbf{31}H_4]^{4+}[CF_3COO]_4^-$ from a chloroform/benzene/TFA slow evaporation (figure 4.8).

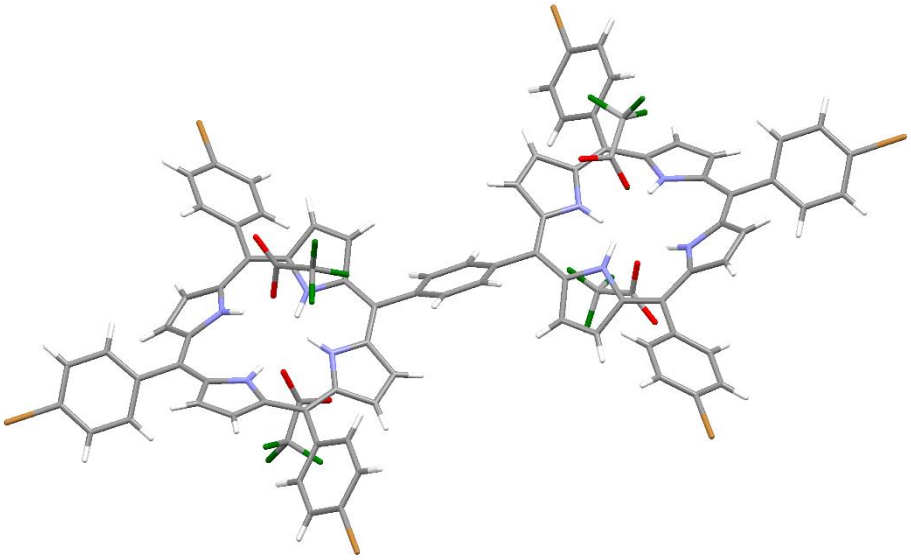


Figure 4.8 Crystal structure of porphyrin dimer salt $[\mathbf{31}H_4]^{4+}[CF_3COO]^-_4$.

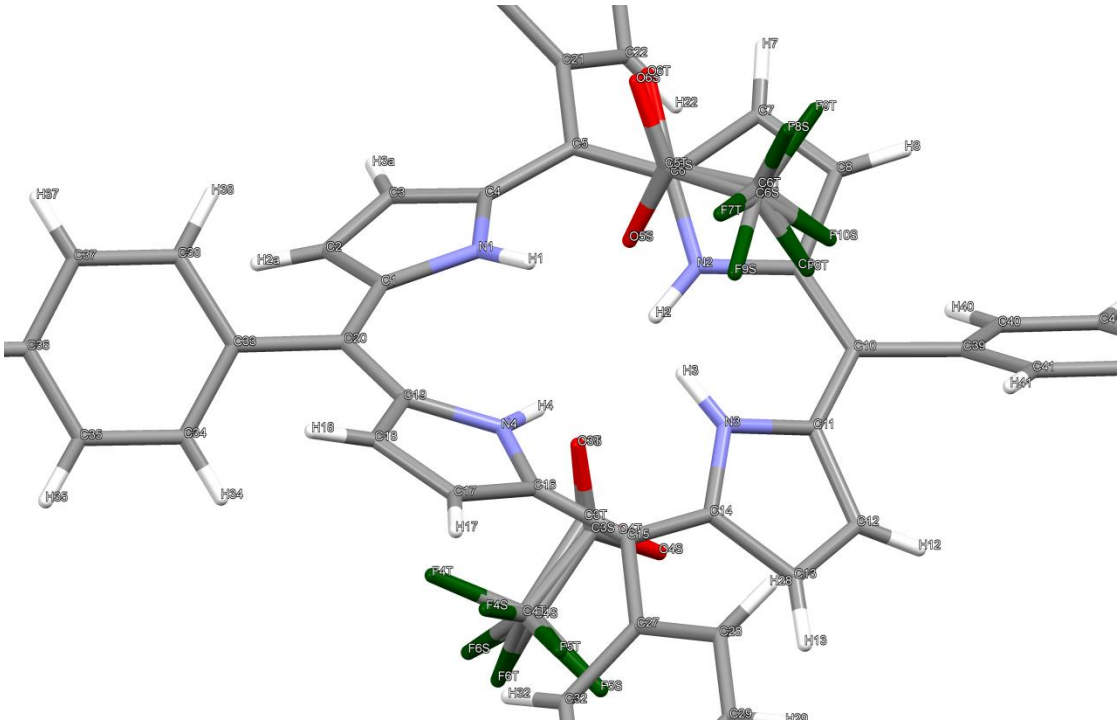


Figure 4.9 Disorder of TFA anions in the crystal structure data obtained for $[\mathbf{31}H_4]^{4+}[CF_3COO]^-_4$.

The data collected indicated that there was some disorder of the TFA anions, shown in figure 4.9. There are two TFA anions each with an occupancy of approximately 0.5 below the ring and two more TFA anions with an occupancy of approximately 0.5 above the ring. The position of the oxygen atom involved in hydrogen bonding (labelled (O3S/O3T for the anion positioned below and O5S/O5T for the anion positioned above) remains in a very similar position for both occupancies of the anion. The disorder of the anions can be seen as a rotation in position of the fluorine atoms and a slight lateral movement of the adjoining carbon atom. The hydrogen bonding interactions of these atoms are listed in table 4.1 below.

Table 4.1 Hydrogen bonding interactions for $[31H_4]^{4+}[CF_3COO]^-_4$.

	D-H (Å)	H…A (Å)	D…A (Å)	<(DHA) (°)
N2-H2...O3T	0.88	2.01	2.859(4)	161.2
N2-H2...O3S	0.88	2.01	2.859(4)	161.2
N1-H1...O5T	0.88	2.04	2.881(4)	159.7
N1-H1...O5S	0.88	2.04	2.881(4)	159.7
N4-H4...O3T	0.88	2.03	2.794(4)	145.1
N4-H4...O3S	0.88	2.03	2.794(4)	145.1
N3-H3...O5T	0.88	2.00	2.831(4)	156.5
N3-H3...O5S	0.88	2.00	2.831(4)	156.5

Figure 4.9 shows significant distortion of the porphyrin ring due to the protonation of the core-nitrogen atoms. The charged species and distorted conformation is then stabilised by interactions with the TFA anions.[44] In the following figures 4.10-4.15, the presence of the TFA anions is omitted for clarity. A plane was created using the pyrrolic carbons C1, C2, C3, C4 seen in red referred to as pyrrole ring A. Similarly, planes were

created for pyrrole ring B; comprised of C6, C7, C8, C9 (green), pyrrole ring C; C11, C12, C13, C14 (orange) and pyrrole ring D; C16, C17, C18, C19 (blue). There is a centre of symmetry in this structure so that the interactions and bending of both of the porphyrin rings in the dimer are the same.

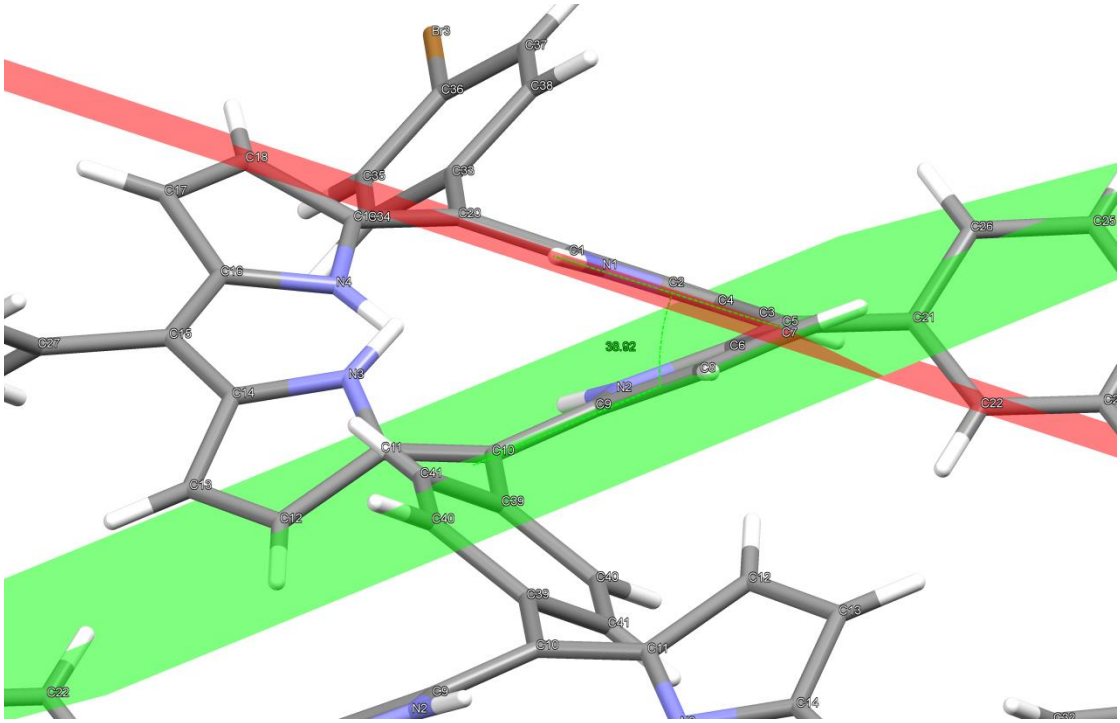


Figure 4.10 Twisting angle 38.92° between pyrrole rings A and B for $[31H_4]^{4+}[CF_3COO]^-_4$.

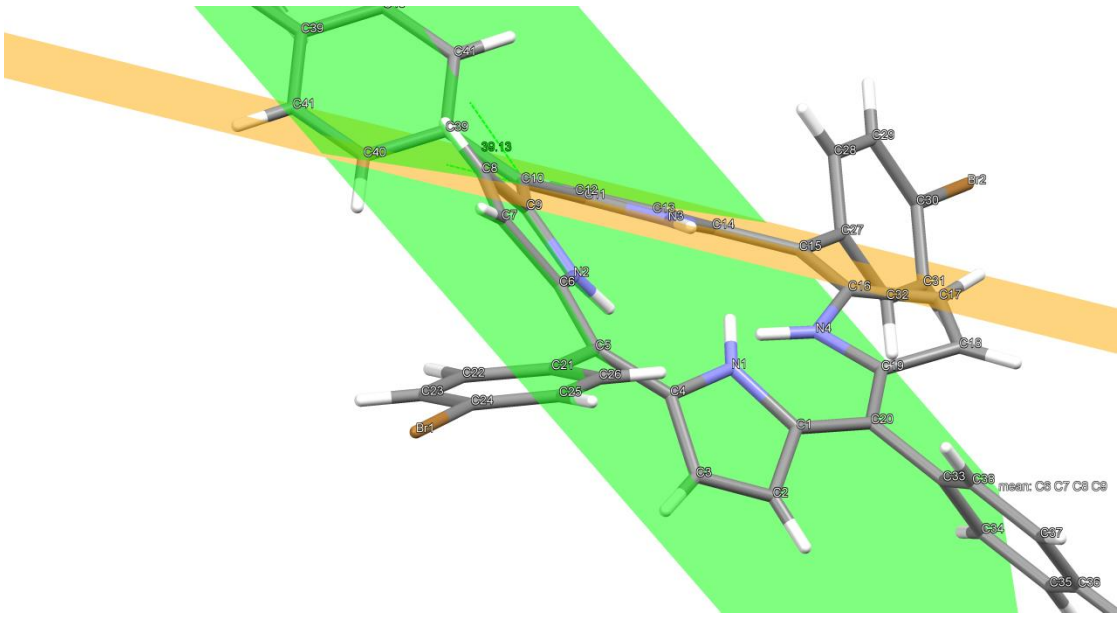


Figure 4.11 Twisting angle 39.13° between pyrrole rings B and C for $[31H_4]^{4+}[CF_3COO]^-_4$.

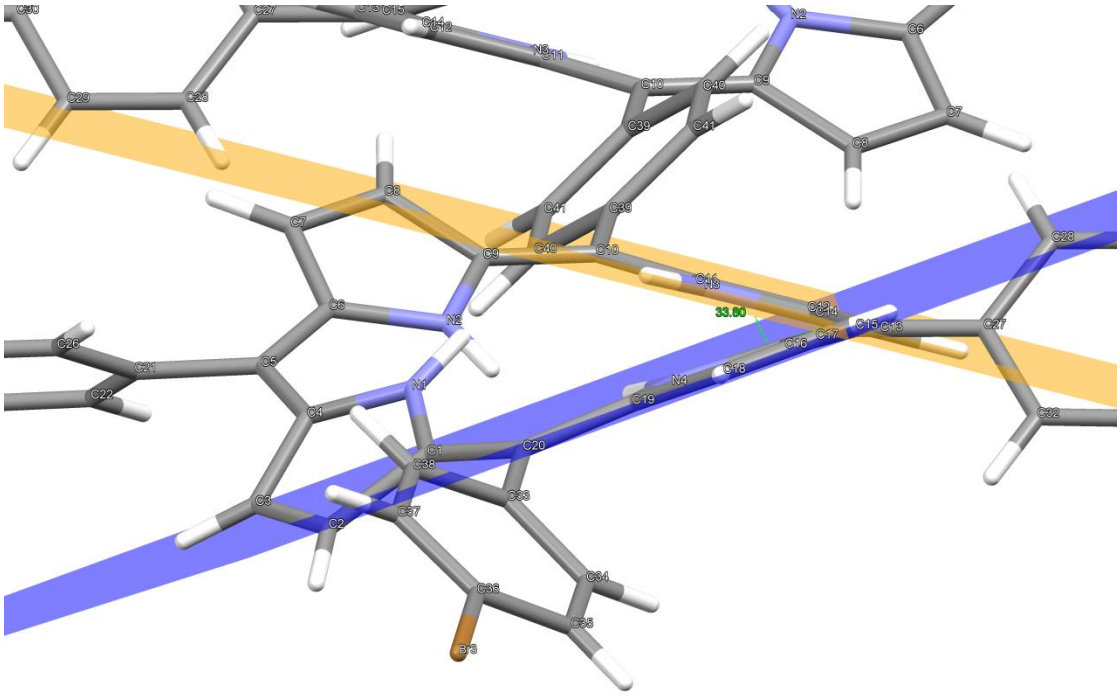


Figure 4.12 Twisting angle 33.80° between pyrrole rings C and D for $[31H_4]^{4+}[CF_3COO]^-_4$.

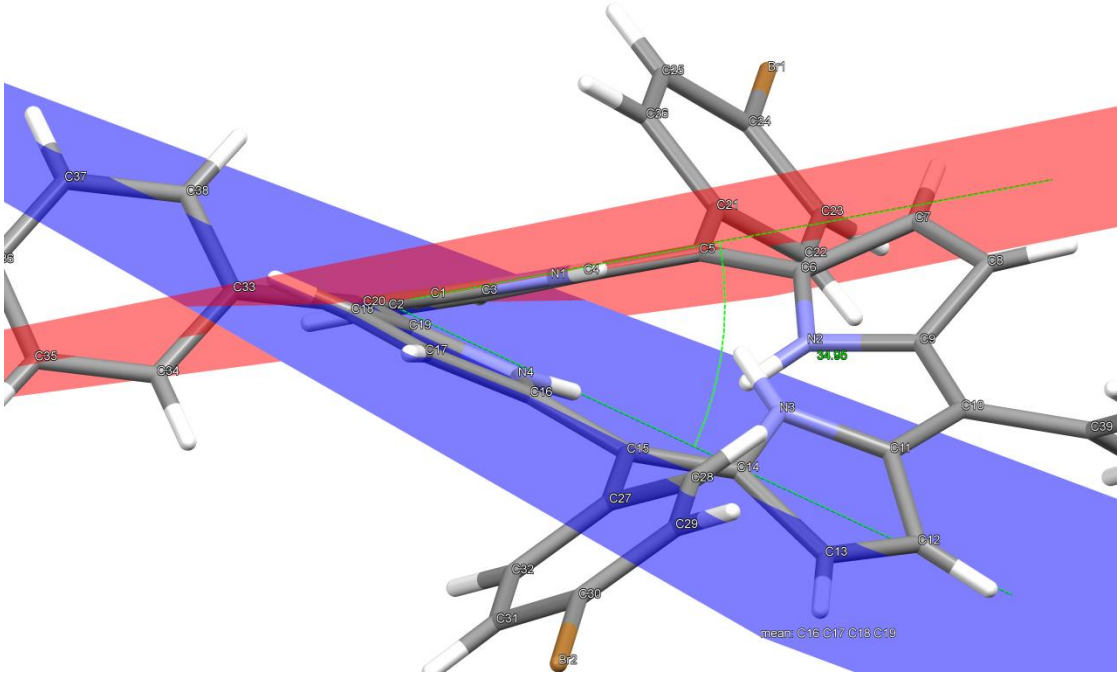


Figure 4.13 Twisting angle 34.95° between pyrrole rings D and A for $[31H_4]^{4+}[CF_3COO]^-_4$.

The angle at which planes created from pyrrolic groups at opposing sides of the ring intersect was also measured. The shorter length of hydrogen bonds with the TFA anion above the porphyrin ring (an indication of a stronger interaction) pictured by the red and orange planes intersecting corresponds with a larger angle of distortion (55.28°) compared to the longer hydrogen bond lengths with TFA anions below the porphyrin ring (50.03°). The twisting and bending angles measured are summarised in table 4.2.

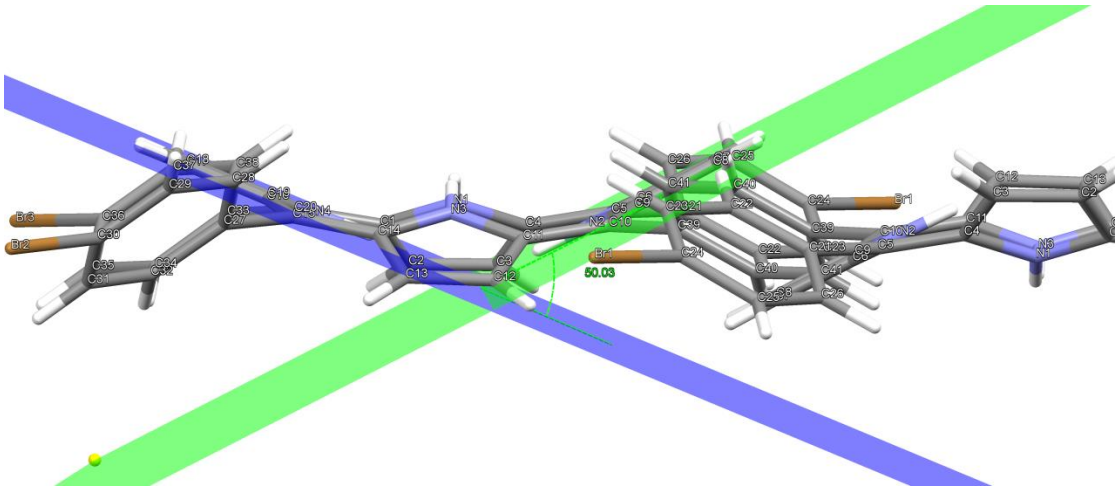


Figure 4.14 Bending angle 50.03° between pyrrole rings A and C for $[31H_4]^{4+}[CF_3COO]^-_4$.

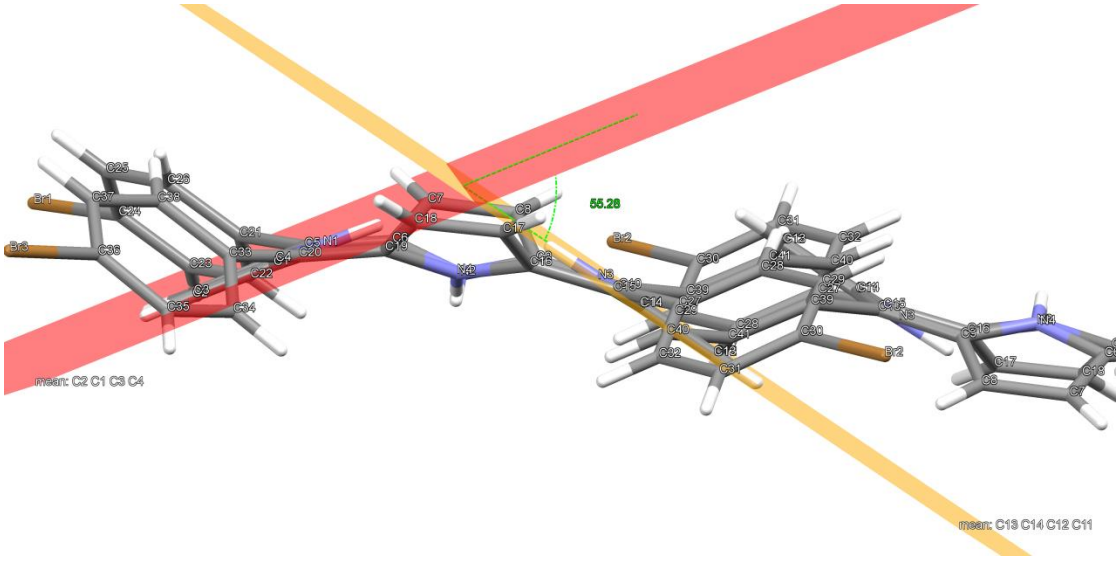


Figure 4.15 Bending angle 55.26° between pyrrole rings B and D for $[31H_4]^{4+}[CF_3COO]^-_4$.

Table 4.2 Summarising angles measured for figure 4.10-4.15.

Twisting angle from planes A and B	38.92°
Twisting angle from planes B and C	39.13°
Twisting angle from planes C and D	33.80°
Twisting angle from planes D and A	34.95°
Bending angle from planes A and C	50.03°
Bending angle from planes B and D	55.26°

Crystallographic Analysis of 32

Single crystals of salts suitable for X-ray diffraction were grown of $[\mathbf{32}H_4]^{4+}[CF_3COO]_4^-$ from chloroform/TFA slow evaporation. Although there is potentially a centre of inversion in **32**, the crystal grown of the salt $[\mathbf{32}H_4]^{4+}[CF_3COO]_4^-$ loses that symmetry as the TFA anions coordinate differently to each of the porphyrin rings as shown in Figure 4.16.

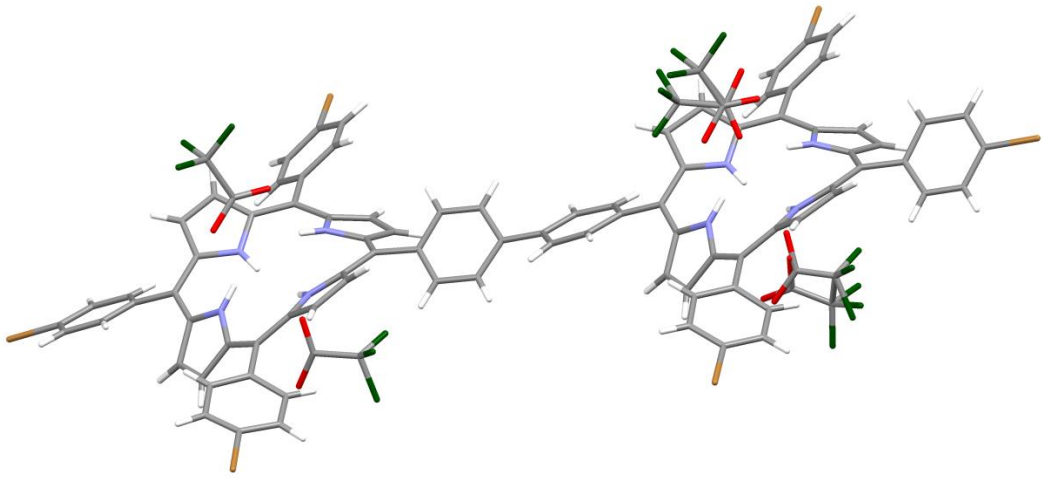


Figure 4.16 Crystal structure of porphyrin dimer salt $[32H_4]^{4+}[CF_3COO]_4^-$.

Figure 4.17 is labelled to identify the atoms involved with hydrogen bonding (interactions listed in table 4.3); it shows that there is one TFA anion located above and one TFA

anion located below the leftmost porphyrin ring (referred to as porphyrin ring A). Porphyrin ring B shown in figure 4.18 has some disorder associated with the TFA anions which interact with it. Above porphyrin ring B there are two TFA anions, each with an occupancy of 0.5. Below porphyrin ring B there is another pair of TFA anions, one at an occupancy of 0.2 containing the O10T atom involved in hydrogen bonding the other at an occupancy of 0.8 containing the O12T atom involved in hydrogen bonding.

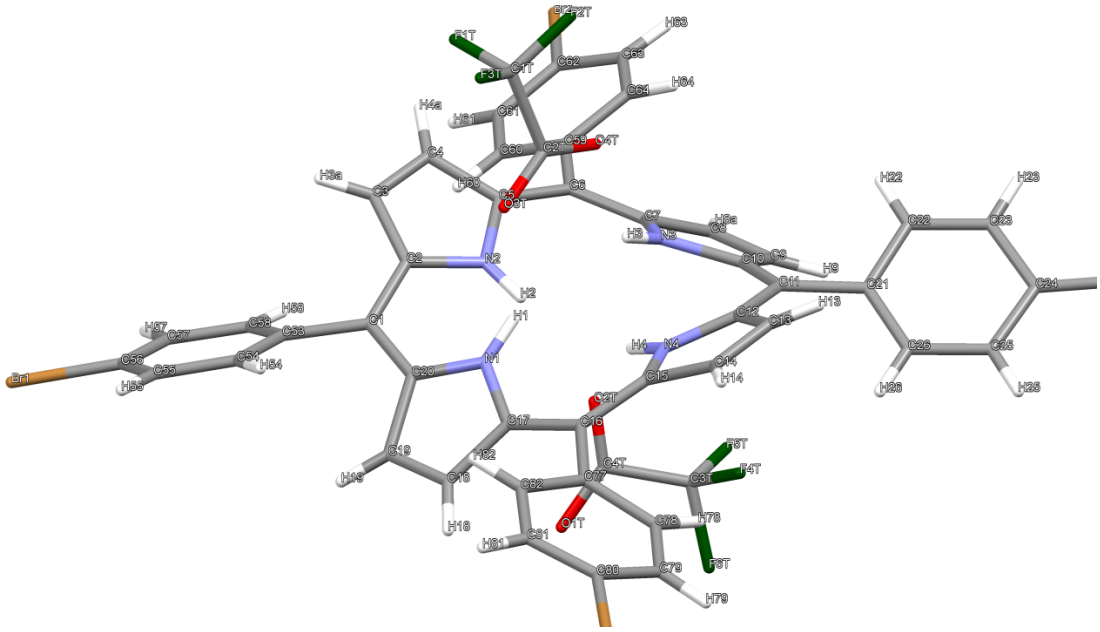


Figure 4.17 Porphyrin ring A and location of TFA anions for $[32H_4]^{4+}[CF_3COO]^-_4$.

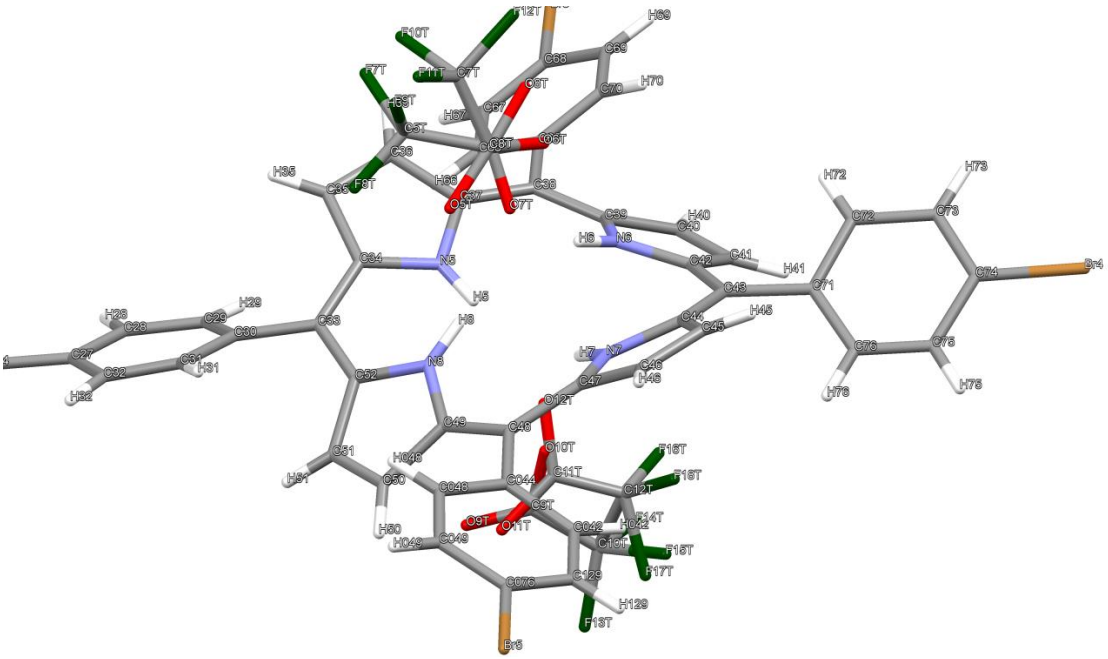


Figure 4.18 Porphyrin ring B and location and disorder of TFA anions for $[32H_4]^{4+}[CF_3COO]^-_4$.

Table 4.3 Hydrogen bonding interactions for porphyrin dimer salt $[32H_4]^{4+}$ $[CF_3COO]^-_4$.

	D-H (Å)	H...A (Å)	D...A (Å)	<DHA (°)
N1-H1...O3T	0.88	2.09	2.732(15)	129.3
N2-H2...O2T	0.88	2.17	2.993(18)	155.3
N3-H3...O4T	0.88	2.04	2.685(18)	129.2
N4-H4...O2T	0.88	2.03	2.824(16)	149.5
N5-H5...O12T	0.88	2.12	2.96(2)	158.7
N6-H6...O6T	0.88	2.09	2.69(7)	125.1
N6-H6...O7T	0.88	2.12	2.97(2)	161.2
N7-H7...O10T	0.88	2.47	3.19(5)	139.5
N7-H7...O12T	0.88	2.02	2.844(17)	155.3
N8-H8...O5T	0.88	2.15	2.80(7)	130
N8-H8...O7T	0.88	2.16	3.00(2)	160.7

As with the previous structure, the data collected for $[\mathbf{32}H_4]^{4+}[CF_3COO]^-_4$, showed significant distortion of the porphyrin rings from the usual planar conformation. Figures 4.19-4.24 analyse the distortion of porphyrin ring A, the pyrrolic carbons C2, C3, C4, C5 were used to create a plane shown in red, referred to as pyrrole ring A. Similarly, planes were created for pyrrole ring B; comprised of C7, C8, C9, C10 (green), pyrrole ring C; C12, C13, C14, C15 (orange) and pyrrole ring D; C17, C18, C19, C20 (blue). Figures 4.25-4.30 analyse the distortion of porphyrin ring B and planes were created using C34, C35, C36, C37 (red) for pyrrole ring A; C39, C40, C41, C42 (green) for pyrrole ring B; C44, C45, C46, C47 (orange) for pyrrole ring C; C49, C50, C51, C52 (blue) for pyrrole ring D. The twisting and bending angles measured are summarised in tables 4.4 and 4.5.

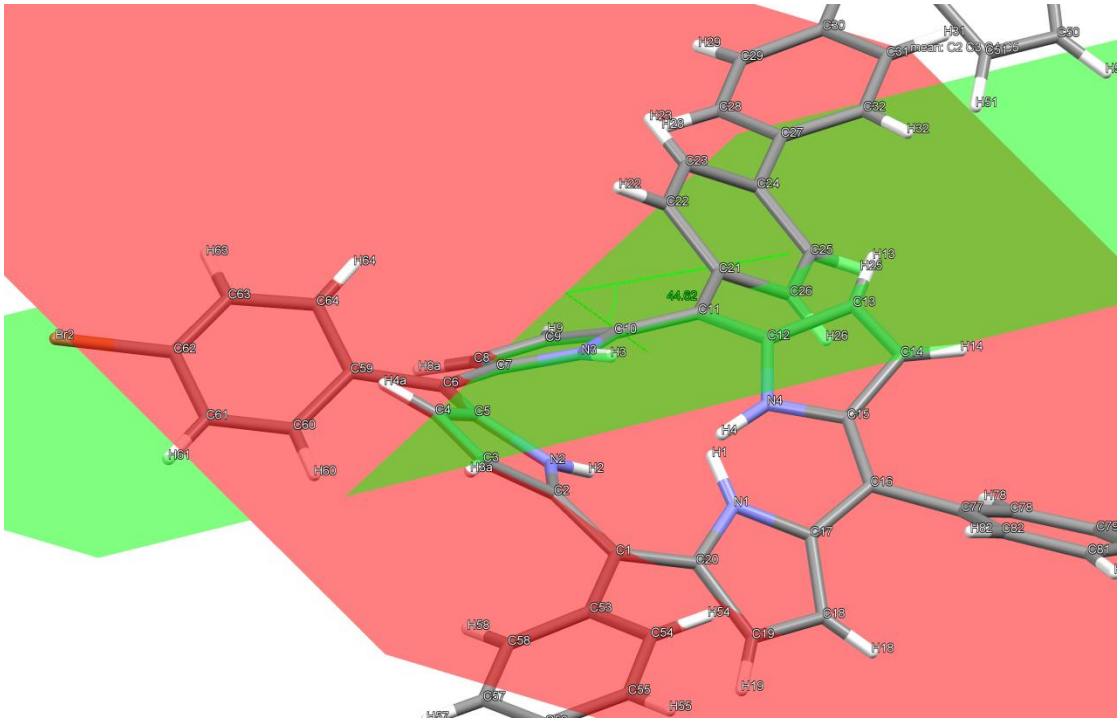


Figure 4.19 Twisting angle 44.62° between pyrrole rings A and B on porphyrin ring A of $[32H_4]^{4+}[CF_3COO]^-_4$.

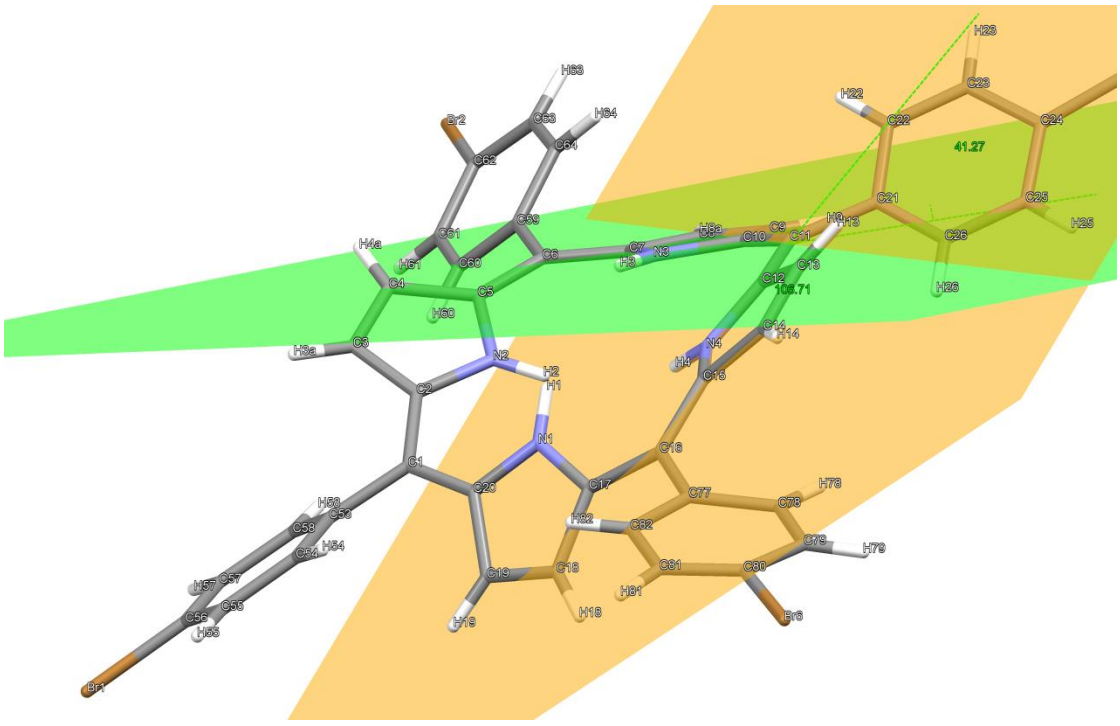


Figure 4.20 Twisting angle 41.27° between pyrrole rings B and C on porphyrin ring A of $[32H_4]^{4+}[CF_3COO]^-_4$.

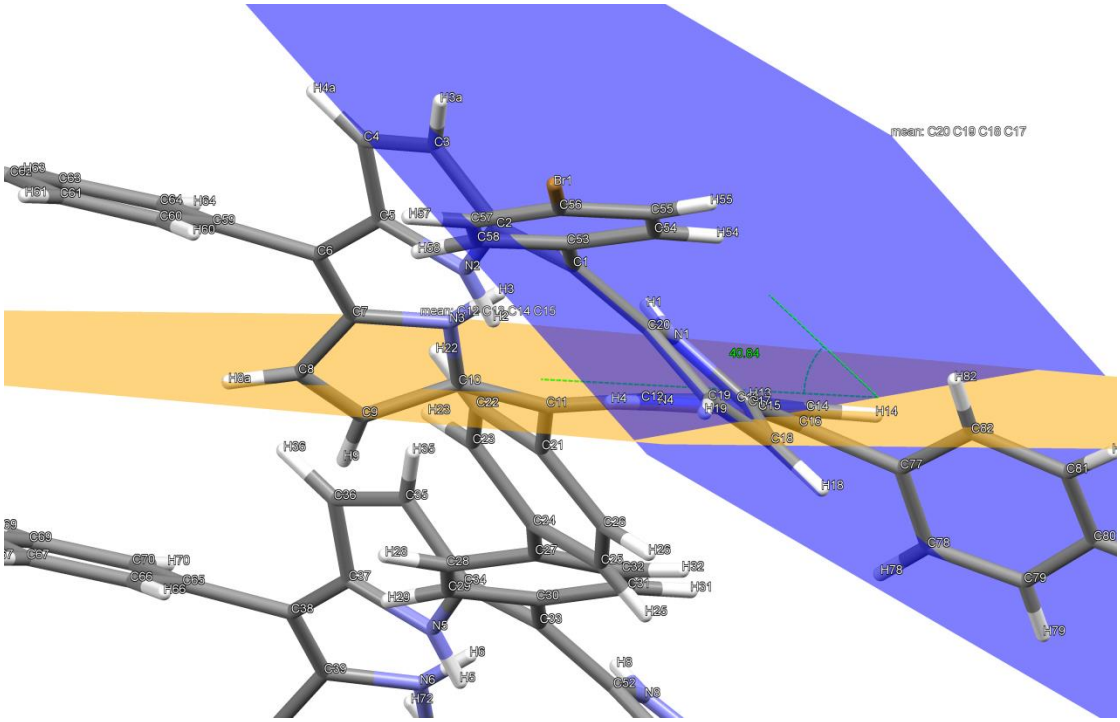


Figure 4.21 Twisting angle 40.84° between pyrrole rings C and D on porphyrin ring A of $[32H_4]^{4+}[CF_3COO]^-_4$.

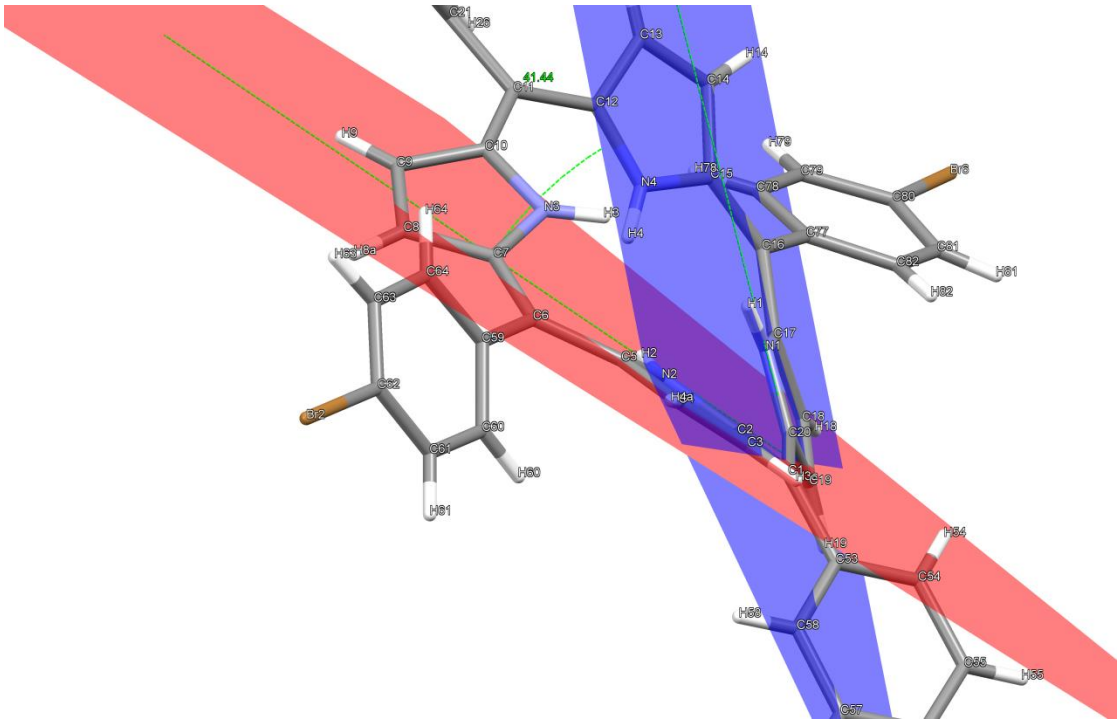


Figure 4.22 Twisting angle 41.44° between pyrrole rings D and A on porphyrin ring A of $[32H_4]^{4+}[CF_3COO]^-_4$.

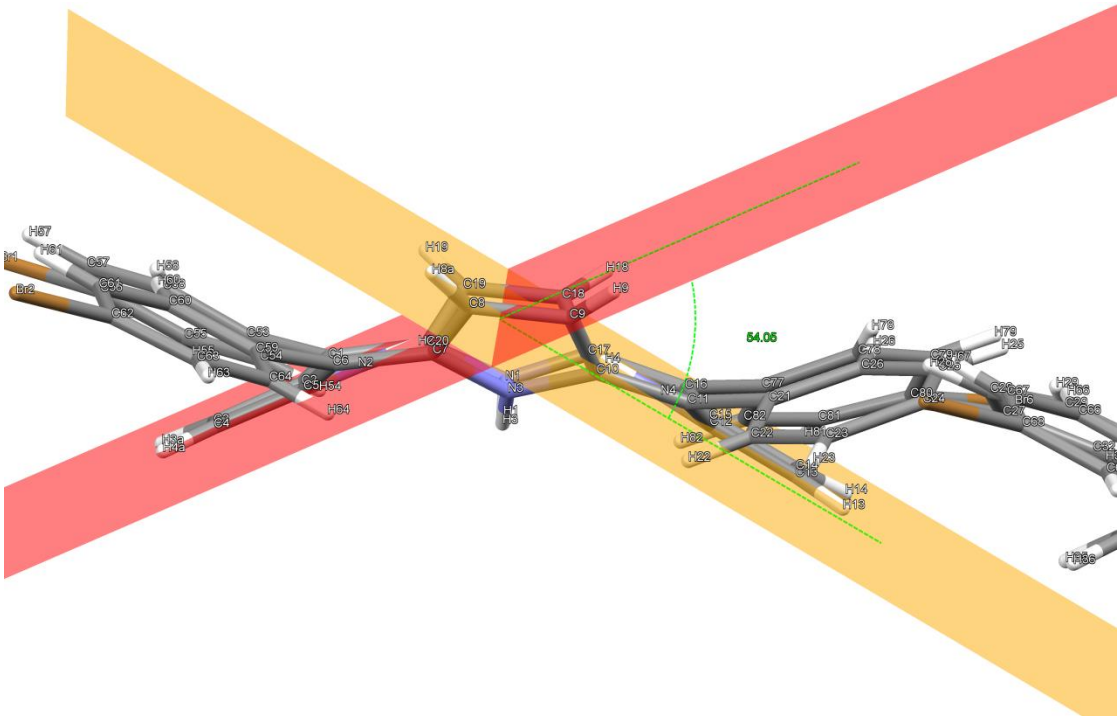


Figure 4.23 Bending angle 54.05° between pyrrole rings A and C on porphyrin ring A of $[32H_4]^{4+}[CF_3COO]^-_4$.

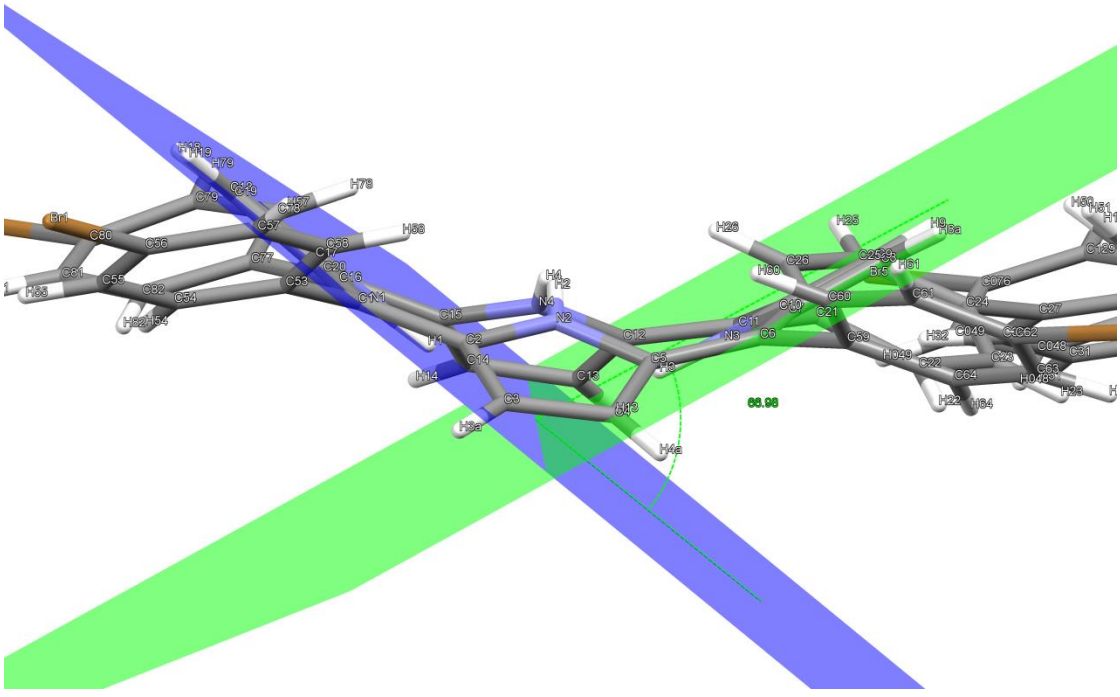


Figure 4.24 Bending angle 66.96° between pyrrole rings B and D on porphyrin ring A of $[32H_4]^{4+}[CF_3COO]^-_4$.

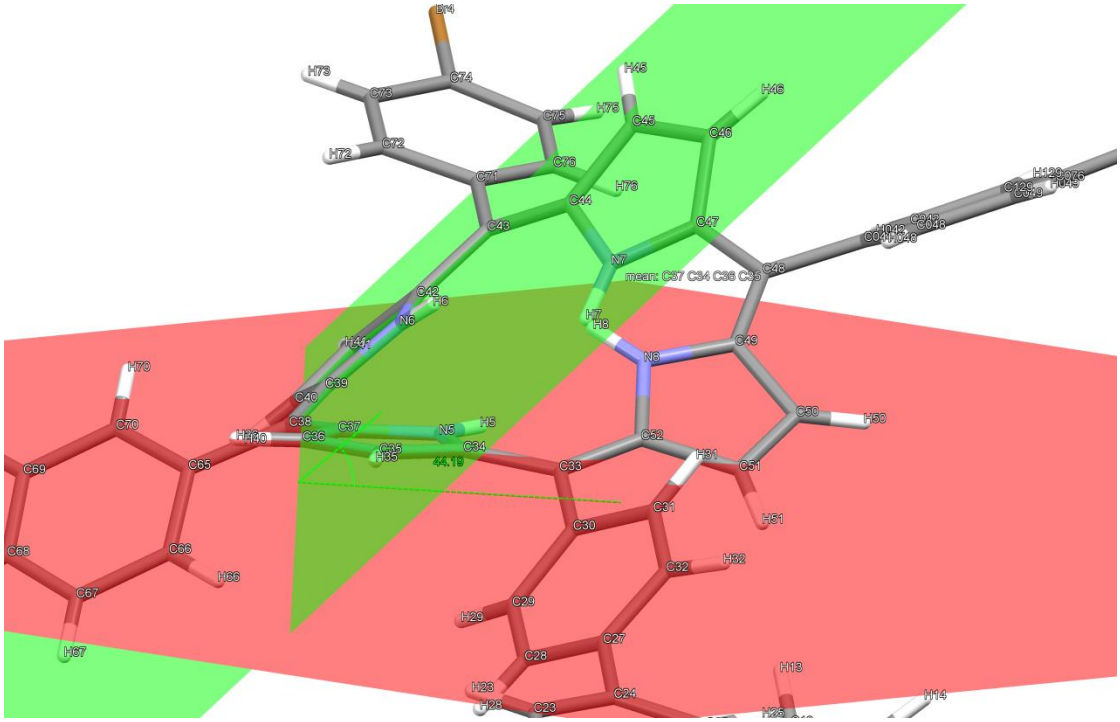


Figure 4.25 Twisting angle 44.19° between pyrrole rings A and B on porphyrin ring B of $[32H_4]^{4+}[CF_3COO]^-_4$.

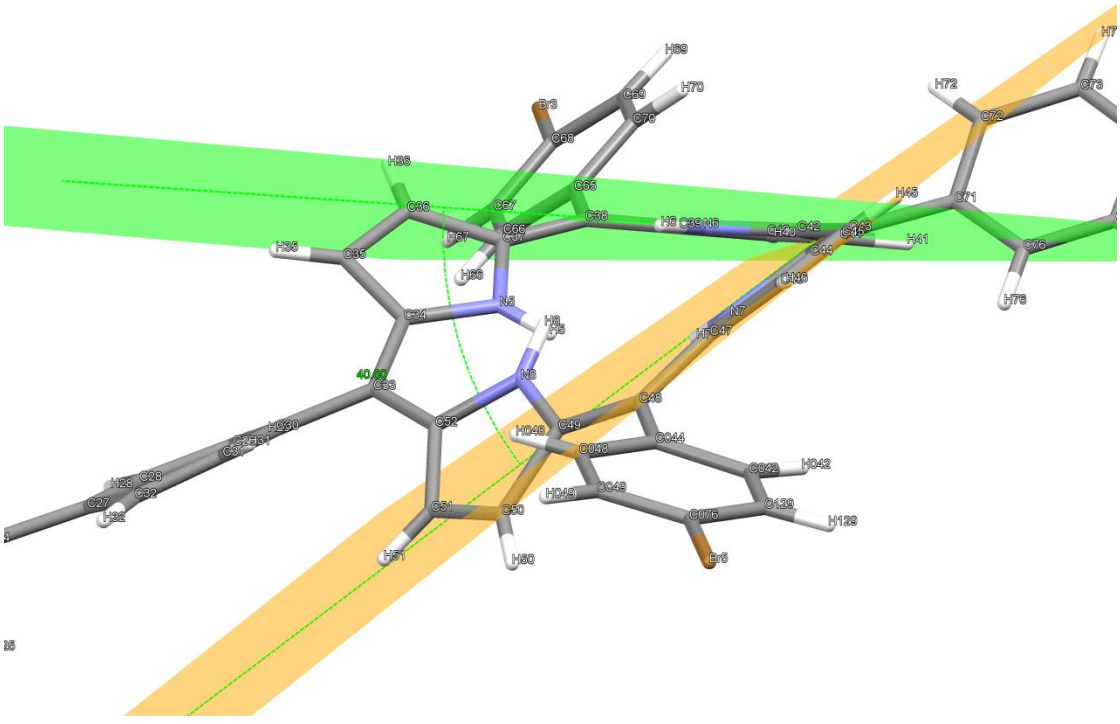


Figure 4.26 Twisting angle 40.80° between pyrrole rings B and C on porphyrin ring B of $[32H_4]^{4+}[CF_3COO]^-_4$.

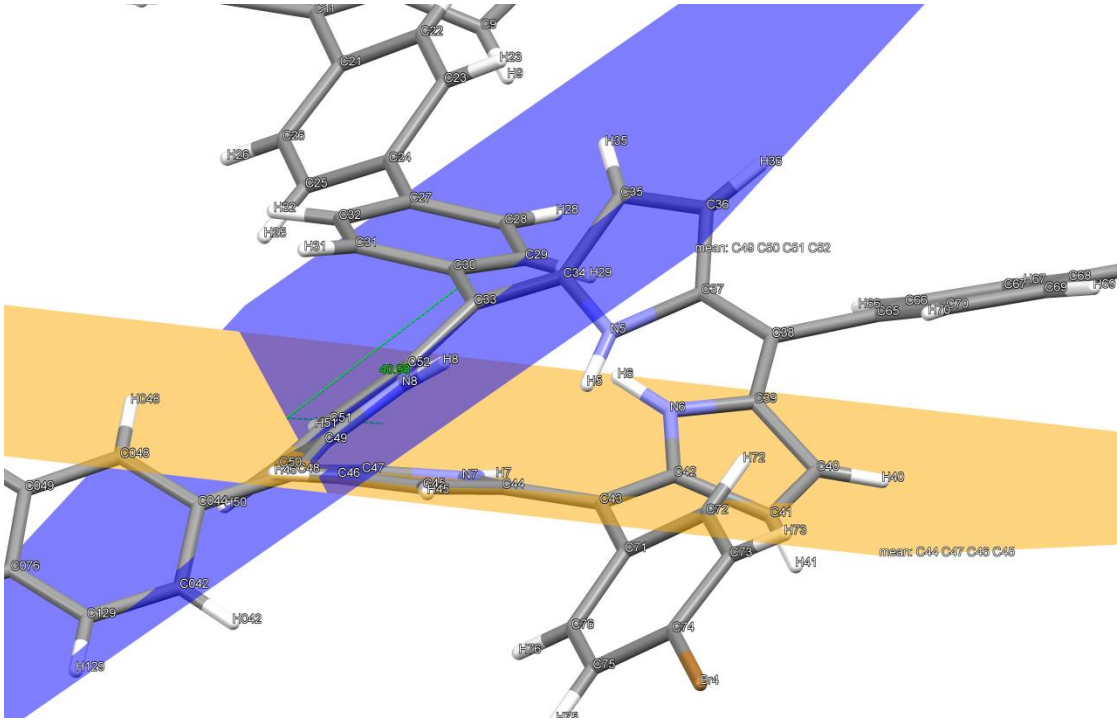


Figure 4.27 Twisting angle 40.98° between pyrrole rings C and D on porphyrin ring B of $[32H_4]^{4+}[CF_3COO]^-_4$.

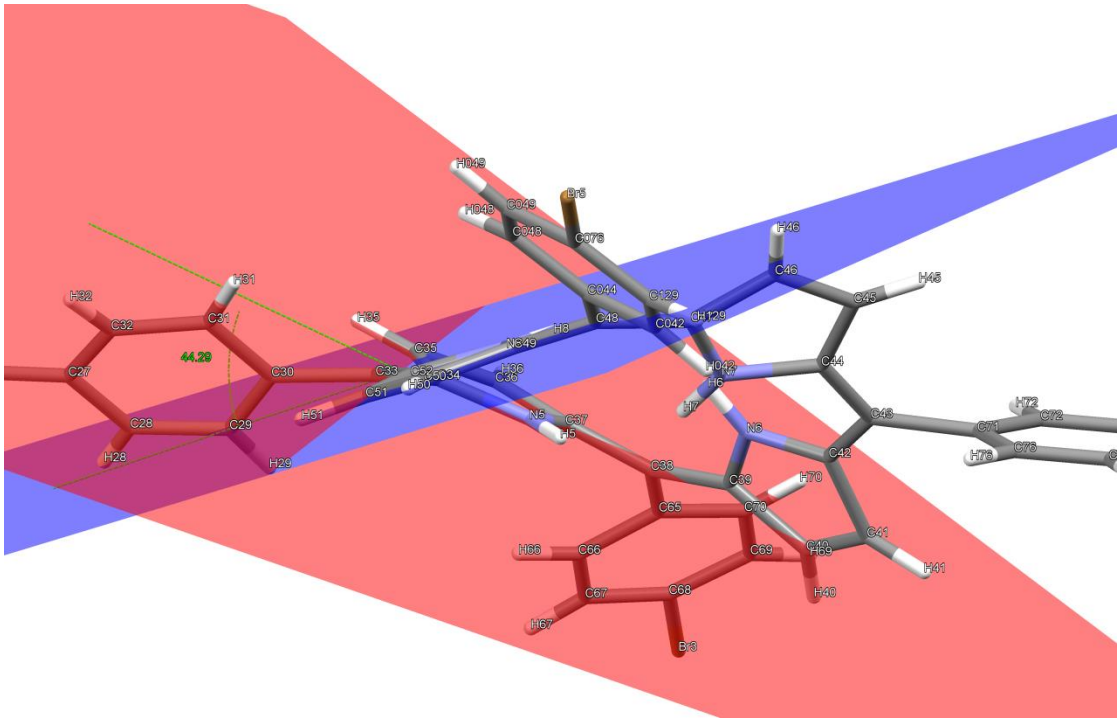


Figure 4.28 Twisting angle 44.29° between pyrrole rings D and A on porphyrin ring B of $[32H_4]^{4+}[CF_3COO]^-_4$.

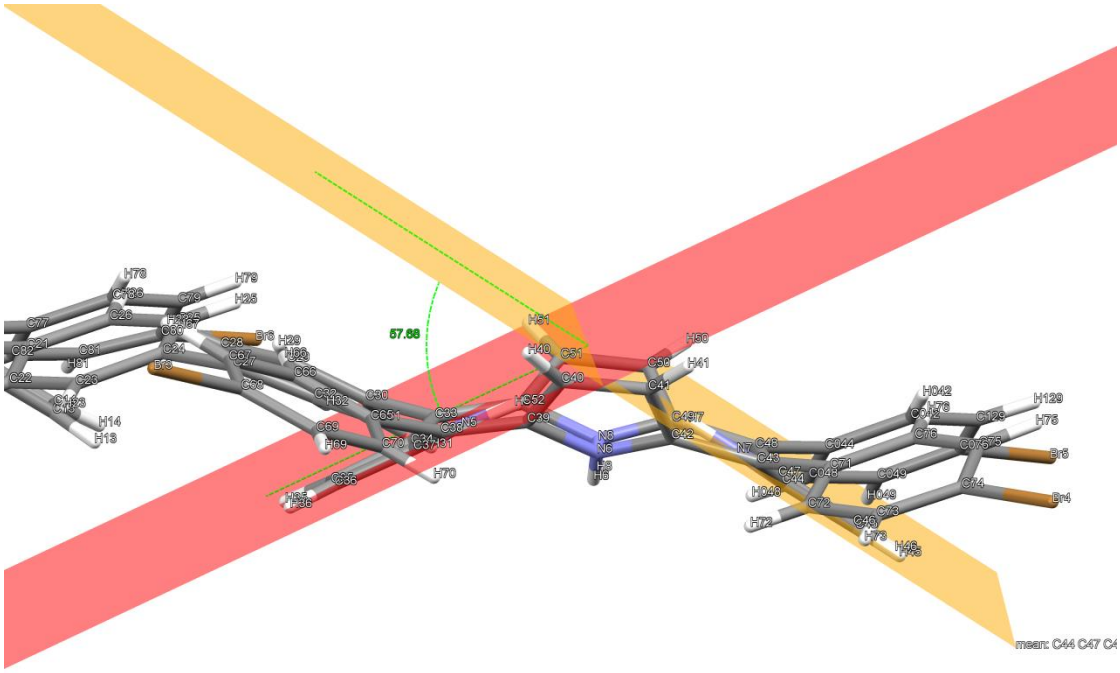


Figure 4.29 Bending angle 57.68° between pyrrole rings A and C on porphyrin B of $[32H_4]^{4+}[CF_3COO]^-_4$.

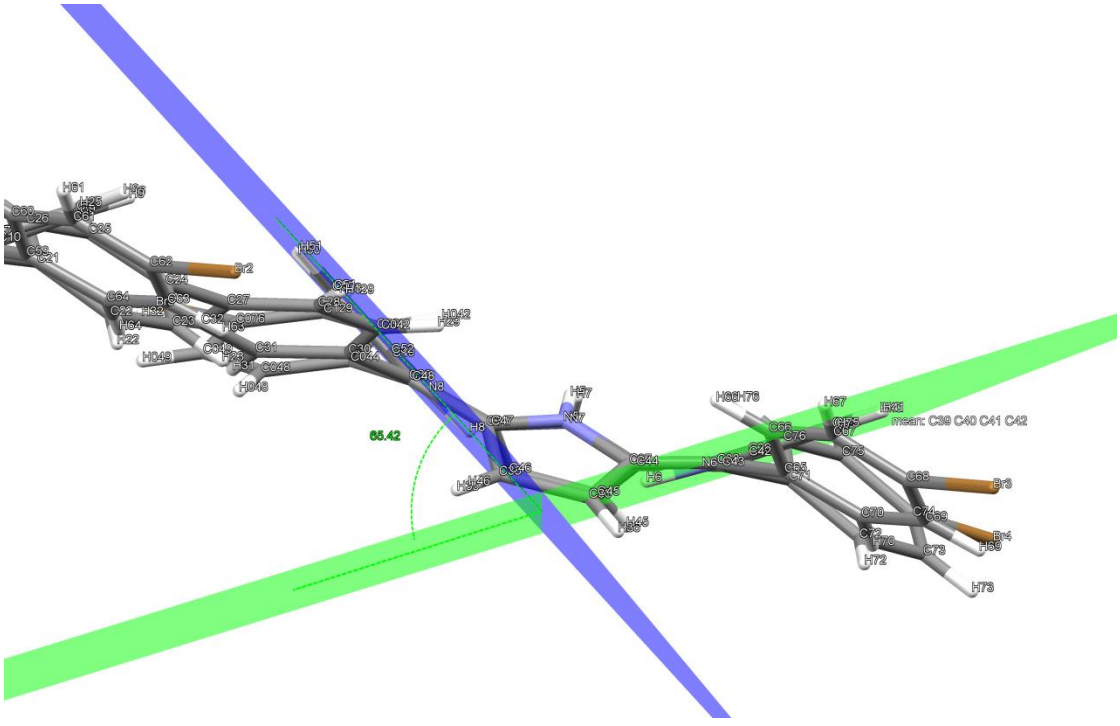


Figure 4.30 Bending angle 65.42° between pyrrole rings B and D on porphyrin B of $[32H_4]^{4+}[CF_3COO]^-_4$.

Table 4.4 Summarising angles measured for figures 4.19-4.24 Ring A.

Twisting angle from planes A and B	44.62°
Twisting angle from planes B and C	41.27°
Twisting angle from planes C and D	40.84°
Twisting angle from planes D and A	41.44°
Bending angle from planes A and C	54.05°
Bending angle from planes B and D	66.98°

Table 4.5 Summarising angles measured for figures 4.25-4.30 Ring B.

Twisting angle from planes A and B	44.19°
Twisting angle from planes B and C	40.80°
Twisting angle from planes C and D	40.98°
Twisting angle from planes D and A	44.29°
Bending angle from planes A and C	57.68°
Bending angle from planes B and D	65.42°

For comparison, the distortion in a crystal structure[45] of tetraphenylporphyrin (TPP) without TFA protonation was analysed, see figures 4.31-4.34. As before, planes were created for each of the pyrrole rings. The twisting angle between adjacent pyrrolic groups is the same for whichever pair is selected, measured at 7.45°, which is much lower than the angles measured in this research for structures with TFA present. The twist observed in TPP results in one of the central protons tilting upwards from the porphyrin ring plane and one central proton tilted downwards. The bending angle of the porphyrin ring is measured as 0° for the A and C pyrrolic groups as the planes are parallel to each other. Similarly the planes created for pyrrolic groups B and D are also parallel.

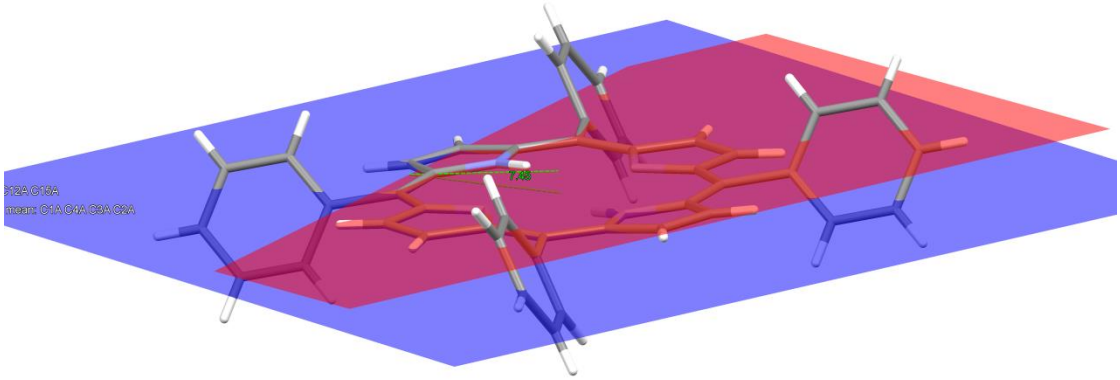


Figure 4.31 Twisting angle 7.45° between pyrrole rings A and B for TPP.

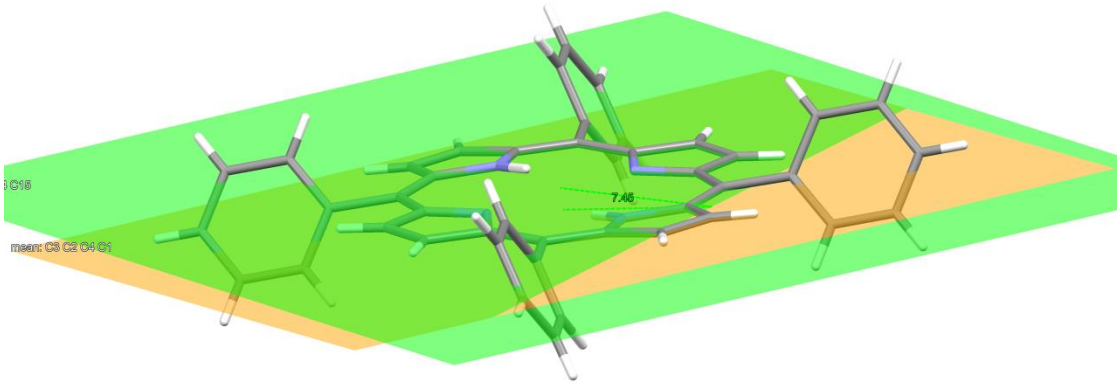


Figure 4.32 Twisting angle 7.45° between pyrrole rings B and C for TPP.

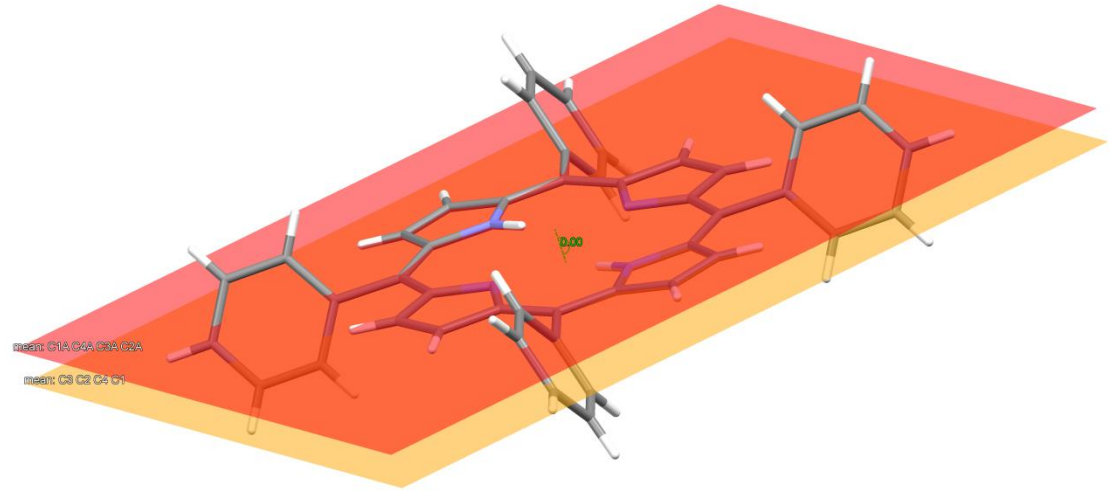


Figure 4.33 Planes created for pyrrole rings A and C.

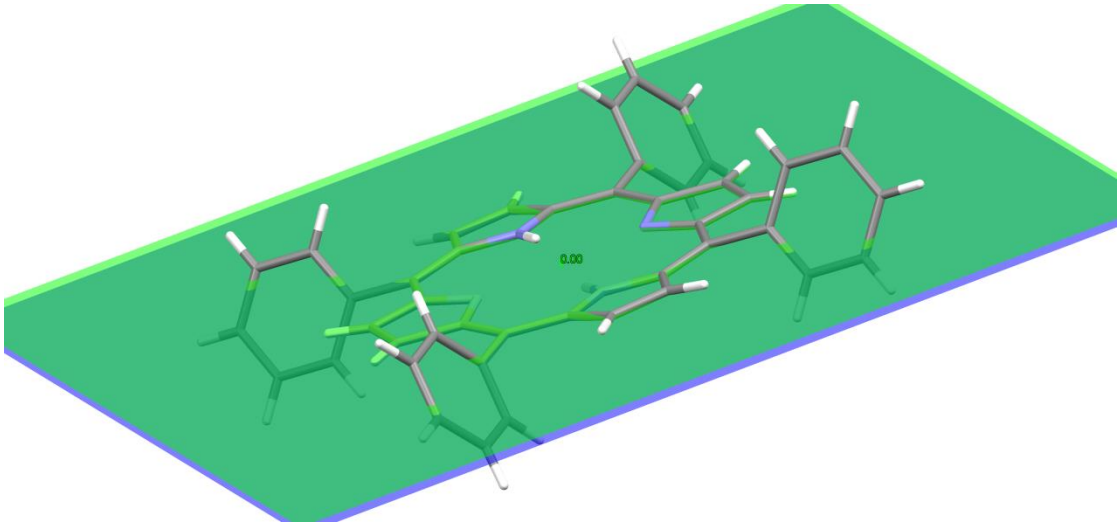


Figure 4.34 Planes created for pyrrole rings B and D.

The distortion observed in the salts $[\mathbf{31}H_4]^{4+}[CF_3COO]^-_4$ and $[\mathbf{32}H_4]^{4+}[CF_3COO]^-_4$ from the almost planar configuration observed for our comparison porphyrin, TPP, provides an indication of how the presence of TFA in a solution of a porphyrin dimer increases the solubility of that dimer; protonation from the TFA causes a buckling of planar conformation of the porphyrin ring. Hydrogen bonds between the TFA anions to the porphyrin centre can then form, this is a strong interaction which inhibits nearby porphyrin dimer molecules from forming π-π interactions. The position of the TFA is directly over the porphyrin rings when hydrogen bonded to the porphyrin dimer, blocking further interactions between nearby porphyrin molecules, preventing aggregation.

For the salt $[\mathbf{31}H_4]^{4+}[CF_3COO]^-_4$ a plane was created using C5, C10, C15, C20 (purple), which intersected with the other porphyrin ring as the crystal displayed a centre of

inversion. A plane was created using C40, C40', C41, C41', (yellow) of the bridging phenyl ring. These two planes intersect at an angle of 33.99°(figure 4.35).

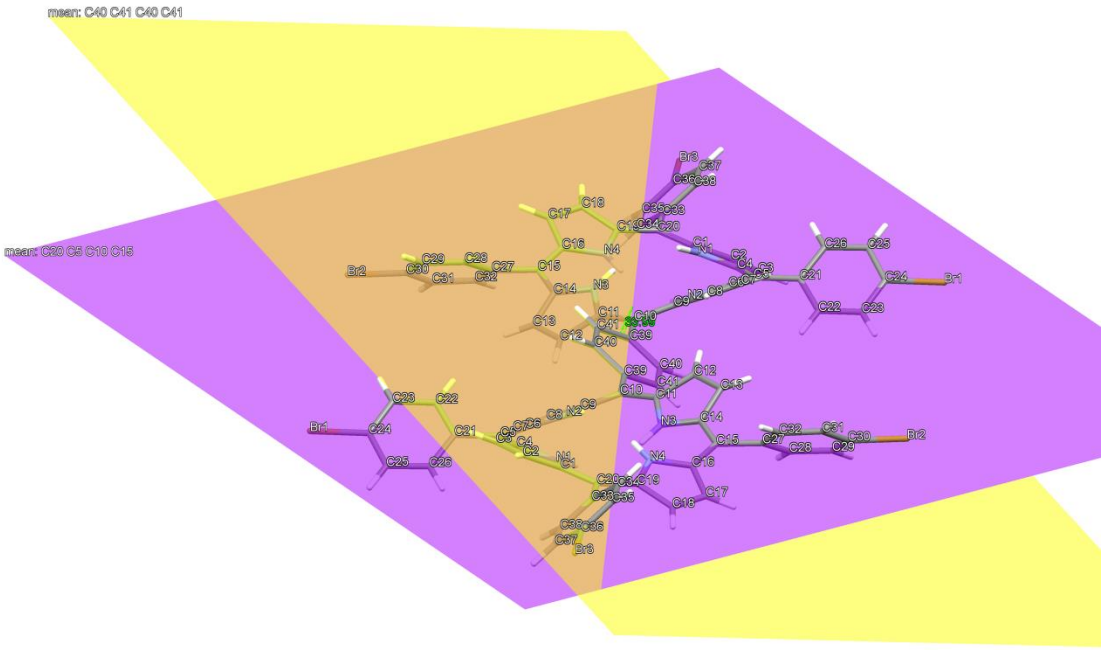


Figure 4.35 Intersection angle 33.99° for phenyl plane and porphyrin plane for $[\mathbf{31}H_4]^{4+}[CF_3COO]^-_4$.

Similarly, as seen in figures 4.36 and 4.37, a plane was created for $[\mathbf{32}H_4]^{4+}[CF_3COO]^-_4$ using carbons labelled C1, C6, C11, C16 on porphyrin ring A and another plane for porphyrin ring B was constructed using C33, C38, C43, C48. These two planes were found deviate from each other by 0.48°. Subsequently the angles of the bridging phenyl rings are reported for both porphyrin rings. Planes were also constructed for bridging phenyl ring A (closest to porphyrin ring A) using C22, C23, C25, C26 (yellow) and for bridging phenyl ring B using C28, C29, C30, C31 (light blue). Porphyrin ring A intersected with bringing phenyl A at 25.59° and bridging phenyl B at 19.54°. Porphyrin ring B intersected with bridging phenyl A at 25.45° and bridging phenyl B at 19.73°. The planes of the bridging phenyl groups intersected at 45.09° (figure 4.38).

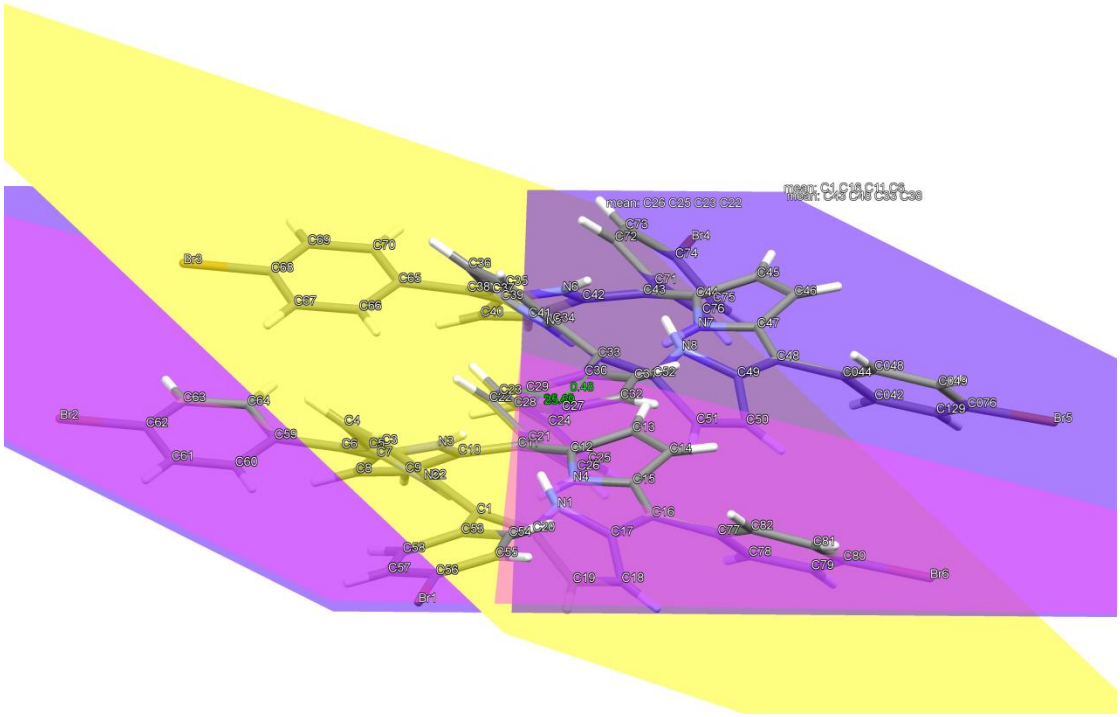


Figure 4.36 Intersection angles 25.59°, 25.45° for phenyl A and porphyrin planes for $[32H_4]^{4+}[CF_3COO]^-_4$.

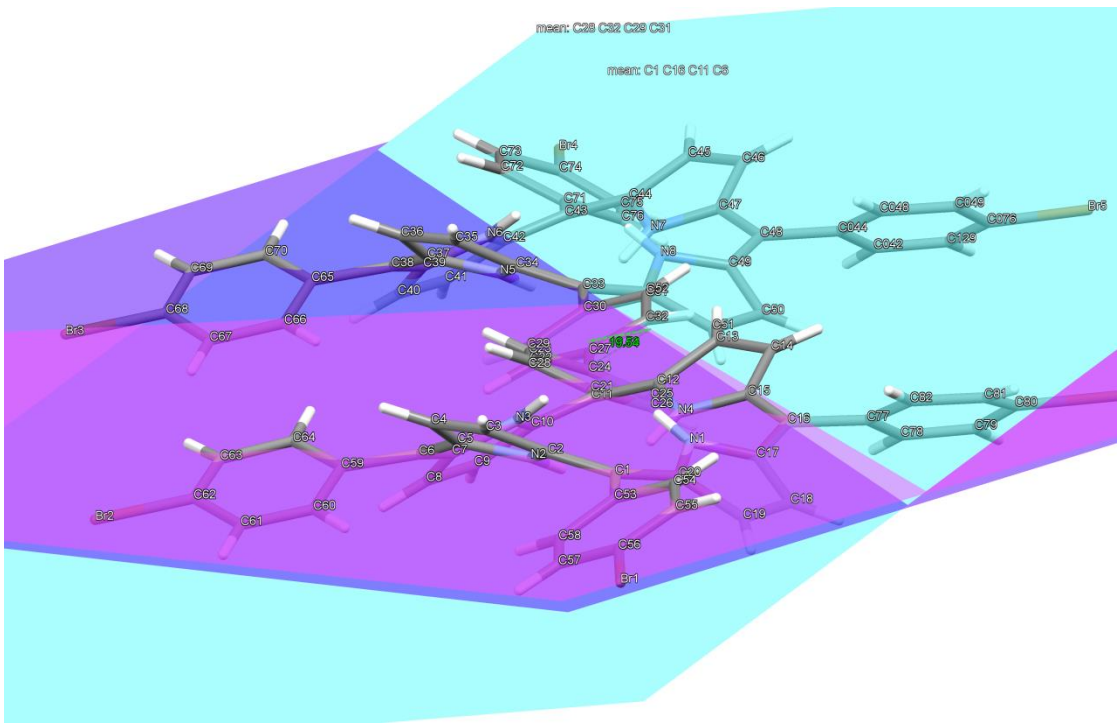


Figure 4.37 Intersection angles 19.54°, 19.73° for phenyl B and porphyrin planes for $[32H_4]^{4+}[CF_3COO]^-_4$.

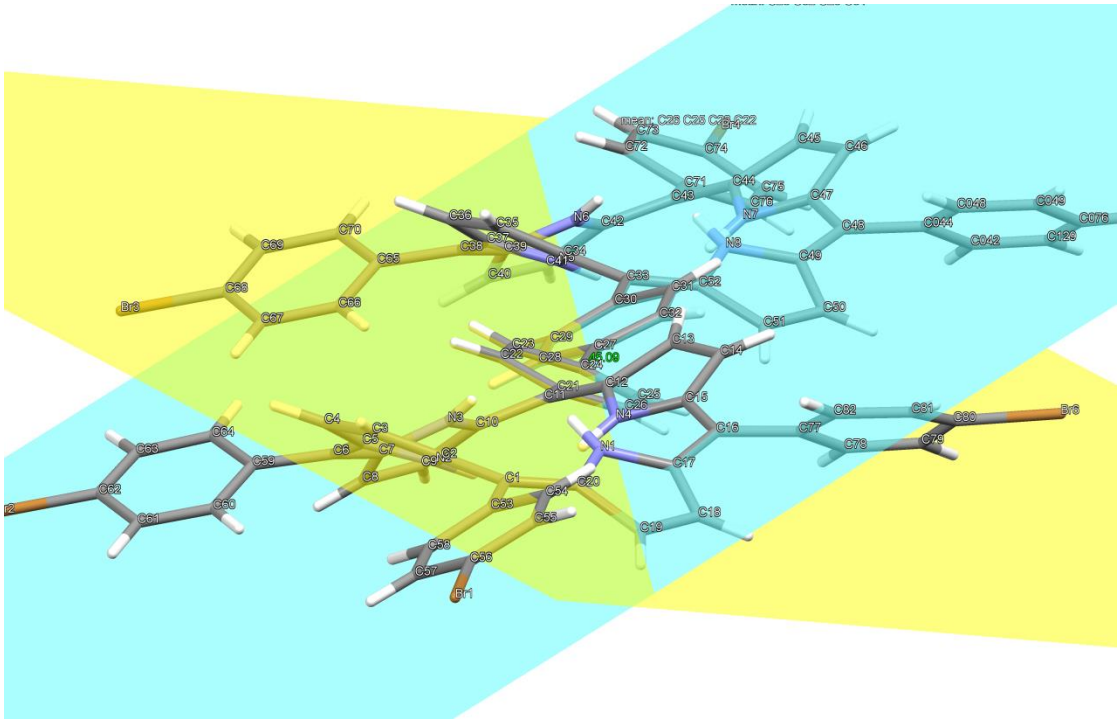


Figure 4.38 Intersection angle 45.09° for phenyl A and B planes.

UV/Vis Spectroscopy for 31 and 32

Figure 4.39 shows the UV/Vis spectra for the neutral species **31** and **32**. There is a split Soret band in dimer **31**, having peaks at 419 nm 285,000 M^{-1} cm^{-1} and 426 nm 303,000 M^{-1} cm^{-1}, indicating two different absorptions which is unusual for such a symmetric molecule. Soret splitting of symmetric porphyrins that theory states should not experience splitting have previously been attributed to stacking, having aggregations form in the solvent system.[46] There is no split Soret band observed for dimer **32**. The extinction coefficient was measured to be 528,000 $M^{-1}cm^{-1}$ at 423 nm.

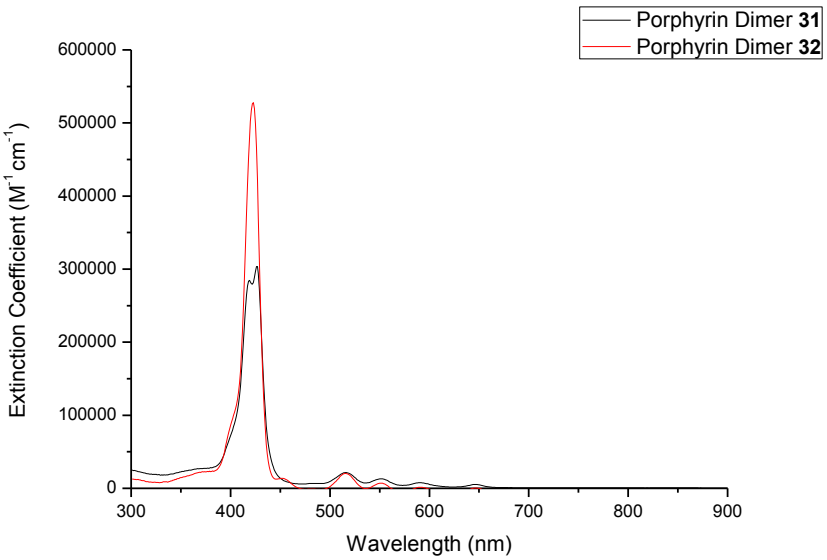


Figure 4.39 UV/Vis spectra for 31 and 32.

This difference in behaviour for these two seemingly similar molecules is not easy to explain. Given that the only structural difference is the number of phenyl rings linking the two porphyrin units together, it is thought that the additional phenyl ring allows a greater degree of rotation for dimer **32**, making π-interactions with other molecules less likely and so decreasing the chance of forming aggregates.

To assess whether any stacking was occurring for these compounds in solution, a series of concentrations was prepared. When stacking occurs, aggregations exist within the solution which absorb light less efficiently than fully solvated molecules, lowering the extinction coefficient. If stacking is present, when absorbance is plotted against concentration a curved line should form. Figure 4.40 shows that porphyrin dimer **31** was found to follow the Beer-Lambert law as the data closely fits the linear line. This would suggest that there is no stacking, which is at odds with the previous hypothesis. It is not entirely clear then how the split Soret band arises, but it is possible that it is due to electronic coupling between the two porphyrin rings,[47] in this case facilitated by the

bridging phenyl ring. Figure 4.41 shows that porphyrin dimer **32** also follows the Beer-Lambert law indicating again that there is no stacking.

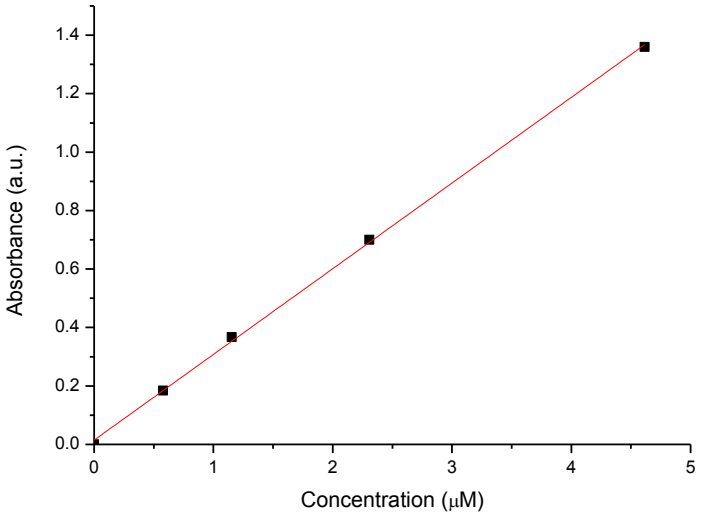


Figure 4.40 Plotting peak Soret band absorbance (427 nm) against concentration for 31.

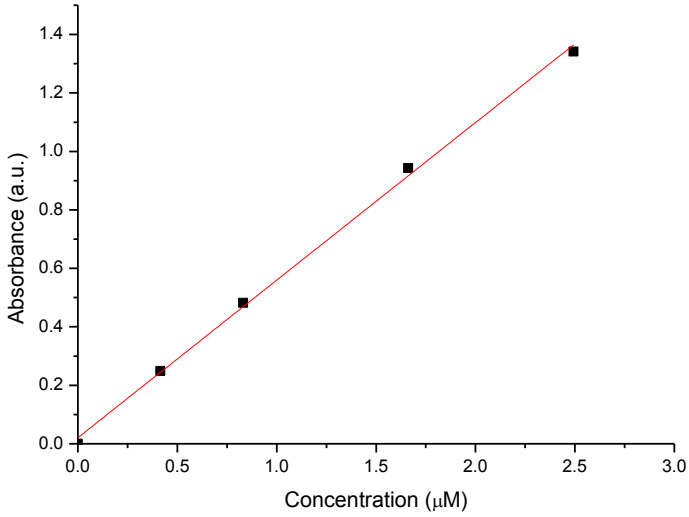


Figure 4.41 Plotting peak Soret band absorbance (423 nm) against concentration for 32.

Conclusions

The porphyrin dimer **31** was successfully synthesised from **12** and **15** *via* an adaptation of the procedure outlined by Lindsey and co-workers.[48] The porphyrin dimer **32** was successfully synthesised from **13** and **15** using the same adaptation as employed for the synthesis of compound **31**.

Whilst the reduction reaction to form the dicarbinol species proceeded very efficiently, very low yields were recorded for the synthesis of **31** and **32**. This has been attributed to unwanted intermolecular reactions occurring during the porphyrinogen formation stage which are compounded for these dimeric molecules compared to the monomeric porphyrins synthesised in the previous chapter.

Single crystals suitable for X-ray diffraction were grown for $[\mathbf{31}H_4]^{4+}[CF_3COO]_4^-$ from a chloroform/benzene/TFA slow evaporation. The solved structure showed significant distortion of the usually planar porphyrin ring with twisting angle between adjacent pyrrollic groups ranging between 33.80° and 39.13° and the bending angle between opposing pyrrolic groups measured as 50.03° and 55.26°. This distortion has been attributed to strong hydrogen bond interactions between central protons of the porphyrin ring and nearby TFA anions.

Single crystals of salts suitable for X-ray diffraction were grown for $[\mathbf{32}H_4]^{4+}[CF_3COO]_4^-$ from chloroform/TFA slow evaporation. The solved structure showed significant distortion of the usually planar porphyrin ring with twisting angle between adjacent pyrrollic groups ranging between 40.80° and 44.62°. The bending angle between opposing pyrrolic groups has been measured as 54.05° and 66.98° for ring A and 57.68°

and 65.42° for ring B. This also shows distortion of the porphyrin plane due to hydrogen bonding interactions with nearby TFA anions.

The hydrogen bond lengths (H…A) for [**32**H_4]$^{4+}$[CF_3COO]$_4^-$ cover a much larger range than those for [**31**H_4]$^{4+}$[CF_3COO]$_4^-$ (2.02 Å - 2.47Å compared with 2.00 Å - 2.04 Å). The angles of hydrogen bonding for [**32**H_4]$^{4+}$[CF_3COO]$_4^-$ also cover a wider range than those for [**31**H_4]$^{4+}$[CF_3COO]$_4^-$ (125.1° - 160.7° compared to 145.1° - 161.2°). The reason for the greater distortion in [**32**H_4]$^{4+}$[CF_3COO]$_4^-$ is a combination of these factors; in short, the TFA anions are located further away from the porphyrin ring so the individual pyrrolic groups have bend out of plane further in order to be at an angle that accommodates hydrogen bonding.

Experimental

1-(5,10,15-tri(4-bromophenyl)-20-porphyrinyl)-4-(5,10,15-tri(4-bromophenyl-20-porphyrinyl)phenyl (31)

1,9-Bis(4-bromobenzoyl)-5-(4-bromophenyl)dipyrromethane (500 mg, 0.749 mmol) was dissolved in THF (75 mL) and methanol (11 mL) and sodium borohyride (1.20 g, 31.7 mmol) was added. The reaction mixture was stirred at room temperature for 1 h after which a saturated aqueous ammonium chloride/DCM mixture (1:1, 100 mL) was added. The organics were collected and washed with water (100 mL), brine (100 mL) and then dried over anhydrous magnesium sulfate. The resulting mixture was filtered and the solvent removed *in vacuo*. The residue and **12** (140 mg, 0.382 mmol) were stirred in acetonitrile (750 mL) to obtain a homogenous solution. TFA (680 μL, 8.88 mmol) was added and the solution was stirred at RT for 1 h. DDQ (510 mg, 2.25 mmol) was added and the solution was stirred for a further 1 h at RT after which, the solvent was removed *in vacuo*. The residue was dissolved in DCM and filtered through a silica column to collect the porphyrinic species. Purification was achieved by column chromatography (silica, 99:1, DCM/TFA). Fractions containing the desired material were collected together, neutralised with NaOH solution (2 M, 200 mL), washed with water, brine, dried with magnesium sulfate, filtered and solvents removed producing a purple solid (27 mg, 16.7 μmol, 4%). NMR data was collected of the TFA salt as porphyrin dimer **31** was insufficiently soluble in common deuterated solvents to obtain reasonable data.

^{1}H NMR ($CDCl_3$/TFA, 400 MHz): δ = 9.26 (s, 4 H), 9.09 (d, *J* = 4.5 Hz, 4 H), 8.86 (d, *J* = 4.5 Hz, 4 H), 8.78 (s, 8 H), 8.43 - 8.53 (m, 12 H), 8.24 (d, *J* = 7.4 Hz, 12 H), -0.48 (br, s, 4 H), -0.61 (br, s, 4 H) ppm. MS: (MALDI-TOF) m/z calculated for [$C_{82}H_{48}Br_6N_8$]: 1623.90. Found: 1623.84. UV/Vis λ_{abs} (CH_2Cl_2)/nm (ε/$dm^3mol^{-1}cm^{-1}$): 419 (285,000), 426 (304,000), 516 (21,600).

4-(5,10,15-tri(4-bromophenyl)-20-phenylporphyrin)-4'-(5,10,15-tri(4-bromophenyl)-20-phenylporphyrin)biphenyl (32)

1,9-Bis(4-bromobenzoyl)-5-(4-bromophenyl)dipyrromethane (250 mg, 0.375 mmol) was dissolved in THF (60 mL) and methanol (10 mL) and sodium borohyride (700 mg, 18.5 mmol) was added. The reaction mixture was stirred at room temperature for 30 min after which a saturated aqueous ammonium chloride/DCM mixture (1:1, 100mL) was added. The organics were collected and washed with water (100 mL), brine (100 mL) and then dried over anhydrous magnesium sulfate. The resulting mixture was filtered and the solvent removed *in vacuo*. The orange residue and **13** (85 mg, 0.192 mmol) were stirred in acetonitrile (375 mL) to obtain a homogenous solution. TFA (250 μL, 3.26 mmol) was added and the solution was stirred at room temperature for 1 h. DDQ (375 mg, 1.65 mmol) was added and the solution was stirred for a further 1 h at RT after which, the solvent was removed *in vacuo*. The residue was dissolved in DCM and filtered through a silica column to collect the porphyrinic species. Purification was achieved by column chromatography (silica, 100:5:1, chloroform/ethyl acetate/TFA). Fractions containing the desired material were collected together, neutralised with NaOH solution (2M, 200 mL), washed with water, brine, dried with magnesium sulfate, filtered and solvents removed producing a purple solid (20 mg, 11.8 μmol, 6%). NMR data was collected of the TFA salt as porphyrin dimer **32** was insufficiently soluble in common deuterated solvents to obtain reasonable data.

^{1}H NMR ($CDCl_3$/TFA, 400 MHz): δ = 8.99 (d, *J* = 7.9 Hz, 4H), 8.66 (d, *J* = 7.9 Hz, 4H), 8.61 (d, *J* = 4.5 Hz, 4H), 8.36 - 8.30 (m, 12H), 8.30 - 8.24 (m, 12H), 8.04 – 7.97 (m, 12H), -0.40 (br, s, 4H), -0.56 (br, s, 4H) ppm. MS: (MALDI-TOF) *m*/*z* calculated for $[C_{88}H_{52}Br_6N_8]^+$: 1695.9389. Found: 1695.9472. UV/Vis λ_{abs} (CH_2Cl_2)/nm (ε/$dm^3mol^{-1}cm^{-1}$): 423 (528,000), 516 (21,300).

References

1. S. S. Han, H. Furukawa, O. M. Yaghi and W. A. Goddard, III, *J. Am. Chem. Soc.*, 2008, **130**, 11580-11581.

2. Q. Fang, S. Gu, J. Zheng, Z. Zhuang, S. Qiu and Y. Yan, *Angew. Chem. Int. Ed.*, 2014, **53**, 2878-2882.

3. H. Furukawa and O. M. Yaghi, *J. Am. Chem. Soc.*, 2009, **131**, 8875-8883.

4. O. M. Yaghi, M. O'Keeffe, N. W. Ockwig, H. K. Chae, M. Eddaoudi and J. Kim, *Nature*, 2003, **423**, 705-714.

5. L. Stegbauer, M. W. Hahn, A. Jentys, G. Savasci, C. Ochsenfeld, J. A. Lercher and B. V. Lotsch, *Chem. Mater.*, 2015, **27**, 7874-7881.

6. B. Lukose, A. Kuc, J. Frenzel and T. Heine, *Beilstein J. Nanotechnol.*, 2010, **1**, 60-70.

7. D. J. Tranchemontagne, J. L. Mendoza-Cortes, M. O'Keeffe and O. M. Yaghi, *Chem. Soc. Rev.*, 2009, **38**, 1257-1283.

8. M. P. Suh, H. J. Park, T. K. Prasad and D.-W. Lim, *Chem. Rev.*, 2012, **112**, 782-835.

9. Z. Wang and S. M. Cohen, *Chem. Soc. Rev.*, 2009, **38**, 1315-1329.

10. M. Eddaoudi, D. B. Moler, H. L. Li, B. L. Chen, T. M. Reineke, M. O'Keeffe and O. M. Yaghi, *Acc. Chem. Res.*, 2001, **34**, 319-330.

11. S. J. Rowan, S. J. Cantrill, G. R. L. Cousins, J. K. M. Sanders and J. F. Stoddart, *Angew. Chem. Int. Ed.*, 2002, **41**, 898-952.

12. M. E. Belowich and J. F. Stoddart, *Chem. Soc. Rev.*, 2012, **41**, 2003-2024.

13. H. M. El-Kaderi, J. R. Hunt, J. L. Mendoza-Cortes, A. P. Cote, R. E. Taylor, M. O'Keeffe and O. M. Yaghi, *Science*, 2007, **316**, 268-272.

14. E. L. Spitler, B. T. Koo, J. L. Novotney, J. W. Colson, F. J. Uribe-Romo, G. D. Gutierrez, P. Clancy and W. R. Dichtel, *J. Am. Chem. Soc.*, 2011, **133**, 19416-19421.

15. L. Ascherl, T. Sick, J. T. Margraf, S. H. Lapidus, M. Calik, C. Hettstedt, K. Karaghiosoff, M. Doeblinger, T. Clark, K. W. Chapman, F. Auras and T. Bein, *Nat. Chem.*, 2016, **8**, 310-316.

16. D. Er, L. Dong and V. B. Shenoy, *J. Phys. Chem. C*, 2016, **120**, 174-178.

17. P. J. Waller, F. Gandara and O. M. Yaghi, *Acc. Chem. Res.*, 2015, **48**, 3053-3063.

18. R. W. Tilford, S. J. Mugavero, III, P. J. Pellechia and J. J. Lavigne, *Adv. Mater.*, 2008, **20**, 2741-2746.

19. L. M. Lanni, R. W. Tilford, M. Bharathy and J. J. Lavigne, *J. Am. Chem. Soc.*, 2011, **133**, 13975-13983.

20. F. J. Uribe-Romo, J. R. Hunt, H. Furukawa, C. Klock, M. O'Keeffe and O. M. Yaghi, *J. Am. Chem. Soc.*, 2009, **131**, 4570-4571.

21. F. J. Uribe-Romo, C. J. Doonan, H. Furukawa, K. Oisaki and O. M. Yaghi, *J. Am. Chem. Soc.*, 2011, **133**, 11478-11481.

22. A. P. Cote, A. I. Benin, N. W. Ockwig, M. O'Keeffe, A. J. Matzger and O. M. Yaghi, *Science*, 2005, **310**, 1166-1170.

23. S. Wei, D.-X. Lu, J. Sun, Y. He, L. Zhu, Y.-L. Zhang and F.-S. Xiao, *Colloid. Surface. A*, 2012, **414**, 327-332.

24. S. Kuecken, J. Schmidt, L. Zhi and A. Thomas, *J. Mater. Chem. A*, 2015, **3**, 24422-24427.

25. P. Kuhn, M. Antonietti and A. Thomas, *Angew. Chem. Int. Ed.*, 2008, **47**, 3450-3453.

26. P. Katekomol, J. Roeser, M. Bojdys, J. Weber and A. Thomas, *Chem. Mater.*, 2013, **25**, 1542-1548.

27. L. K. Ritchie, A. Trewin, A. Reguera-Galan, T. Hasell and A. I. Cooper, *Micropor. Mesopor. Mat.*, 2010, **132**, 132-136.

28. H. Wei, S. Chai, N. Hu, Z. Yang, L. Wei and L. Wang, *Chem. Comm.*, 2015, **51**, 12178-12181.

29. N. L. Campbell, R. Clowes, L. K. Ritchie and A. I. Cooper, *Chem. Mater.*, 2009, **21**, 204-206.

30. N. A. A. Zwaneveld, R. Pawlak, M. Abel, D. Catalin, D. Gigmes, D. Bertin and L. Porte, *J. Am. Chem. Soc.*, 2008, **130**, 6678-6679.

31. C. Z. Guan, D. Wang and L. J. Wan, *Chem. Comm.*, 2012, **48**, 2943-2945.

32. J. W. Colson, A. R. Woll, A. Mukherjee, M. P. Levendorf, E. L. Spitler, V. B. Shields, M. G. Spencer, J. Park and W. R. Dichtel, *Science*, 2011, **332**, 228-231.

33. P. Kissel, D. J. Murray, W. J. Wulftange, V. J. Catalano and B. T. King, *Nat. Chem.*, 2014, **6**, 774-778.

34. Y.-B. Zhang, J. Su, H. Furukawa, Y. Yun, F. Gandara, A. Duong, X. Zou and O. M. Yaghi, *J. Am. Chem. Soc.*, 2013, **135**, 16336-16339.

35. S.-Y. Ding and W. Wang, *Chem. Soc. Rev.*, 2013, **42**, 548-568.

36. S. Wan, F. Gandara, A. Asano, H. Furukawa, A. Saeki, S. K. Dey, L. Liao, M. W. Ambrogio, Y. Y. Botros, X. Duan, S. Seki, J. F. Stoddart and O. M. Yaghi, *Chem. Mater.*, 2011, **23**, 4094-4097.

37. J. Karnbratt, M. Gilbert, J. K. Sprafke, H. L. Anderson and B. Albinsson, *J. Phys. Chem. C*, 2012, **116**, 19630-19635.

38. X. Feng, L. L. Liu, Y. Honsho, A. Saeki, S. Seki, S. Irle, Y. P. Dong, A. Nagai and D. L. Jiang, *Angew. Chem. Int. Ed.*, 2012, **51**, 2618-2622.

39. L. Chen, Y. Yang and D. Jiang, *J. Am. Chem. Soc.*, 2010, **132**, 9138-9143.

40. A. M. Shultz, O. K. Farha, J. T. Hupp and S. T. Nguyen, *Chem. Sci.*, 2011, **2**, 686-689.

41. L. Grill, M. Dyer, L. Lafferentz, M. Persson, M. V. Peters and S. Hecht, *Nat. Nanotechnol.*, 2007, **2**, 687-691.

42. T. Zambelli, *Int. J. Nanosci. Ser.*, 2004, **3**, 331-341.

43. L. Lafferentz, V. Eberhardt, C. Dri, C. Africh, G. Comelli, F. Esch, S. Hecht and L. Grill, *Nat. Chem.*, 2012, **4**, 215-220.

44. M. J. Webb and N. Bampos, *Chem. Sci.*, 2012, **3**, 2351-2366.

45. S. J. Silvers and A. Tulinsky, *J. Am. Chem. Soc.*, 1967, **89**, 3331-3337.

46. P. Z. El-Khoury, K. Honkala and W. P. Hess, *J. Phys. Chem. A*, 2014, **118**, 8115-8123.

47. I. Dragomir, A. Hagarman, C. Wallace and R. Schweitzer-Stenner, *Biophys. J.*, 2007, **92**, 989-998.

48. P. D. Rao, S. Dhanalekshmi, B. J. Littler and J. S. Lindsey, *J. Org. Chem.*, 2000, **65**, 7323-7344.

Chapter 5:

Porphyrin Tetris

Introduction

Synthesis of Porphyrin Arrays

There have been many different methods for synthesising porphyrin dimers and larger arrays reported in the literature, linked at either the β-[1] or *meso*-[2] positions or both[3]. Of particular interest are conjugated arrays as these have desirable properties that make them potential candidates in the fields of photovoltaic devices,[4] NIR dyes[5] and nanoelectronics.[6]

A strategy of synthesising *meso-meso* linked porphyrin arrays shown in figure 5.1 was described by Osuka and Shimidzu in which zinc(II) 5,15-di(3,5-di-tert-butylphenyl)porphyrin underwent oxidative coupling when exposed to an Ag(I) salt such as $AgPF_6$ forming appreciable amounts of dimeric and trimeric products, noting that the reaction was accelerated by the addition of I_2.[7] In another study, they reported that by using Zn(II) 3,5-dioctyloxyphenylporphyrin as the starting molecule the same reaction could be repeated successively to result in a 128-mer molecule.[8]

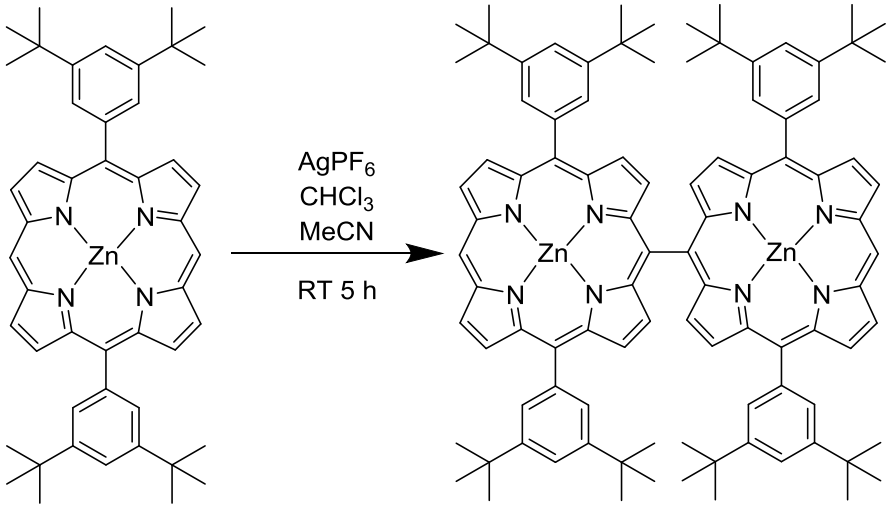


Figure 5.1 Oxidative coupling of porphyrins *via* an Ag(I) salt.

Porphyrins may also be fused together either directly[9] or through a bridging unit such as benzene.[10] When fused, the individual porphyrin units are forced into a coplanar formation which can have a striking effect on their photophysicial properties.[11] Porphyrin tapes such as the one shown in figure 5.2, are fused porphyrin oligomers which are linked at the β-β, *meso-meso*, β-β positions.[12] Porphyrin tapes can be formed by an oxidation reaction of *meso-meso* linked porphyrins. using $FeCl_3$[13] or DDQ[14] in the presence of a scandium catalyst such as $Sc(OTf)_3$.

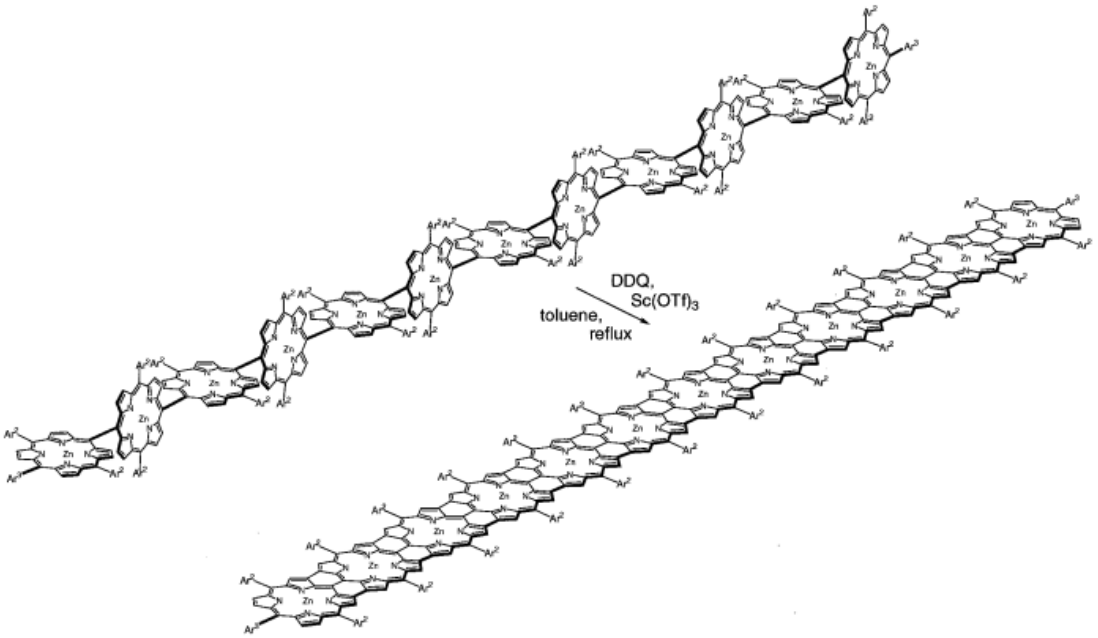
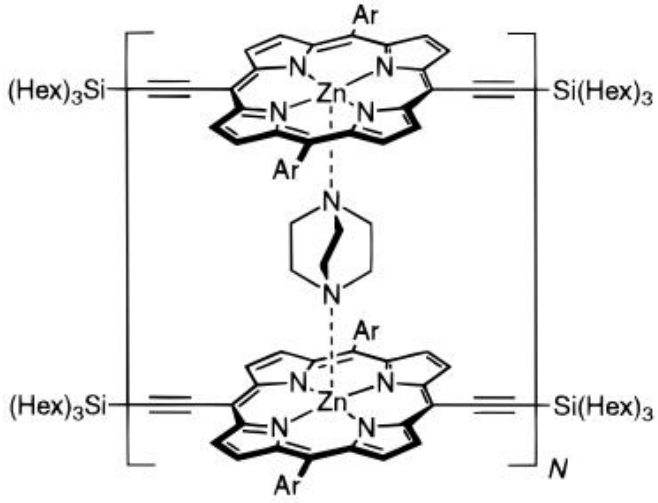


Figure 5.2 Porphyrin tape formed by scandium (III) catalysed oxidation of *meso*-linked porphyrin array.[12]

One of the most common methods of creating porphyrin arrays, and the one selected to conduct this research is through Sonogashira coupling reactions. The coupling takes place between porphyrins containing terminal alkyne and bromine moieties to produce porphyrins linked by alkyne bridges. Using Sonogashira coupling reactions in the field of porphyrin chemistry was first introduced to the scientific community by Therien and co-workers in 1994.[15] As systems synthesised in this manner are conjugated, they have been considered and examined for use as photonic wires and as light harvesting arrays.[16, 17] By performing successive coupling reactions, arrays of up to seven porphyrin units capable

of charge transport have been reported.[18] Similarly, butadiyne linked porphyrin array have been shown to be able to transport electrons over distances up to 10 nm with low attenuation, giving further evidence to the claim that prophyrin wires could be useful in nanoelectronic devices.[19]

Porphyrin arrays are not just limited to one-dimensional wire configurations, a number of 2D and 3D structures have been reported. Chains of metallated porphyrins can be linked together by a coordinating molecule such as DABCO or Bipy to create structures known as porphyrin ladders as seen in figure 5.3.[20]



$\mathbf{1}_2$·(DABCO) to $\mathbf{6}_2$·$(DABCO)_6$; *N* = 1 to 6; Ar = 3,5-di(*t*-butyl)phenyl

Figure 5.3 Series of porphyrin ladders designed by Anderson and co-workers.[21]

Porphyrin rings may be synthesised in the same way as linear chains, separating out the cyclised from the linear products.[22] Alternatively, a more directed, templated approach can be taken as demonstrated by Anderson and co-workers. Expanding on their own work, a template-assisted synthesis of porphyrin nanotubes was achieved in which six molecules of zinc-coordinated butadiyene linked porphyrin dimer were held in place with metal coordination bonds by the template so that Glaser couplings could take place between the molecules to result in new butadiyene links (figure 5.4).[23]

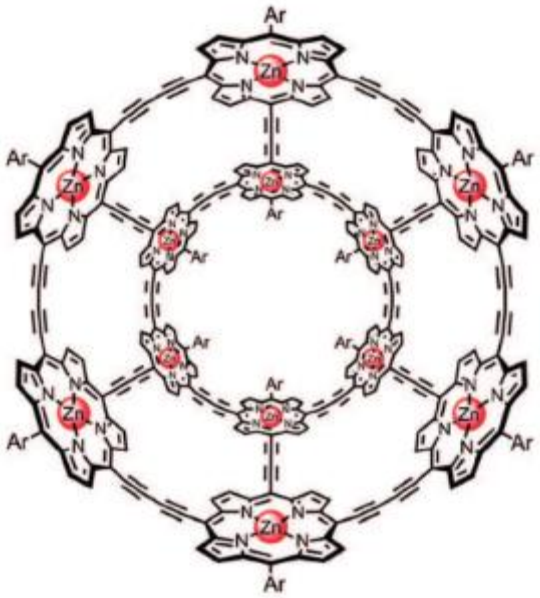


Figure 5.4 Porphyrin nanotube synthesised by Anderson and co-workers.[23]

Another 3D structure, porphyrin boxes, have been synthesised and act as porous organic cages. The porphyrin box created by Hong *et al.* using the components shown in figure 5.5 has a very high surface area (1370 $m^2 g^{-1}$) and moderate CO_2 uptake (7.32 wt%). They were also able to create a second porphyrin box using tri(2-aminoethyl)amine as the linker which demonstrated a greater CO_2 uptake (12.43 wt%) and also selective gas sorption, preferentially absorbing CO_2 over N_2 and CH_4 at 273 K at 1 bar.[24]

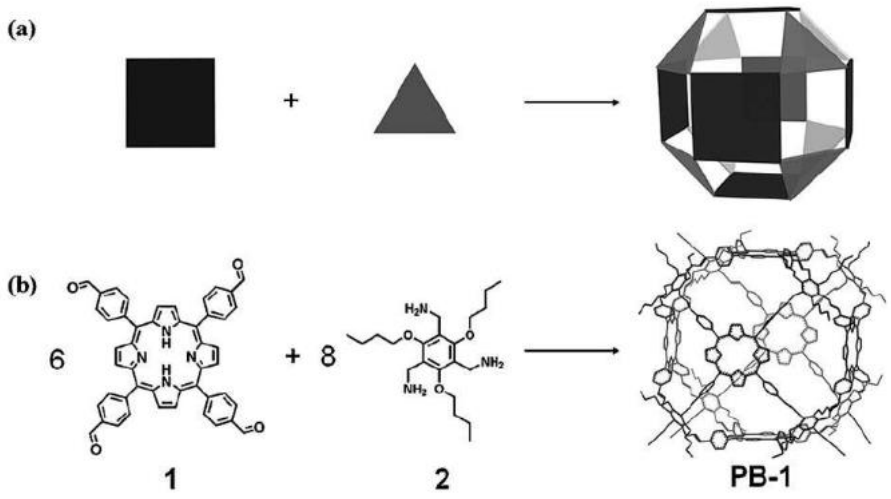


Figure 5.5 Porphyrin box designed by Hong *et al.*[24]

Results and Discussion

Porphyrin Tetris

The game Tetris is still as popular now as it was when it was first released in 1984. Designed and programmed by Alexey Pajitnov, the game features 7 different shapes known as 'Tetriminos' called I, J, L, O, S, T and Z corresponding to the letter of the alphabet that they look like (figure 5.6).

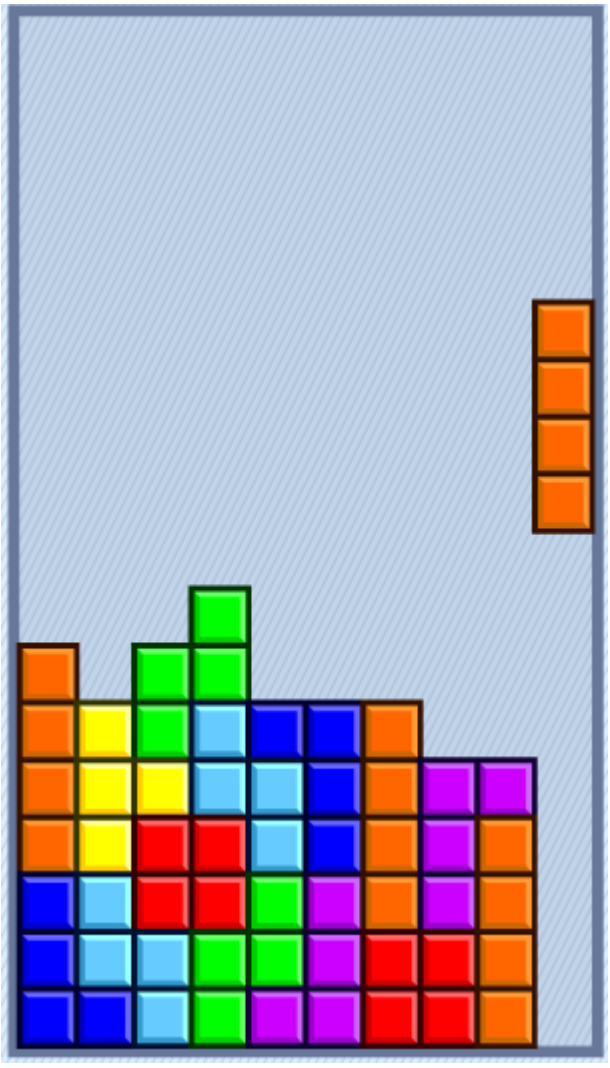


Figure 5.6 Screenshot of Tetris game showing I, J, L, O, S, T and Z Tetriminos.

The S and Z Tetriminos and the J and L Tetriminos in the 2D world of Tetris are enantiomers of each other. When these are transposed into the 3D world of real life, they

are able to rotate along the z-axis so that the chirality is lost and they effectively become the same shape. For this reason, only five different molecules are required for a complete set of molecular Tetris pieces. As these Tetris molecules are composed of porphyrin rings which themselves are planar, a planar arrangement for the Tetris molecules should be possible, making them suitable for surface deposition. Once deposited on a surface, we can observe any tiling effects that may occur[25] and 'play' porphyrin Tetris (figure 5.7).

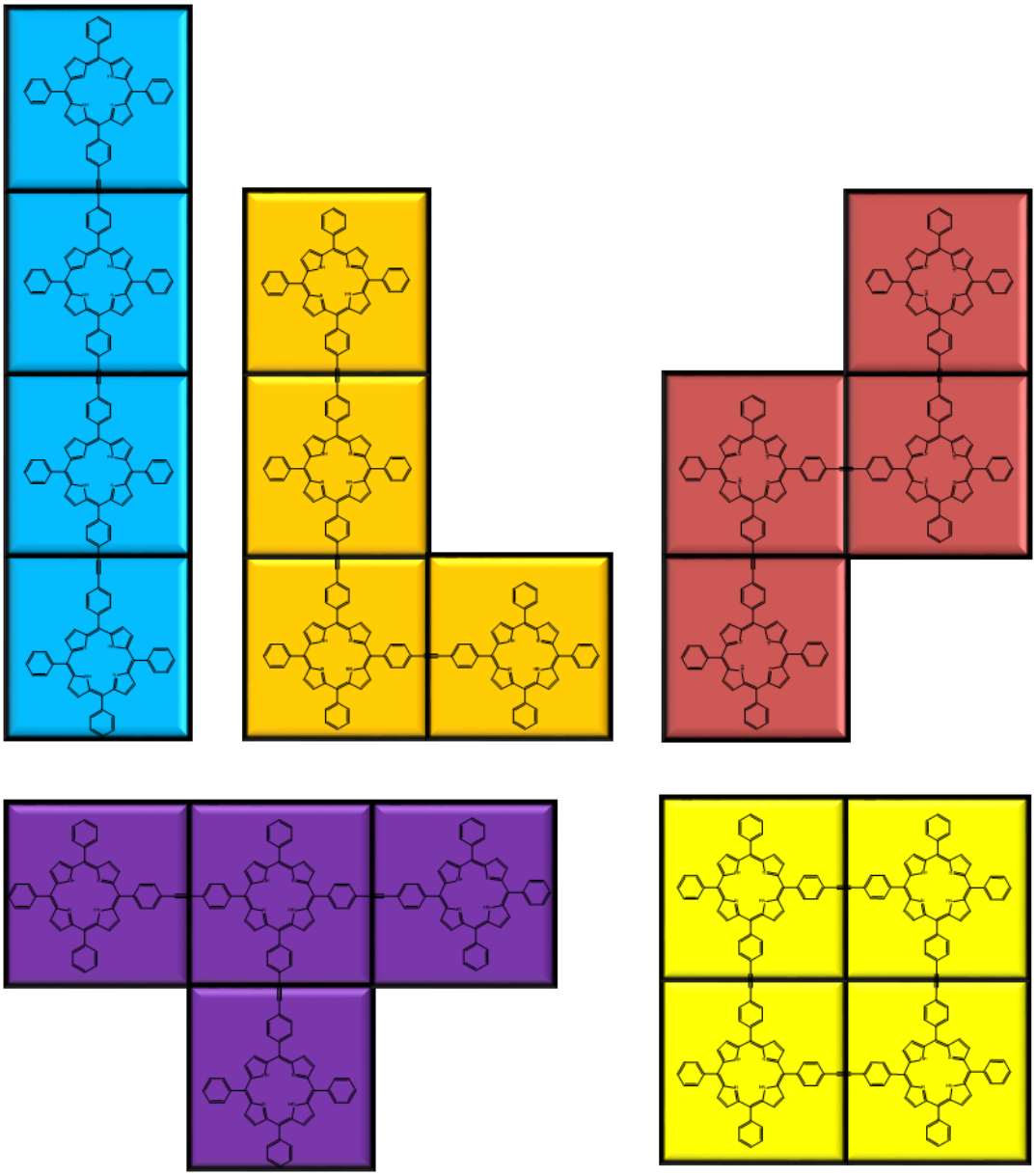


Figure 5.7 Tetris Tetriminos (coloured in accordance with The Tetris Company's standardised scheme) with the target porphyrin molecules overlaid.

The porphyrin molecule TPP is highly symmetric and can be described as square-like in shape. The chosen target molecules for the Tetris pieces consist of TPP units connected together through ethynyl bridges at the 4- position of specifically chosen phenyl groups.

Previous literature used the different reactivity of bromo- and iodo- substituents on the porphyrin units to successfully undergo multiple Sonogashira reactions. However, reactions involving porphyrins with both bromo- and iodo- substituents had to be carried out at low temperature (22 °C) to avoid unwanted bromo-coupling.[17] To evade the potential for unwanted coupling altogether, the porphyrin units in this research were designed so that a Sonogashira reaction could be performed at moderate temperature with a bromo- and alkyne- terminated porphyrin to result in a protected dimeric species. A deprotection reaction could then be performed to yield terminal alkyne species which could then undergo an additional Sonogashira coupling reaction to produce the desired porphyrinic Tetrimino. In this manner, the five target molecules are able to be produced from eight different monomeric porphyrins (**23**-**30** figure 5.8), the synthesis of which was discussed in chapter 3. Table 5.1 below summarises the porphyrin units required to synthesise each of the Tetrimino targets.

Table 5.1 Summarising the monomeric porphyrin units required to synthesise the Tetris pieces.

Target Tetris Tetrimino	First Sonogashira coupling reaction	Second Sonogashira coupling reaction
T	**24**, **25**	-
I	**26**, **27**	**23**
S/Z	**28**, **29**	**23**
J/L	**27**, **28**	**23**
O	**29**, **30**	**30**

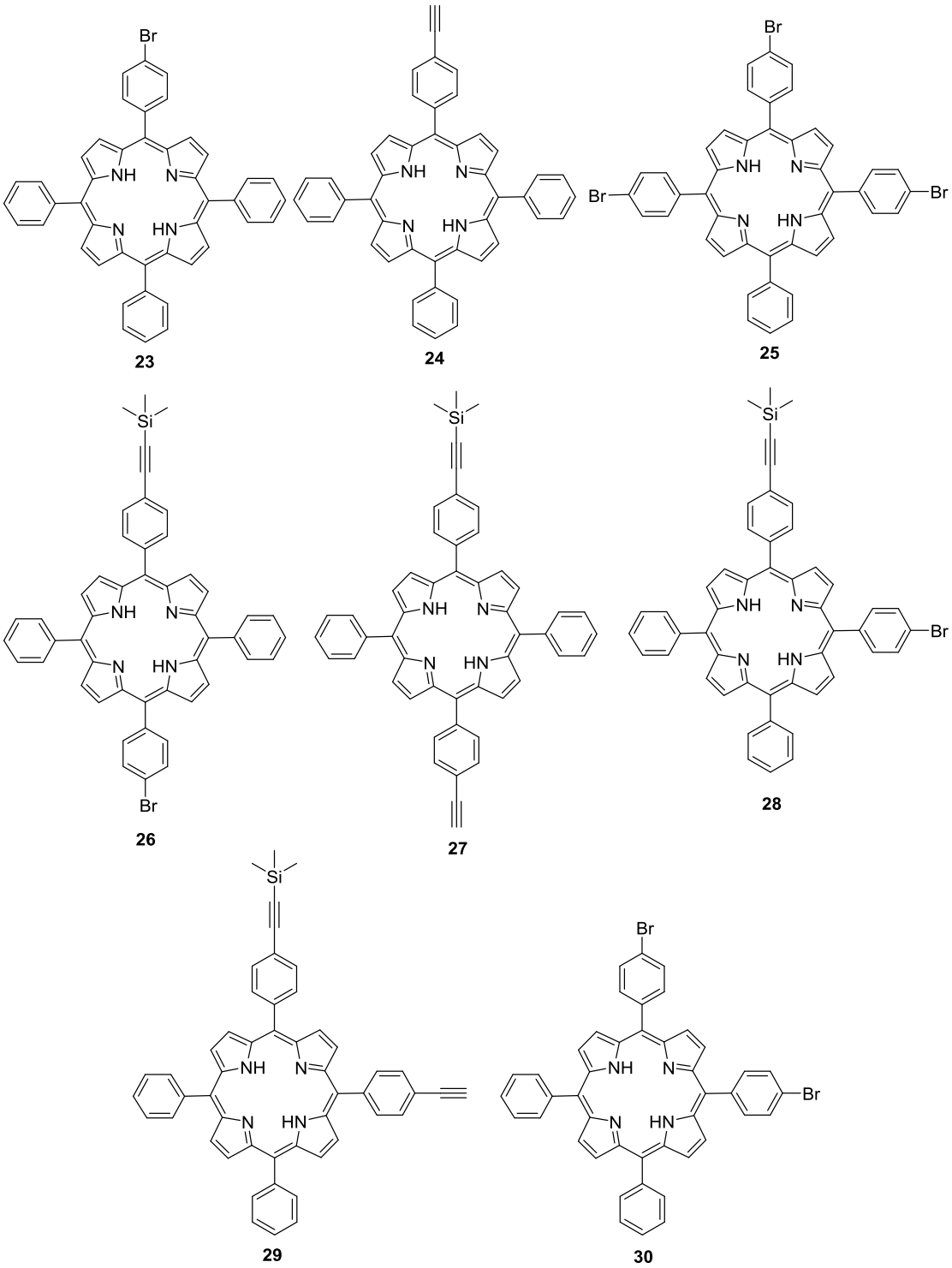


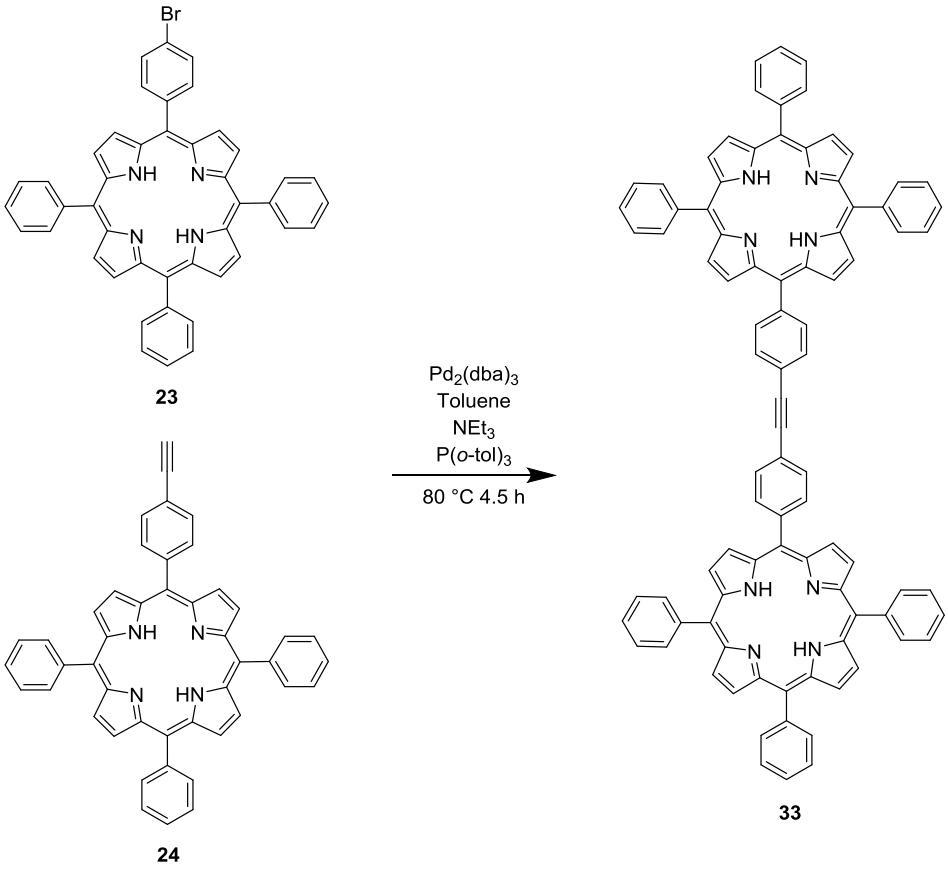
Figure 5.8 Structures of porphyrins 23-30.

The MALDI-TOF data discussed in this section was usually collected from a non-calibrated spectrometer as the data was used for an initial assessment of the success or failure of a reaction. The data cannot be regarded as high accuracy and so *m/z*, peaks are

usually quoted to the nearest integer during the discussion. Once purified, the desired product was confirmed by calibrating the spectrometer with polyethylene glycol (PEG) to collect high-accuracy data.

Synthesis of Porphyrin Dimers 33 and 34

The synthetic route to the target Tetris pieces requires successive Sonogashira coupling reactions. Previous literature[26] indicated that the coupling reaction proceeded efficiently when there were solubilising groups on the *meso-* phenyl groups, however as there are no such groups on the target molecules, the reaction conditions were first tested on the dimer below to check suitability for this study (scheme 5.1).



Scheme 5.1 Synthesis of porphyrin dimer 33.

A copper-free Sonogashira coupling reaction was conducted using porphyrins **23** and **24** in a 1:1 ratio with $Pd_2(dba)_3$ as the catalyst and P(o-tol)$_3$ as the phosphine ligand. The

reaction was conducted in toluene and triethylamine at 80 °C for 4.5 h. The reaction employed a 20% loading of palladium catalyst and the ratio of catalyst to phosphine ligand was approximately 1:6. The reaction mixture was analysed by MALDI-TOF MS as seen in figure 5.9.

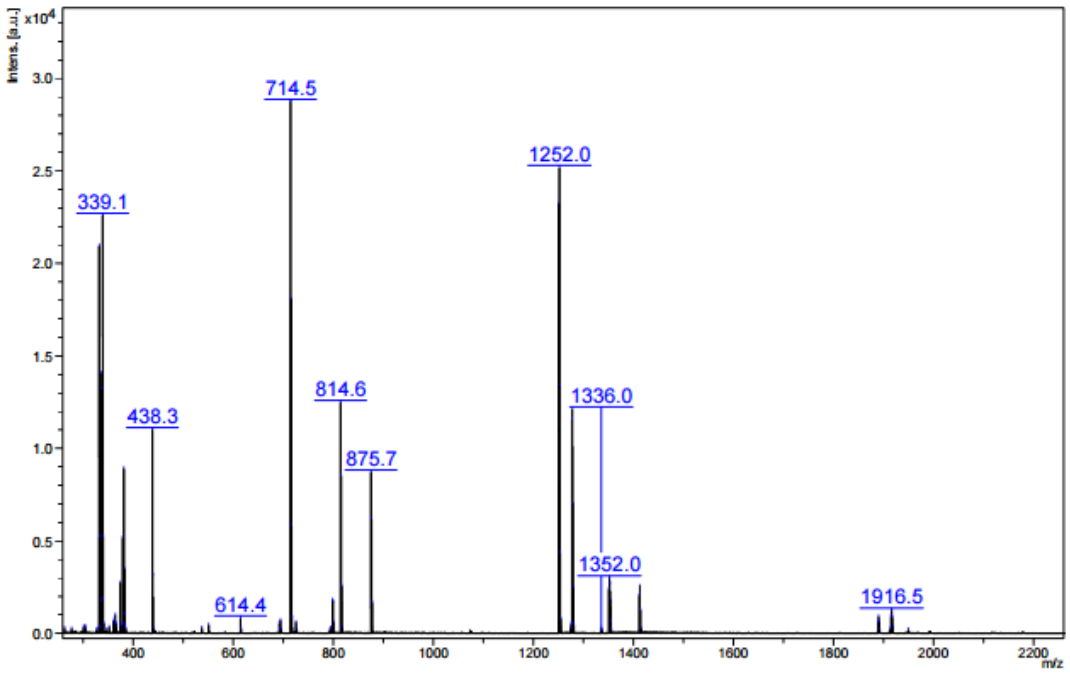


Figure 5.9 MALDI-TOF MS data for crude product mix produced during synthesis of 33.

The peak observed at 1252 *m/z* in the spectrum corresponds to the desired ethyne linked porphyrin dimer product **33**. A small amount of palladium insertion was detected in one porphyrin ring only (corresponding with at peak at 1354 *m/z*) with no evidence of palladium insertion in both porphyrin rings (predicted peak at 1464 *m/z*). Also observed is a peak at 1270 *m/z*, although we were unable to isolate this during purification, the most likely product responsible for this peak is an enyne-linked dimer (shown in figure 5.10).[26] The data also presents some peaks relating to higher molecular weight materials (HMWM[27]) around 1917 *m/z*, which corresponds to an unknown product containing three porphyrin rings as well as a number of unidentified lower mass peaks.

Purification of **33** consisted of silica column chromatography in a 2:1 hexane/chloroform mix, slowly increasing the amount of chloroform until it was eluted with 100% chloroform. Using those conditions, one column chromatogram was insufficient to obtain acceptable spectroscopic data. Upon repeating the column chromatography a second time, the purity of **33** was determined to be satisfactory through NMR analysis.

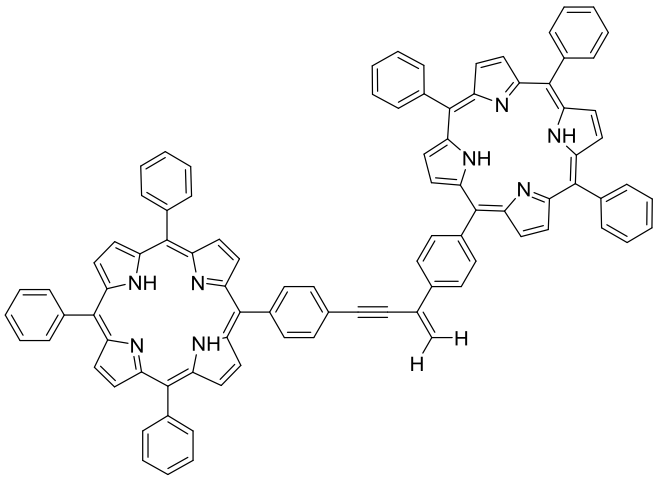
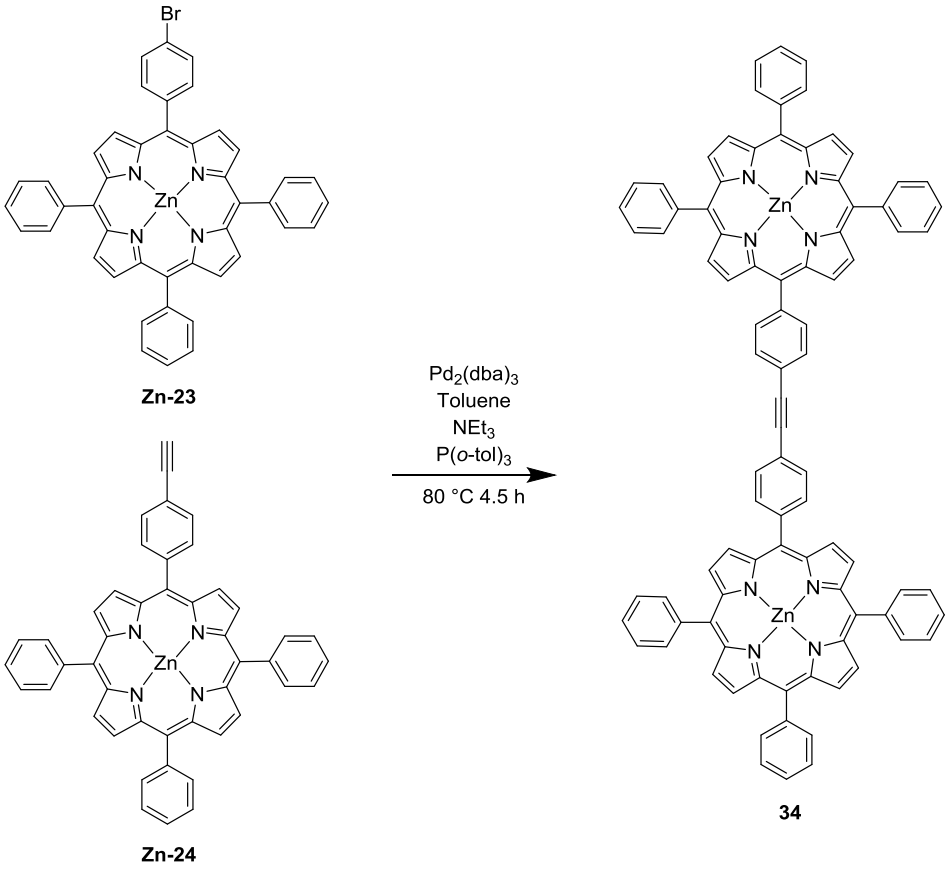


Figure 5.10 Enyne-linked porphyrin dimer.

A similar Sonogashira coupling reaction was performed with Zn-coordinated porphyrins **Zn-23** and **Zn-24**, shown in scheme 5.2.

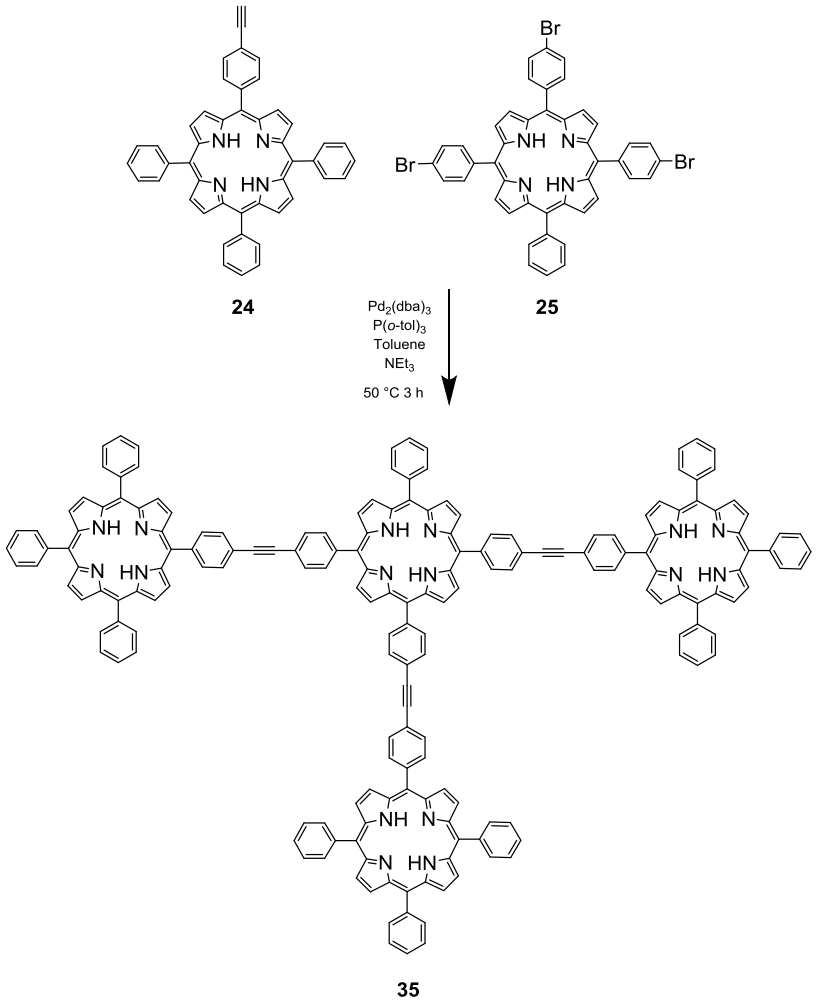


Scheme 5.2 Synthesis of porphyrin dimer 34.

No demetallation or transmetallation was observed in the products generated. The Zn-coordinated porphyrin dimer **34** was less soluble than the freebase porphyrin dimer **33**. The purification process was modified so that preparative TLC plates were used instead of standard column chromatography. Although some separation was achieved, there was excessive streaking of the product. MS and NMR analysis could confirm the presence of **34**, but small amounts of impurities were still present despite repeated attempts at purification.

As the Sonogashira coupling reactions form **33** and **34** were successful, albeit in low yields (*c.a.* 15%), the synthesis of the more complex Tetris compounds was attempted using the same reaction procedures.

Synthesis of Tetrimino T



Scheme 5.3 Synthesis of Tetrimino T.

As seen in table 5.1, the synthesis of Tetrimino T only requires one reaction from the porphyrin monomer units, unlike the other Tetris shapes which require three reaction steps each. Tetrimino T was synthesised from just two porphyrin monomers by coupling **24** and **25**. The first conditions tried for the Sonogashira coupling reaction were identical to those used in the synthesis of the dimer **33**. The reaction was conducted in toluene and triethylamine at 80 °C for 4.5 h. The reaction used a 20% loading of palladium catalyst and the ratio of catalyst to phosphine ligand was approximately 1:6. As three Sonogashira coupling reactions were occurring, a ratio in excess of 3:1 of **24** to **25** was used. After a review of the literature,[17] these conditions were later refined to a 15% palladium catalyst

loading at a 1:8 ratio catalyst: phosphine ligand, heated at 50 °C for 3 h with a second batch of catalyst and ligand added at the midway point. These conditions improved the yield from *c.a.* 15% to 34% and were used in subsequent Sonogashira coupling reactions throughout this study.

Once the coupling reaction had completed and solvents removed, MALDI-TOF MS analysis showed that several products had formed as seen in figure 5.11. The desired Tetrimino T compound is seen at 2528 m/z, a couple of peaks at higher m/z represent the HMWM generated, there are also peaks at lower m/z representing trimeric, dimeric, monomeric species.

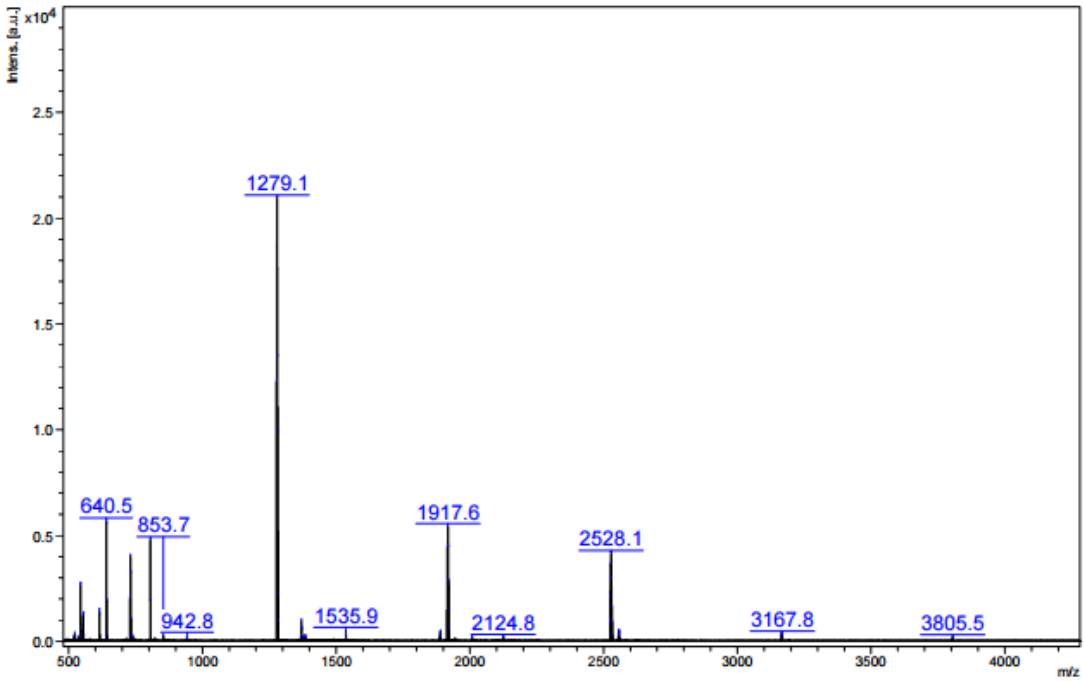


Figure 5.11 MALDI-TOF MS data for crude Tetrimino T reaction.

Column chromatography was used in the initial attempt of purification for Tetrimino T. However, this had only limited success in removing the impurities generated from the desired product so alternative purification techniques were investigated. Size exclusion chromatography (SEC) is able to purify mixtures of compounds by their size, with larger compounds eluting first and smaller compounds eluting later. The polarity of the

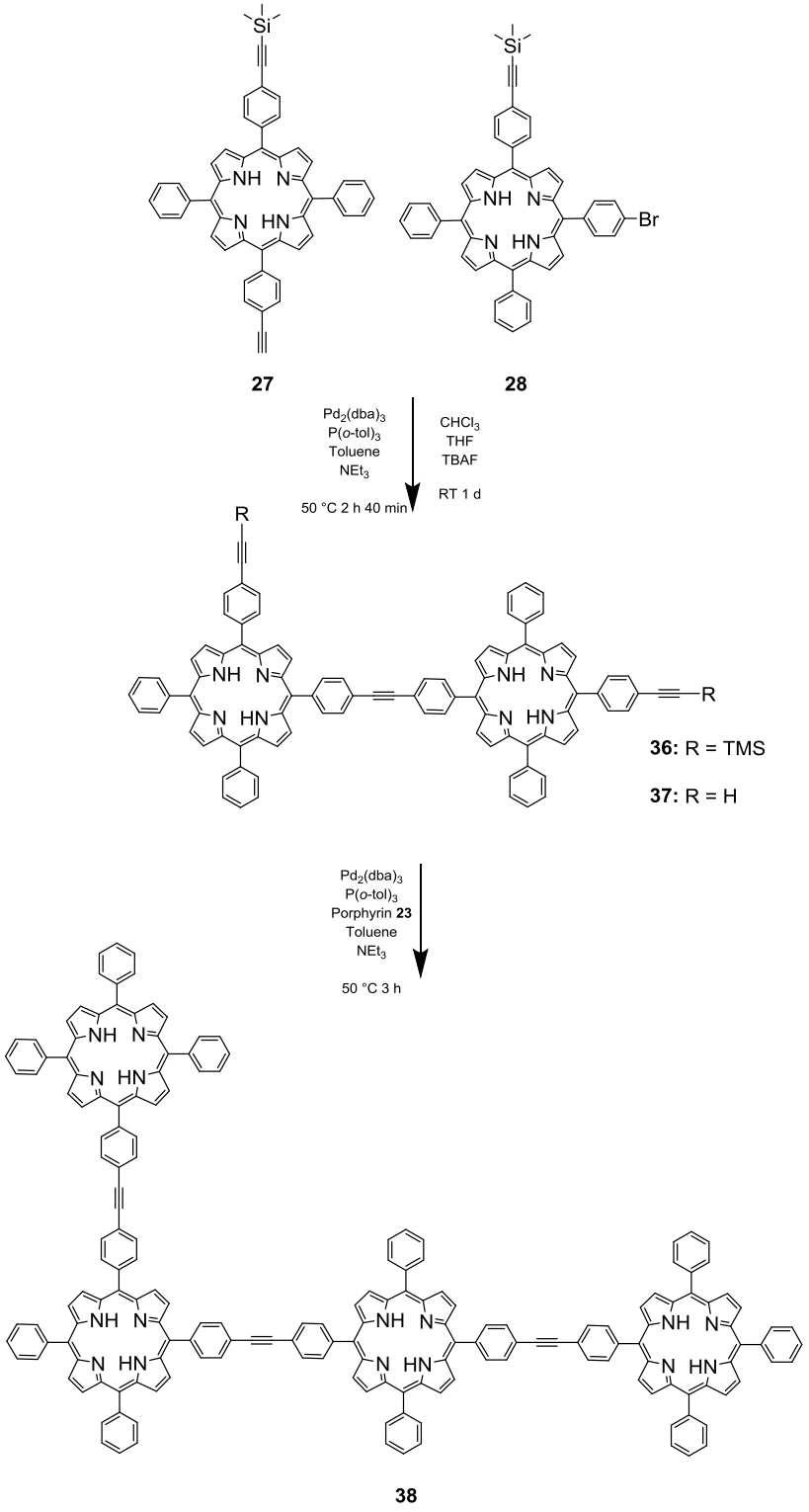
compounds is unimportant in this technique and so if there is a mixture of compounds with very similar polarities but with a large difference in size (as there is in the Tetrimino T product mix), the technique of SEC is appropriate.

SEC was performed with the product mix from the Tetrimino T reaction using Bio-Beads SX-1 in toluene. The crude mix was dissolved in toluene and loaded onto the column in one 5 mL loading, filtered through a 0.45 μm PTFE filter. Several different fractions eluted from the column. First to elute was a broad, ill-defined band containing the HMWM. The second band to elute contained the desired Tetrimino T compound. Following this were smaller bands for trimeric, dimeric and monomeric species. Some purple material in the Tetrimino T fractions precipitated from solution after being eluted from the column. This material was collected, analysed and confirmed to be the desired product.

A significant amount of product was stuck on the PTFE filter so this was washed off with 99:1 chloroform/TFA solution. MALDI-TOF MS analysis showed that this material also contained the desired Tetrimino T compound. This solution was neutralised with aqueous NaOH, washed with water, brine dried and filtered. All fractions containing Tetrimino T were combined and solvents removed. Addition of toluene (15 mL) resulted in a suspended precipitate in a light purple solution which was collected by filtration. The collected material was dissolved in chloroform and solvents removed to give a purple solid. The light purple solution was concentrated to approximately 5 mL and loaded onto the SEC column. The fractions containing the desired compound were collected and solvents removed. MS and NMR analysis confirmed that the solids collected were the desired Tetrimino T compound. However, the solids contained a small amount of toluene solvent despite exposure to vacuum. The solids were dissolved in chloroform and

loaded onto a short silica column acting as a plug. After several washings with chloroform, during which the Tetrimino T compound was not eluted, 5% MeOH was added to the solvent mix. The Tetrimino T compound quickly eluted, solvents were removed and NMR analysis showed that the toluene solvent had been removed.

Synthesis of Tetrimino J/L



Scheme 5.4 Synthesis of Tetrimino J/L.

A Sonogashira coupling reaction was performed using porphyrins **27** and **28** with a second batch of palladium catalyst and phosphine ligand added 1 h 20 min into the

reaction (scheme 5.4). The mixture was cooled after a further 1 h 20 min and concentrated to dryness. Toluene (5 mL) was added to the residue and this was passed through a PTFE filter, the filtrate was loaded onto an SEC column (Bio-Beads SX-3) and the fractions containing the desired species (identified by mass spectrometry) were collected. The material that was trapped on the PTFE filter was washed off with DCM, solvents were removed and toluene (5 mL) was added to the residue again to repeat the process. A total of three loadings of 5 mL were required before all the crude material had passed through the column once. The fractions containing the J/L protected precursor were collected together, solvents removed and then subjected to silica column chromatography to produce the pure dimeric J/L protected precursor **36**.

The deprotection reaction was performed in 1:2 chloroform/THF with the addition of TBAF, stirring at RT for 1 d. The reaction was quenched, washed, dried and filtered. Solvents were removed and NMR analysis shown in figure 5.12 on the resultant purple solid showed that the product **37** was of acceptable purity.

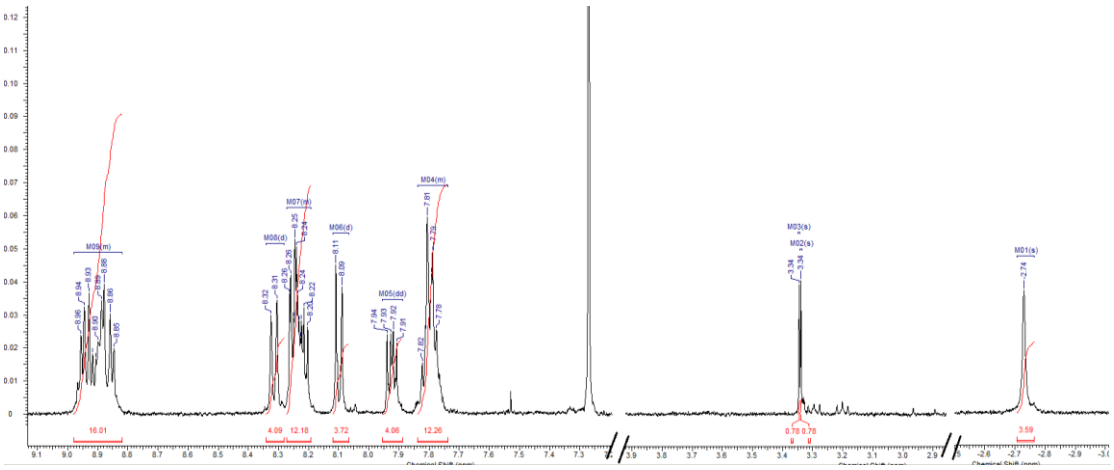


Figure 5.12 ^{1}H NMR of 37.

The synthesis of Tetrimino J/L required a Sonogashira coupling reaction using porphyrins **37** and **23.** The porphyrins were reacted together for a total of 3 h, with a second batch of catalyst was added at the 1.5 h time point. Solvents were then removed *in*

vacuo to give a crude solid. MALDI-TOF MS analysis on this solid showed a peak at 2522 *m/z* corresponding to the J/L Tetrimino compound as well as a significant amount of enyne linked product at 2548 *m/z* (figure 5.13).

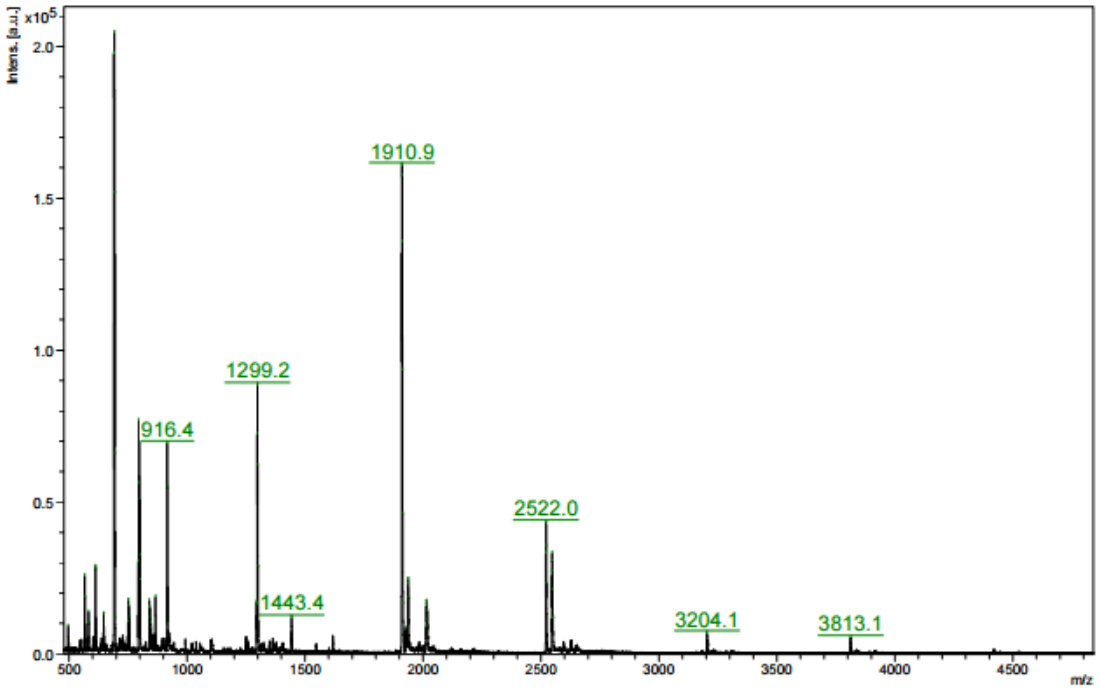
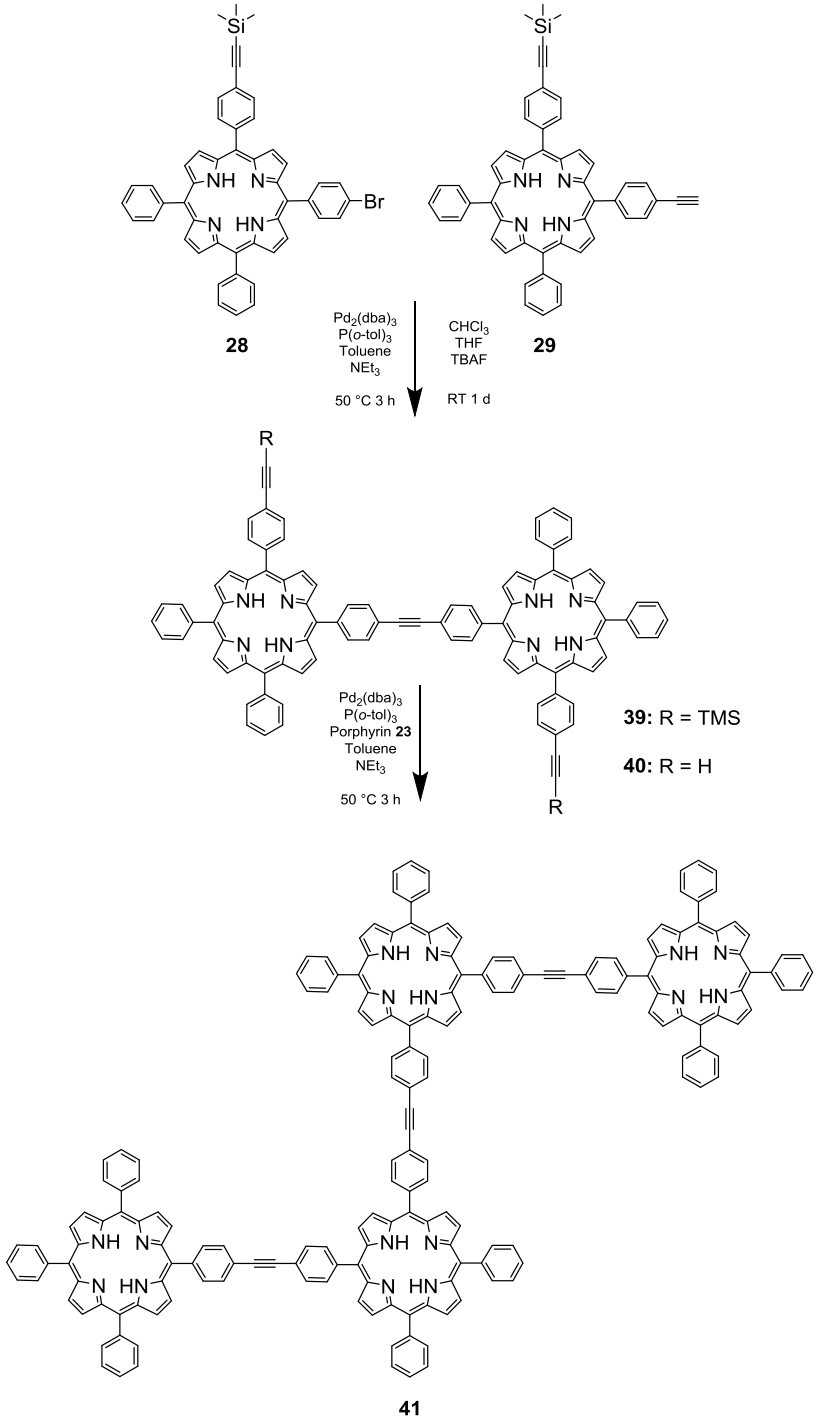


Figure 5.13 MALDI-TOF MS data for crude Tetrimino J/L product mix.

The compound mixture created a suspension when toluene was added, indicating poor solubility. Solvents were removed and chloroform was added which created a solution. This solution was passed through a PTFE filter and loaded onto a column containing Bio-Beads SX-1 using chloroform as the eluent. The main fractions eluted were HMWM, Tetrimino J/L product and enyne impurity, unreacted dimer and porphyrin **23**. The fractions containing the desired product and enyne impurity were collected together and solvents were removed. Toluene was added, creating a suspension which was separated out using a centrifuge. The collected solids were dissolved in chloroform and loaded onto a silica column. After several elutions with chloroform, removing the undesired products and solvent residues, the eluent was changed to 95:5 chloroform/MeOH to collect the desired Tetrimino J/L compound.

Synthesis of Tetrimino S/Z



Scheme 5.5 Synthesis of Tetrimino S/Z.

Following a Sonogashira reaction between **28** and **29**, the mixture was cooled and concentrated to dryness (scheme 5.5). The residue was dissolved in toluene and loaded onto a SEC column containing Bio-Beads SX-3 as the stationary media. This caused three

main bands to separate. The first to elute was the HMWM, next was the desired protected dimer **39** and finally monomeric products were eluted.

The deprotection step was performed in a THF/chloroform mix with TBAF stirring at RT for 1 d. This reaction proceeded very efficiently with no detectable protecting groups remaining in MALDI-TOF MS analysis. After the reaction solution was worked-up, the resultant purple solid was determined by NMR to be of acceptable purity.

The final step in the synthesis of Tetrimino S/Z was a Sonogashira coupling reaction using an excess of porphyrin **23** with S/Z deprotected precursor **40**. Solvents were removed, dissolved in chloroform and loaded onto a column for SEC. The fraction containing the desired Tetrimino S/Z compound was collected and solvents were removed. Toluene was added to the solid, creating a suspension which was collected *via* centrifuge. The solid was analysed by MALDI-TOF MS to give the spectrum in figure 5.14. Unlike the previous reactions, some palladium insertion was detected as evidenced by the peaks at 2632 *m/z* and 2734 *m/z*. Addition of TFA to a solution of this removed all traces of palladium insertion, the solution was the neutralised using aqueous NaOH solution, dried and solvents removed.

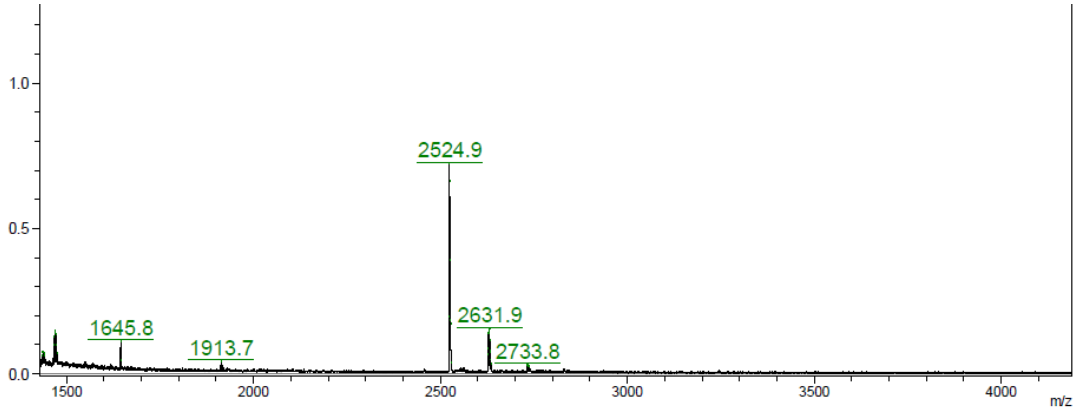
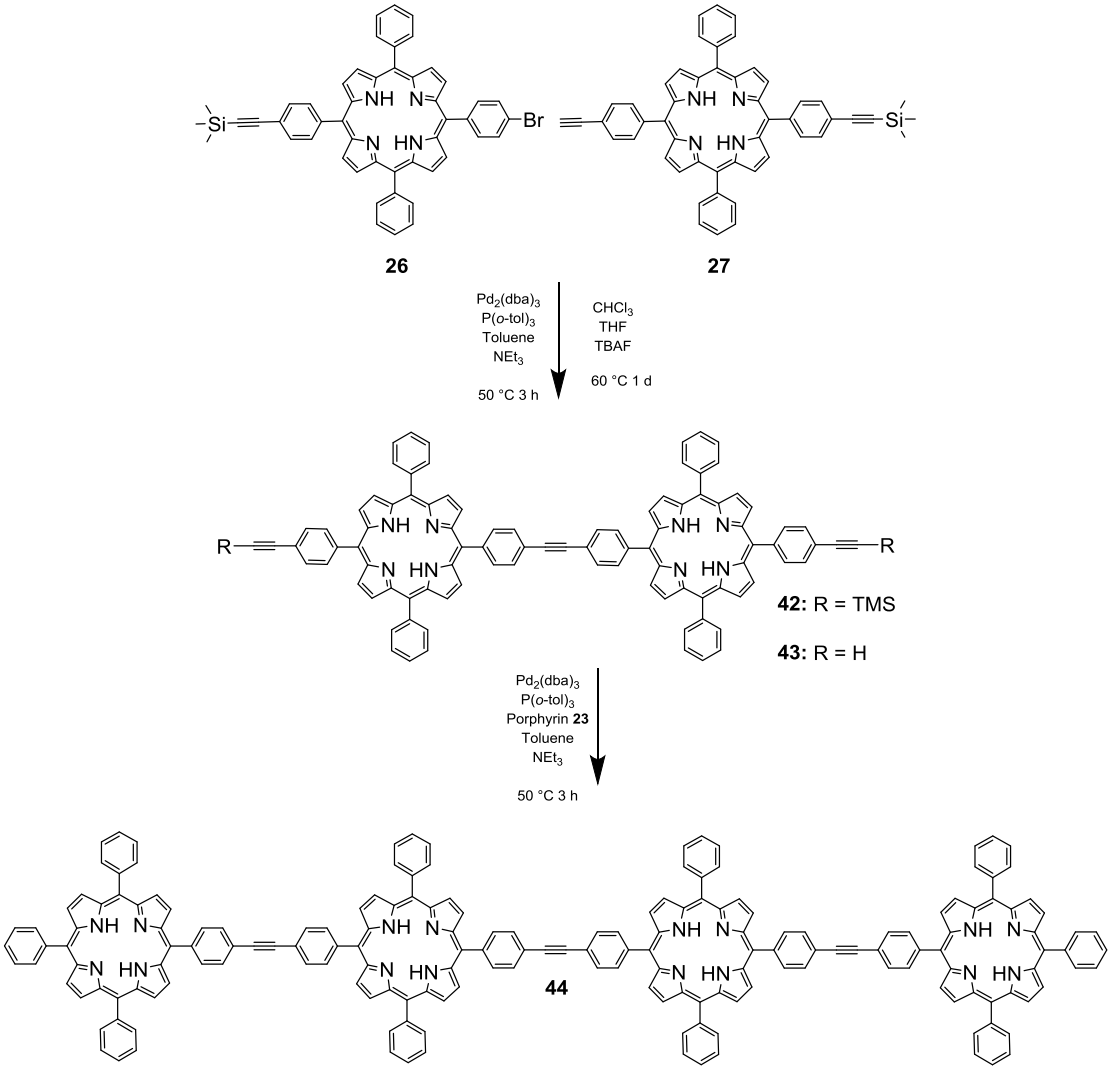


Figure 5.14 MALDI-TOF MS data collected for Tetrimino S/Z.

Synthesis of Tetrimino I



Scheme 5.6 Synthesis of Tetrimino I.

As with the previous Tetrimino J/L and S/Z compounds the protected dimeric species was formed *via* a Sonogashira coupling reaction, this time between porphyrins **26** and **27** (scheme 5.6). In this instance, after the reaction was complete and solvents removed, purification was achieved by adding DCM (100 mL) to the crude product and filtering through a PTFE filter. The desired porphyrin product was only sparsely soluble in DCM and so created a suspension which was trapped in the filter whereas the monomeric and oligomeric by-products were reasonably soluble and were able to pass through in solution. The solvent from the filtrate was removed to create a solid. DCM (20 mL) was

added to this solid which was again passed through a PTFE filter. The desired porphyrin was then extracted from the PTFE filters by eluting with a solution of 99:1 DCM/TFA. The solution was neutralised with 2 M NaOH, washed with water and brine and the solvents were removed. The product was analysed by MALDI-TOF MS to give the spectrum in figure 5.15 with the large peak at 1443 m/z suggesting that the sample mainly consists of the Tetrimino I protected precursor. Despite the extremely low solubility, ^{1}H NMR data was collected in chloroform and confirmed the purity of **42** was high enough to continue without further purification.

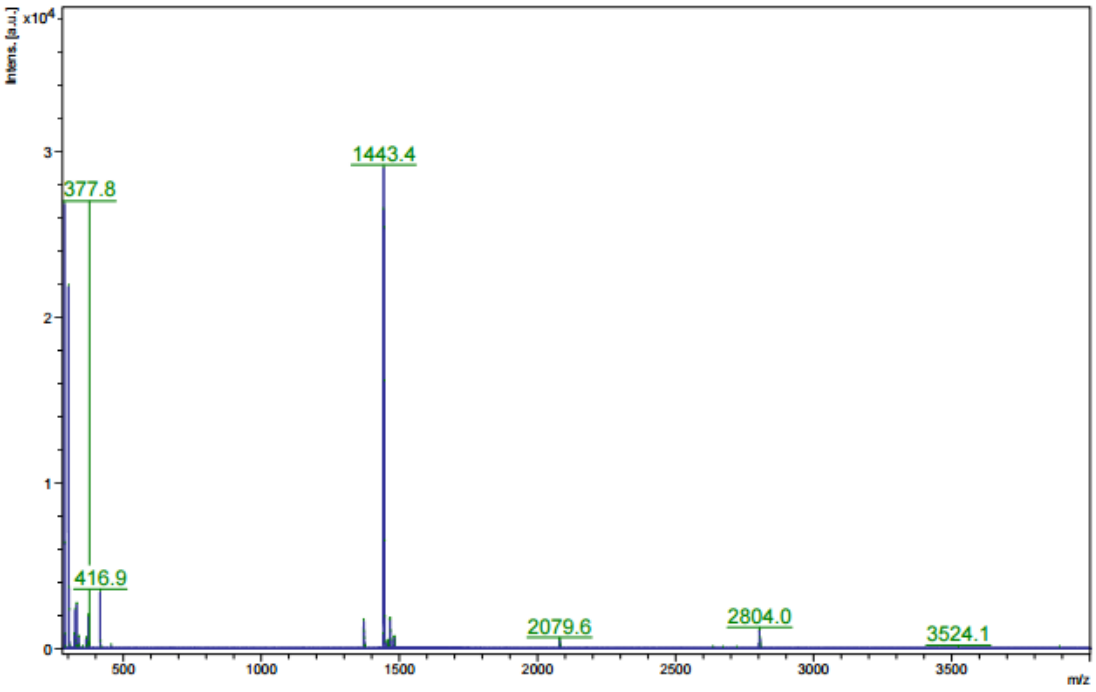
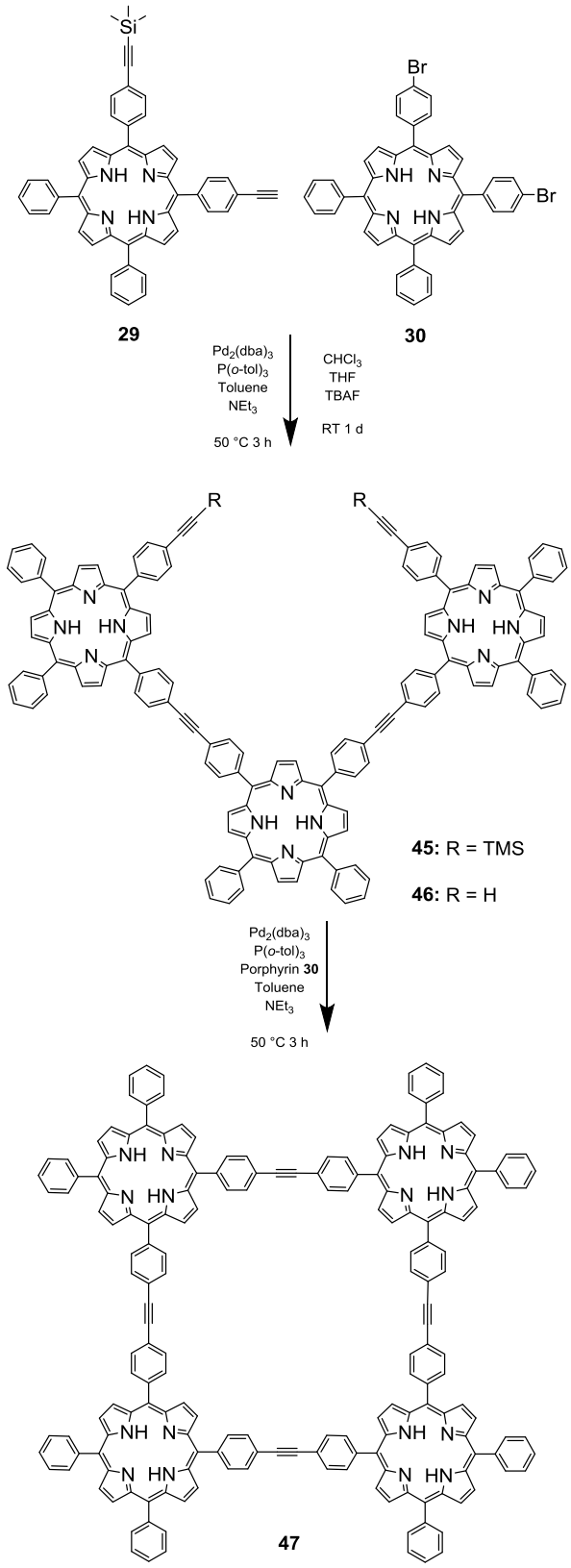


Figure 5.15 MALDI-TOF MS data for material collected from PTFE filter during purification of 42.

The Tetrimino I protected precursor compound **42** underwent a deprotection reaction to produce the terminal-alkyne species required for the final Sonogashira coupling reaction. As **42** had very low solubility, a large amount of solvent (THF and chloroform, 2:1, 225 mL) at an elevated temperature (60 °C) was required to dissolve the reactants. TBAF was added to this and the solution was stirred at 60 °C for 24 h to produce the Tetrimino I deprotected precursor **43**, which also exhibited very low solubility.

The coupling reaction of **43** with **23** was conducted in a lower concentration than for the previous Tetris compounds due to the very low solubility of **43** in the *c.a.* 1 mmol concentration conditions used for the previous Tetris compounds. The reaction was very low yielding, with the major component of the product mix being unreacted porphyrin dimer **43**. Suggesting that despite increased solvent volume, **43** was not completely in solution. As with its precursor compounds **42** and **43**, Tetrimino I was very insoluble. The majority of the reaction by-products could be removed by adding DCM to the product mix and passing the suspension through a PTFE filter, with a subsequent washing of 99:1 DCM/TFA. After neutralising, and removing solvents, SEC was performed using 99.9:0.1 DCM/TFA as the eluent. The separation achieved in this system was sufficient to entirely remove the presence of the unreacted dimer from the desired Tetrimino I compound but the presence of TFA within the eluent caused both compounds to elute more quickly than expected.

Synthesis of Tetrimino O



Scheme 5.7 Synthesis of Tetrimino O.

The Tetrimino O compound offered perhaps the most choice in terms of developing a synthetic route. A similar porphyrin square was synthesised from two monomeric porphyrins in a yield of 7%[28] Alternatively, the target could be built up one porphyrin ring at a time, *via* successive Sonogashira coupling and deprotection reactions, although this would be time and resource intensive, it would decrease the chance of unwanted products. The target could also be formed by a homocoupling of two dimers, this would result in HMWM being generated but that could easily be removed *via* SEC. A coupling of two different protected dimers followed by a deprotection reaction and subsequent coupling is also viable. The route chosen, shown in scheme 5.7 is a hybrid of these approaches; two Sonogashira coupling reactions are required in the synthesis but the potential for unwanted products forming is fairly low, with polymerisation not occurring in the formation of the trimeric species and only occurring in the formation of the Tetrimino O compound when the intermolecular reaction is favoured over the intramolecular reaction.

The first Sonogashira coupling reaction in the Tetrimino O synthesis is between porphyrins **29** and **30**. These two porphyrins were kept at approximately 1:1 ratio as the porphyrin which would otherwise be in excess (porphyrin **29**) was particularly challenging to synthesise so efforts were made to use it as sparingly as possible. The reaction mixture was held at 50 °C for a total of 3 h after which solvents were removed. The residue was purified by dissolving it in toluene and loading onto a column containing Bio-Beads SX-1 for SEC. The fractions containing the protected Tetrimino O precursor **45** were collected together and solvents removed. The ESI MS data collected for **45** is shown in figure 5.16.

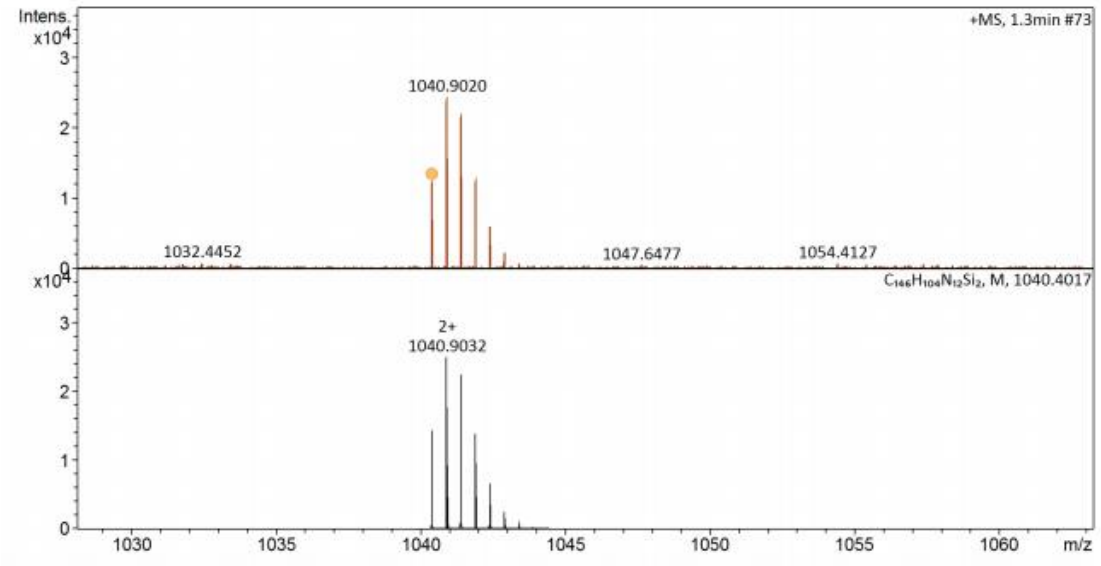


Figure 5.16 MS (ESI) collected for 45 (top) and predicted specrum (bottom).

The deprotection step was performed in the same manner as for the other Tetrimino precursor molecules. Despite repeated attempts at column chromatography, purification proved very challenging. NMR analysis confirmed the wanted material had been produced but it could not be completely isolated from other, unknown non-porphyrinic materials. The final coupling reaction was performed using the porphyrin trimer **46** in this slightly impure state.

The Sonogashira coupling reaction between **46** and **30** was conducted at 50 °C for 3 h. After this time, solvents were removed to produce a crude solid. Purification was attempted using similar techniques as with previous Tetris compounds. SEC was performed in toluene after filtering through a PTFE filter, however, no fractions were found to contain the desired product. Material was washed off the filter using 99:1 chloroform/TFA solution and found to contain the desired product, along with some impurities. A second SEC column was performed using 99.9:0.1 DCM/TFA as the eluent. A couple of bands eluted, indicating some success in separation. The fractions containing the desired Tetrimino O compound were collected together. Analysis showed

that impurities were still present, as evidenced by the MALDI-TOF MS data shown in figure 5.17. The small amount of material to work with impeded the purification process and so an analytically pure sample could not be obtained.

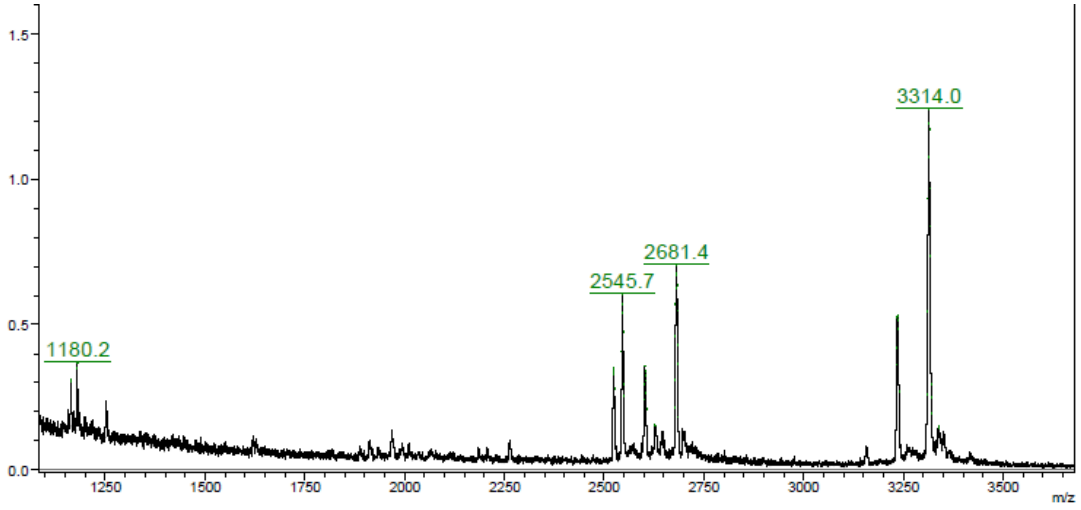


Figure 5.17 MALDI-TOF MS data for Tetrimino O.

NMR Spectra of Tetris Products

All of the Tetriminos are isomers of each other, except for the O Tetrimino which has an additional alkyne group, giving it by mass two extra carbon atoms and two fewer hydrogen atoms. Additionally, the precursor molecules to the I, S/Z and J/L Tetriminos are also isomers. On initial glance at the NMR spectra, they appear to be very similar to each other, however closer inspection reveals some differences.

To help identify the peaks, the aromatic region of the NMR spectra for the protected I dimer **42** and dimer **33** is compared in figure 5.18. The spectrum recorded for **43** is largely similar to that collected for **42**, however differences between the two are also highlighted. The most downfield peaks at roughly 8.9 ppm present themselves as a multiplet of 16 protons and correspond to the pyrrolic β-protons (labelled A and circled in red). The multiplet relating to the β-protons can be partially resolved and this is below.

The 12 protons in the multiplet at 7.8 ppm observed for compound **42** are from three terminal protons on each of the four phenyl rings at the 10-, 20- and 10'-, 20'- positions of the porphyrin rings in the Tetrimino I precursor molecule. This multiplet increases to 18 protons in dimer **33** as there are also terminal phenyl groups at the 5- and 15'-positions which contribute an additional three protons each (labelled E, circled in dark blue). The other two protons on these phenyl groups can be found in the multiplet at approximately 8.25 ppm, representing 8 protons for **42** and 12 protons for dimer **33** (labelled C, circled in dark green).

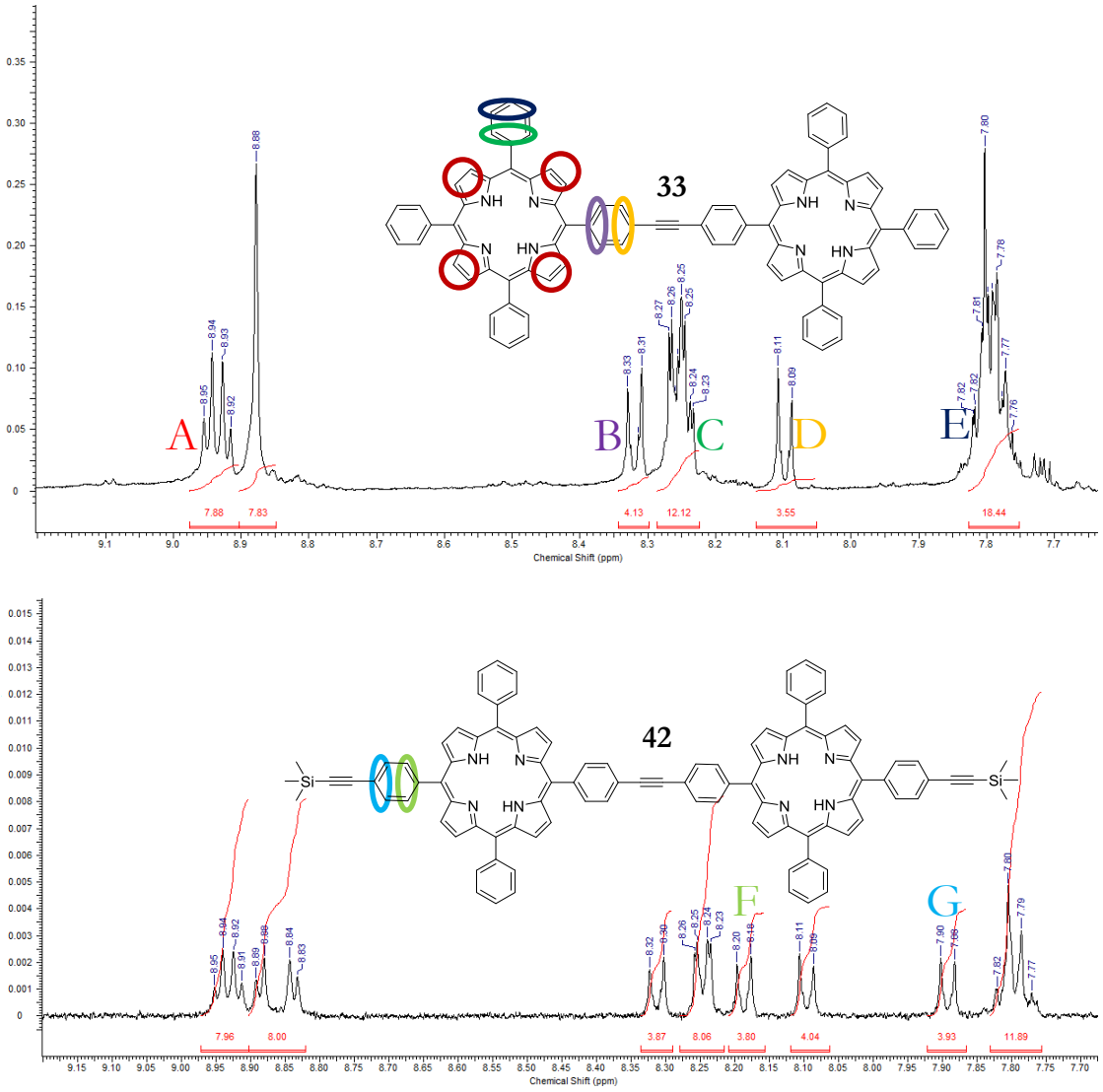


Figure 5.18 ^{1}H NMR Spectra of 33 (top) and 42 (bottom).

The phenyl groups linked by an ethynyl group have two sets of 4 protons associated with them appearing as two doublets. The group of 4 protons closest to the ethynyl group are at approximately 8.10 ppm (labelled D, circled in yellow) whereas the group of 4 protons further away are at approximately 8.31 ppm (labelled B, circled in purple). This was established by performing 2D COSY NMR experiments. Finally, there are two environments seen in the I precursor molecules that are not observed in dimer **33**, these relate to the protons on the phenyl rings with either the TMS-protected ethynyl group for **42** or the terminal ethynyl group for **43**. The set of four phenyl protons further away from the ethynyl group are found as a doublet at 8.19 ppm for the TMS-protected molecule and 8.21 ppm for the deprotected molecule (labelled F, circled in light green). The other set of four phenyl protons closer to the ethynyl group is at 7.89 ppm for the protected molecule and 7.92 ppm for the deprotected molecule (labelled G, circled in light blue). This assignment was also established from 2D COSY NMR data.

The position of the terminal ethynyl groups on the molecule has a small but noticeable effect on the NMR with respect to the signal labelled G in figure 5.18. The Tetrimino I deprotected precursor is a very symmetric molecule, having a C_2 axis running through all of the ethynyl groups and perpendicular C_2 axes through the central ethynyl group. This means that the terminal ethynyl groups are in the same environment as each other and so the signal relating to the 'G' protons is resolved as a doublet. Likewise, the Tetrimino S/Z deprotected precursor has a C_2 axis through its central ethynyl group so its terminal ethynyl groups are also in the same environment as each other, also resulting in a doublet.

The Tetrimino J/L deprotected precursor **37** has one terminal ethynyl group in the same position as the I precursor **43** and one in the same position as the S/Z precursor **40**. This means that the 'G' protons are no longer in the same environment as each other. This

can be seen from the more complicated splitting pattern which is a superposition of one doublet at 7.92 ppm from the I precursor position and another doublet at 7.93 ppm from the S/Z precursor position (figure 5.19). The other set of protons on those phenyl groups (labelled F in figure 5.18) either resolve themselves distinctly as in the I precursor or are moved downfield due to the shifting ethynyl group, merging with the protons forming multiplet 'C'.

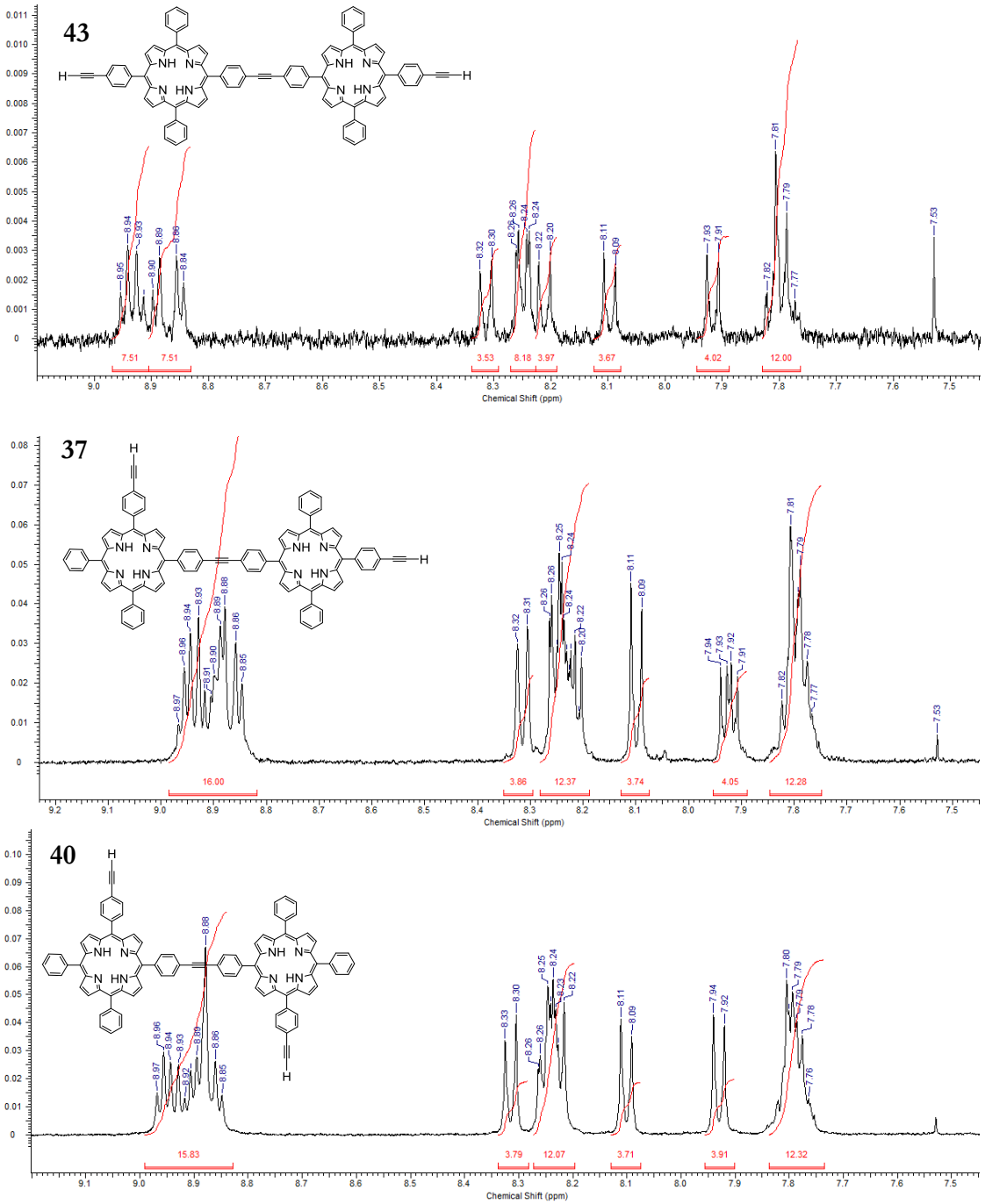


Figure 5.19 ^{1}H NMR spectra of 43 (top), 37 (middle) and 40 (bottom).

The peak at 7.53 ppm observed in each of the spectra is due to the satellite peaks of ^{1}H from the chloroform solvent interacting with a ^{13}C nucleus. This illustrates the differences in solubility between the isomers. The NMR spectrum collected for Tetrimino I deprotected precursor **43** was a saturated solution and is still clearly much less concentrated than the S/Z and J/L isomers. The other difference can be found in the pyrrolic β-protons. The multiplet of 16 protons appears different for each isomer and the peaks can partly be resolved to explain this.

The comparison between the pyrrolic β-protons can be made using the final Tetrimino compounds. Tetrimino I was not sufficiently soluble in chloroform to obtain useful NMR data; instead TFA had to be used as the solvent, making direct comparison with the other pieces difficult. Tetrimino O could not be purified sufficiently to obtain good data. NMR data for the T, S/Z and J/L Tetriminos are shown in figure 5.20. These spectra are similar to those collected for **33** as there are no longer terminal ethynyl groups on the molecule.

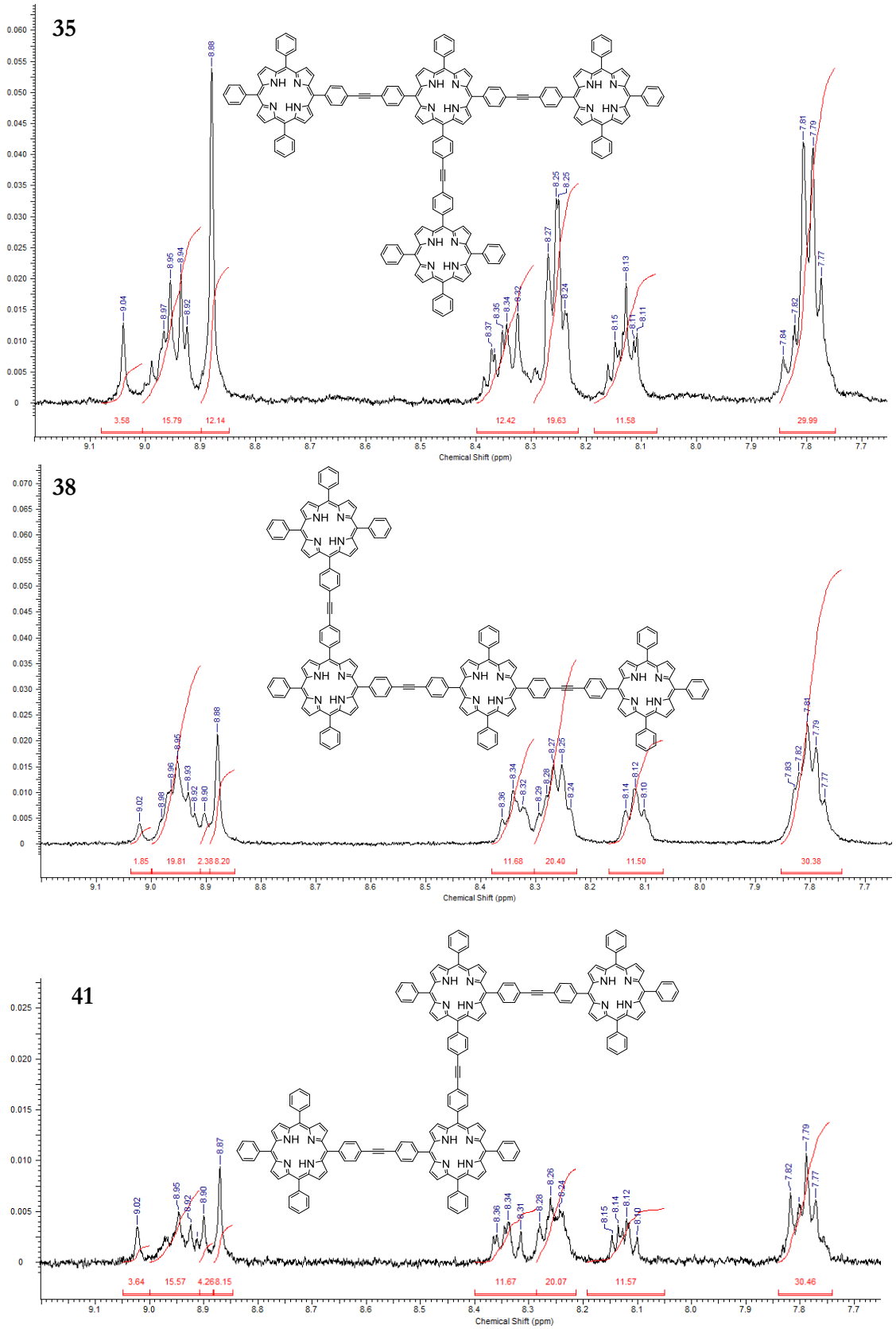


Figure 5.20 ^{1}H NMR spectra of Tetrimino T (top), Tetrimino J/L (middle) and Tetrimino S/Z (bottom).

Focusing on the pyrrolic group protons for each compound (roughly 9.04-8.87 ppm), we are able to deduce that the ethynyl groups on the compounds have a deshielding effect on nearby protons. The most downfield peak for Tetrimino T can be resolved into a singlet representing 4 protons. In figure 5.21 these four protons have been circled in red as there are the only four protons located in proximity to two ethynyl groups. Conversely, the most upfield peak at 8.88 ppm representing 12 protons (circled in purple) relates to the protons located furthest away from an ethynyl group. The remaining 16 protons (circled in green) appear as a multiplet that could not be resolved.

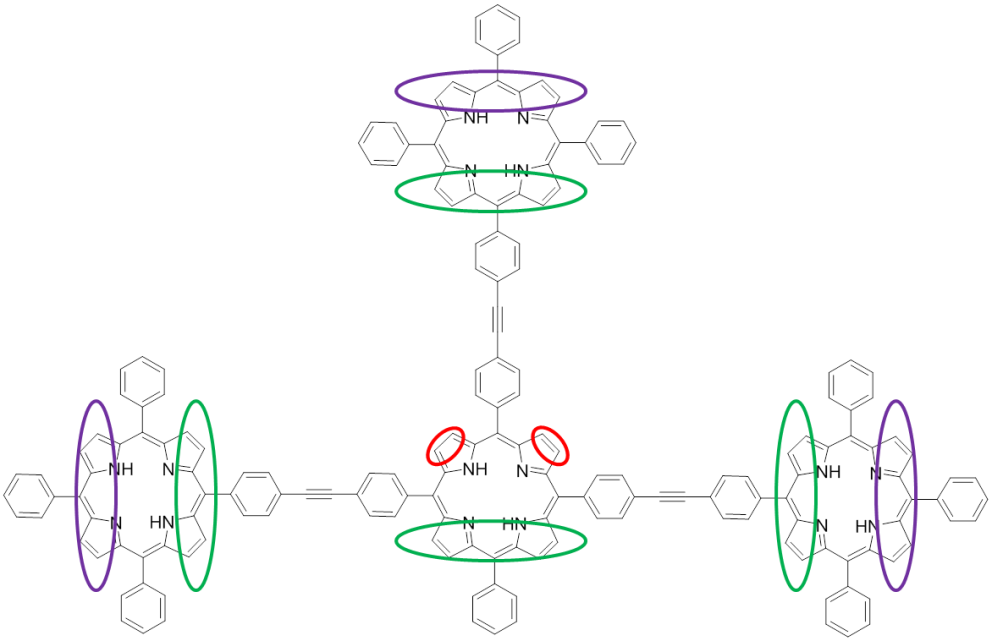


Figure 5.21 Pyrrolic proton environments for Tetrimino T.

Building on the assignments for Tetrimino T, the most downfield peak for Tetrimino J/L integrates to 2 protons (circled in red figure 5.22), as there are only two β- pyrrolic protons in close proximity to two ethynyl groups this correlates to what we expect. The peak has shifted upfield very slightly (0.02 ppm), which may be due to the fact that there is no longer a third ethynyl group deshielding the β-protons in question. Also in keeping with Tetrimino T is the set of 8 protons in the same environment of being far away from the ethynyl group (circled in purple). The remaining 20 protons have an appearance of a

multiplet in-between these two singlets. This multiplet can partly be resolved to reveal another singlet, relating to 2 protons. These two protons are on the pyrrolic group opposite to the pyrrolic group with ethynyl groups either side of it (circled in blue). They are in closer proximity to the ethynyl groups than the protons circled in purple which explains why they are found downfield with respect to them.

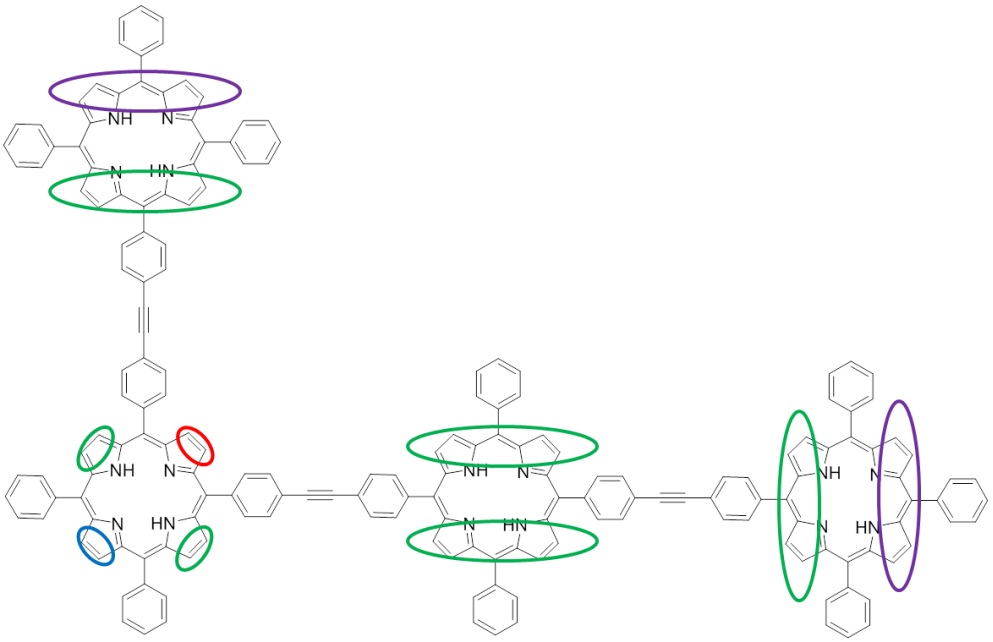


Figure 5.22 Pyrrolic proton environments for Tetrimino J/L.

Further evidence for these assignments can be found by examining the spectrum recorded for the Tetrimino S/Z compound. As with Tetrimino J/L, we would expect 8 protons for the environment circled in purple which are observed. We would expect 4 protons relating to protons in close proximity to two ethynyl links (circled in red figure 5.23), which are also observed. In this spectrum, the central multiplet can also be partially resolved, giving a third singlet relating to 4 protons. These 4 protons are in the same environment as those seen in the Tetrimino J/L compound (circled in blue). The remaining 16 protons make up the multiplet and are circled in green.

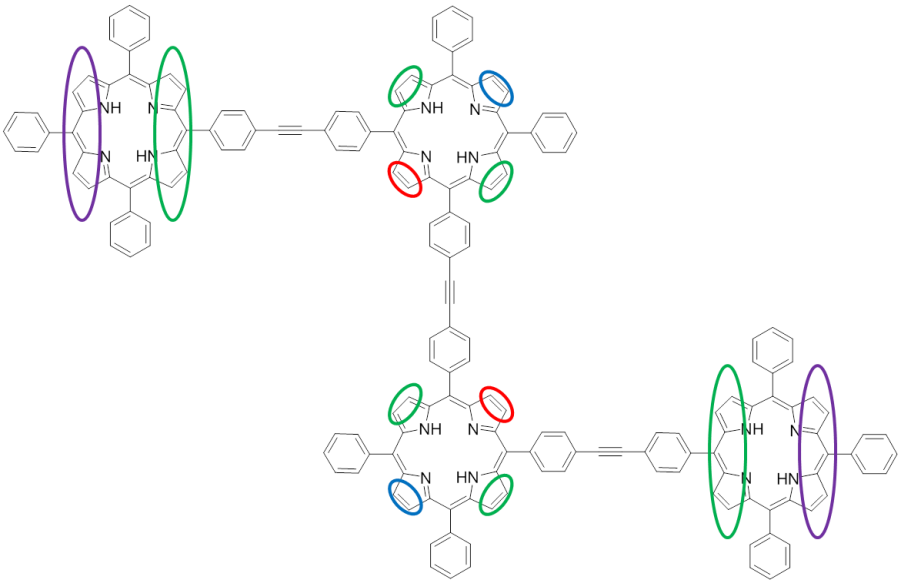


Figure 5.23 Pyrrolic proton environments for Tetrimino S/Z.

Conclusions

A series of Tetris themed molecules has been successfully synthesised by adapting procedures presented by Lindsey *et al.*[17]

The reactions forming the protected dimeric precursor molecules tended to go in moderate yields (31% - 49%) whereas the reaction forming the protected trimeric precursor for Tetrimino O was slightly lower at 22%. The reactions forming the Tetrimino compounds were also low-moderate yield ranging from (14 - 51%).

Size exclusion chromatography was effective at separating out the desired compound from the HMWM, and lower mass species. Bio-Beads SX-3 proved to be most effective at separating out the dimeric species whereas Bio-Beads SX-1 was more effective for the final Tetris compounds. In many cases, the purification process was aided by the insolubility of the Tetris compounds in toluene compared to the impurities which could not be separated by SEC, which were fairly soluble in toluene.

The Tetris pieces with lower solubility, Tetrimino I and Tetrimino O proved to be the most challenging to synthesise and purify. Alternative solvent systems, higher reaction temperatures or longer reaction times may have to be investigated to increase the yields of these products to more acceptable levels.

NMR analysis has shown that despite being isomers there are subtle differences in the spectra for the J/L, S/Z, T, and I Tetris compounds which help confirm the compound synthesised.

Experimental

1,2-bis(4-(10,15,20-triphenylporphyrin-5-yl)phenyl)ethyne (33)

Porphyrins **24** (50 mg, 78.3 μmol) and **25** (50 mg, 72.0 μmol), $Pd_2(dba)_3$ (15 mg, 16.4 μmol) and $P(o\text{-}tol)_3$ (28 mg, 92.0 μmol) were placed in a Schlenk flask purged with N_2. A degassed solution of toluene (30 mL) and triethylamine (6 mL) was added in a single portion. The mixture was stirred and heated at 80 °C for 4.5 h, cooled and filtered through a pad of alumina. The porphyrinic material was purified by column chromatography (silica, 2:1, hexane:chloroform → chloroform) x 2 to produce the title compound as a purple solid (14 mg, 11.2 μmol, 16%).

^1H NMR (400 MHz, $CDCl_3$) δ = 8.84 - 8.99 (m, 16 H), 8.32 (d, *J* = 8.22 Hz, 4 H), 8.22 - 8.28 (m, 12 H), 8.10 (d, *J* = 8.22 Hz, 4 H), 7.75 - 7.82 (m, 18 H), -2.72 (br. s., 4 H) ppm. MS: (MALDI-TOF, DCTB/MeCN) *m/z* calculated for $[C_{90}H_{58}N_8]^+$: 1250.4779. Found: 1250.4832.

Zn_2-1,2-bis(4-(10,15,20-triphenylporphyrin-5-yl)phenyl)ethyne (34)

Zn-5-(4-ethynylphenyl)-10,15,20-tri(phenyl)porphyrin (50 mg, 71.2 μmol), Zn-5-(4-bromophenyl)-10,15,20-tri(phenyl)porphyrin (50 mg, 66.0 μmol), $Pd_2(dba)_3$ (15 mg, 16.4 μmol) and $P(o\text{-}tol)_3$ (28 mg, 92.0 μmol) were placed in a Schlenk flask purged with N_2. A degassed solution of toluene (30 mL) and triethylamine (6 mL) was added in a single portion. The mixture was stirred and heated under reflux for 4.5 h, cooled and filtered through a pad of alumina. The porphyrinic material was purified by preparative TLC (chloroform) to produce the title compound as a purple solid (10 mg, 7.26 μmol, 11%).

^{1}H NMR (400 MHz, $CDCl_3$) δ = 8.88 - 9.04 (m, 16 H), 8.31 (d, *J* = 8.28 Hz, 4 H), 8.21 - 8.27 (m, 12 H), 8.03 - 8.10 (m, 4 H), 7.73 - 7.81 (m, 18 H) ppm. MS: (MALDI-TOF, DCTB/MeCN) *m/z* calculated for $[C_{90}H_{54}N_8Zn]^+$: 1374.3049. Found: 1374.3114.

Tetrimino T (35)

Porphyrins **24** (30 mg, 47.0 μmol), and **25** (10 mg, 11.7 μmol), $Pd_2(dba)_3$ (6 mg, 6.6 μmol) and P(o-tol)$_3$ (15 mg, 49.3 μmol) were placed in a Schlenk flask purged with N_2. A degassed solution of toluene (7.5 mL) and triethylamine (1.5 mL) was added in a single portion. The mixture was stirred and heated to 50 °C for 1 h 30 min after which a second batch of $Pd_2(dba)_3$ (6 mg, 6.6 μmol) and P(o-tol)$_3$ (15 mg, 49.3 μmol) was added. The mixture was stirred for an additional 1 h 30 min, cooled, and solvents removed. Toluene (5 mL) was added to the residue, this was then passed through a PTFE filter and loaded onto a column for size exclusion chromatography (Bio-Beads SX-1, toluene). Fractions containing the desired product were collected together. Material trapped on the PTFE filter was washed off with chloroform/TFA, neutralised with aqueous NaOH, dried with magnesium sulfate, filtered and added to the desired fractions. Solvents were removed, 15 mL toluene was added to create a suspension which was then collected by filtration to produce the title compound as a purple solid (10 mg, 3.96 μmol, 34%).

^{1}H NMR (400 MHz, $CDCl_3$) δ = 9.04 (s, 4 H), 8.90 - 9.01 (m, 16 H), 8.88 (s, 12 H), 8.30 - 8.39 (m, 12 H), 8.22 - 8.30 (m, 20 H), 8.09 - 8.17 (m, 12 H), 7.75 - 7.85 (m, 30 H), -2.66 (s, 2 H), -2.72 (s, 6 H) ppm. MS: (ESI) *m/z* calculated for $[C_{182}H_{114}N_{16} + H_2]^{2+}$: 1262.4779. Found: 1262.4770. UV/Vis λ_{abs} (CH_2Cl_2)/nm: 424, 516, 551, 591, 647.

Tetrimino J/L protected precursor (36)

Porphyrins **27** (38 mg, 51.7 μmol) and **28** (38 mg, 48.1 μmol) were reacted together in toluene (15 mL) and triethylamine (3 mL), $Pd_2(dba)_3$ (8 mg, 8.7 μmol) and P(o-tol)$_3$

(19 mg, 62.4 μmol) were placed in a Schlenk flask purged with N_2. A degassed solution of toluene (15 mL) and triethylamine (3 mL) was added in a single portion. The mixture was stirred and heated to 50 °C for 1 h 30 min after which a second batch of $Pd_2(dba)_3$ (8 mg, 8.7 μmol) and $P(o\text{-}tol)_3$ (19 mg, 62.4 μmol) was added. The mixture was stirred for an additional 1 h 30 min, cooled, and solvents removed. Toluene (5mL) was added to the residue and this was passed through a PTFE filter and loaded onto a column for size exclusion chromatography (Bio-Beads SX-3, toluene). Fractions containing the desired product were collected together. Material stuck on the PTFE filter was washed off with chloroform and solvents removed. The process was repeated twice more so that all of the crude material from the reaction had been loaded onto the column. Fractions containing the desired product were collected together and solvents removed to produce the title compound as a purple solid (34 mg, 23.5 μmol, 49%).

^{1}H NMR (400 MHz, $CDCl_3$) δ = 8.82 - 8.98 (m, 16 H), 8.29 - 8.34 (m, 4 H), 8.22 - 8.27 (m, 8 H), 8.20 (dd, *J* = 7.97, 4.96 Hz, 4 H), 8.10 (d, *J* = 7.91 Hz, 4 H), 7.91 (d, *J* = 7.97 Hz, 2 H), 7.89 (d, J = 7.97 Hz, 2 H), 7.75 - 7.83 (m, 12 H), 0.37 - 0.42 (m, 18 H), -2.74 (s, 4 H) ppm. MS: (ESI) *m/z* calculated for: $[C_{100}H_{74}N_8Si_2 + H]^+$: 1443.5648. Found: 1443.5614. UV/Vis λ_{abs} (CH_2Cl_2)/nm (ε/$dm^3mol^{-1}cm^{-1}$): 422 (659,000), 516 (38,000), 552 (22,400), 590 (11,800), 647 (10,400).

Tetrimino J/L deprotected precursor (37)

42 (20 mg, 13.9 μmol) was dissolved in chloroform (5 mL) and THF (10 mL). TBAF (1 M in THF, 160 μL, 160 μmol) was added and the solution was stirred at RT for 24 h before being quenched with aqueous NH_4Cl. Chloroform (100 mL) was added, the organic layer collected and washed with water and brine. This was then dried, filtered and solvents removed to produce the title compound as a purple solid (16 mg, 12.3 μmol, 88%).

^{1}H NMR (400 MHz, $CDCl_3$) δ = 8.82 - 8.98 (m, 16 H), 8.31 (d, *J* = 7.65 Hz, 4 H), 8.19 - 8.27 (m, 12 H), 8.10 (d, *J* = 8.16 Hz, 4 H), 7.93 (d, *J* = 8.09, 2 H), 7.92 (d, J = 8.09 Hz, 2 H), 7.74 - 7.84 (m, 12 H), 3.34 (s, 1 H), 3.34 (s, 1 H), -2.74 (s, 4 H) ppm. MS: (ESI) *m/z* calculated for $[C_{94}H_{58}N_8 + H]^+$: 1299.4857. Found: 1299.4846. UV/Vis λ_{abs} (CH_2Cl_2)/nm (ε/$dm^3mol^{-1}cm^{-1}$): 422 (702,000), 516 (37,000), 552 (20,800), 591 (11,900), 647 (10,000).

Tetrimino J/L (38)

Porphyrins **43** (15 mg, 11.5 μmol) and **23** (24 mg, 34.6 μmol), $Pd_2(dba)_3$ (4 mg, 4.4 μmol) and P(o-tol)$_3$ (10 mg, 32.9 μmol) were placed in a Schlenk flask purged with N_2. A degassed solution of toluene (7.5 mL) and triethylamine (1.5 mL) was added in a single portion. The mixture was stirred and heated to 50 °C for 1 h 30 min after which a second batch of $Pd_2(dba)_3$ (4 mg, 4.4 μmol) and P(o-tol)$_3$ (10 mg, 32.9 μmol) was added. The mixture was stirred for an additional 1 h 30 min, cooled, and solvents removed. Chloroform (5 mL) was added to the residue passed through a PTFE filter and loaded onto a column of SEC (Bio-Beads SX-1, chloroform). The fractions containing the desired material were combined and solvents were removed to produce the title compound as a purple solid (15 mg, 5.9 μmol, 51%).

^{1}H NMR (400 MHz, $CDCl_3$) δ = 9.02 (s, 2 H), 8.91 - 8.99 (m, 20 H), 8.90 (br. s., 2 H), 8.88 (s, 8 H), 8.30 - 8.38 (m, 12 H), 8.22 - 8.30 (m, 20 H), 8.06 - 8.17 (m, 12 H), 7.76 - 7.87 (m, 30 H), -2.69 (br. s., 4 H), -2.72 (s, 4 H) ppm. MS: (MALDI-TOF, DCTB/MeCN) calculated for $[C_{182}H_{114}N_{16}]^+$: 2523.9446. Found: 2523.918. UV/Vis λ_{abs} (CH_2Cl_2)/nm: 425, 516, 552, 591, 647.

Tetrimino S/Z protected precursor (39)

Porphyrins **28** (40 mg, 50.6 μmol) and **29** (40 mg, 54.4 μmol), $Pd_2(dba)_3$ (15 mg, 16.4 μmol) and P(o-tol)$_3$ (28 mg, 92.0 μmol) were placed in a Schlenk flask purged with

N_2. A degassed solution of toluene (30 mL) and triethylamine (6 mL) was added in a single portion. The mixture was stirred and heated to 50 °C for 1 h 20 min after which a second batch of $Pd_2(dba)_3$ (6 mg, 6.6 μmol) and $P(o\text{-}tol)_3$ (15 mg, 49.3 μmol) was added. The mixture was stirred for an additional 1 h 20 min, cooled, and solvents removed. Toluene (3 mL) was added to the residue, which was then passed through a PTFE filter and loaded onto a column for size exclusion chromatography (Bio-Beads SX-3, toluene). Fractions containing the desired product were collected together, solvents were removed to produce the title compound as a purple solid (23 mg, 15.9 μmol, 31 %).

^{1}H NMR (400 MHz, $CDCl_3$) δ = 8.83 - 8.98 (m, 16 H), 8.31 (d, *J* = 7.91 Hz, 4 H), 8.18 - 8.27 (m, 12 H), 8.10 (d, *J* = 7.91 Hz, 4 H), 7.90 (d, *J* = 8.03 Hz, 4 H), 7.75 - 7.83 (m, 12 H), 0.40 (s, 18 H), -2.74 (s, 4 H) ppm. MS: (ESI) *m/z* calculated for $[C_{100}H_{74}N_8Si_2 + H]^+$: 1443.5648. Found: 1443.5657. UV/Vis λ_{abs} (CH_2Cl_2)/nm: 423, 516, 552, 591, 646.

Tetrimino S/Z deprotected precursor (40)

39 (12 mg, 8.3 μmol) was dissolved in chloroform (5 mL) and THF (10 mL). TBAF (1 M in THF, 80 μL, 80 μmol) was added and the solution was stirred at RT for 24 h before being quenched with aqueous NH_4Cl. Chloroform (100 mL) was added, the organic layer collected and washed with water and brine. This was then dried, filtered and solvents removed to produce the title compound as a purple solid (10 mg, 7.7 μmol, 93%).

^{1}H NMR (400 MHz, $CDCl_3$) δ = 8.83 - 8.99 (m, 16 H), 8.31 (d, *J* = 8.16 Hz, 4 H), 8.20 - 8.27 (m, 12 H), 8.10 (d, *J* = 8.16 Hz, 4 H), 7.93 (d, *J* = 8.16 Hz, 4 H), 7.74 - 7.84 (m, 12 H), 3.35 (s, 2 H), -2.74 (s, 4 H) ppm. MS (ESI) *m/z* Calculated for $[C_{94}H_{58}N_8 + H]^+$: 1299.4857. Found: 1299.4841. UV/Vis λ_{abs} (CH_2Cl_2)/nm: 422, 516, 552, 591, 646.

Tetrimino S/Z (41)

Porphyrins **37** (10 mg, 7.7 μmol) and **23** (16 mg, 23.1 μmol), $Pd_2(dba)_3$ (4 mg, 4.4 μmol) and $P(o\text{-}tol)_3$ (10 mg, 32.9 μmol) were placed in a Schlenk flask purged with N_2. A degassed solution of toluene (7.5 mL) and triethylamine (1.5 mL) was added in a single portion. The mixture was stirred and heated to 50 °C for 1 h 30 min after which a second batch of $Pd_2(dba)_3$ (4 mg, 4.4 μmol) and $P(o\text{-}tol)_3$ (10 mg, 32.9 μmol) was added. The mixture was stirred for an additional 1 h 30 min, cooled, and solvents removed. Toluene (5 mL) was added to the residue; this was then passed through a PTFE filter and loaded onto a column for size exclusion chromatography (Bio-Beads SX-1, toluene). The material on the PTFE filter was washed off with chloroform (20 mL) and combined with fractions from the column containing the desired material. Solvents were removed, toluene (10 mL) was added, creating a suspension which was collected *via* centrifuge. Solvents were removed to produce the title compound as a purple solid (9 mg, 3.6 μmol, 47%).

^{1}H NMR (400 MHz, $CDCl_3$) δ = 9.02 (s, 4 H), 8.88 - 9.00 (m, 20 H), 8.87 (s, 8 H), 8.29 - 8.40 (m, 12 H), 8.21 - 8.29 (m, 20 H), 8.05 - 8.19 (m, 12 H), 7.74 - 7.84 (m, 30 H), -2.69 (s, 4 H), -2.73 (s, 4 H) ppm. MS: (MALDI-TOF, DCTB/MeCN) calculated for $[C_{182}H_{114}N_{16}]^+$: 2523.9446. Found: 2523.907. UV/Vis λ_{abs} (CH_2Cl_2)/nm: 423, 516, 551, 591, 647.

Tetrimino I protected precursor (42)

Porphyrins **26** (40 mg, 50.6 μmol) and **27** (40 mg, 54.4 μmol), $Pd_2(dba)_3$ (8 mg, 8.7 μmol) and $P(o\text{-}tol)_3$ (19 mg, 62.4 μmol) were placed in a Schlenk flask purged with N_2. A degassed solution of toluene (30 mL) and triethylamine (6 mL) was added in a single portion. The mixture was stirred and heated to 50 °C for 1 h 30 min after which a second batch of $Pd_2(dba)_3$ (8 mg, 8.7 μmol) and $P(o\text{-}tol)_3$ (19 mg, 62.4 μmol) was added. The

mixture was stirred for an additional 1 h 30 min, cooled, and solvents removed. DCM (10 mL) was added to the residue, creating a suspension which was passed through a PTFE filter, this was then washed with DCM (100 mL). The suspension was collected by passing 99:1 DCM/TFA solution (50 mL) through the filter. The solution was neutralised with NaOH solution (2 M) and then washed with water and brine. Solvents were removed to give the title compound as a purple solid (27 mg, 18.7 μmol, 37%).

^{1}H NMR (400 MHz, $CDCl_3$) δ = 8.90 - 8.97 (m, 8 H), 8.89 (d, *J* = 4.4 Hz, 4 H), 8.84 (d, *J* = 4.4 Hz, 4 H), 8.31 (d, *J* = 8.2 Hz, 4 H), 8.25 (dd, *J* = 7.6, 1.6 Hz, 8 H), 8.19 (d, *J* = 8.2 Hz, 4 H), 8.10 (d, *J* = 8.2 Hz, 4 H), 7.89 (d, *J* = 8.2 Hz, 4 H), 7.76 - 7.83 (m, 12 H), 0.39 (s, 18 H), -2.75 (s, 4 H) ppm. MS: (FD) calculated for $[C_{100}H_{74}N_8Si_2 + H]^+$: 1443.5648 Found: 1443.5514. UV/Vis λ_{abs} (CH_2Cl_2)/nm: 424, 516, 552, 591, 648.

Tetrimino I deprotected precursor (43)

THF (150 mL) and chloroform (75 mL) were added to **39** (20 mg, 13.9 μmol). The fine suspension was dissolved by heating the mixture to 60 °C. Following this TBAF (1 M in THF, 320 μL, 320 μmol) was added and the solution was stirred at 60 °C for 24 h. MALDI-TOF MS analysis showed that there was no remaining starting material and the solution was allowed to cool to room temperature. Aqueous NH_4Cl (100 mL) and chloroform (100 mL) was added, the organic phase collected, washed with water, brine and dried over anhydrous magnesium sulfate. The mixture was filtered and solvents removed to produce a purple solid (17 mg, 13.1 μmol, 94%).

^{1}H NMR (400 MHz, $CDCl_3$) δ = 8.90 - 8.97 (m, 8 H), 8.83 - 8.90 (m, 8 H), 8.31 (d, *J* = 8.03 Hz, 4 H), 8.25 (dd, *J* = 7.53, 1.63 Hz, 8 H), 8.21 (d, *J* = 8.16 Hz, 4 H), 8.10 (d, *J* = 8.16 Hz, 4 H), 7.92 (d, *J* = 8.03 Hz, 4 H), 7.76 - 7.83 (m, 12 H), 3.34 (s, 2 H), -2.74 (s, 4 H) ppm. MS: (ESI) *m/z* calculated for $[C_{94}H_{58}N_8 + H]^+$: 1299.4857. Found: 1299.4849. UV/Vis λ_{abs} (CH_2Cl_2)/nm: 423, 516, 553, 590, 647.

Tetrimino I (44)

Porphyrins **40** (15 mg, 11.5 μmol) and **23** (24 mg, 34.6 μmol), $Pd_2(dba)_3$ (4 mg, 4.4 μmol) and P(o-tol)$_3$ (10 mg, 32.9 μmol) were placed in a Schlenk flask purged with N_2. A degassed solution of toluene (30 mL) and triethylamine (6 mL) was added in a single portion. The mixture was stirred and heated to 50 °C for 1 h 30 min after which a second batch of $Pd_2(dba)_3$ (4 mg, 4.4 μmol) and P(o-tol)$_3$ (10 mg, 32.9 μmol) was added. The mixture was stirred for an additional 1 h 30 min, cooled, and solvents removed. Chloroform (25 mL) was added to the residue, this was then passed through a PTFE filter followed by additional chloroform (50 ml). The material on the filter was washed off with 99:1 chloroform/TFA solution (10 mL) and loaded onto a column for size exclusion chromatography (Bio-Beads SX-1, 99.9:0.1 DCM/TFA) in two, separate 5 mL loadings. Fractions containing the desired material were collected together, neutralised with NaOH solution (2 M, 100 mL) then washed with water and brine. Solvents were removed to produce the title compound as a purple solid (4 mg, 1.6 μmol, 14%).

^{1}H NMR (400 MHz, TFA) δ = 8.80 - 8.95 (m, 32 H), 8.71 (m, 12 H), 8.55 - 8.66 (m, 20 H), 8.34 - 8.45 (m, 12 H), 8.00 - 8.10 (m, 30 H) ppm. MS: (MALDI-TOF, DCTB/MeCN) calculated for $[C_{182}H_{114}N_{16}]^+$: 2523.9446. Found: 2523.978. UV/Vis λ_{abs} (CH_2Cl_2)/nm: 425, 516, 553, 591, 647.

Tetrimino O protected precursor (45)

Porphyrins **29** (35 mg, 47.6 μmol) and **30** (17 mg, 22.0 μmol) $Pd_2(dba)_3$ (7 mg, 7.6 μmol) and P(o-tol)$_3$ (17 mg, 55.9 μmol) were placed in a Schlenk flask purged with N_2. A degassed solution of toluene (7.5 mL) and triethylamine (1.5 mL) was added in a single portion. The mixture was stirred and heated to 50 °C for 1 h 30 min after which a second batch of $Pd_2(dba)_3$ (7 mg, 7.6 μmol) and P(o-tol)$_3$ (17 mg, 55.9 μmol) was added. The mixture was stirred for an additional 1 h 30 min, cooled, and solvents removed. Toluene

(5 mL) was added to the residue, this was then passed through a PTFE filter and loaded onto a column for size exclusion chromatography (Bio-Beads SX-1, toluene). Fractions containing the desired product were collected together; solvents were removed to produce the title compound as a purple solid (10 mg, 4.8 μmol, 22%).

^{1}H NMR (400 MHz, $CDCl_3$) δ = 9.02 (s, 2 H), 8.80 - 9.00 (m, 22 H), 8.32 (d, *J* = 8.16 Hz, 4 H), 8.35 (d, *J* = 8.16 Hz, 4 H), 8.19 - 8.29 (m, 16 H), 8.12 (dd, *J* = 8.16, 5.90 Hz, 8 H), 7.91 (d, *J* = 8.16 Hz, 4 H), 7.75 - 7.84 (m, 18 H), 0.40 (s, 18 H), -2.69 (br. s., 2 H), -2.74 (s, 4 H) ppm. MS: (ESI) *m/z* calculated for $[C_{146}H_{102}N_{12}Si_2 + H_2]^{2+}$: 1040.4017 Found: 1040.4001. UV/Vis λ_{abs} (CH_2Cl_2)/nm (ε/$dm^3mol^{-1}cm^{-1}$): 423 (1,220,000), 516 (78,800), 552 (51,700), 591 (33,800), 647 (28,300).

Tetrimino O deprotected precursor (46)

45 (11 mg, 5.3 μmol) was dissolved in chloroform (5 mL) and THF (10 mL). TBAF (1 M in THF, 80 μL, 80 μmol) was added and the solution was stirred at RT for 24 h before being quenched with aqueous NH_4Cl. Chloroform (100 mL) was added, the organic layer collected and washed with water and brine. This was then dried, filtered and solvents removed to produce the title compound as a purple solid (10 mg, 5.2 μmol, 98%).

^{1}H NMR (400 MHz, $CDCl_3$) δ = 9.02 (s, 2 H), 8.81 - 9.00 (m, 22 H), 8.29 - 8.38 (m, 8 H), 8.20 - 8.29 (m, 16 H), 8.12 (dd, *J* = 7.65, 4.77 Hz, 8 H), 7.93 (d, *J* = 7.91 Hz, 4 H), 7.75 - 7.84 (m, 18 H), 3.34 (s, 2 H), -2.69 (br. s., 2 H), -2.74 (br. s., 4 H) ppm. MS: (ESI) *m/z* calculated for $[C_{140}H_{86}N_{12} + H_2]^{2+}$: 968.3622. Found: 968.3603. UV/Vis λ_{abs} (CH_2Cl_2)/nm: 423, 516, 552, 591, 647.

Tetrimino O (47)

Porphyrins **46** (10 mg, 5.2 μmol) and **25** (10 mg, 11.76 μmol), $Pd_2(dba)_3$ (3 mg, 3.3 μmol) and P(o-tol)$_3$ (8 mg, 26.3 μmol) were placed in a Schlenk flask purged with N_2. A

degassed solution of toluene (7.5 mL) and triethylamine (1.5 mL) was added in a single portion. The mixture was stirred and heated to 50 °C for 1 h 30 min after which a second batch of $Pd_2(dba)_3$ (3 mg, 3.3 μmol) and $P(o\text{-}tol)_3$ (8 mg, 26.3 μmol) was added. The mixture was stirred for an additional 1 h 30 min, cooled, and solvents removed. Toluene (5 mL) was added to the residue and was passed through a PTFE filter and loaded onto a column for SEC (Bio-Beads SX-1, toluene). No fractions were found to contain the wanted material. Chloroform (10 mL) was passed through the filter resulting in a light pink solution. 99:1 chloroform/TFA solution was passed through the PTFE filter resulting in a dark green solution. This solution was neutralised with NaOH solution (2 M, 50 mL) washed with water and brine and solvents removed. A second SEC column was attempted (Biobeads SX-1, 99.9:0.1, TFA), the fractions containing Tetrimino O were collected together, neutralised with NaOH, washed with water, brine and solvents removed The resulting pink solid was unable to be purified for satisfactory spectroscopic data collection.

MS: (MALDI-TOF) calculated for $C_{184}H_{112}N_{16}$ 2545.9289. Found: 2545.7.

References

1. H. W. Jiang, T. Tanaka and A. Osuka, *Chem. Sci.*, 2015, **6**, 6102-6105.

2. A. Nakano, A. Osuka, T. Yamazaki, Y. Nishimura, S. Akimoto, I. Yamazaki, A. Itaya, M. Murakami and H. Miyasaka, *Chem. Eur. J.*, 2001, **7**, 3134-3151.

3. D. Kim and A. Osuka, *J. Phys. Chem. A*, 2003, **107**, 8791-8816.

4. T. Hasobe, H. Murata, S. Fukuzumi and P. V. Kamat, *Mol. Cryst. Liq. Cryst.*, 2007, **471**, 39-51.

5. T. V. Duncan, K. Susumu, L. E. Sinks and M. J. Therien, *J. Am. Chem. Soc.*, 2006, **128**, 9000-9001.

6. A. Pramanik and H. S. Kang, *J. Chem. Phys.*, 2011, **134**, 6.

7. A. Osuka and H. Shimidzu, *Angew. Chem. Int. Ed.*, 1997, **36**, 135-137.

8. N. Aratani, A. Osuka, Y. H. Kim, D. H. Jeong and D. Kim, *Angew. Chem. Int. Ed.*, 2000, **39**, 1458-1462.

9. C.-L. Mai, W.-K. Huang, H.-P. Lu, C.-W. Lee, C.-L. Chiu, Y.-R. Liang, E. W.-G. Diau and C.-Y. Yeh, *Chem. Comm.*, 2010, **46**, 809-811.

10. N. Kobayashi, M. Numao, R. Kondo, S. Nakajima and T. Osa, *Inorg. Chem.*, 1991, **30**, 2241-2244.

11. H. Mori, T. Tanaka, S. Lee, J. M. Lim, D. Kim and A. Osuka, *J. Am. Chem. Soc.*, 2015, **137**, 2097-2106.

12. A. Tsuda and A. Osuka, *Science*, 2001, **293**, 79-82.

13. G. Sedghi, L. J. Esdaile, H. L. Anderson, S. Martin, D. Bethell, S. J. Higgins and R. J. Nichols, *Adv. Mater.*, 2012, **24**, 653-657.

14. H. S. Cho, D. H. Jeong, S. Cho, D. Kim, Y. Matsuzaki, K. Tanaka, A. Tsuda and A. Osuka, *J. Am. Chem. Soc.*, 2002, **124**, 14642-14654.

15. V. S. Y. Lin, S. G. Dimagno and M. J. Therien, *Science*, 1994, **264**, 1105-1111.

16. R. W. Wagner, T. E. Johnson and J. S. Lindsey, *J. Am. Chem. Soc.*, 1996, **118**, 11166-11180.

17. R. S. Loewe, R. K. Lammi, J. R. Diers, C. Kirmaier, D. F. Bocian, D. Holten and J. S. Lindsey, *J. Mater. Chem.*, 2002, **12**, 1530-1552.

18. K. Susumu, P. R. Frail, P. J. Angiolillo and M. J. Therien, *J. Am. Chem. Soc.*, 2006, **128**, 8380-8381.

19. G. Sedghi, V. M. Garcia-Suarez, L. J. Esdaile, H. L. Anderson, C. J. Lambert, S. Martin, D. Bethell, S. J. Higgins, M. Elliott, N. Bennett, J. E. Macdonald and R. J. Nichols, *Nat. Nanotechnol.*, 2011, **6**, 517-523.

20. H. L. Anderson, *Inorg. Chem.*, 1994, **33**, 972-981.

21. P. N. Taylor and H. L. Anderson, *J. Am. Chem. Soc.*, 1999, **121**, 11538-11545.

22. L. H. Yu and J. S. Lindsey, *J. Org. Chem.*, 2001, **66**, 7402-7419.

23. P. Neuhaus, A. Cnossen, J. Q. Gong, L. M. Herz and H. L. Anderson, *Angew. Chem. Int. Ed.*, 2015, **54**, 7344-7348.

24. S. Hong, M. R. Rohman, J. Jia, Y. Kim, D. Moon, Y. Kim, Y. H. Ko, E. Lee and K. Kim, *Angew. Chem. Int. Ed.*, 2015, **54**, 13241-13244.

25. B. C. Barnes, D. W. Siderius and L. D. Gelb, *Langmuir*, 2009, **25**, 6702-6716.

26. R. W. Wagner, T. E. Johnson, F. Li and J. S. Lindsey, *J. Org. Chem.*, 1995, **60**, 5266-5273.

27. R. W. Wagner, Y. Ciringh, C. Clausen and J. S. Lindsey, *Chem. Mater.*, 1999, **11**, 2974-2983.

28. R. W. Wagner, J. Seth, S. I. Yang, D. Kim, D. F. Bocian, D. Holten and J. S. Lindsey, *J. Org. Chem.*, 1998, **63**, 5042-5049.

Chapter 6:

Anthracenes

Introduction

Anthracenes consist of three benzene rings fused together; compounds that contain them have been cited as being promising candidates in the field of organic electronics. This is in part due to their conjugation and planar shape facilitating packing within crystal structures which in turn permits the system to possess charge carrying abilities.[1] Tetracenes[2] and pentacenes[3] also possess charge carrying abilities (to a greater extent even) but their limited chemical stability, lower solubility and light sensitivity contribute to anthracenes becoming an attractive alternative.[4]

The charge carrying capabilities possessed by anthracene compounds make them suitable for a variety of applications. There are many examples of anthracene based compounds being used for organic thin film transistors (OTFTs) or semiconductors.[5-7] To expand on this slightly, research conducted by Kwon and co-workers[8] resulted in the compound BPEA (figure 6.1).

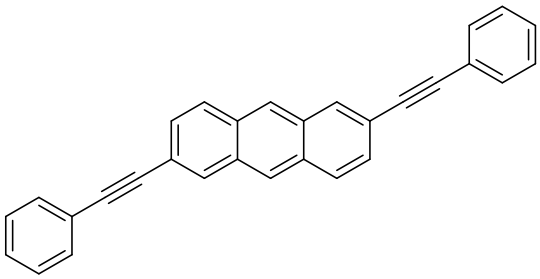


Figure 6.1 BPEA compound used in OTFT devices.

OTFT devices containing BPEA were prepared by first spin coating a mixture of poly(4-vinylphenol) with cross linking agent poly(melamine-co-formaldehyde) in propylene glycol monomethyl ether acetate onto a substrate. The source and drain electrodes (formed using gold) were then positioned on the device and finally the organic semiconductor BPEA deposited, followed by annealing. The same process was used to make devices with pentacene as the organic semiconductor. The team found that

compared to pentacene, BPEA had twice the field effect mobility (0.42 cm^2/Vs compared to 0.21 cm^2/Vs), less standard deviation and greater stability.

Another important area of molecular electronic is molecular wires. Molecular wires often feature (poly)acetylenes as these groups are capable of charge transport.[9,10] Combine this with the knowledge that anthracenes are also capable of charge transport and we speculate that compounds containing both of these features may have some interesting characteristics useful in the field of organic electronics. A series of 9,9'-dianthrylpoly-ynes was synthesised by Nakagawa and Akiyama[11] but have yet to be assessed for charge carrying capabilities.

When exposed to light ranging from UV-blue, anthracenes can undergo a cyclisation reaction with a nearby anthracene. This photodimerisation reaction has been known for a long time,[12] but only recently have there been efforts to make 2D materials using the photodimerised product as a central motif.[13,14] One of the more successful attempts was reported by King and co-workers[15] when they were able to prepare a 2D COF by irradiating single crystals of 'fantrip' monomer with 460 nm light to form the fantrip dimer molecule followed by irradiation at 400 nm to from the polymer (figure 6.2).

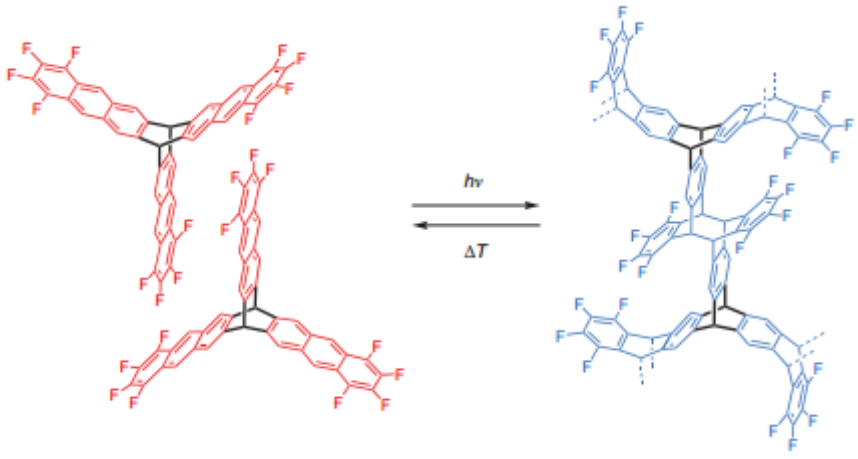


Figure 6.2 The photopolymerisation reaction of fantrip monomer.[15]

During the process, the single crystals remained intact so impressively, they were able to monitor the process *via* X-ray crystallography. The corresponding 2D sheets were created by treating the crystals with 1-methyl-2-pyrrolidine (NMP) at either room temperature or 50 °C. Exfoliation began within a few minutes of treatment and the process was monitored by AFM, TEM and SEM with individual monolayers first observed after several days.

Another study by Schlüter and co-workers[16] presented an equally impressive demonstration of forming a 2D polymer from the photodimerisation of anthracene. In their system, the monomer (shown in figure 6.3) was irradiated with 465 nm light. Again, the process could be monitored *via* X-ray crystallography. To form the 2D nanosheets, the crystals were treated with NMP at 50 °C for 2-3 weeks.

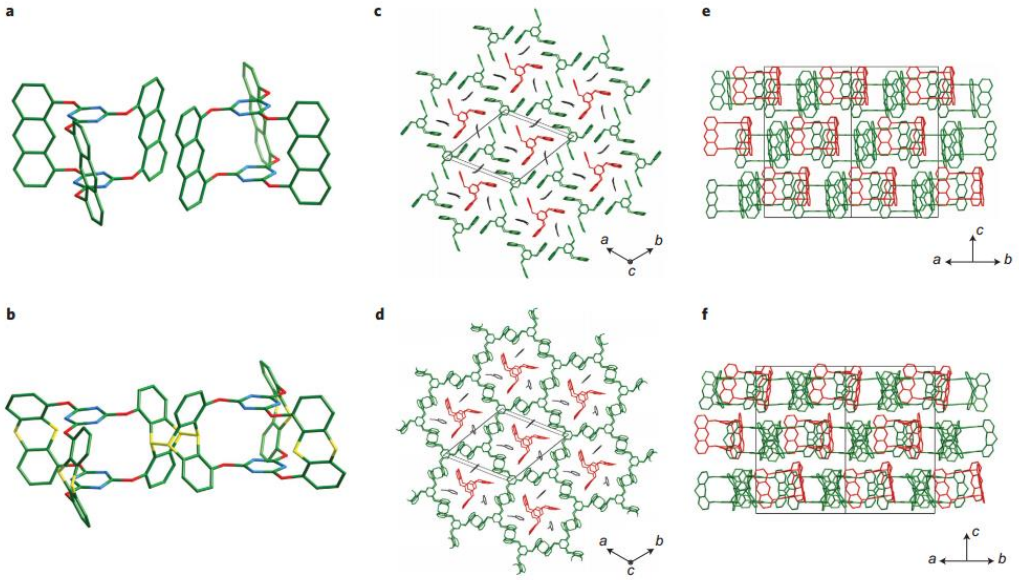


Figure 6.3 (a) Crystal structure of two monomers (b) crystal structure after photodimerisation (c,e) top and side view of bulk monomer packing (d,f) top and side view of bulk polymer.[16]

The main aims of this chapter are to discuss the synthesis of the poly(acetylene) anthracene dimer series (figure 6.4) and to determine the electrochemical and

fluorescence properties of these molecules . This series was designed as these molecules have potential use as molecular wires in the field of organic electronics.

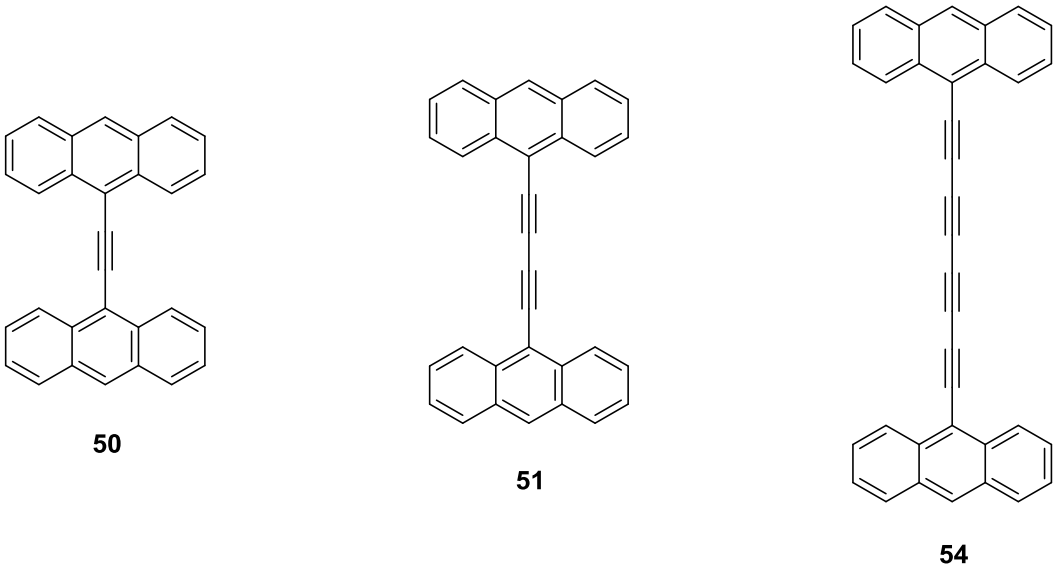
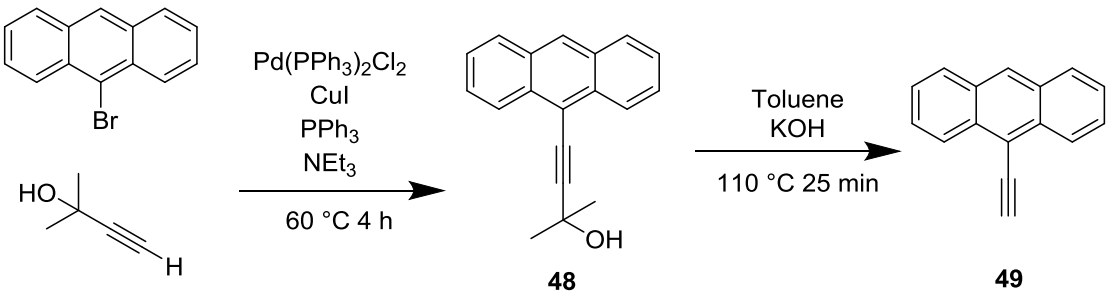


Figure 6.4 Target compounds in poly(acetylene) anthracene dimer series

Results and Discussion

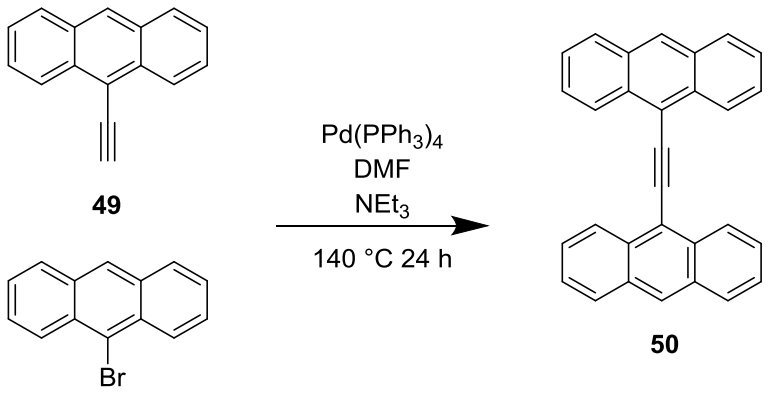
The route chosen to synthesise a series of anthracene dimer compounds, **50**, **51** and **54** and the anthracene trimer compound **55** uses 9-ethynyl anthracene (**49**), the synthesis of which has been taken from the literature and is shown in scheme 6.1 below.[17]



Scheme 6.1 Synthesis of 49 *via* 48.

Commercially available 9-bromoanthracene is used without further purification along with 2-methylbut-3-yn-2-ol in a Sonogashira coupling reaction. $Pd(PPh_3)_2Cl_2$ and CuI were used of the catalytic cycle, with PPh_3 used as the phosphine ligand. The reaction was conducted in thoroughly degassed triethylamine for 4 h at reflux. During this time the mixture developed a distinctive reddish-orange colour. Purification by column chromatography produced **48** as a yellow crystalline solid.

The tertiary alcohol protecting group is cleaved from the anthracene by adding KOH to a refluxing solution of **48** in toluene to give **49**. This reaction was very time and moisture sensitive, toluene was stored over a potassium mirror and degassed with dinitrogen before use. Extending the reaction time past 30 minutes caused the solution to change colour from light yellow-orange to a dark reddish-brown and lowered the yield substantially.



Scheme 6.2 Synthesis of 50.

The synthesis of 1,2-di(9-anthracenyl)ethyne (**50**) was first attempted using $Pd(PPh_3)_4$ and CuI as a co-catalyst (scheme 6.2). Although this generated the desired product, a significant amount of the Glaser coupling product (**51**) was also produced. These were found to be inseparable by column chromatography under the conditions used. Crystallisation of the product mixture in toluene resulted in the formation of two distinct crystal types. The first type presented itself as small, red-orange blocks whereas the second type had the appearance of long, thin yellow-orange needles. Given the stark differences in dimensions between the two types of crystal, a manual separation technique was attempted (figure 6.5).

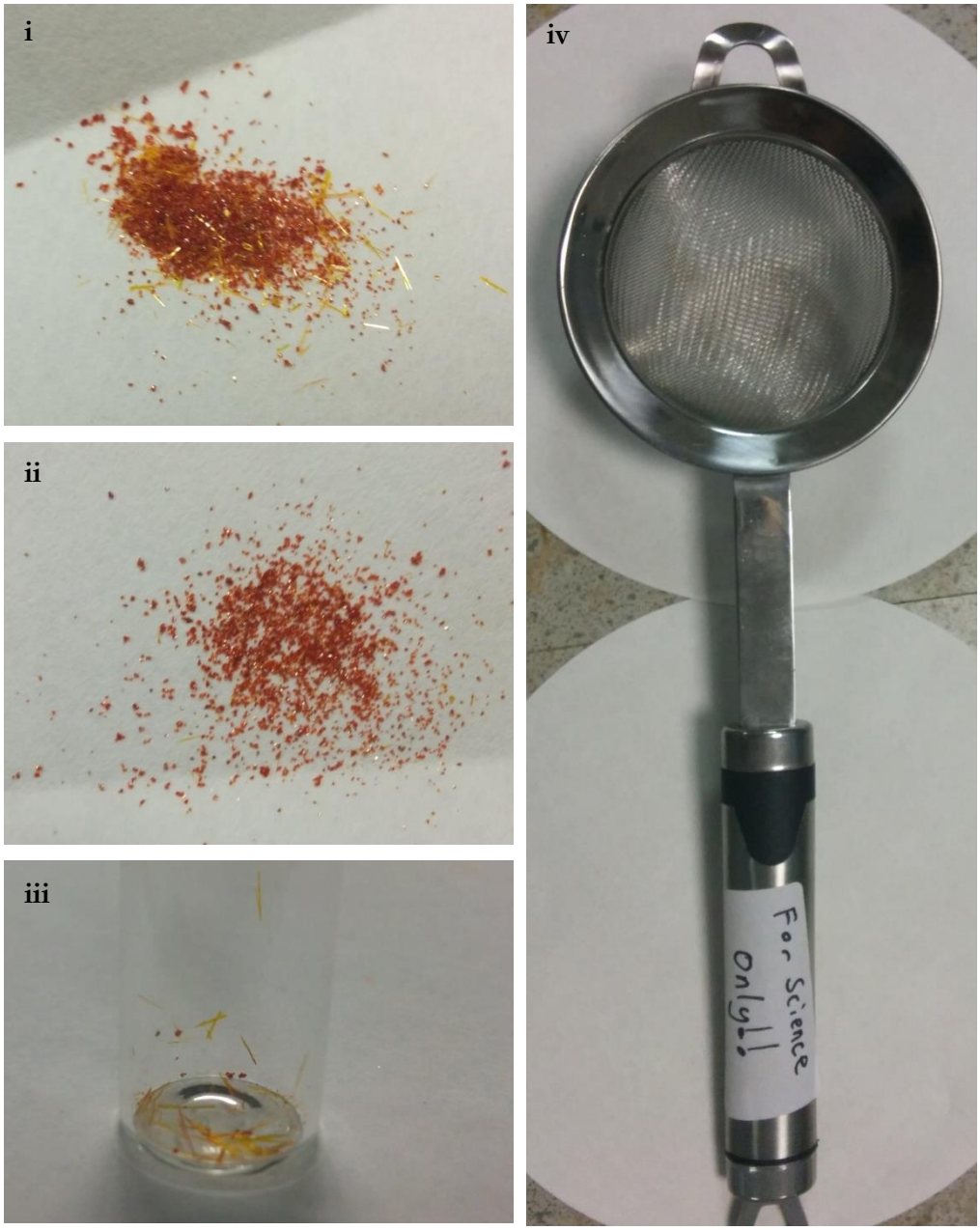
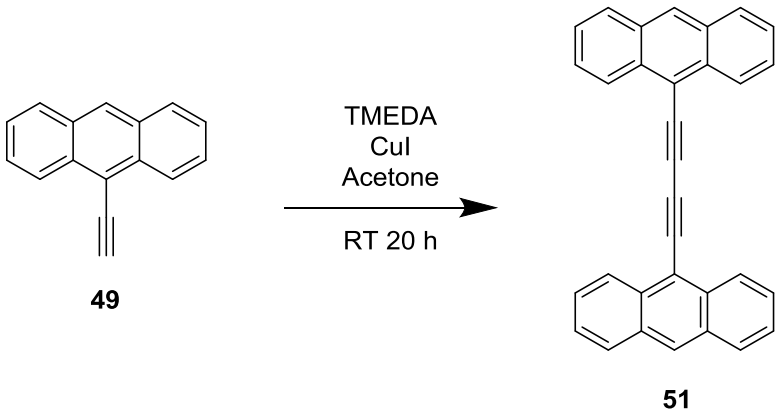


Figure 6.5 Manual separation of 50 and 51.

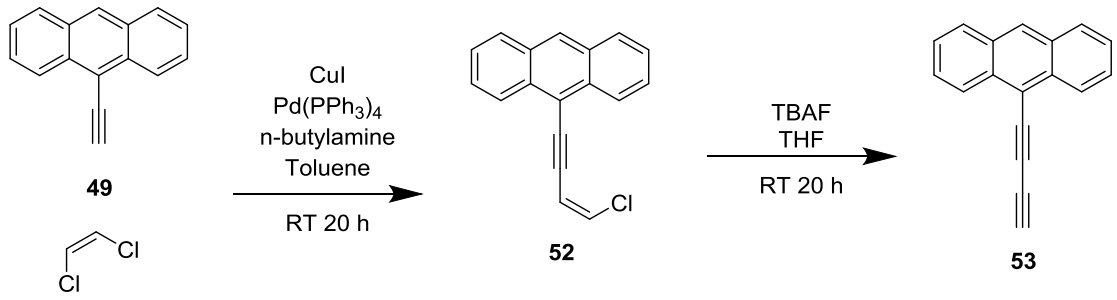
The assortment of crystals (i) were placed into a hand-operated fine mesh sieve (iv). The sieve was gently shaken so that crystals would fall through the mesh (ii). The crystals that remained in the sieve were collected and stored separately (iii). As is evident from (ii) and (iii) this method was very effective at removing the yellow needles from the red blocks, but less effective *vice versa*. X-ray diffraction experiments were able to show that the red blocks were crystals of **51** (yielding 35% from this reaction) and the yellow needles were crystals of **50**. As this method still gave an unsatisfactory purity of **50** and a very low yield

(<10%), an alternative method of synthesis was investigated. The reaction was repeated with the exclusion of copper iodide with the other conditions remaining the same. As expected, this resulted in the Glaser product **51** being absent from any analysis with the desired anthracene dimer **50** being the major component of the crude reaction mixture and easily isolatable by column chromatography.



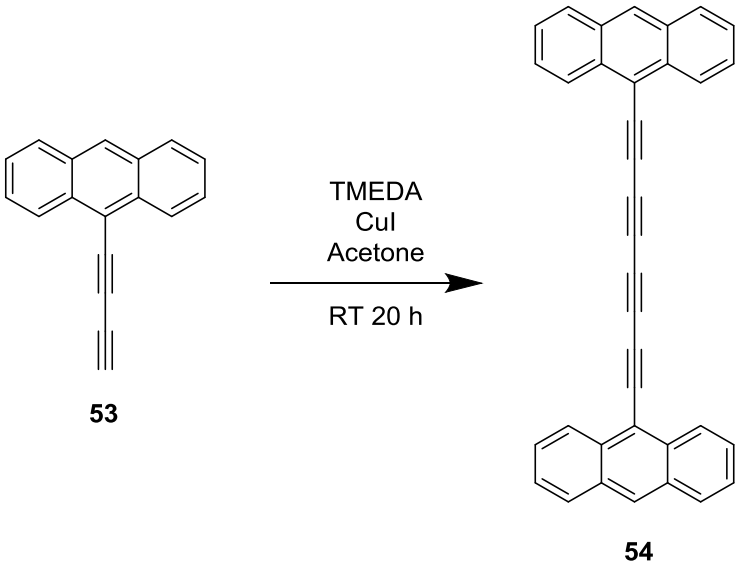
Scheme 6.3 Synthesis of 51.

Although the synthesis of **51** had already been achieved *via* an unwanted Glaser coupling reaction in an attempt to synthesise **50**, an alternative synthetic method was investigated to assess the more efficient route. A modification of the Glaser coupling reaction, the Hay coupling reaction[18] was chosen as the reaction could be carried out at room temperature without the need for dry solvents. After purification, this method generated **51** in 30% yield. This is comparable to the previous yield (35%) due to the Glaser coupling product in the synthesis of **50**.



Scheme 6.4 Synthesis of 52 and 53.

52 and **53** were synthesised using a method previously published in the literature (scheme 6.4).[19] **49** and *cis*-1,2-dichloroethene are coupled together using Sonogashira conditions performed at RT for 20 h with the exclusion of light. There was some evidence for an additional reaction having taken place between **49** and **53** in MS analysis, but this was not confirmed by other spectroscopic methods. **52** was readily purified by column chromatography using hexane as the eluent. The reaction to form **53** was very simple, **52** was dissolved in anhydrous THF and TBAF was added to this solution. The reaction was stirred again at RT for 20 h with the exclusion of light.

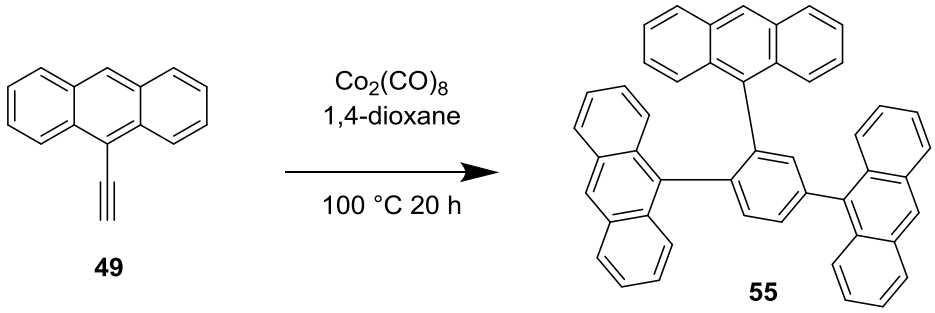


Scheme 6.5 Synthesis of 54.

The route chosen for the synthesis of **54** was the same as the route for **51**, *i.e.* a Hay coupling reaction (scheme 6.5). The resultant product was very insoluble and had to be

crystallised from hot toluene twice before crystals suitable for X-ray diffraction were grown.

In an effort inspired by the recent literature provided by King[15] and Schlüter[16] to create a compound suitable for creating anthracene based 2D COFs formed by photodimerisation reactions, the synthesis of 1,3,5-tri(9,9',9"-anthracenyl)benzene was attempted. It was thought that as the target compound would be similar to the previously reported compounds in terms of being 3-fold symmetric, a similar 2D structure may arise if the same photodimerisation methodology was used. Cobalt complexes such as dicobalt octacarbonyl [$Co_2(CO)_8$] have been used extensively in the literature[20-22] in trimerisation reactions of compounds containing an alkyne group and so it was thought appropriate to use for the system studied herein. $Co_2(CO)_8$ was added to **49** and stirred in dioxane at 100 °C for 20 h.



Scheme 6.6 Synthesis of 55.

Initially, it was assumed that the product formed would be substituted in the 1-, 3- and 5-positions due to the bulky sterics of the anthracene group. However once the product had been purified by column chromatography NMR evidence suggested that the 1-, 2-, 4-isomer had been produced with no evidence for the 1-, 3-, 5- isomer. Single crystals suitable for X-ray diffraction were obtained from cooling of a hot solution in toluene with the data confirming that the 1-, 2-, 4- isomer had been produced (figure 6.6).

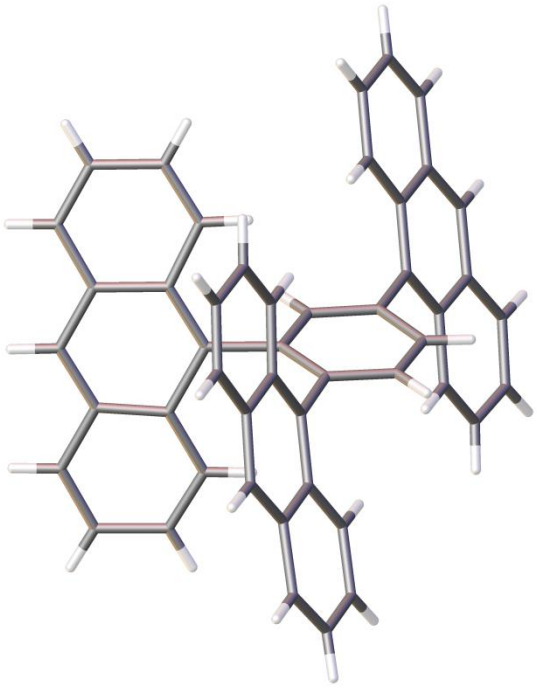


Figure 6.6 Crystal structure of 55.

Following this the synthesis of 1,2,3,4,5,6-hexa(9,9',9",9"',9"",9"""-anthracenylbenzene) was attempted. This heavily substituted structure does not lend itself well to standard schematic representation so instead the proposed structure of this is shown below (figure 6.7).

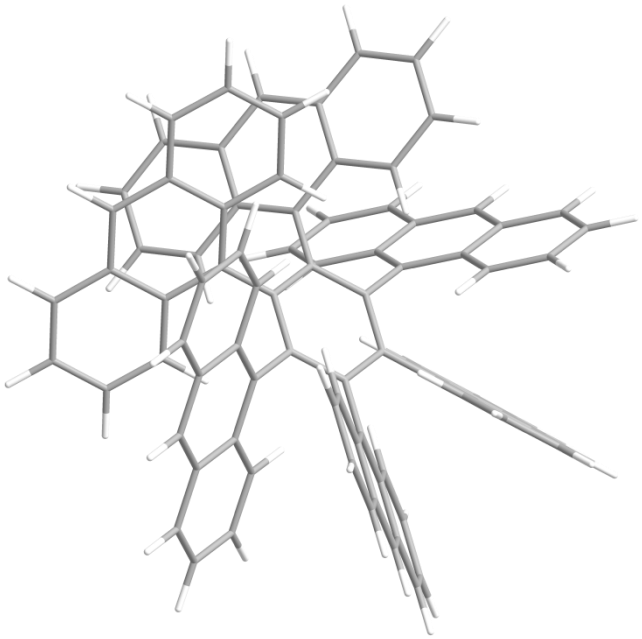


Figure 6.7 Structure generated using ChemBio3D Ultra.

The first conditions used mimicked the successful synthesis of **55**; a solution of **50** in dioxane was treated with 30% loading of $Co_2(CO)_8$, heated to reflux and stirred for 24 h. The reaction was cooled, and the product mixture was analysed, revealing that no reaction had occurred. A microwave synthesis was also attempted, with dioxane and $Co_2(CO)_8$ holding at 1.4 bar for 20 h. This resulted in a product that was quite insoluble, only partially dissolving in DMF. MS analysis showed that the desired product had not formed.

An alternative metal catalyst was also investigated, $RhCl_3$, as this has also been used extensively in reported trimerisation reactions.[23-25] Use of $RhCl_3$ in a reaction to form **55** from **49** was proven to be successful so the same conditions were used in the attempted synthesis of hexa-anthracenyl benzene. **50** was dissolved in a mixture of xylene and diisopropylethylamine with an 8% loading of $RhCl_3$. The mixture was heated to reflux and stirred for 24 h. Analysis showed again that the desired compound had not formed. The reaction was repeated in a solvothermal synthesis bomb. The reaction vessel was held at 200 °C and 4.5 bar for 24 h. Analysis showed that this reaction had also failed.

It was theorised that as to form the desired compound, a reaction has to take place with an extremely sterically hindered intermediate, perhaps the reason for failure so far was simply that the molecules could not approach closely enough in solution to react. To eliminate the need for solvent, a mechanical reaction was attempted by placing **50** in a ball mill along with the catalyst $Co_2(CO)_8$ but this was also unsuccessful. Finally, with the assistance of Dr. Thomas Chamberlain, a melt phase reaction was performed in a sealed glass ampule under an atmosphere of N_2. The glass ampule was heated to 400 °C for 24 h using $Co_2(CO)_8$ as the catalyst. MALDI-TOF MS analysis showed some interesting peaks corresponding to cobalt complexes but no evidence was found of the desired product.

The substantial crowding of the benzene ring required for the hexa-anthracenyl product to form is probably the best indication of why the reactions failed.

Crystallographic Analysis of 50

Crystals of **50** were obtained from a hot to cold recrystallisation performed in toluene (figure 6.8). The compound displayed some polymorphism, with the majority of the crystals obtained being bright orange in colour with the appearance of thin needles (polymorph α) but also a small amount of crystals having the appearance of yellow planks (polymorph β). A previous study conducted by Becker *et al.*[26] found that in the orange needle like crystals, the anthracene moieties were coplanar, this was confirmed by the data collected during this research. Another study by Thamattoor[27] was able to grow 'yellow, block-like crystals'. Their description of their crystal structure data indicates that it is the same polymorph β as the polymorph grown during this research.

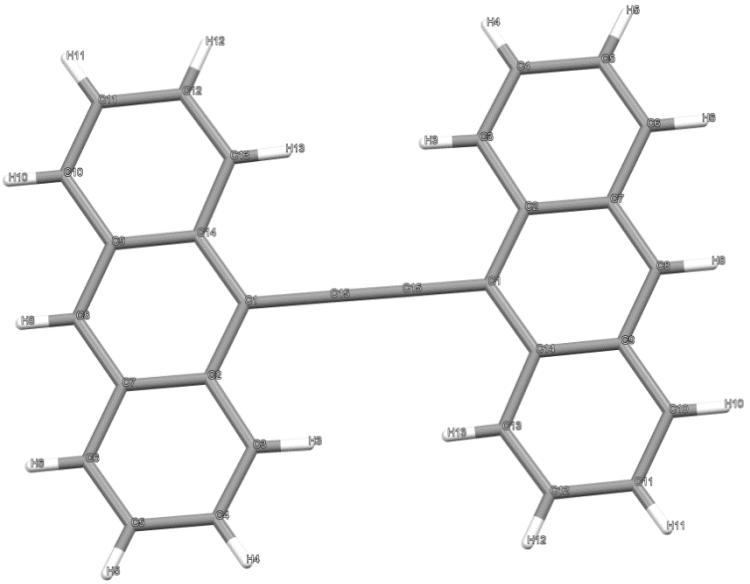


Figure 6.8 Crystal structure of polymorph α of 50.

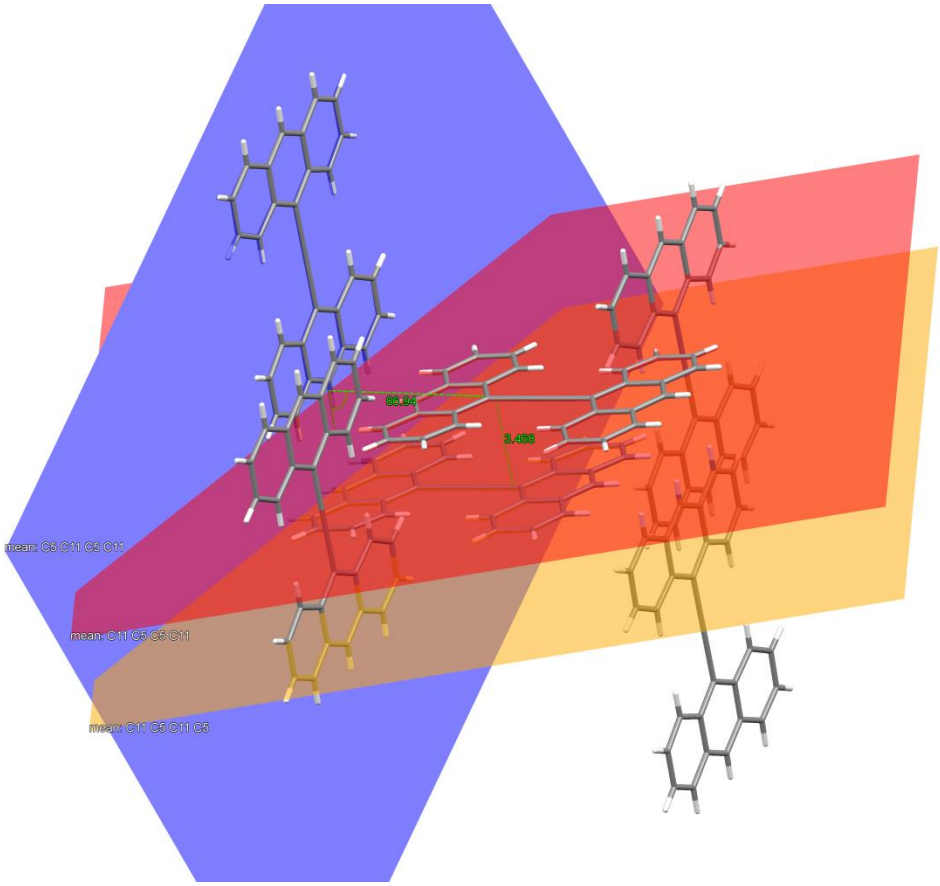


Figure 6.9 Packing structure of polymorph α of 50.

The crystal structure obtained for the α polymorph was centrosymmetric through the middle of the linking alkyne bond. The length of the alkyne bond C15-C15 is 1.215(3) Å and the angle measured for C1-C15-C15 was 179.4(2)°. The two anthracene units are not completely co-planar but are essentially parallel. Their planes, calculated from C4, C5, C11, and C12 are separated by a small step (0.315 Å) and diverge from each other at an angle <0.01°. It is also worth noting that the anthracene units are not in a direct face-to-face orientation with those of an adjacent molecule but rather are in a staggered formation so that the anthracene of one molecule sits over the alkyne bond of another as shown in figure 6.9. Planes were also created using atoms C5, C11, C5 and C11 of the anthracene molecules. The distance measured between two of these planes for two anthracenes in a 'staggered' face-to-face orientation is 3.47 Å indicating a π-π interaction

and the angle of intersection of the equivalent anthracene plane in the second orientation is 86.94°.

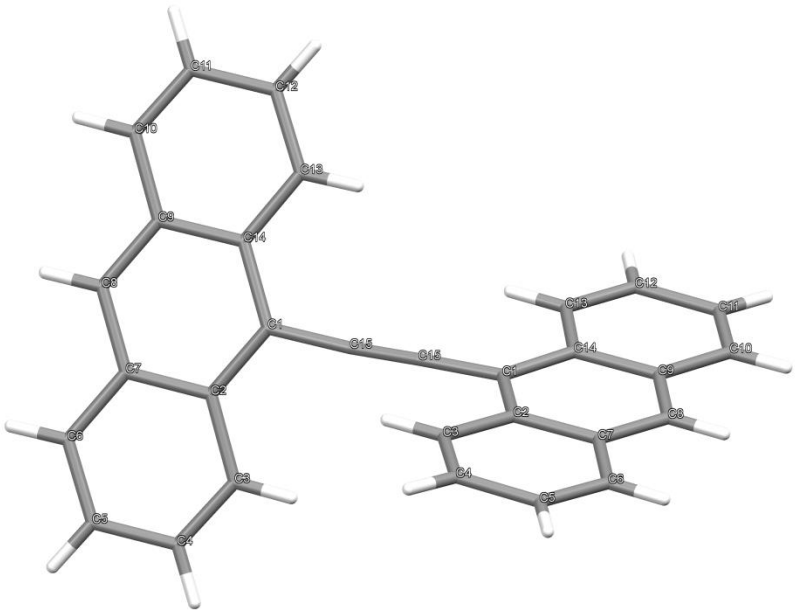


Figure 6.10 Crystal structure of 50 polymorph β.

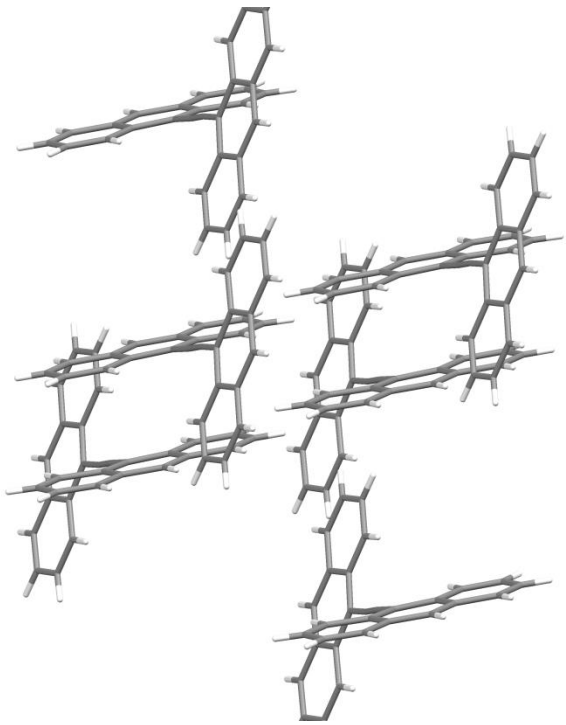


Figure 6.11 Packing of 50 polymorph β.

The crystal structure obtained for the β polymorph (Figures 6.10 and 6.11) was centrosymmetric through the middle of the linking alkyne bond. The length of the alkyne bond was measured to be 1.2055(18) Å and it was slightly bent, so that the angle measured for C1-C15-C15 was 175.04(12)°. A plane was generated using C4, C5, C11 and C12 of one anthracene group. Another plane, using the carbons in the same position on the other anthracene group was also generated. These two planes have an angle of 66.52° with respect to each other. The distance between two face to face anthracene groups on adjacent molecules is 3.47 Å, again indicating a π-π interaction (figure 6.12).

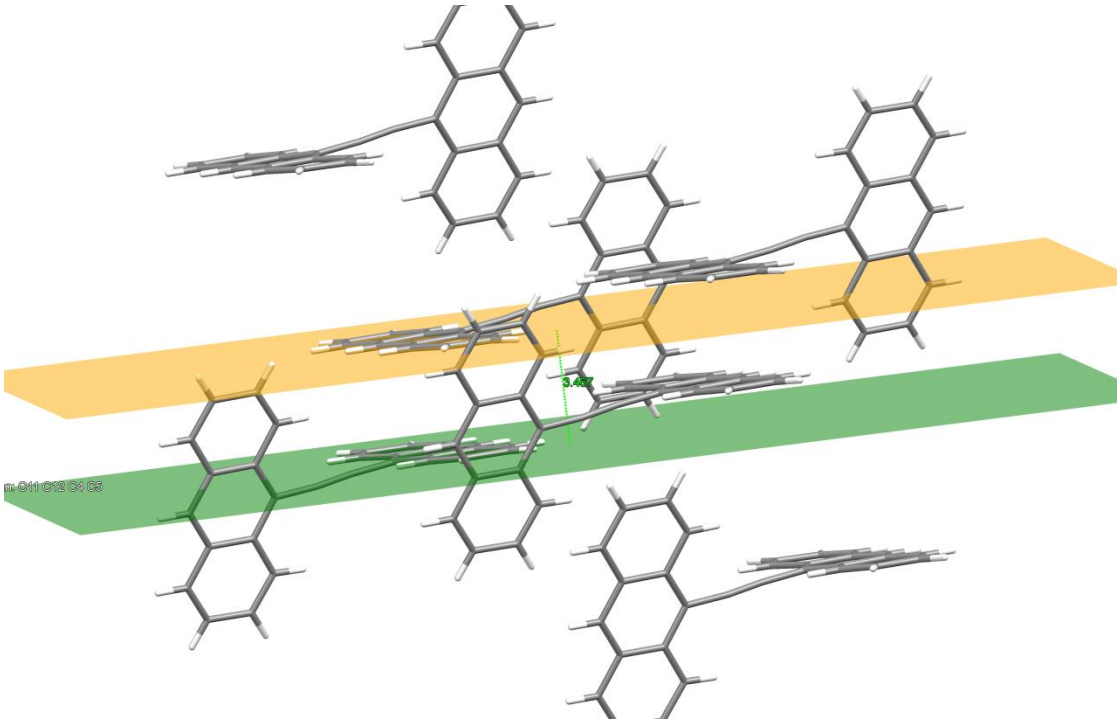


Figure 6.12 Average distance between two face-to-face anthracene groups.

Crystallographic Analysis of 51

Crystals of **51** were also obtained from a hot to cold recrystallisation performed in toluene (figure 6.13 and 6.14). The crystals obtained were red-orange in colour and block-like in shape. The crystal structure obtained for **51** was not a direct analogue of either polymorph of **50**.

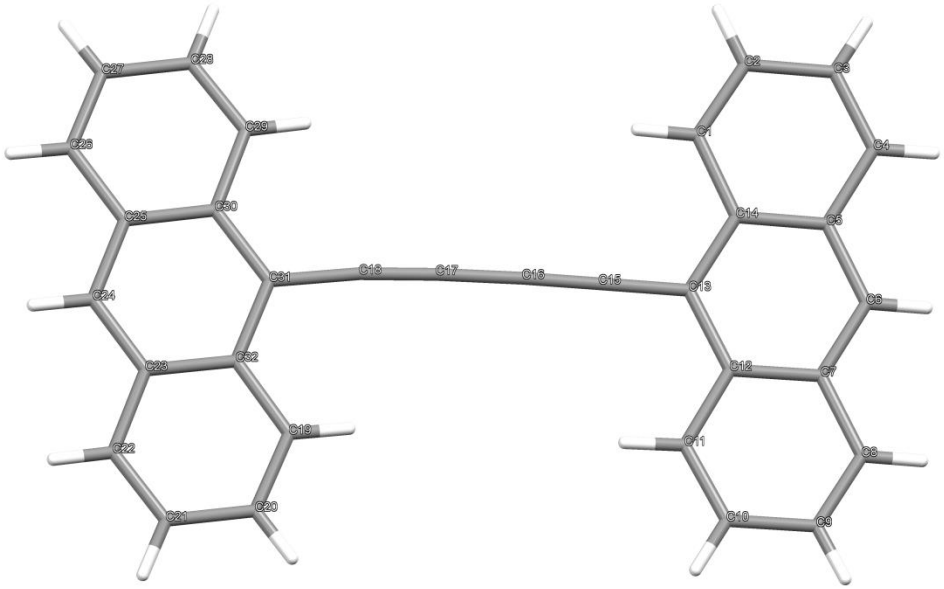


Figure 6.13 Crystal structure of 51.

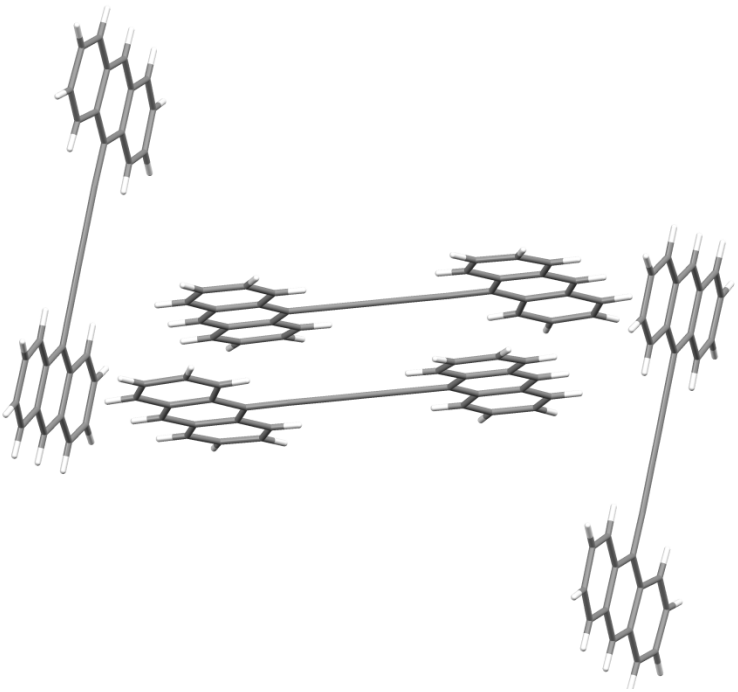


Figure 6.14 Packing of 51.

Unlike the previous structure obtained for **50**, the two sides of the molecule have slightly different properties, *i.e.* there is no inversion centre. The two alkyne bonds that link the

two anthracene groups need to be described separately. The bond between C17 and C18 had a measured length of 1.2059(14) Å and was at an angle of 174.86(11)° when measured against C31. The other alkyne bond between C15 and C16 was measured to be 1.2078(14) Å at an angle of 179.83(12)° to C13. When packing, the molecules orientate themselves so that the shorter alkyne bond of one molecule is in closer proximity to the next molecules longer alkyne bond. The most striking difference between this structure and the one obtained for **50** is that in this case, the anthracene moieties are nearly coplanar. If planes are generated in the same way as before (*i.e.* C2, C3, C9 and C10 on one anthracene and C20, C21, C27, C28 on the other anthracene) the angle separating the two planes on the same molecule is just 3.91°.

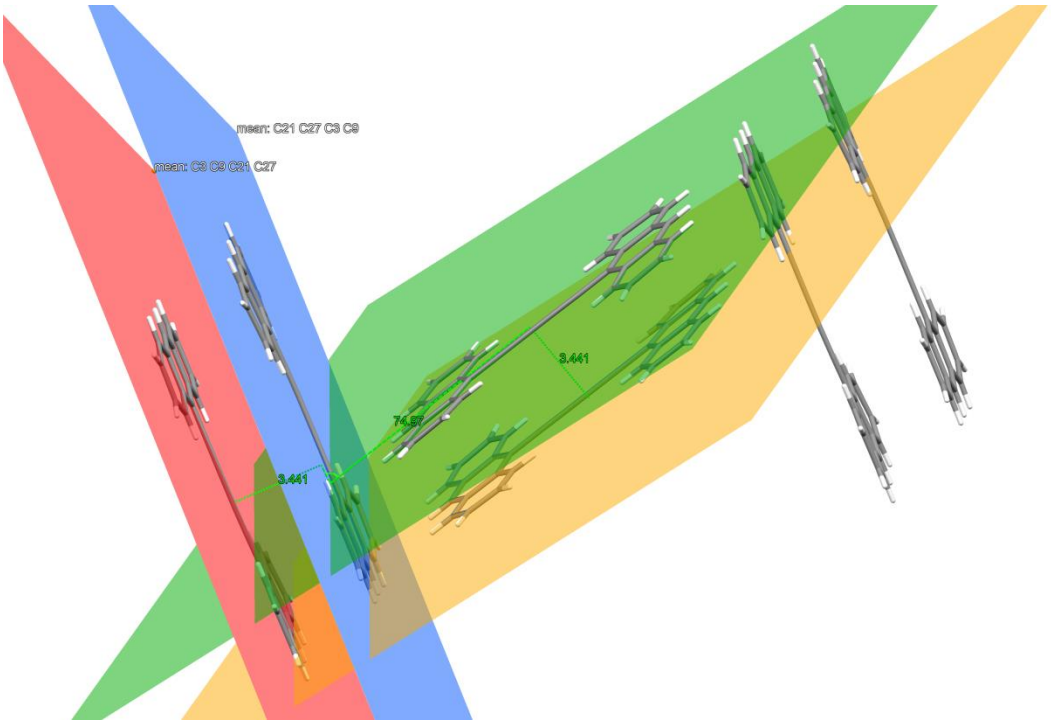


Figure 6.15 Packing of 51.

There is a mean average distance of 3.44 Å between molecules in the (slightly offset) face-to-face orientation (figure 6.15). This was determined by creating an average plane for each of the anthracene molecules, using C3 C9, C21 and C27. A second orientation of the molecule can be seen at 74.97° when comparing planes created by the anthracene

units compared to the first orientation. The face-to-face anthracenes in this orientation also have an average distance of 3.44 Å.

Crystallographic Analysis of 54

Crystals of **54** were obtained from two successive hot to cold recrystallisations performed in toluene (figures 6.16 and 6.17). The crystals obtained were red-brown in colour and needle like in shape.

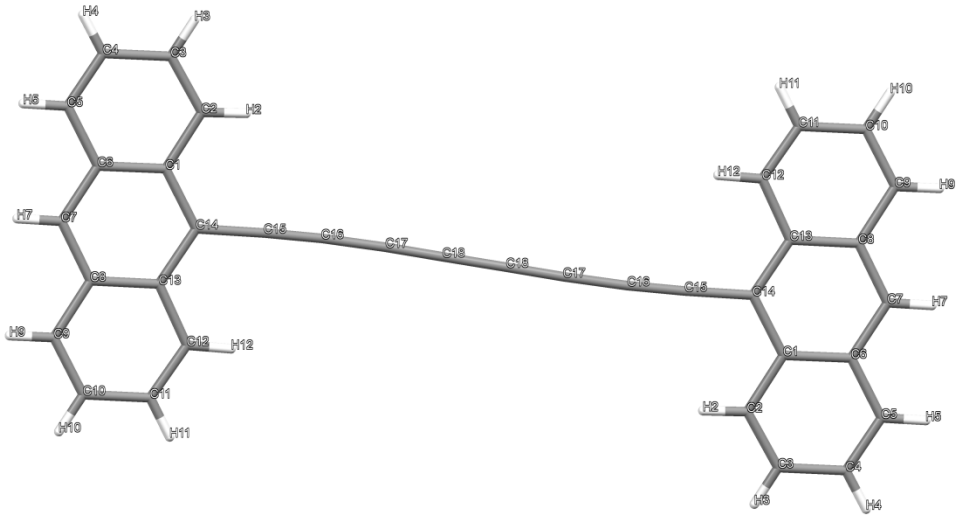


Figure 6.16 Crystal structure of 54.

The crystal structure had a centre of inversion so that only two alkyne bonds need to be described. The first alkyne bond, between C15 and C16 has length 1.215(5) Å and an angle of 177.8(4)° when measured from C14. The second alkyne bond between C17 and C18 marginally longer 1.221(5) Å and has a very similar angle when measured to C16, 177.5(4)°.

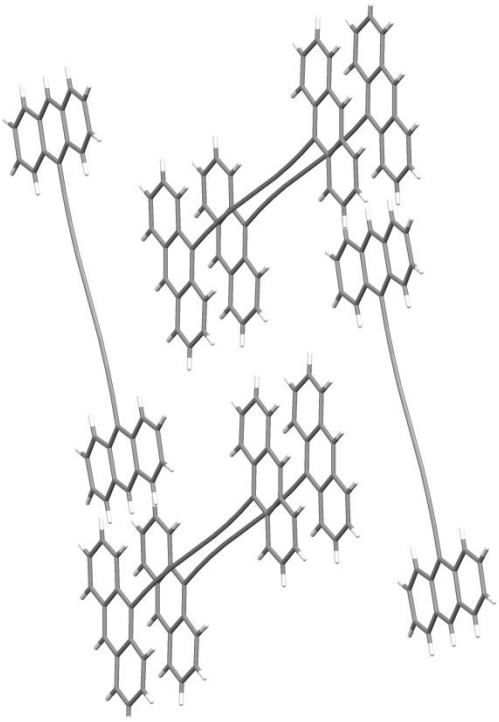


Figure 6.17 Packing of 54.

The packing again is different to that encountered in the previous molecules in this series. Two molecules face each other but the anthracene units are offset slightly. Planes were calculated using C4, C10, C4 and C10. These two molecules are separated by 3.45 Å in the crystal lattice. There is a second orientation of molecules within the crystals at an interplanar angle of 8.34° (figure 6.18).

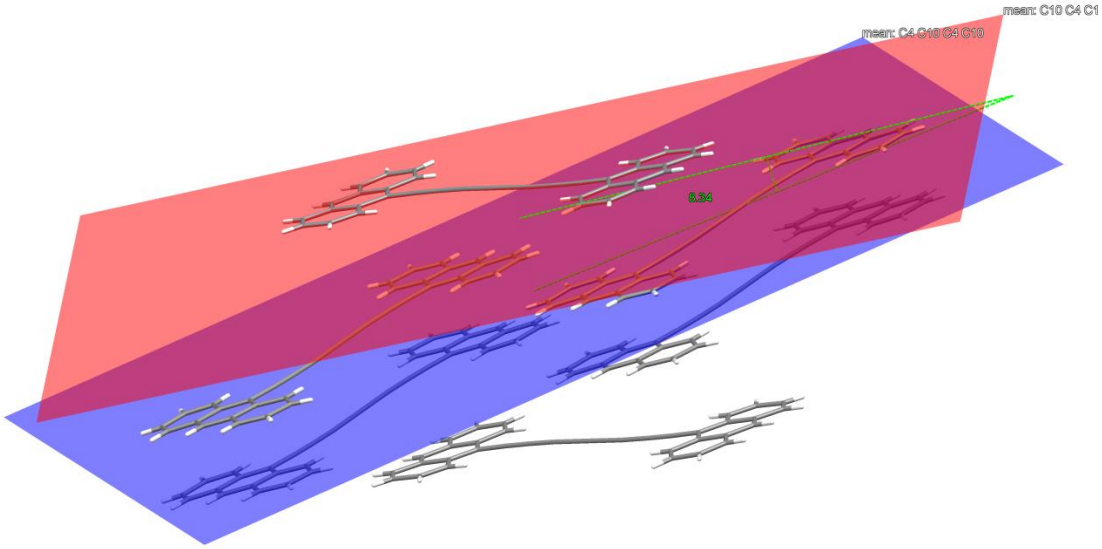


Figure 6.18 Orientation of anthracene units within the crystal.

Cyclic Voltammetry

Cyclic Voltammograms (CVs) were recorded for the protected anthracene compound **48** (figure 6.19), the anthracene dimer compounds **50**, **51** and the anthracene trimer compound **55 (**figures 6.20, 6.21, and 6.22 respectively). Compound **54** in the (poly)acetylene anthracene dimer series was insufficiently soluble to obtain CV data. The experiments were conducted at room temperature in DCM with 0.4 M $[^{n}Bu_4N][BF_4]$ supporting electrolyte.

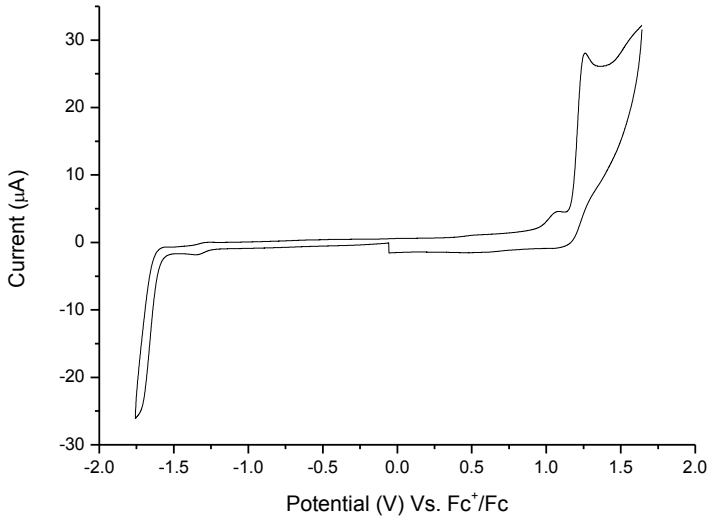


Figure 6.19 Cyclic voltammogram of 48 recorded in DCM with $[^{n}Bu_4N][BF4]$ (0.4 M) supporting electrolyte recorded at scan rate 0.1 V s^{-1}.

The CV recorded for **48** shows that there are no electrochemical reversible processes (whether oxidative or reductive) for the swept potential range.

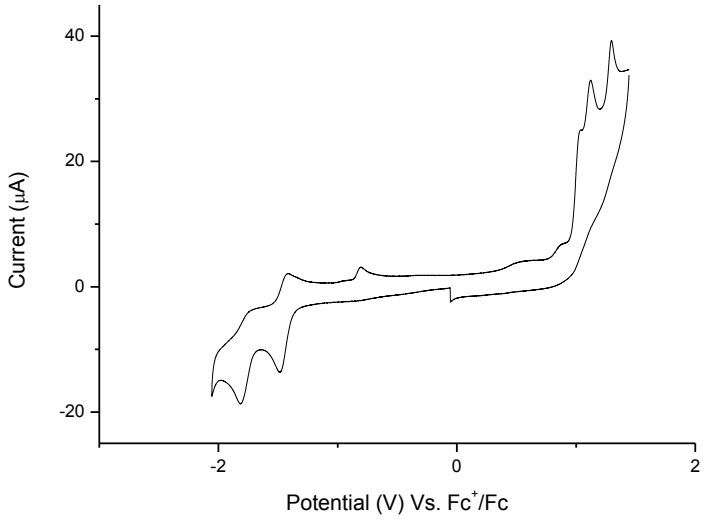


Figure 6.20 Cyclic voltammogram of 50 recorded in DCM with [^{n}Bu$_4$N][BF4] (0.4 M) supporting electrolyte recorded at scan rate 0.1 V s^{-1}.

The first reductive process E_p is at -1.45 V and is reversible. For a fully reversible one-electron process $E_{pa} - E_{pc}$ = 59 mV.[28] This process was measured as $E_{pa} - E_{pc}$ = 62 mV, so corresponds to a one electron reduction with deviation from the theoretical value within the expected range due to experimental limitations. The second reduction at E_p -1.78 V is also a one electron reversible process, $E_{pa} - E_{pc}$ = 76 mV. The CV also presents several oxidation processes that are irreversible.

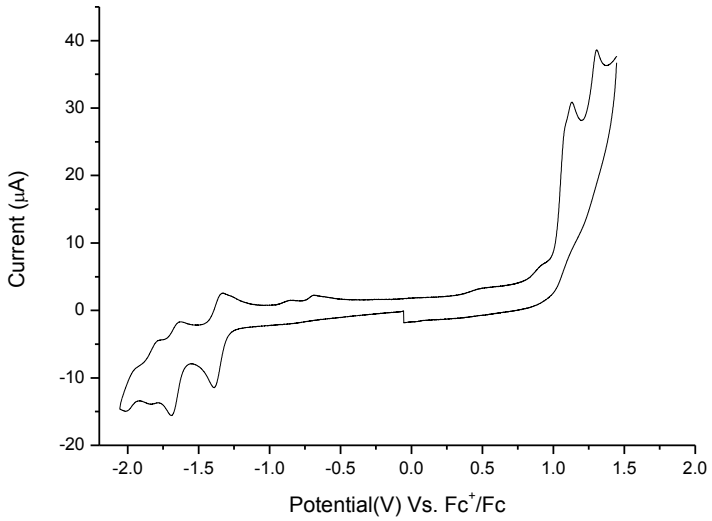


Figure 6.21 Cyclic voltammogram of 51 recorded in DCM with [^{n}Bu$_4$N][BF4] (0.4 M) supporting electrolyte recorded at scan rate 0.1 V s^{-1}.

The CV recorded for **51** looks similar to that collected for **50**. It possess a reversible reduction at E_p = 1.36 V, $E_{pa} - E_{pc}$ = 58 mV, another one at 1.66 V, , $E_{pa} - E_{pc}$ = 58 mV and a third resolvable at -1.81 V, $E_{pa} - E_{pc}$ = 53 mV. As with **50**, there are several oxidative processes that are irreversible.

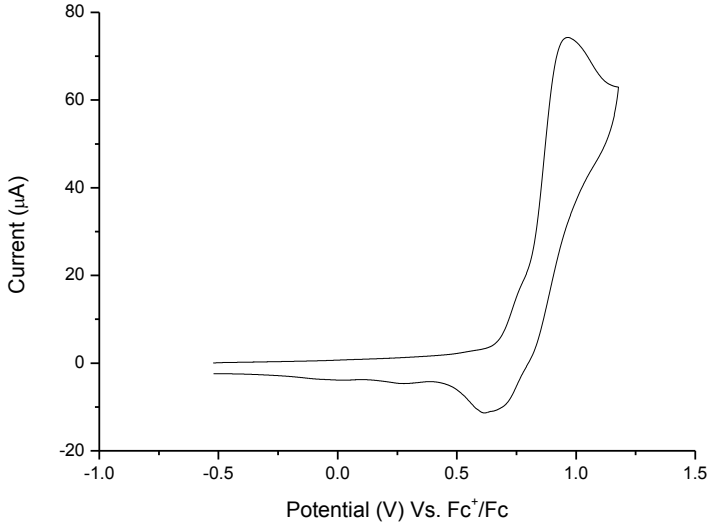


Figure 6.22 Cyclic voltammogram of 55 recorded in DCM with [^{n}Bu$_4$N][BF4] (0.4 M) supporting electrolyte recorded at scan rate 0.1 V s^{-1}.

The CV data collected for **55** shows that there are no reductive processes occurring. There is one reversible oxidation process. The $E_{pa} - E_{pc}$ = 31 mV which corresponds well with a 2 electron process.

Fluorescence Measurements

Fluorescence measurements were taken for the compounds **48**, **50**, **51**, and **54** (figures 6.23, 6.24, 6.25 and 6.26 respectively). For many of the spectra recorded, the excitation and emission spectra are not the typical mirror image of each other. The peak intensities of **51** and **54** appear to have been reversed and the clearly resolvable peaks of **50** in the excitation spectrum have merged into a single observable peak in the emission spectrum. These deviations in the emission spectra from the expected mirror image shape indicate that there is additional photophysical processes occurring. The most likely cause of these additional processes is photodimerisation of the anthracene moieties. The photodimerisation process of anthracene compounds is initiated by blue - UV light.[29] As the fluorescence spectra were recorded using excitation wavelengths 372 nm (for **48**) 417 nm (for **50** and **51**) and 450 nm (for **54**), it is reasonable to suggest that these excitation wavelengths are causing part of the sample compound to photodimerise whilst fluorescence measurements were being taken, and that the multiple species that would arise from the photodimerisation process are responsible for the complicated emission spectra obtained.

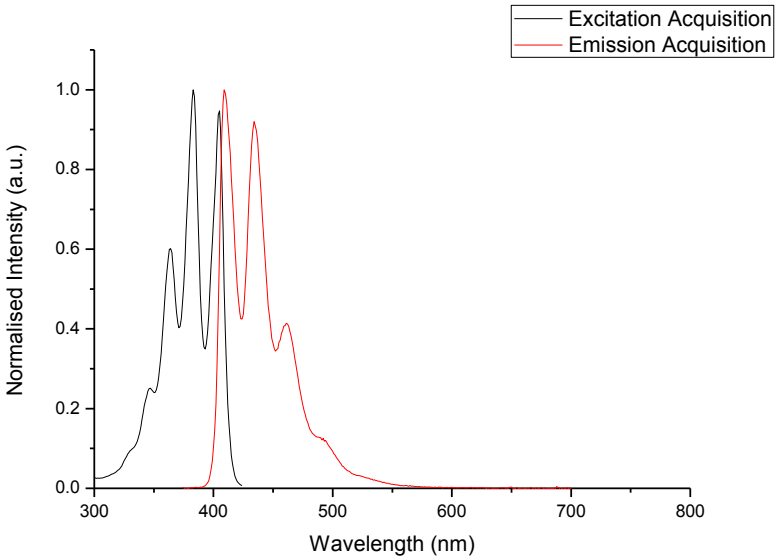


Figure 6.23 Excitation and fluorescence spectra for 48.

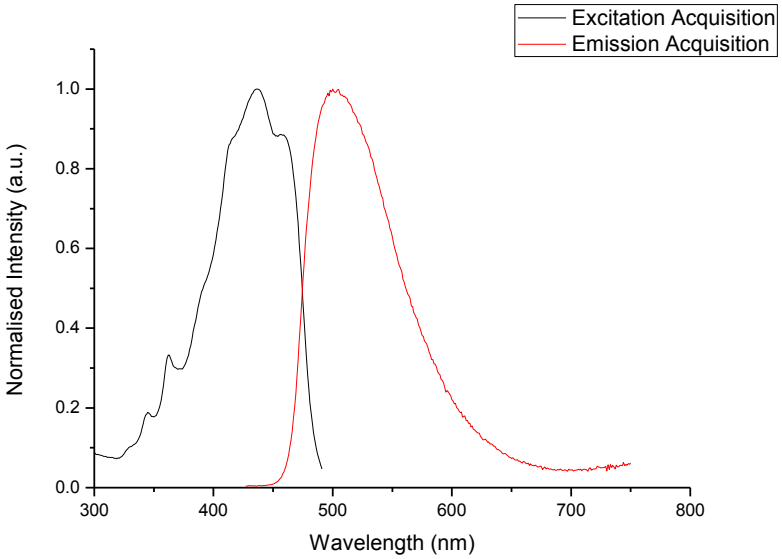


Figure 6.24 Excitation and fluorescence spectra for 50.

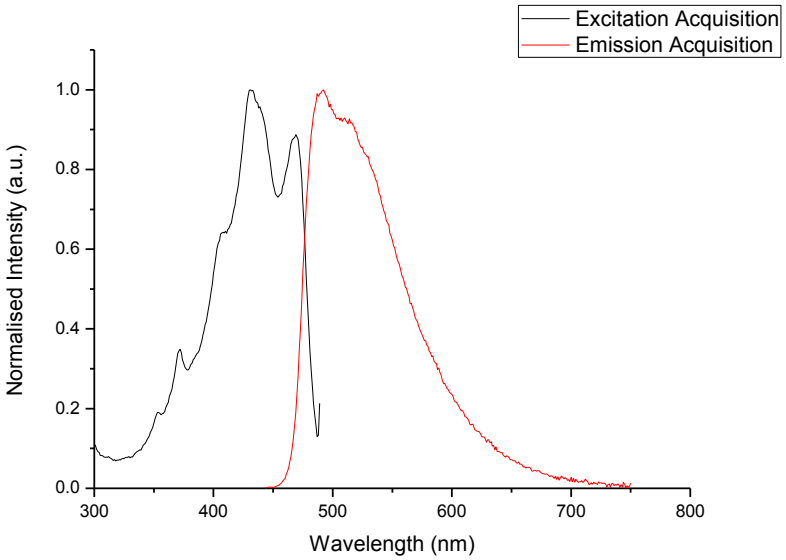


Figure 6.25 Excitation and fluorescence spectra for 51.

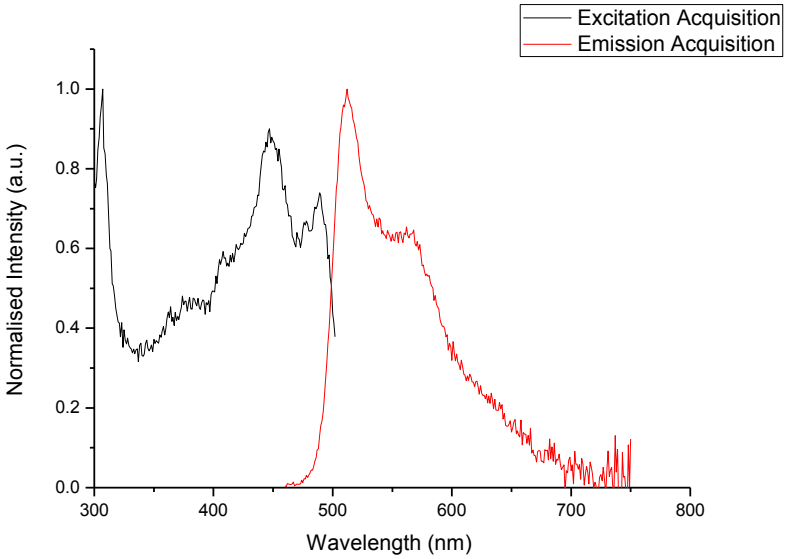


Figure 6.26 Excitation and fluorescence spectra for 54.

Quantum yields were calculated using the equation for compounds **48**, **50**, **51** and **54** using comarin-153 as the standard compound. Solutions of the target compounds were prepared in DCM whereas solutions of coumarin-153 were prepared in ethanol.

$$\Phi_x = \Phi_{ST}\left(\frac{Grad_x}{Grad_{ST}}\right)\left(\frac{\eta_x^2}{\eta_{ST}^2}\right)$$

Where Φ_x is the quantum yield of compound x, Φ_{ST} is the quantum yield of the standard compound, Grad is the gradient of the plot integrated fluorescence intensity Vs. absorbance and η the refractive index of the solvent.

Table 6.1 Summary of fluorescence measurements for compounds 48, 50, 51 and 54.

Compound	λ_{abs} (nm)	λ_{em} (nm)	Stokes shift (nm)	Quantum Yield
48	405	409	4	0.476768
50	456	500	44	0.014494
51	469	492	23	0.016438
54	489	512	23	0.002455

We can see from these results that the protected anthracene compound **48** is very fluorescent. The anthracene dimers **50** and **51** have a much lower quantum yield and anthracene dimer **54** has almost zero fluorescence.

Conclusions

A series of (poly)acetylene anthracene dimers has been successfully synthesised and crystal structures have been solved for each member of the series.

Two polymorphs were present in the recrystallisation attempts performed by cooling a hot solution of **50** in toluene. The vast majority of crystals obtained were that of polymorph α, but a small amount *c.a.* 2% were of polymorph β. Both polymorphs had a centre of inversion around the middle of the alkyne bond. Polymorph β is the most unusual structure throughout this series as the two anthracene planes of the molecule are not co-planar/parallel but are instead twisted, with the angle the planes intersect measured as 66.52°.

The crystal structure obtained from cooling of a hot solution of **51** in toluene, although had potential for a centre of inversion, did not present one.

The Tetra-acetylene anthracene dimer **54** required two successive recrystallisations before crystals suitable for X-Ray diffraction were obtained. The crystal structure showed a much more 'flat' packing than **50** and **51**, with planes of the different orientations of dimer molecules intersecting at 8.34° compared with 86.94° (**50**) and 74.97° (**51**) respectively.

Fluorescence measurements were also taken of these compounds, along with the protected anthracene **48**. The emission spectra obtained were slightly unusual in that they were not mirror images of the excitation spectra, indicating that additional photophysical processes were also occurring. This is most likely due to the photodimerisation of

anthracenes initiated by UV-blue light, as this range of light was used to collect the fluorescence data.

The attempted synthesis of 1,3,5-tri(9,9',9"-anthracenyl)benzene actually resulted in the production of 1,2,4-tri(9,9',9"-anthracenyl)benzene, with the structure being confirmed by X-ray diffraction studies performed on a crystal grown from cooling a hot solution of **54** in toluene.

Experimental

4-(Anthracen-9-yl)-2-methylbut-3-yn-2-ol (48)

9-Bromoanthracene (5.00 g, 19.4 mmol), $Pd(PPh_3)_2Cl_2$ (38 mg, 54.1 μmol), CuI (50 mg, 0.263 mmol) and PPh_3 (78 mg, 0.297 mmol) were placed in a Schlenk flask purged with N_2. Degassed triethylamine (25 mL) was added, the mixture was stirred and heated to reflux. 2-methyl-but-3-yn-2-ol (4.47 mL, 46.1 mmol) was added and the mixture was allowed to reflux for a further 4 h before cooling to RT. The mixture was filtered and the solvents were removed *in vacuo*. The residue was subjected to column chromatography (silica, DCM) to produce the title compound as a yellow crystalline solid (3.40 g, 13.1 mmol, 68%).

^{1}H NMR (400 MHz, $CDCl_3$) δ = 8.51 (dd, *J* = 8.72, 0.94 Hz, 2 H), 8.42 8.00 (d, *J* = 8.41 Hz, 1 H), 7.58 (ddd, *J* = 8.44, 6.74, 1.25 Hz, 2 H), 7.50 (m, 2 H), 2.36 (s, 1 H), 1.86 (s, 6 H) ppm. ^{13}C NMR (101 MHz, $CDCl_3$) δ = 132.58, 131.08, 128.64, 127.70, 126.60, 126.52, 125.61, 116.58, 105.19, 78.86, 66.24, 31.85 ppm. MS: (ESI) *m/z* calculated for $[C_{19}H_{16}O + H]^+$: 261.1274. Found: 261.1266. Elemental analysis calculated for $C_{19}H_{16}O$: C, 87.66; H, 6.20; N,0.00. Found: C, 87.56; H, 6.25; N, 0.00.

9-Ethynylanthracene (49)

A solution of **48** (1.00 g, 3.84 mmol) in degassed toluene (35 mL) was prepared and heated to reflux. Potassium hydroxide (270 mg, 4.81 mmol) was added, the reaction mixture stirred and heated under reflux for 25 mins. The mixture was cooled, filtered and the solvents removed *in vacuo*. The crude product was purified by column chromatography (silica, hexane) to produce the title compound as a light yellow crystalline solid (600 mg, 2.97 mmol, 77%).

^{1}H NMR (400 MHz, $CDCl_3$) δ = 8.56 - 8.62 (m, 2 H), 8.47 (s, 1 H), 8.00 - 8.07 (m, 2 H), 7.60 (ddd, *J* = 8.73, 6.61, 1.32 Hz, 2 H), 7.49 - 7.55 (m, 2 H), 4.00 (s, 1 H) ppm. ^{13}C NMR (101 MHz, $CDCl_3$) δ = 133.16, 131.01, 128.65, 128.22, 126.82, 126.54, 125.67, 116.01, 88.18, 80.32 ppm. MS: (EI) *m/z* calculated for $[C_{16}H_{10}]^+$: 202.0777. Found: 202.0772.

1,2-Di(9-anthrancenyl)ethyne (50)

9-Bromoanthracene (350 mg, 1.36 mmol), **49** (494 mg, 2.44 mmol) and $Pd(PPh_3)_4$ (203 mg, 0.176 mmol) were placed in a Schlenk flask purged with N_2. DMF (70 mL) and triethylamine (3.5 mL) were degassed and added to the mixture in a single portion. The mixture was stirred and heated under reflux for 24 h. The mixture was cooled, filtered and the solvents removed *in vacuo*. The residue was subjected to column chromatography (silica, 4:1, hexane/DCM) and finally crystallised from toluene to produce crystalline orange needles (350 mg, 0.925 mmol, 68%).

^{1}H NMR (400 MHz, $CDCl_3$) δ = 8.93 (dd, *J* = 8.66, 0.88 Hz, 4 H), 8.54 (s, 2 H), 8.10 (d, *J* = 8.41 Hz, 4 H), 7.64 - 7.70 (m, 4 H), 7.55 - 7.61 (m, 4 H) ppm. ^{13}C NMR ($CDCl_3$, 101 MHz): δ = 132.8, 131.4, 128.8, 128.0, 126.9, 126.9, 125.8, 117.7, 97.4, ppm. MS: (EI) *m/z* calculated for $[C_{30}H_{18}]^+$: 378.14030. Found: 378.13881. Elemental analysis calculated for $C_{30}H_{18}$: C, 95.21; H, 4.79; N,0.00. Found: C, 95.12; H, 4.80; N, 0.00.

1,4-Di(9-anthracenyl)1,3-butadiyne (51)

9-Ethynylanthracene (100mg, 0.494 mmol) was dissolved in acetone (10 mL), followed by an addition of TMEDA (74 μL, 0.494 mmol). CuI (5 mg, 0.0263 mmol) was added and the mixture was stirred at RT for 20 h. Chloroform (50 mL) was added and the solution washed with saturated NH_4Cl solution, water and brine. The organic phase was dried with magnesium sulfate, filtered and solvents removed *in vacuo*. The residue was purified

by column chromatography (silica, 4:1, hexane/chloroform) to produce the title compound as a bright orange solid (30 mg, 0.0745 mmol, 30%).

^{1}H NMR (400 MHz, $CDCl_3$) δ = 8.72 (dd, *J* = 8.62, 0.88 Hz, 4 H), 8.51 (s, 2 H), 8.07 (d, *J* = 8.48 Hz, 4 H), 7.69 (ddd, *J* = 8.70, 6.58, 1.24 Hz, 4 H), 7.57 (ddd, *J* = 8.22, 6.76, 1.10 Hz, 4 H) ppm. ^{13}C NMR (101 MHz, $CDCl_3$) δ = 134.04, 131.13, 128.94, 128.91, 127.28, 126.68, 125.94, 115.80, 85.08, 81.66 ppm. MS: (FD) *m/z* calculated for $[C_{32}H_{18}]^+$: 402.1403. Found: 402.14044.

9-((Z)-4-Chlorobut-3-en-1-ynyl)anthracene (52)

CuI (60 mg, 0.315 mmol), $Pd(PPh_3)_4$ (180 mg, 0.156 mmol), 1,2-dichloroethylene (0.478 mL, 6.31 mmol) and n-butylamine (1.56 mL, 15.6 mmol) were added to a solution of **49** (630 mg, 3.11 mmol) in toluene (10 mL). The reaction mixture was then stirred at RT in darkness for 24 h. The mixture was then washed with water and brine, dried with magnesium sulfate and solvents removed *in vacuo*. Column chromatography (silica, hexane) afforded the target compound as a bright yellow solid (526 mg, 2.00 mmol, 64%).

^{1}H NMR (400 MHz, $CDCl_3$) δ = 8.66 (d, *J* = 8.66 Hz, 2 H), 8.47 (s, 1 H), 8.03 (dd, *J* = 8.40, 0.70 Hz, 2 H), 7.57 - 7.65 (m, 2 H), 7.49 - 7.56 (m, 2 H), 6.62 (d, *J* = 7.28 Hz, 1 H), 6.39 - 6.48 (m, 1 H) ppm. ^{13}C NMR (101 MHz, $CDCl_3$) δ = 132.74, 131.10, 128.65, 128.44, 128.28, 126.89, 126.71, 125.74, 116.69, 112.48, 94.62, 94.44 ppm.

9-(Buta-1,3-diynyl)anthracene(53)

Bu_4NF (1M in THF, 1 mL 1 mmol) was added to a solution of **52** (100 mg, 0.381 mmol) in degassed THF (10 mL). The solution was covered to exclude light and stirred for 24 h before being quenched with aqueous NH_4Cl solution. The mixture was extracted with diethyl ether, washed with water and brine and then dried with magnesium sulfate. After

filtration, the solvents were removed *in vacuo* and the residue purified by column chromatography (silica, hexane) to give the title compound as a yellow solid (50 mg, 0.221 mmol, 58%).

^{1}H NMR (400 MHz, $CDCl_3$) δ = 8.54 (d, *J* = 8.78 Hz, 2 H), 8.49 (s, 1 H), 8.03 (d, *J* = 8.41 Hz, 2 H), 7.59 - 7.65 (m, 2 H), 7.50 - 7.56 (m, 2 H), 2.80 - 2.85 (m, 1 H) ppm. ^{13}C NMR (101 MHz, $CDCl_3$) δ = 134.35, 130.98, 129.23, 128.88, 127.39, 126.35, 125.90, 114.69, 84.15, 74.01, 72.70, 68.49 ppm.

1,8-Di(9-anthracenyl)1,3,5,7octatetrayne (54)

53 (40 mg, 0.177 mmol) was dissolved in acetone (10 mL). To this, TMEDA (36 μL, 0.241 mmol) and CuI (3 mg, 0.016 mmol) were added causing an immediate colour change from golden-yellow to red-orange and the mixture was left to stir, after 5 minutes some precipitate was starting to form. After 1 h, a significant amount of precipitate had formed and the mixture was brown in colour. DCM (200 mL) was added to dissolve this precipitate, this was the washed with water, brine, dried with magnesium sulfate, filtered and solvents removed *in vacuo* to produce an orange brown solid. Single crystals were grown by recrystallizing the solid in toluene twice to afford the title compound (4 mg, 8.88 μmol, 10%). This solid was not soluble enough to collect ^{13}C NMR data.

^{1}H NMR (400 MHz, $CDCl_3$) δ = 8.56 (d, *J* = 7.63 Hz, 4 H), 8.52 (s, 2 H), 8.06 (d, *J* = 8.39 Hz, 4 H), 7.63 - 7.70 (m, 4 H), 7.56 (m, 4 H) ppm.

1,2,4-Tri(9,9',9''-anthracenyl)benzene (55)

49 (400 mg, 1.98 mmol) and $Co_2(CO)_8$ (205 mg, 0.600 mmol) were placed in a Schlenk flask. Degassed 1,4-dioxane (120 mL) was introduced and the mixture was heated under reflux with stirring for 20 h. The mixture was cooled, filtered and the solvents removed *in vacuo*. The residue was purified by column chromatography (silica, 1:1,

chloroform/hexane) followed by a crystallisation from toluene to produce small, block-like, light yellow crystals (90 mg, 0.148 mmol, 22%). This solid was not soluble enough to collect ^{13}C NMR data.

^{1}H NMR (400 MHz, $CDCl_3$) δ = 8.58 (s, 1 H), 8.23 - 8.27 (m, 2 H), 8.13 (s, 1 H), 8.10 - 8.12 (m, 2 H), 8.07 - 8.10 (m, 2 H), 8.05 - 8.06 (m, 1 H), 8.04 (d, J = 8.41 Hz, 1 H), 8.01 (s, 1 H), 7.90 - 7.93 (m, 3 H), 7.67 (d, J = 8.41 Hz, 2 H), 7.53 - 7.63 (m, 6 H), 7.19 - 7.24 (m, 2 H), 7.12 - 7.17 (m, 4 H), 7.04 - 7.09 (m, 2 H) ppm. MS: (MALDI-TOF) m/z calculated for $[C_{48}H_{30}]^{+}$: 606.2342. Found: 606.2326. Elemental analysis calculated for $C_{48}H_{30}$: C, 95.02; H, 4.98; N, 0.00. Found: C, 94.95; H, 5.10; N, 0.00.

References

1. S. Mery, D. Haristoy, J. F. Nicoud, D. Guillon, H. Monobe and Y. Shimizu, *J. Mater. Chem.*, 2003, **13**, 1622-1630.

2. D. Kotowski, B. Kutrzeba-Kotowska, M. Obarowska, R. Signerski and J. Godlewski, *Org. Electron.*, 2005, **6**, 193-199.

3. D. J. Yun, J. Chung, C. Jung, H. S. Han, J. Lee, B. Anass, S. Lee, Y. Kyung and S. H. Park, *J. Electrochem. Soc.*, 2013, **160**, 436-442.

4. L. Jiang, J. H. Gao, E. J. Wang, H. X. Li, Z. H. Wang and W. P. Hu, *Adv. Mater.*, 2008, **20**, 2735-2740.

5. H. S. Kim, Y. H. Kim, T. H. Kim, Y. Y. Noh, S. Pyo, M. H. Yi, D. Y. Kim and S. K. Kwon, *Chem. Mater.*, 2007, **19**, 3561-3567.

6. H. Meng, F. P. Sun, M. B. Goldfinger, F. Gao, D. J. Londono, W. J. Marshal, G. S. Blackman, K. D. Dobbs and D. E. Keys, *J. Am. Chem. Soc.*, 2006, **128**, 9304-9305.

7. H. Lee, J. A. Hur, M. J. Cho, D. H. Choi and T. D. Kang, *J. Korean. Phys. Soc.*, 2013, **62**, 930-936.

8. S. O. Kim, M. W. Lee, S. H. Jang, S. M. Park, J. W. Park, M. H. Park, S. H. Kang, Y. H. Kim, C. K. Song and S. K. Kwon, *Thin Solid Films*, 2011, **519**, 7998-8002.

9. J. H. Yao, Y. W. Li, Z. G. Zou, J. W. Yang and Z. L. Yin, *Physica B Condens. Matter*, 2011, **406**, 3969-3974.

10. D. Psiachos, *Chem. Phys.*, 2014, **436**, 8-16.

11. S. Akiyama and M. Nakagawa, *Bull. Chem. Soc. Jpn.*, 1970, **43**, 3561-3566.

12. A. S. Cherkasov and T. M. Vember, *Opt. Spektrosk.*, 1959, **7**, 321-325.

13. R. Bhola, P. Payamyar, D. J. Murray, B. Kumar, A. J. Teator, M. U. Schmidt, S. M. Hammer, A. Saha, J. Sakamoto, A. D. Schluter and B. T. King, *J. Am. Chem. Soc.*, 2013, **135**, 14134-14141.

14. P. Payamyar, M. Servalli, T. Hungerland, A. P. Schutz, Z. K. Zheng, A. Borgschulte and A. D. Schluter, *Macromol. Rapid. Comm.*, 2015, **36**, 151-158.

15. P. Kissel, D. J. Murray, W. J. Wulftange, V. J. Catalano and B. T. King, *Nat. Chem.*, 2014, **6**, 774-778.

16. M. J. Kory, M. Worle, T. Weber, P. Payamyar, S. W. van de Poll, J. Dshemuchadse, N. Trapp and A. D. Schluter, *Nat. Chem.*, 2014, **6**, 779-784.

17. L. Gutierrez-Arzaluz, C. A. Guarin, W. Rodriguez-Cordoba and J. Peon, *J. Phys. Chem. B*, 2013, **117**, 12175-12183.

18. R. Umeda, H. Tabata, Y. Tobe and Y. Nishiyama, *Chem. Lett.*, 2014, **43**, 883-884.

19. Q. Xiao, R. T. Ranasinghe, A. M. P. Tang and T. Brown, *Tetrahedron*, 2007, **63**, 3483-3490.

20. V. Gandon, D. Leca, T. Aechtner, K. P. C. Vollhardt, M. Malacria and C. Aubert, *Org. Lett.*, 2004, **6**, 3405-3407.

21. A. Kalogerakis and U. Groth, *Org. Lett.*, 2003, **5**, 843-844.

22. G. Chouraqui, M. Petit, P. Phansavath, C. Aubert and M. Malacria, *Eur. J. Org. Chem.*, 2006, 1413-1421.

23. K. Tanaka, Y. Takahashi, T. Suda and M. Hirano, *Synlett*, 2008, 1724-1728.

24. K. M. Oberg, E. E. Lee and T. Rovis, *Tetrahedron*, 2009, **65**, 5056-5061.

25. R. T. Yu and T. Rovis, *J. Am. Chem. Soc.*, 2006, **128**, 2782-2783.

26. H. D. Becker, B. W. Skelton and A. H. White, *Aust. J. Chem.*, 1985, **38**, 1567-1570.

27. R. I. Goldstein, R. Guo, C. Hughes, D. P. Maurer, T. R. Newhouse, T. J. Sisto, R. R. Conry, S. L. Price and D. M. Thamattoor, *Crystengcomm*, 2015, **17**, 4877-4882.

28. J. Phelps and A. J. Bard, *J. Electroanal. Chem.*, 1976, **68**, 313-335.

29. H. Bouas-Laurent, A. Castellan, J. P. Desvergne and R. Lapouyade, *Chem. Soc. Rev.*, 2000, **29**, 43-55.

Chapter 7:

Conclusions

This thesis primarily explores how simple building blocks can be used to create complex molecular architectures. As the complexity of the final target compounds increases, the need for reliable, high yielding reactions early on in the synthetic pathway becomes ever more paramount. This need is illustrated particularly well with the Tetrimino S/Z compound. If we count the one-pot reduction, condensation and oxidation reactions performed to make each porphyrin from the dicarbonyl species as a single reaction, then the porphyrins that are needed in the synthesis of Tetrimino S/Z (**28** and **29** and **23**) take 7, 9 and 4 reactions respectively to make. The Sonogashira coupling and deprotection reactions add 3 more to the total giving a final count of 23 reactions.

This number of reactions for a single product may seem to be slightly unwieldly, but rather than being 23 reactions in a linear synthesis, the Tetris compounds were designed to be products of a convergent synthetic route, so that the longest 'chain' of reactions is actually 12. The nature of this research also meant that many of the early stage reactions were used towards several different products and so with this in mind, the total number of reaction to form Tetrimino S/Z falls to 20 reactions. This is a small improvement but if we consider that usually each of the porphyrin monomers were used in the synthesis of multiple Tetris compounds then the benefits of this convergent synthesis route become more pronounced.

Although only eight different porphyrin monomers were discussed in chapter 3, the wide range of dipyrromethanes synthesised in chapter 2 would allow many more porphyrins to be synthesised. Any combination of a 1,9-diacylated dipyrromethane and another dipyrromethane can be combined to form a porphyrin by just an additional reduction, condensation, and oxidation reaction. Additionally, the results discussed in chapter 2 show that the reactions forming the dipyrromethane building blocks (for the most part)

proceeded fairly efficiently and can be made in the gram scale using relatively cheap starting materials. This in turn means that the porphyrin monomers themselves can be made in relatively large quantities (several 100 mg) so that plenty of material is available to perform coupling reactions. The versatility of the system designed whereby the dipyrromethanes involved in the porphyrin forming reaction could be freely interchanged is very appealing. Such a system allows for the architecture of larger porphyrinic systems to be encoded by carefully selecting the dipyrromethanes which would result in porphyrin units with substituents in the desired positions.

The coupling reaction between the porphyrin monomers proved to be amongst the lowest yielding reactions presented in this thesis. Although figuring out the purification process did consume a lot of time and materials, once the procedure was in place it was quite efficient and did not lose much material. The low yields therefore come from the generation of unwanted by-products. Evidence of an unwanted enyne product was apparent in many of the reactions, which was fortunately separable from the desired product but should this research be continued, efforts should be made to reduce the amount generated of this unwanted by-product. The SEC performed during the purification of the Tetris compounds also showed the generation of HMWM, eluting as a fairly prominent band before the desired material.

The Tetris compounds admittedly, do not have any immediate applications associated with them although it would be interesting to deposit these Tetris compounds onto a surface to observe how they tile with respect to each other, mimicking the 2D nature of the computer game. The Tetris T, J/L O and I Tetrimino compounds are all examples of rep-tiles introduced in chapter 1. If we discover that the tilings produce a hierarchical structure as often seen in rep-tile tilings, then this could be very interesting indeed.

The methodology used to synthesise the porphyrin dimers discussed in chapter 4 was successful but low yielding. The low yields have been attributed to the need for two cyclisation reactions occurring during the condensation stage, rather than the usual one which increases the chances of undesirable intermolecular reactions occurring. These porphyrin dimers were terminated with bromoaryl groups that make them suitable for later incorporation into covalent organic frameworks. The compounds have yet to be deposited onto a surface for characterisation as SCOFs. The data collected from the crystals grown show how the presence of TFA anions within the crystal structure distort the planar configuration of the porphyrin rings into a puckered conformation.

This thesis has also presented the synthesis of a number of anthracene compounds along with analysis of their crystal structures. We were able to observe that changing the number of alkyne groups in the (poly)acetylene anthracene dimer series, significant changes to the packing of the molecules occurred within the crystal structure. These types of molecules containing anthracene and acetylene groups have previously been used as components in organoelectronic devices.